The field relationships and mineral chemistry of mafic and ultramafic intrusions in the Loch Uisg area, Isle of Mull.

James Alexander Westland
BSc. (Hons), St. Andrews

Thesis presented for the degree of Master of Science

University of Glasgow

School of Geographical & Earth Sciences

August 2014

Abstract

The Loch Uisg Granite-Gabbro Intrusion, previously known as the Loch Uisg Granophyre and Gabbro, is a 2-component intrusion, which crops out in the south-east of the Island of Mull. It was first described in the Mull Memoir of the BGS (Bailey *et al*, 1924). It comprises an extensive granitic component and two smaller gabbroic units, intruded into folded basaltic lava country rocks. The latter gabbroic units are slightly different to one another in terms of their field characteristics and their mineral chemistry, but are thought to comprise one gabbroic intrusion. The granite and the gabbro were re-mapped and samples taken for optical and SEM analysis. As a result of this work, a new model for emplacement is proposed based on field relationships of the units and the mineral chemistry. Interaction between the felsic and the mafic components is considered in detail. By detailed examination of the field relationships and the mineral chemistry it is proposed that the granite was intruded first and that the gabbro was intruded soon after.

Intruded into the Loch Uisg Granite-Gabbro Intrusion and the surrounding basaltic country rocks are two very different suites of mafic and ultramafic rocks. These are described in this work as the "Loch Uisg Picrite Suite" and the "Miscellaneous Minor Intrusions".

The Loch Uisg Picrite Suite comprises three intrusions: an irregular dyke-like intrusion and two sill-like intrusions of very fresh picrite, rich in magnesian olivine (up to $Fo_{91.5}$). These figures place the LUPS rocks in the same category as the Baffin Island Picrites, the Horingbaai dykes from Namibia, the Gorgona komatiites, and the M9 dyke of Rum. Due to the highly magnesian nature of these rocks, these intrusions are unusual within the British Palaeogene Igneous Province. The dyke-like body, known as the Gleann Beag Intrusion after its location, displays very pronounced igneous layering. Layering is also present in the sill-like bodies. The mineral chemistry is described in detail and a petrogenetic model is proposed for the origin of these unusual rocks. Because of the unusual nature of these rocks, the igneous history of SE Mull has been re-assessed. It is proposed that ultramafic activity in SE Mull recommenced at a late stage in the overall history of the Palaeogene magmatism. Due to the freshness of the LUPS rocks, it is proposed that the emplacement of the

intrusions of this particular suite may represent some of the very last igneous events in Mull.

The third suite of mafic rocks is composed of several altered medium to coarse-grained dykes and dyke-like bodies which cross the area, broadly following the regional NW-SE trend where they are found cutting the Loch Uisg Granite-Gabbro Intrusion and the basalt country rocks towards the eastern end of Loch Uisg. Their geographical extent is limited to a small area of approximately 1 km^2. They are distinct from the dykes of the Mull Dyke Swarm and display a wide variety of textures, mineralogy and grain size. The field relationships of these dykes are described and optical and SEM analysis provides an insight into the makeup of these rocks. All the members of this dyke suite have been extensively altered by hydrothermal action. It is proposed that they were intruded in a similar way to the Mull Dyke Swarm, from a similar basic to ultrabasic source magma. An explanation is given for the difference in grain size and mineral chemistry between these "Miscellaneous Minor Intrusions" and the dykes of the Mull Dyke Swarm.

Declaration

The material presented in this thesis summarises the results of three years of independent research carried out in the field on the Isle of Mull and at the Department of Geographical and Earth Sciences, University of Glasgow.

The research was supervised by Dr. Brian Bell (University of Glasgow) and Dr. John Faithfull (Hunterian Museum, University of Glasgow).

This thesis is the result of my own research and any published or unpublished work of other researchers has been given full acknowledgement in the text.

James A. Westland, 2014

Acknowledgements

The author would like to thank the following people for their help and input over the course of this work.

Dr Brian Bell and Dr John Faithfull both of Glasgow University for their invaluable input and encouragement. Also to the external examiner, Dr Brian O'Driscoll of Keele University and the internal examiner Dr David Brown of Glasgow University. Their contribution is greatly appreciated and gratefully acknowledged. Also a big "thank you" to other staff members at Glasgow University, in the Gregory Building and at Thurso Street for help and assistance.

To Rachael Ellen - thanks for words of support and encouragement. Keep in touch!

Thanks go to Jim and Patience Corbett of the Lochbuie Estate, for their assistance and willingness to have me working all over the estate. I would also like to thank the other residents of the Lochbuie / Loch Uisg area for their help when required.

My mother needs a special word of thanks for being a pillar of wisdom and encouragement all these years and for stressing to me from an early age the need for good education. Glasgow University has indeed been an inspiring place of good education!

A special "thank you" needs to go to my parents-in-law, Duncan and Morag MacGilp for allowing me to use their spare room as a study. Very much appreciated!

Finally, a massive "thank you" goes to my wife Moira for putting up with my frequent forays both to the field area and to Glasgow. Fitting a part time research degree round a busy family life is not easy. Many thanks for your words of encouragement and for helping me to find the time to do this work.

Table of Contents

List of Figures

Chapter 1

Chapter 2

Chapter 3

List of Tables

List of Abbreviations

BGS	British Geological Survey
BPIP	British Palaeogene Igneous Province
FoV	Field of View
GBI	Gleann Beag Intrusion
GGF	Great Glen Fault
HFoV	Horizontal Field of View
LIP	Large Igneous Province
LLF	Long Loch Fault (Rum)
LUG	Loch Uisg Gabbro
LUGGI	Loch Uisg Granite-Gabbro Intrusion
LUPS	Loch Uisg Picrite Suite
MCC	Mull Central Complex
MMI	Miscellaneous Minor Intrusions
MORB	Mid Ocean Ridge Basalt
NAIP	North Atlantic Igneous Province
NNO	Nickel-Nickel Oxide Buffer
OFB	Ocean Floor Basalt
OIB	Ocean Island Basalt
QFM	Quartz-Fayalite-Magnetite Buffer
SEM	Scanning Electron Microscope
*T*p	Mantle source potential temperature

VAB	Volcanic Arc Basalt
WPA	Within Plate Alkali Basalt
WPT	Within Plate Tholeiite

Chapter 1: Introduction

1.1 Introduction and definition of project

The research presented in this thesis is based upon a field and laboratory re-investigation of various intrusions that crop out in the southern portion of the Palaeogene Centre 1 (Glen More) of the Mull Central Complex (MCC), western Scotland (Bailey *et al*. 1924; BGS 1923, 1992). No detailed study of these rocks has been undertaken since the original survey by the British Geology Survey in the early 1920s.

In its regional context, the MCC is one of many foci of intrusive activity associated with the Palaeogene proto-Icelandic Plume (Saunders *et al*. 1997). This major magmatic event resulted in the development of voluminous lava fields throughout the northern Atlantic, together with localized foci of intrusive activity, one of which is the MCC (Figure 1.1).

The MCC comprises a myriad of intrusions, many with ring-shaped outcrop patterns (ring-dykes and cone-sheets), emplaced at relatively shallow depths, estimated to be less than 2 km (Emeleus & Bell 2005). The country-rocks to these intrusions comprise a thick sequence of Palaeogene lavas overlying various Mesozoic strata (Cretaceous, Jurassic and Triassic), and below which are Palaeozoic units (Devonian lavas and conglomerates) and Proterozoic metamorphic rocks. The terrane boundary defined by the Great Glen Fault separates the Moine Supergroup to the NW from the Dalradian Supergroup to the SE.

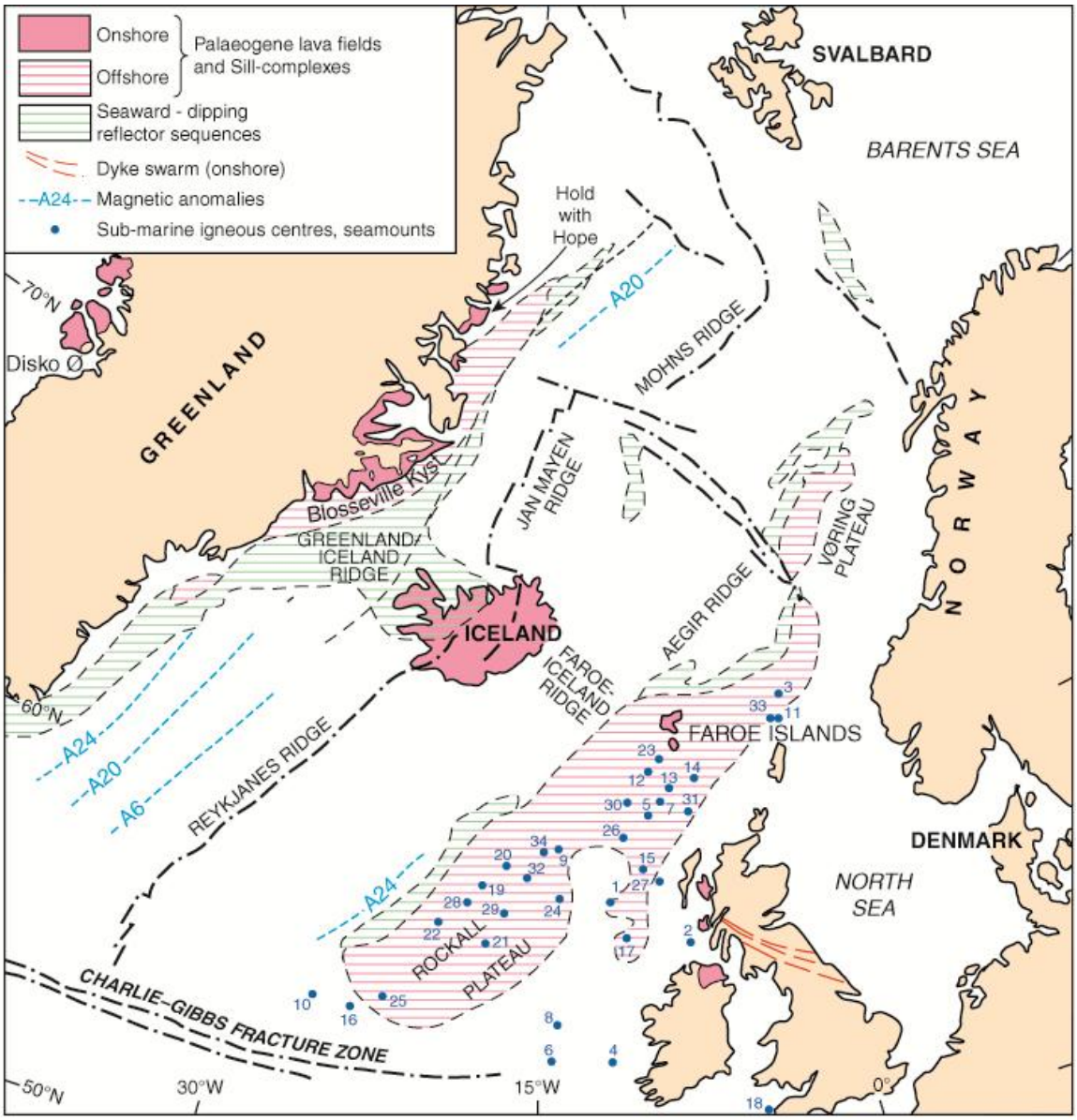

1 Anton Dohrn
2 Blackstones
3 Brendan (Shetland)
4 Brendan (Ireland)
5 Darwin
6 Donn
7 Drekaegya
8 Drol
9 East George Bligh
10 Eriador
11 Erlend
12 Faroe Bank
13 Faroe Bank Channel Knoll
14 Fraenir
15 Geikie
16 Gondor
17 Hebrides Terrace
18 Lundy
19 Lyonesse
20 Mammal
21 Mentone
22 Owlsgard
23 Regin Smidur
24 Rockall
25 Rohan
26 Rosemary Bank
27 St Kilda
28 Sandarro
29 Sandastre
30 Sigmundur
31 Sula Sgeir
32 Swithin
33 West Erlend
34 West George Bligh

Figure 1.1: Simplified geological map of the northern Atlantic, illustrating the distribution of lava fields, locations of offshore central complexes, the approximate positions of magnetic anomaly boundaries, and the present day location of the spreading centres (Reykjanes and Jan Mayen ridges) SW and NE, respectively, of Iceland (from Emeleus & Bell 2005).

Specifically, this research has involved the re-investigation of a composite intrusion referred to as the Loch Uisg Granophyre and Gabbro (Bailey *et al.* 1924), together with various other minor intrusions, mainly gabbroic in character, and gabbroic NW-SE trending dykes that crop out in the Loch Uisg area (Figures 1.2, 1.3 and 1.4).

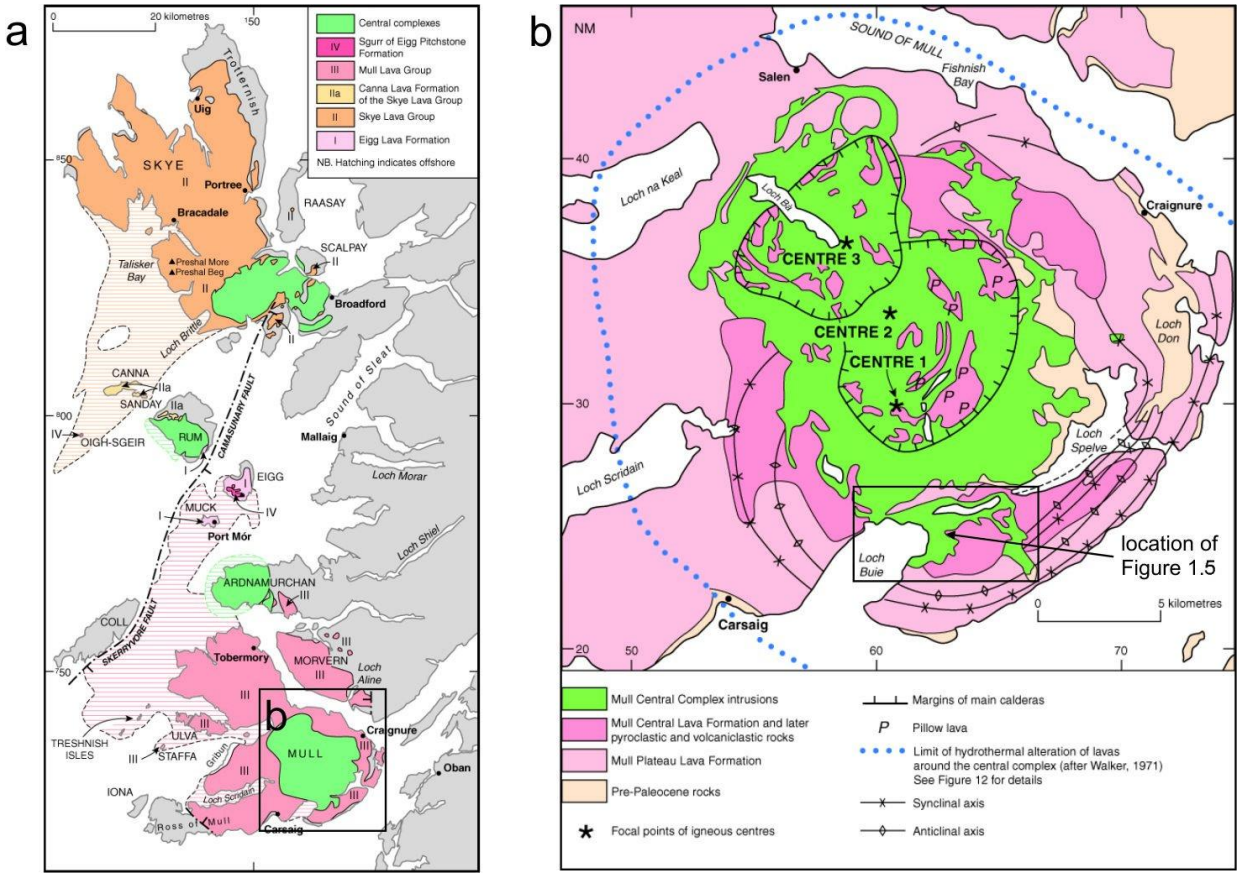

Figure 1.2: a, Simplified geological map showing the outcrops of the Palaeogene lava fields and the locations of the central complexes (Mull, Skye, Rum and Ardnamurchan); **b,** Simplified geological map showing the distribution and foci of intrusive units of the MCC (Centres 1, 2 and 3), the country-rock lithologies (mainly lavas), and the location of Figure 1.3 (from Emeleus & Bell 2005).

1.2 Palaeogene igneous activity in Mull

The main reference for the igneous geology of Mull is still the Mull Memoir (Bailey *et al.* 1924). The authors established the important concepts of magma-type and magma-series, which have been refined since then. (Tilley 1950; Yoder & Tilley 1962). Most research since then has built upon this early work. Although there have been detailed studies of specific aspects of the Mull geology (*e.g.* Kerr *et al.*1998), there are very few works that draw together all aspects of the

igneous geology. There are very few papers in the published literature that deal with the geology of the Loch Uisg – Loch Buie area, the Memoir (Bailey *et al*. 1924) being the main reference although it is brief, the Loch Uisg intrusions occupying only four pages. The origin of the Loch Uisg Granophyre has been studied (Pankhurst *et al*. 1978; Walsh *et al*. 1979) and further work was done on this intrusion as part of a study into the age of various rocks in Mull using radiometric analysis (Mussett 1986). However, there is virtually nothing in the published literature on the Loch Uisg Gabbro or the other mafic and ultramafic intrusions in the area apart from that contained in the Memoir (Bailey *et al*. 1924) and the BGS maps (BGS, 1923, 1992). Good general reviews of the Palaeogene geology of the Isle of Mull are given by Richey(1961) and Emeleus and Bell (2005). In common with many of the other Palaeogene centres, the earliest igneous activity is marked by phases of extrusion of flood basalts, followed by a later focused complex of high level intrusions (Richey, 1961, Skelhorn 1969, Emeleus and Bell, 2005). In Mull, these have been interpreted in terms of three main intrusive centres, having foci in Glen More (Centre 1), Beinn Chaisgidle (Centre 2) and Loch Bà (Centre 3) (Figure1.3).

The migration of the intrusive centres took place over a time of approximately 2 million years. Using radiometric dating, the Staffa Lava Formation, one of the earliest expressions of igneous activity, can be dated at 58.35±0.29 Ma. The Loch Bà Felsite, one of the last intrusions associated with the MCC, has been dated at 58.5±0.1 Ma (Emeleus & Bell, 2005).

Centre 1 includes several large gabbro intrusions, including the Ben Buie Gabbro, the Beinn Bheag Gabbro and the Loch Uisg Gabbro. Also associated with Centre 1 are several large granitic and felsitic intrusions, such as the Loch Uisg Granite, the Derrynaculen Granite and the Glas Bheinn Granite (Figure 1.3). These granitic intrusions have a high degree of crustal assimilation (Pankhurst *et al*, 1978). Several suites of cone sheets are associated with Centre 1 which cut all the major intrusions as well as the lavas. (Bailey *et al*. 1924).

Centre 2 igneous activity, centred on Beinn Chaisgidle, is characterized by a series of arcuate intrusions, traditionally interpreted as ring dykes of gabbro,

granite, felsite, diorite and various hybrid rock types such as quartz-gabbro. Cone sheets are also a feature of Centre 2, occasionally outcropping in such profusion as to obscure the country rocks. The arcuate intrusions of Centre 2 are in turn cut by the Loch Bà ring dyke of Centre 3. Centre 3 is characterized by mainly granitic intrusions ("granophyres"), the formation of which is due to fractionation, rather than crustal assimilation as is the case with the Centre 1 granites (Walsh *et al*. 1979). Palaeogene dykes, trending NW-SE cut across the rocks of all three centres as well as the lavas and are a prominent feature of the Palaeogene igneous activity of Mull.

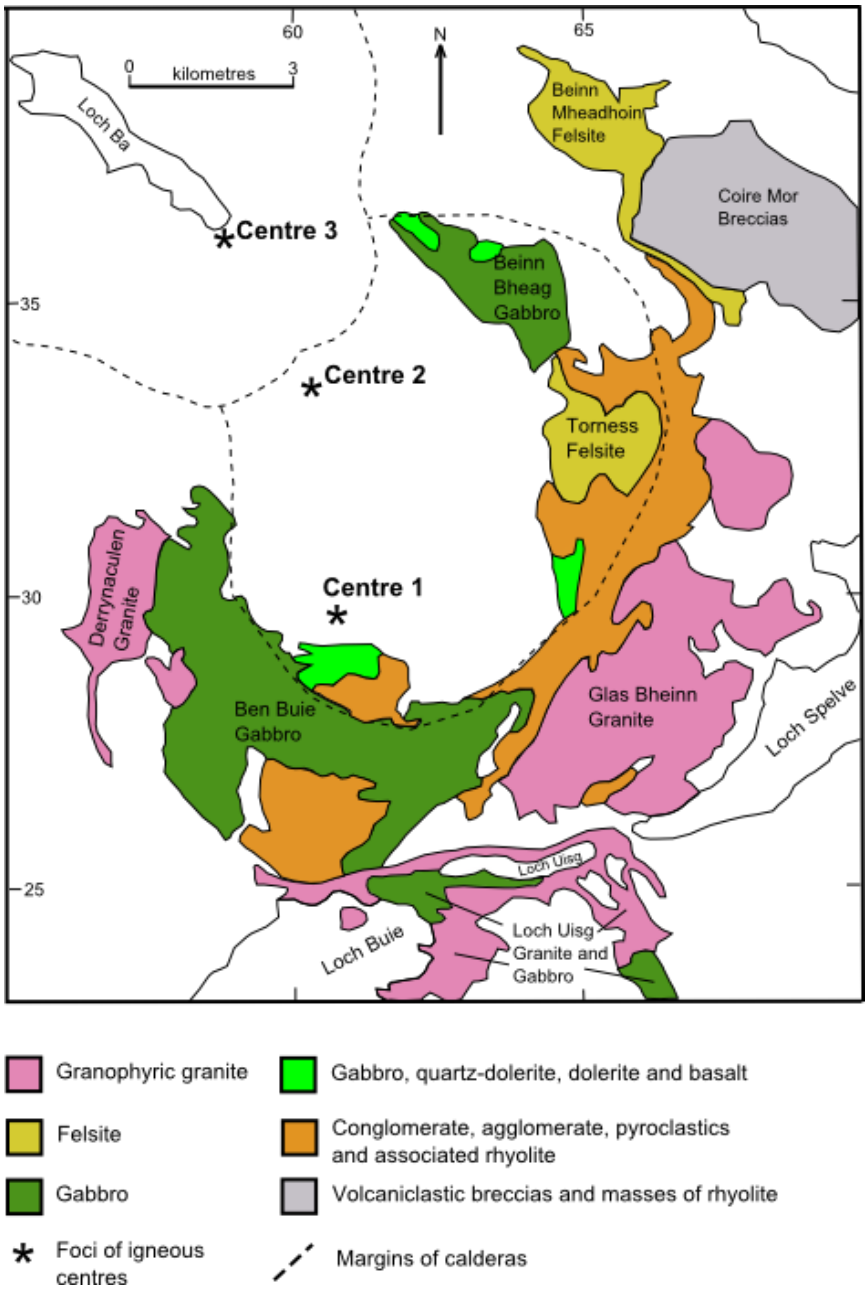

Figure 1.3: Mull Central Complex, showing the intrusions associated with Centre 1 and the foci of the three igneous centres. Cone sheets omitted for clarity.

1.3 Tectonic setting

The Mull Central Complex has deflected the track of the Great Glen Fault (GGF) which runs through SE Mull. As well as being diverted by the MCC, it is believed that the GGF was a factor influencing the location of the igneous activity at the beginning of the Palaeogene (Bailey *et al*, 1924).

The GGF has caused considerable displacement of the crust. Two major displacements have occurred: a sinistral shift of about 133 km in late Lower or early Middle Devonian times and a later dextral shift of *ca.* 29 km in Palaeogene times (Holgate,1969). The latter dextral shift has disrupted some of the early basalt lavas associated with the Palaeogene igneous activity but has had no effect on the Loch Uisg Granite-Gabbro Intrusion which sits astride the GGF.

The line of the fault can be recognised from the topography of the area – the image in Figure 5.35 shows the position and orientation of the fault in SE Mull.

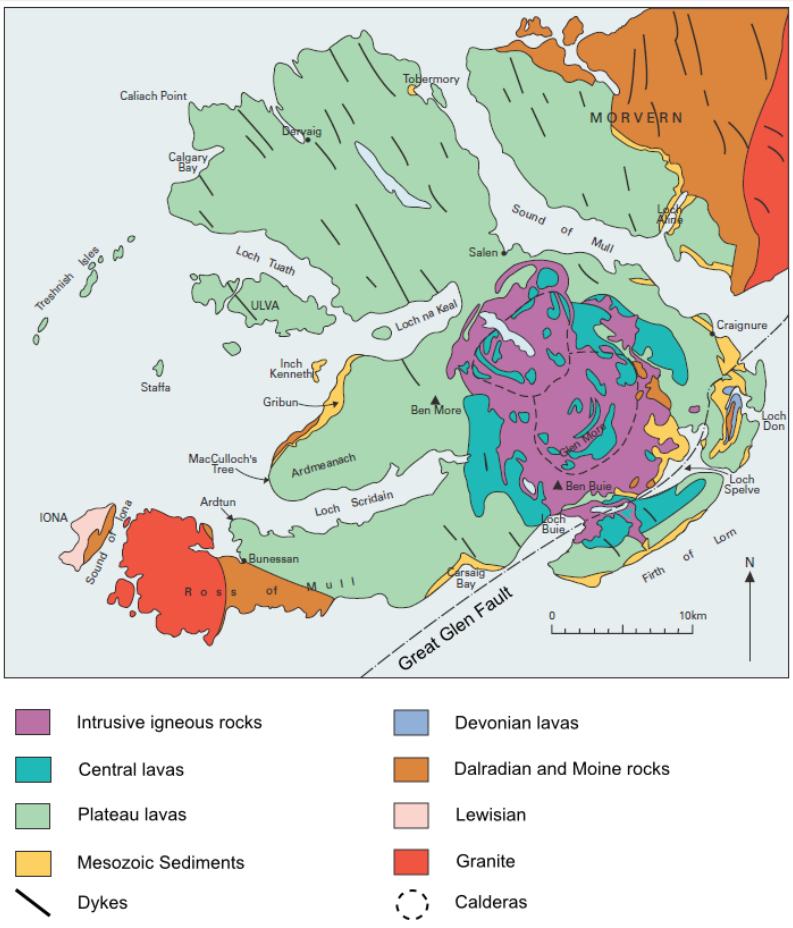

Figure 1.4: Sketch map (modified by the author) from the BGS Publication "A Landscape Fashioned by Geology", SNH Publications, showing the trace of the GGF and how it is deflected by the Mull Igneous Centre.

In addition to the GGF running through the study area, there are numerous small faults which run in a NW – SE direction (the regional trend), and which cut across

the GGF. These manifest themselves as deep gullies and glens cutting across the landscape. These are well seen in aerial photographs such as the image in Figure 2.2 in Chapter 2. Displacement on these faults (e.g. on the Loch Uisg Granite-Gabbro intrusion and basalt lava country rock contacts) appears to be limited, but brecciation, veining and slickensides, which show some lateral displacement can be seen in the stream bed of Allt Lag na Sliseig (Chapter 2).

1.4 The Intrusions

In the Loch Uisg area (Figure 1.5) there are numerous gabbroic intrusions, including the *Loch Uisg Gabbro*. The locations and names of these intrusions are given in Figure 1.5, some of which are simply assigned a number (3, 5 and 7). The *Loch Uisg Gabbro* (1) crops out along the southern and western shores of Loch Uisg and the *Glen Libidil Gabbro* (2) crops out in the valley of that name. In the memoir (Bailey *et al*. 1924), both of these intrusions are grouped together simply as the *Loch Uisg Gabbro*.

Field details of the *Loch Uisg Gabbro* reported by Bailey *et al*. (1924) are sparse when compared to other larger gabbroic intrusions of the MCC, for example the Ben Buie Gabbro that crops out further west. Many of the field details presented here, such as the development of layering and the presence of xenoliths, are not reported at all. Furthermore, petrographic and mineralogical details, for example the very high olivine content of certain intrusions (for example, the Gleann Beag Intrusion), are not recorded in the memoir.

One facet of these rocks considered in detail in this thesis is the picritic (highly magnesian) character of three of these intrusions: 4, 9 and 10, as depicted in Figure 1.5, the so-called Loch Uisg Picrite Suite (LUPS). These rocks are remarkably fresh (being devoid of hydrothermal alteration, typical of many of the intrusions of the MCC), are extremely rich in highly forsteritic olivine (up to $Fo_{91.5}$), and form the main part of this study.

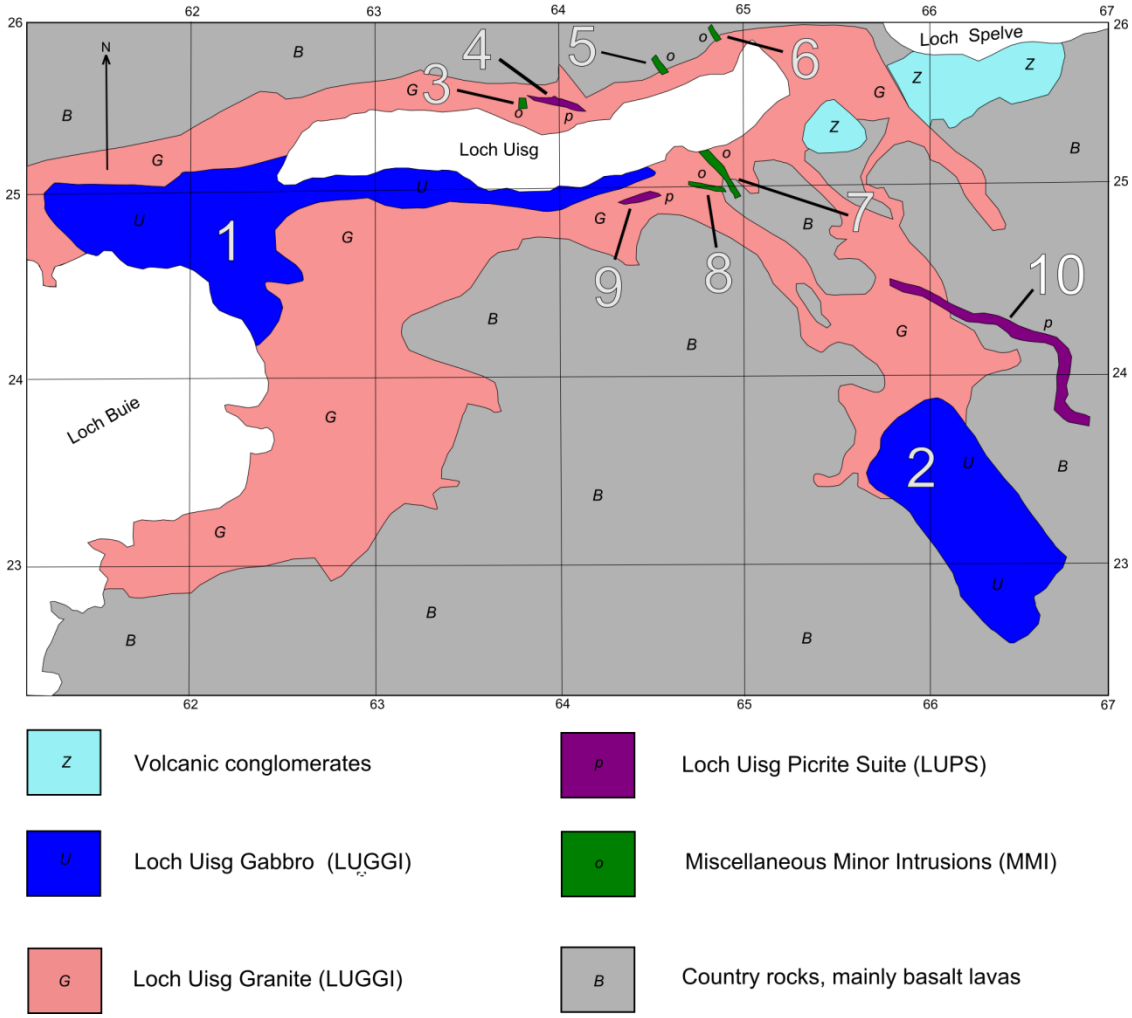

Figure 1.5: Sketch map of the area around and SE of Loch Uisg showing the distribution of the gabbro unit, the granite (granophyre) unit, country-rock basaltic lavas and members of the NW-trending Mull Dyke Swarm. 1: Loch Uisg Gabbro; 2: Glen Libidil Gabbro; 3: unnamed; 4: Loch Uisg Cottage Sheet; 5: unnamed; 6: Sand Quarry Dyke; 7: unnamed; 8: Fence Dyke; 9: Coille Sron nam Boc Sheet; 10: Gleann Beag Intrusion.

1.5 Mapping

A significant part of this study involved re-mapping the outcrop of the *Loch Uisg Gabbro and Granophyre* at a scale of 1:5000 and recording its internal characteristics, including the nature of the boundary between the gabbroic and granitic units. The main body of fieldwork took place over a 2 ½ year period starting in March 2009, although preliminary reconnaissance studies with a view to evaluating the worth of the project were conducted in 2008. Several areas were worked on concurrently in order to accommodate the effects of weather, vegetation and estate management operations (from August until February, deer stalking takes place). Maps were obtained from the EDINA service. The use of a

Garmin GPS unit proved invaluable as a mapping tool as it allowed a high degree of plotting accuracy in relatively featureless areas. Follow-up laboratory work commenced in December 2010 and was completed by January 2012.

1.6 History of research and current understanding

The work of Bailey et al. (1924), the officers of the British Geological Survey (BGS) who produced the so-called *Mull Memoir,* delivered a major step forward in our understanding of the field relationships of a wide variety of intrusive styles and the nature and relationships of the magmas involved. They described classic examples of cone-sheets and ring-dykes, composite intrusions formed by the near-simultaneous emplacement of contrasting magma compositions, for example the *Loch Uisg Gabbro and Granophyre* described in this thesis. The parental character of basaltic magmas was also explored, highlighting the fundamental differences between tholeiitic basalt (the Non-porphyritic Central Type of the Mull Memoir) and alkali basalt (the Plateau Type of the Mull Memoir), and the concept of magmatic evolution (magma series of the Mull Memoir) was discussed.

The *Loch Uisg Gabbro and Granophyre* was not discussed in great detail, running to only four pages and one diagram in the Mull Memoir. The main gabbroic and granitic intrusions have irregular outcrop patterns, a consequence of their geometry, the irregular form of their mutual boundary and the nature of today's topography. Several key features were recognised by Bailey *et al*. (1924) and reconsidered during the present study:

1. The gabbro unit of the Loch Uisg Gabbro-Granite Intrusion ranges between a coarse-grained gabbro and a dolerite.

2. The petrographic differences between the *Loch Uisg Gabbro* outcrop (1 in Figure 1.3) and the *Glen Libidil Gabbro* (2 in Figure 1.3) are considered to be relatively insignificant and hence are treated as being discrete outcrops of the same intrusion.

3. The age relationship between the gabbro and granophyre units could not be determined: there is no evidence of chilled margins or of xenoliths of one unit within the other.

4. The suggestion that "the gabbro may be later than the granophyre, since no trace of gabbro is to be found attached to the roof of the granophyre" (Bailey *et al*. 1924).

5. The granophyre unit has a sheet-like geometry, as shown in Figure 1.4, reproduced from Bailey et al. (1924), although the contact relationships are, in places, not clear; at the west end of Loch Uisg the upper contact dips steeply towards the north.

6. The granophyre unit has thermally altered the folded country-rock basaltic lavas and their mutual contact is transgressive towards the stratification of the lava sequence.

7. The granophyre unit is intruded by cone-sheets attributed to the Early Basic Cone-sheets of Bailey et al. (1924).

8. The gabbro unit is dominated by plagioclase (labradorite) and augite in an ophitic to subophitic textural relationship, pseudomorphs after olivine and spinel (magnetite); hydrothermal alteration of plagioclase is common but not severe.

9. The granophyre unit has a micro-granophyric texture and contains needles of augite (now chlorite).

10. The total combined surface area of the main gabbro and granophyre outcrops is approximately 14-16 km^2.

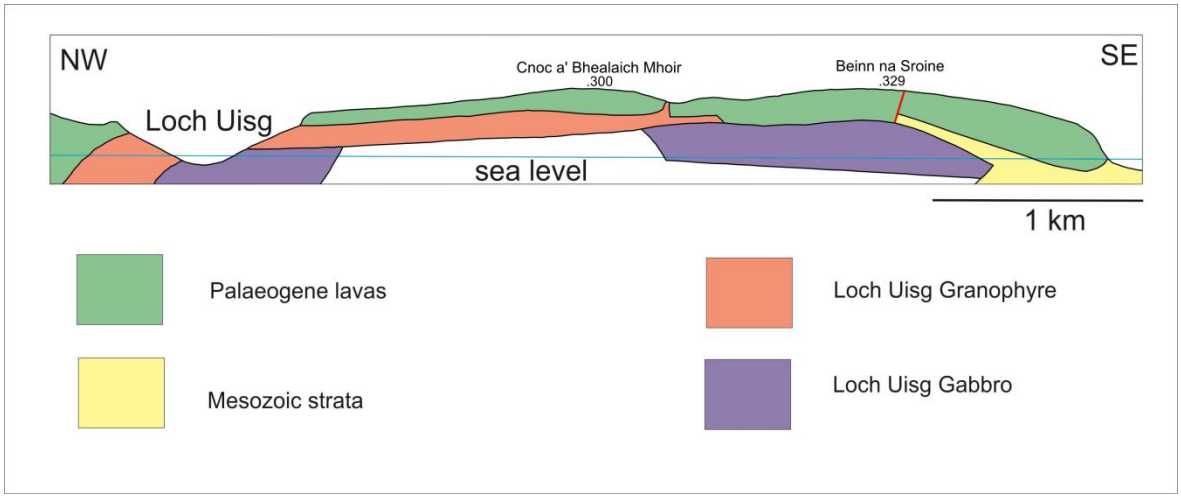

Figure 1.6: Schematic cross-section across the Loch Uisg gabbro and granophyre units (after Bailey *et al*. 1924).

The geochemistry of the granophyre unit was considered by Pankhurst *et al.* (1978), with the following conclusions:

1. The intrusion is of rhyodacite composition (determined by whole-rock geochemistry) and is compositionally relatively homogeneous over its outcrop;

2. Significant alteration by the contemporaneous hydrothermal alteration system is recorded from the oxygen isotope signature of its constituent minerals. $\delta^{18}O$ values vary from -3.7 to +1.49 ‰ indicating considerable variation in the effect of such interaction within the granophyre mass;

3. Sr-isotope data indicate that the parental magma of the granophyres was generated by (partial) melting of basement, possibly Lewisian (Archaean) gneisses or Caledonian (Palaeozoic) granites, but not Moine Supergroup lithologies.

1.7 Project Scope and layout of thesis

1. Field relationships, contact relationships, petrography and petrogenetic model of the gabbro and granophyre units of the Loch Uisg Gabbro-Granite Intrusion.

2. Field relationships, petrography, mineral chemistry and petrogenesis of the Loch Uisg Cottage Intrusion, the Coille Sron nam Boc Intrusion and the Gleann Beag Intrusion (the so-called Loch Uisg Picrite Suite, LUPS) (Figure 1.5).

3. Field relationships, petrography, mineral chemistry and petrogenesis of other minor intrusions.

4. Summary of the findings.

1.8 Note on Nomenclature

Bailey *et al.* (1924 mapped the gabbroic and felsic igneous rocks around Loch Uisg, interpreting them as a lower gabbro (or dolerite) and an overlying "granophyre". Much of the "granophyre" is fine grained or felsitic, but the term "granophyre" is widely used in the literature. The BGS (2012) have recently

revised the nomenclature of lithovolcanic units and recommend replacing "*Loch Uisg Granophyre and Gabbro*" with the expression "*Loch Uisg Granite-Gabbro Intrusion*". The latter is the term which is used throughout the rest of this work.

Chapter 2: The Loch Uisg Granite-Gabbro Intrusion

2.1 State of knowledge prior to this study

Bailey *et al*. (1924) suggested that the gabbro and the granite were closely related, both spatially and temporally. The gabbro crops out in two main areas: along the shores of Loch Uisg and Loch Buie, and in Glen Libidil. Bailey *et al*. (1924) concluded that although the two gabbro "outcrops" are not contiguous, there are reasons for treating them as one body of rock (as they state in the memoir):

(1) The interval between the northern and southern exposure is only a mile;

(2) Both localities show extensive, and sufficiently similar, basic masses at the base of the Loch Uisg Granophyre (sic);

(3) There are no exposures of the base of the Loch Uisg Granophyre where dolerite, or gabbro, does not occur in mass.

(Bailey *et al*. (1924) p 230)

However, Bailey *et al*. (1924) stated that there are mineralogical differences between the two gabbro bodies, so the certainty with which they assert the unity of the two outcrops is perhaps questionable. The work of Bailey *et al*. (1924) represents the only published information on the Loch Uisg Gabbro but much of their research is based on only three thin sections.

Although the Memoir description is quite sparse, running to only four pages (Bailey *et al*. (1924) pp. 230 - 233), several important points are made by the authors, and these points form the starting point of the current investigation:

1) The granite and gabbro are considered "Centre 1" intrusions;
2) The emplacement of the granite has not been affected by the arcuate folding of the lavas, which predates it;
3) The granite has baked the lavas, giving the steep cliff line above the south side of Loch Uisg;

4) The morphology of the granite is sill-like, but the northern contact dips steeply to the north;
5) The two outcrops of gabbro are considered to be parts of a (larger) contiguous body;
6) Contacts between the granite and gabbro are rare, and so their age relationships are unclear;
7) There is limited evidence of magma mingling along the contact zone;
8) Xenoliths and / or back-veining are not seen between the granite and the gabbro.

Little research has subsequently been undertaken on either part of the intrusion. Apart from the Memoir (1924) and map (1923), and the revised map of 1992, the main published work is an investigation of the (geochemistry of the) granite by Pankhurst *et al*. (1978), which provides evidence for its petrogenesis being a combination of crustal contamination and fractional crystallization of basaltic magmas.

2.2 The general field relationships

The Loch Uisg Granite-Gabbro Intrusion belongs to Centre 1 (the Glen More Centre) of the Mull Central Complex (MCC). Both parts are defined in Figure 2.1 (reproduced from Figure 1.4).

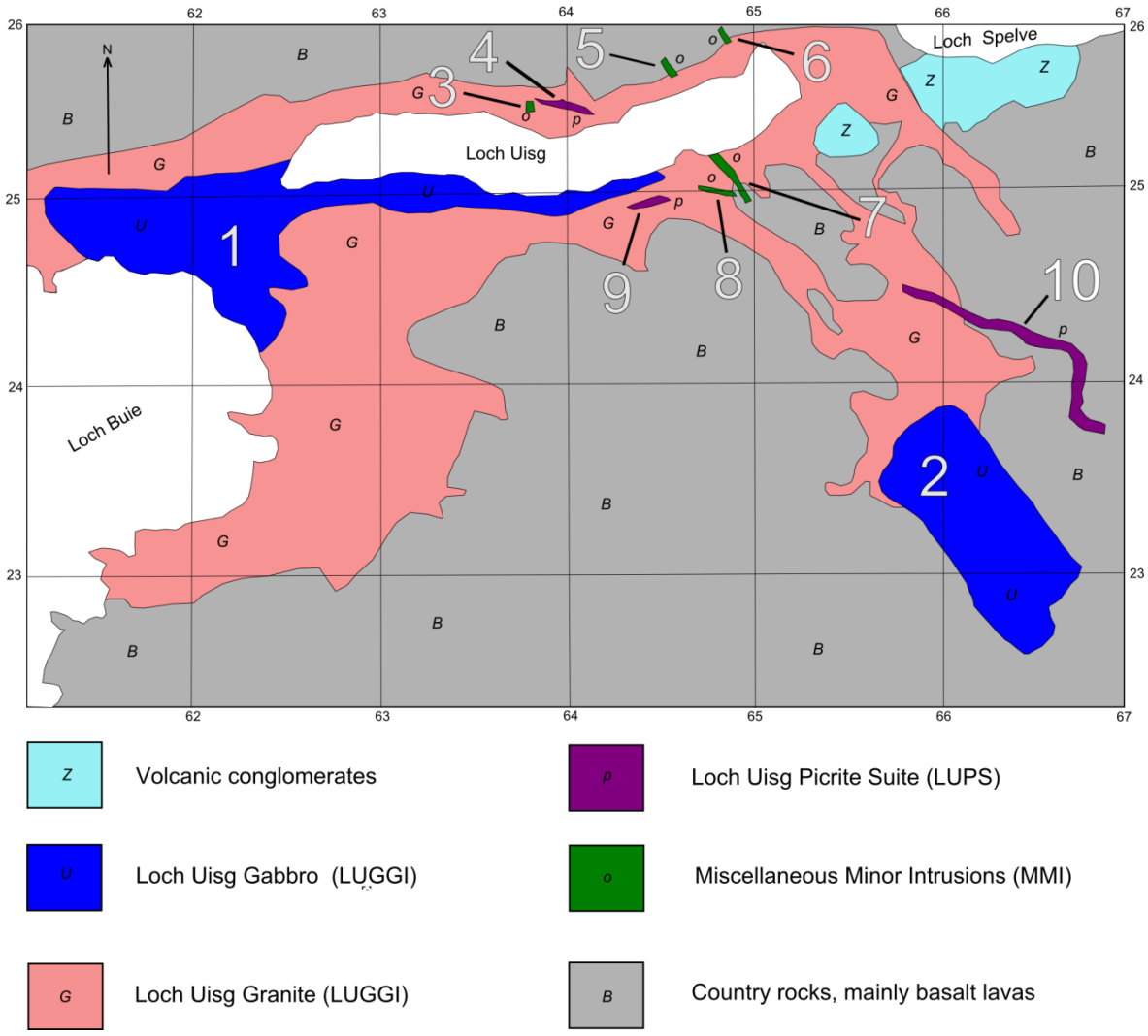

Figure 2.1: Sketch map of the area around and SE of Loch Uisg showing the distribution of the gabbro unit, the granite (granophyre) unit, country-rock basaltic lavas and members of the NW-trending Mull Dyke Swarm. 1: Loch Uisg Gabbro; 2: Glen Libidil Gabbro; 3: unnamed; 4: Loch Uisg Cottage Sheet; 5: unnamed; 6: Sand Quarry Dyke; 7: unnamed; 8: Fence Dyke; 9: Coille Sron nam Boc Sheet; 10: Gleann Beag Intrusion.

The country-rock into which the Loch Uisg Granite-Gabbro Intrusion (LUGGI) was emplaced consists mainly of basaltic lavas of both the Plateau and Central types (Bailey *et al*. 1924). In addition, feldspar-phyric basaltic lavas crop out to the north of Loch Uisg and there are two significant outcrops of a volcaniclastic conglomerate at the eastern end, near Barrachandroman. The lavas display the distinctive arcuate folding (due to the emplacement of the Central intrusions), for which the MCC is famous (Bailey *et al*. 1924). Both the intrusions and the country-rocks are cut by numerous cone-sheets and dykes of the Mull Dyke Swarm. The Great Glen Fault runs through Loch Spelve, Loch Uisg and Loch Buie, but appears to have had no effect on the intrusions (Figure 1.2). The area is

traversed by numerous NW-SE -trending faults that have given rise to steep-sided gullies. These are very noticeable in satellite images of the area (Figure 2.2). Displacement on these faults appears to be minimal, but brecciation, veining and slickensides can be seen in the granite on the south side of Loch Uisg in the bed of Allt Lag na Sliseig at [NM 648 249].

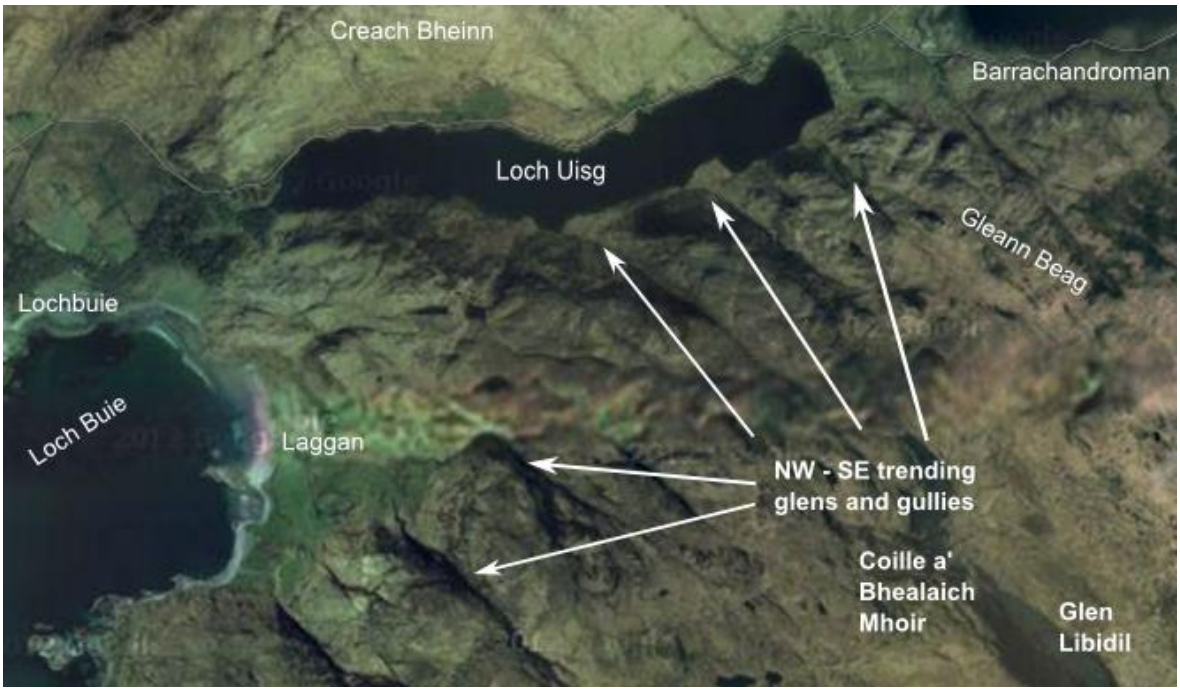

Figure 2.2: Satellite image of the Loch Uisg area, showing the relief and the distinctive gullies and glens that run NW-SE across the area. (Satellite image from Google Maps, 2012).

Exposure is variable. Along the NW and SE shores of Loch Buie, the granite and other minor intrusions are well exposed. The granite is also well exposed in many of the deep glens and gullies that traverse the area. However, a lot of the area is covered in thick vegetation that makes observation difficult. The gabbro is exposed in the cliffs at Laggan on the shore of Loch Buie and also in Glen Libidil. However, the contact zone between the granite and the gabbro is obscured by vegetation for the most part and there are very few places where the contact can be determined with any accuracy.

2.3 Field relationships of the granite

The outcrop of the granite is approximately 7 km^2 in extent (Figure 2.1). The granite is best seen along the shores of Loch Buie, where it locally forms cliffs

(Figure 2.3), and on the sides of the many NW-SE trending glens and gorges on the south side of Loch Uisg. It is also well exposed on the island of Eilean Mor (Figure 2.10), where it is cut by numerous cone-sheets. The granite is also well exposed in the cliffs above Loch Uisg near the contact with the basaltic lavas; in many cases the contact is recognised in the field where it forms a very sharp, clear boundary. However, in the intervening ground, extending up from the shores of lochs Buie and Uisg, the vegetated slopes comprise, mainly, poor exposure. Much of the lower areas are covered in rhododendron that is quite impenetrable, making accurate field observations very difficult.

Figure 2.3: Granite cliff, 20 m in height, near Lochbuie [NM 596 247]. Here, basaltic lavas crop out on the shore in the foreground. In the background, Creach Bheinn is mainly composed of the Ben Buie Gabbro.

The appearance of the granite varies considerably. In places it displays a pseudo columnar structure. Most of the exposures display a distinctive platy fabric. The rock, itself, varies from an aphanitic rock to a much more granular microgranite. Since the majority of the rock has a very fine grained appearance rather than that of a (coarser-grained) granophyre, it is perhaps more accurate to refer to it as a microgranite than a granite. However, in order to maintain consistency with the latest BGS nomenclature (BGS 2012), the rock is referred to as granite throughout this work. Small feldspar phenocrysts are common throughout the outcrop. Locally, the rock is quite dark and can appear very similar to some of the basaltic lavas. In general, it appears darker closer to the contact with the gabbro. Elsewhere, the variation between felsite and a microgranite does not appear to follow any geographic pattern.

2.3.1 Contacts of Loch Uisg Granite with the country-rocks

The granite is intruded, predominantly, into basaltic lavas and volcaniclastic conglomerates (Figure 2.1). Some of the lavas are of the "big feldspar" type (Bailey *et al.* 1924), whereas others are non-porphyritic. Above the south shore of Loch Uisg, the arcuate folds that affect the lavas are noticeable from the dip of the lavas in the field (Figure 1.2a). The granite has caused considerable alteration of the country-rock lavas, as seen in the prominent cliffs above (north and south of) Loch Uisg. Further to the NE, towards the eastern end of the peninsula (Figure 2.2), this alteration is much less discernable.

Throughout much of its outcrop, the granite appears to have a sill-like form. Horizontal and sub-horizontal upper contacts with the country-rock lavas are clearly discernable to the south of Loch Uisg, especially in the cliffs above the loch (Figure 2.4). Inland, in Gleann Beag (at [NM 656 250], similar relationships are evident Figure 2.5). The lower contact of the granite with the gabbro is not well seen in the field but, where inferred, it appears also to be horizontal to sub-horizontal.

The lithologies are also reflected in the exposure: from above the south side of Loch Uisg, as far as Laggan Farm, the granite-dominated slopes are generally broad and grassy with poor exposure. Above the contact, cliffs and crags are prominent.

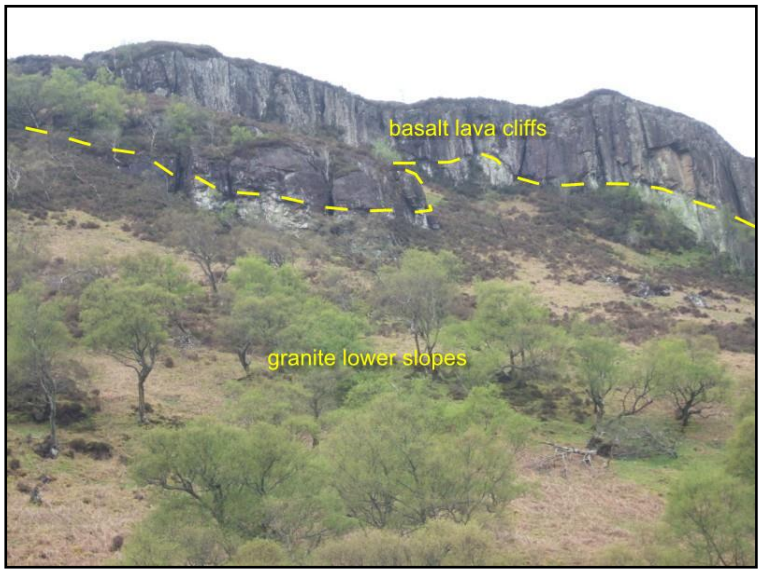

Figure 2.4: Contact of Loch Uisg Granite on the lower tree-covered slopes with the crag-forming country-rock basaltic lavas at Sròn nam Boc [NM 645 248] above Loch Uisg. Cliffs reach up to 40m in height.

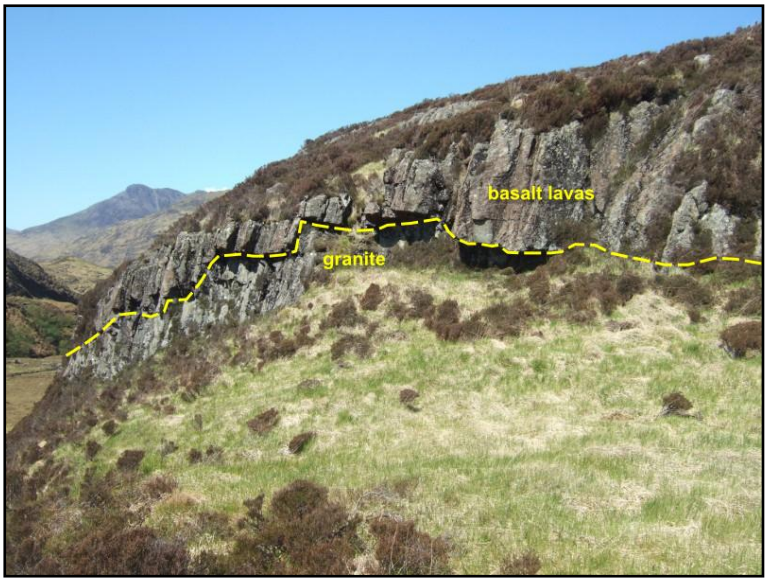

Figure 2.5: Contact between the Loch Uisg Granite (on lower ground) and country-rock lavas in Gleann Beag at [NM 656 250]. Both lithologies form a small cliff 4m in height.

On the north side of Loch Uisg, the contacts are much steeper, for example, near Loch Uisg Cottage where the contact crosses the main Loch Buie road (Figure 2.6). However, at the western end of the intrusion, the "western apophysis" of Bailey *et al.* (1924), exposure is poor and the upper contact with the basaltic lavas of the country-rock is difficult to discern.

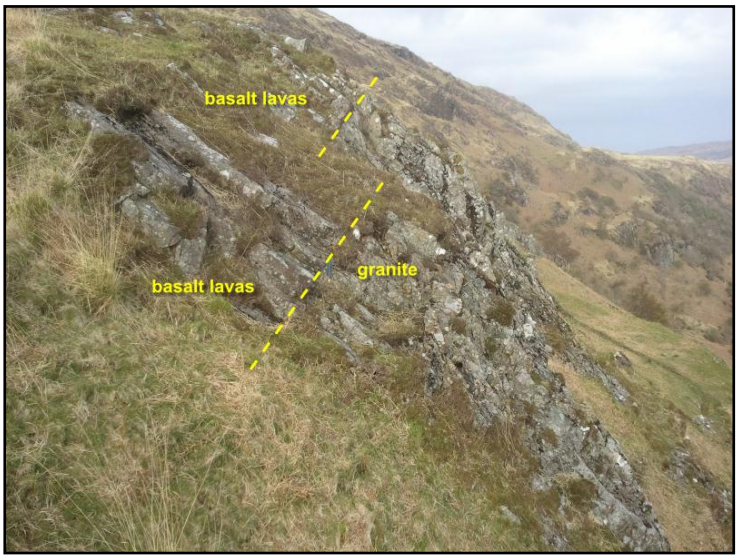

Figure 2.6: Contact between the Loch Uisg Granite and the country-rock basaltic lavas above the western end of Loch Uisg at [NM 626 257], looking east. Contact dips at approximately 60º towards the north.

Elsewhere, the contact relationships are considerably more complex. For example, on the NW shore of Loch Buie, near Eilean a' Chrabhaiche at [NM 595 244], the granite forms a complex network of veins and small dykes cutting the lavas (Figure 2.7). In some of these veins, xenoliths of basalt are prominent. The granite is also intruded along lava unit flow boundaries.

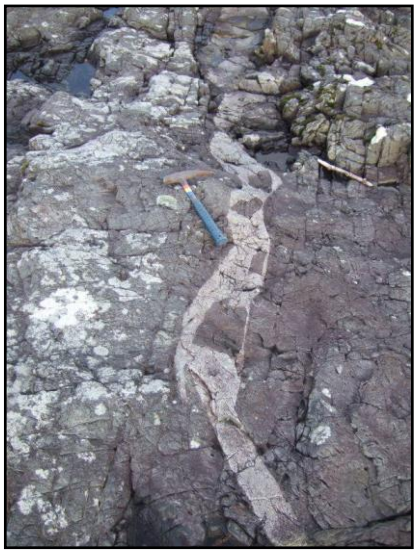

Figure 2.7: At Eilean a'Chrabhaiche, [NM 595 244], a vein of granite bearing basalt xenoliths cuts altered country-rock lava.

Further to the SW, on the shore of Loch Buie at [NM 590 241], there is a prominent plexus of granitic and felsitic dykes, veins and stringers that cut the basaltic lavas, well away from the main exposed mass of the granite (Figure 2.8). This implies that the intrusion is quite close to the surface at this point. If this is the case, then, at no great depth, the Loch Uisg Granite is of greater volumetric extent than is currently exposed.

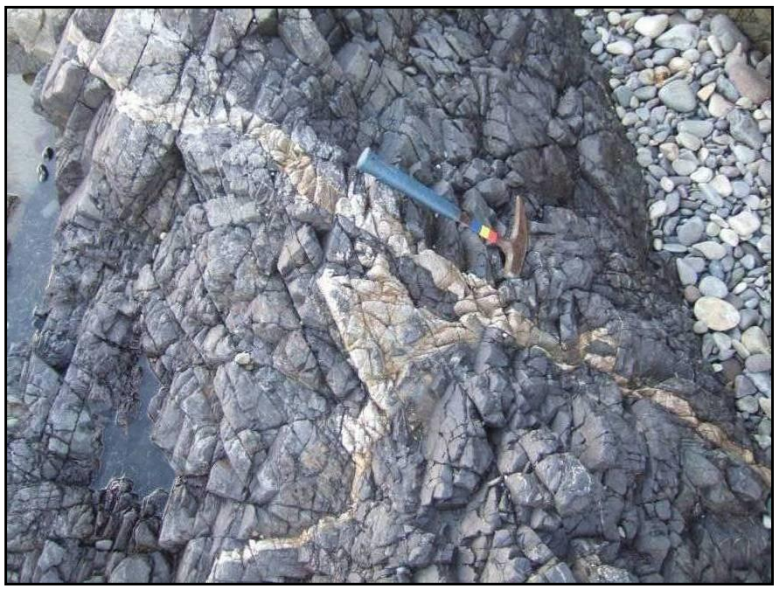

Figure 2.8: Country-rock lava cut by veins of granite on the shore of Loch Buie [NM 590 241].

At Rubh Aoineadh Mheinis [NM 659 212], in a very remote part of the Laggan Peninsula outwith the main study area, there is an outcrop of granite that cuts Jurassic sedimentary rocks that underlie the basaltic lavas (Figure 2.9). This intrusion is indicated on the BGS map (1923, rev. 1992) and may be, at depth, connected to the main Loch Uisg Granite outcrop, again substantially increasing the dimensions of the intrusion at depth. It may however, simply be a separate intrusion.

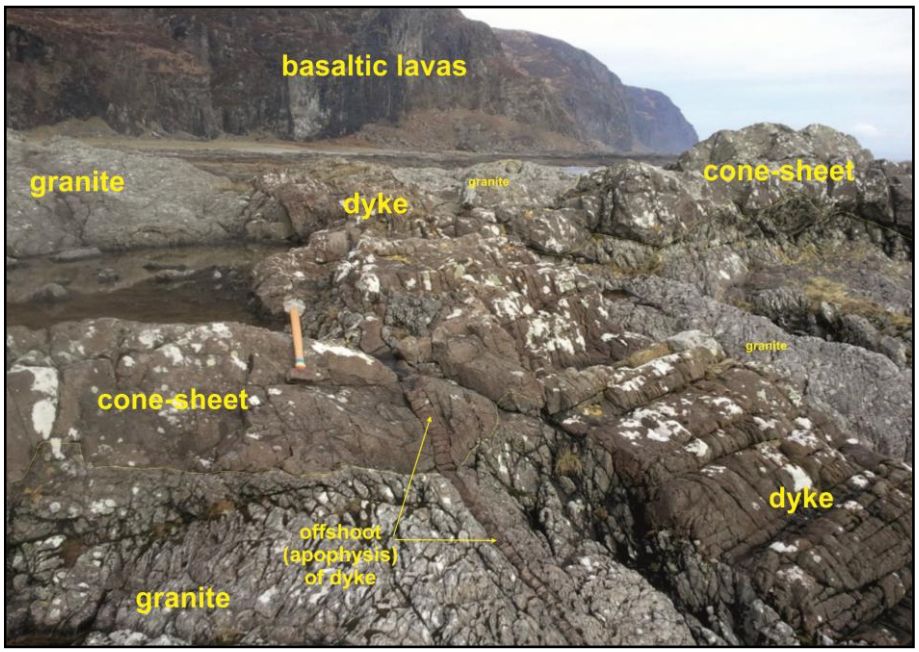

Figure 2.9: Granite cut by a dolerite cone-sheet, both cut by a dolerite dyke. Shore at Rubh Aoineadh Mheinis [NM 659 217] looking NE.

2.3.2 Relationship of Loch Uisg Granite to cone-sheets

There are two main suites of cone-sheets in the area around lochs Uisg and Buie: a suite of early silicic to intermediate cone-sheets and a suite of later basic cone-sheets (Bailey *et al*. 1924). The definition of cone-sheets given in the Mull Memoir (Bailey *et al*. 1924) was used to identify these intrusions in the field – inclined sheets with an orientation that implies a focus on the igneous centres. The basic sheets are mainly dark grey to black fine to medium grained basalt and dolerite. The silicic sheets are predominantly light grey, sometimes cream coloured microgranite.

The older of the two, the silicic and intermediate cone-sheets, occur throughout the country-rock basaltic lavas, but are not evident within the Loch Uisg Granite. Bailey *et al*. (1924) noted that in the poorly exposed "western apophysis" of the intrusion, these early cone-sheets cut, and are cut by, the

Loch Uisg Granite; however, no evidence of this was found during the present study.

The late basic cone-sheets (Bailey *et al*. 1924) cut both the country-rock basaltic lavas and the Loch Uisg Granite in abundance. Many of these cone-sheets are cut by dykes of the Mull Swarm and *vice versa*. Best seen along the shores of Loch Buie, they are particularly prominent on Eilean Mor, the tidal island at the head of Loch Buie at [NM 611 244] (Figure 2.10) and also in the cliffs facing Eilean Uamh Ghuaire [NM 618 232] (Figure 2.11).

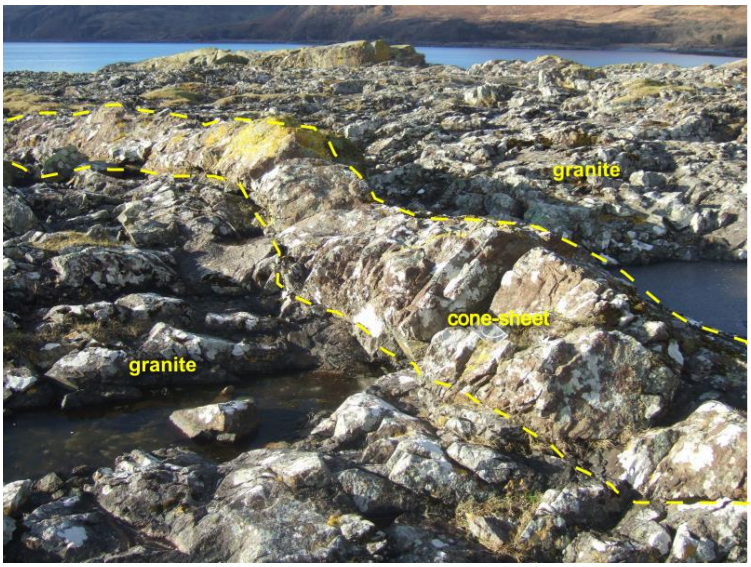

Figure 2.10: Looking NW at a dolerite cone-sheet cutting Loch Uisg Granite on Eilean Mor, Loch Buie (at [NM 611 244]). The cone-sheet is approximately 1m thick.

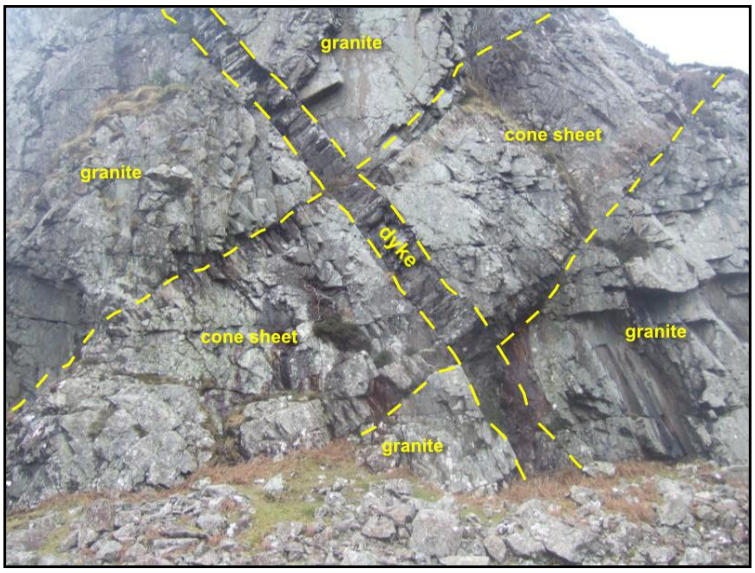

Figure 2.11: Dolerite cone-sheet cutting the Loch Uisg Granite, in turn cut by a dyke of the Mull Dyke Swarm, in the cliffs facing Eilean Uamh Ghuaire [NM 618 232] on the SE shore of Loch Buie. The dyke is approximately 1m thick. The cone-sheet is approximately 5m thick.

2.3.3 Relationship of Loch Uisg Granite to dykes of the Mull Dyke Swarm

Members of the Mull Dyke Swarm occur in abundance in south Mull, typically trend NW-SE, and post-date the Loch Uisg Granite (Figure 2.12). From Eilean a'Chrabhaiche to near Barachandroman, and on the NW and SE shores of Loch Buie, the dykes are particularly conspicuous, where it can be observed that they range considerably in thickness from a few centimetres to over three metres.

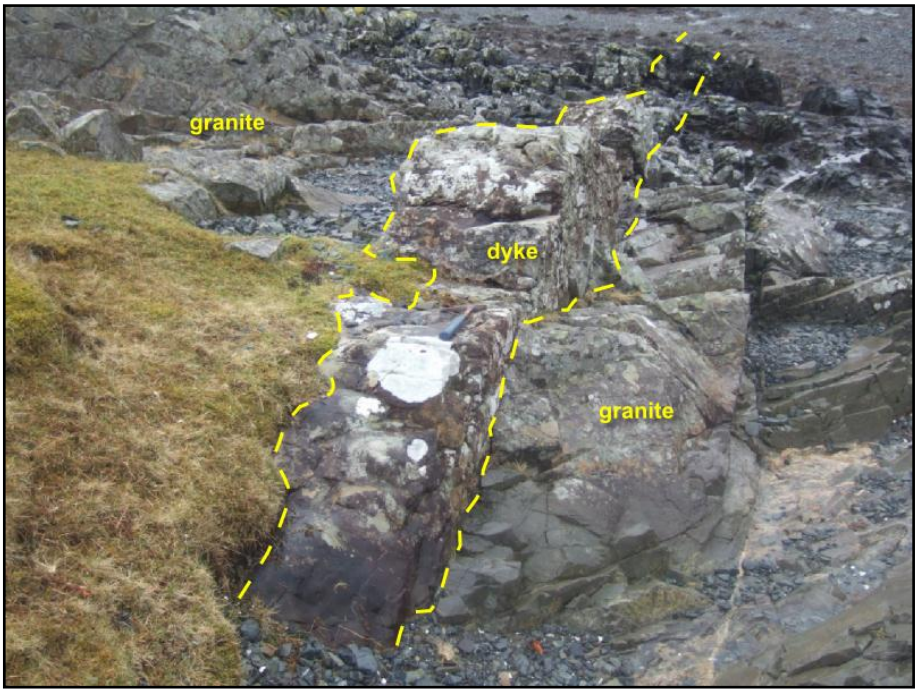

Figure 2.12: A typical dolerite dyke of the Mull Dyke Swarm intruded into the Loch Uisg Granite near the southern end of Laggan Sands beach on Loch Buie at [NM 620 234]. Hammer for scale.

2.4 The Loch Uisg Gabbro

The Loch Uisg Gabbro crops out in two areas, from the south side of Loch Uisg to Laggan, and in Glen Libidil (Figure 2.1).

2.4.1 The Loch Uisg Gabbro - South Loch Uisg to Laggan

The gabbro is shown as a quite extensive body on the map of Bailey *et* al (1923, 1924). However, the outcrop is more restricted than this might suggest, especially along the south shore of Loch Uisg from the prominent alluvial fan at Cluas an Lagain to Laggan (Figure 2.1), where it crops out as a thin strip running along the shore. The rock is better exposed at Laggan Sands where it forms a conspicuous cliff (Figure 2.13) and where reasonable inland exposures occur.

Between the cliffs at Laggan and Loch Uisg, numerous exposures can be seen, but the contact with the Loch Uisg Granite is very difficult to discern.

The BGS map (1923, 1992) shows the contact of the gabbro and the granite extending from Moy Castle at [NM 617 248] to the NW and thence to the shore of Loch Uisg. Exposure is very poor, almost non-existent, apart from some blocks that may not be *in situ* near the Stone Circle at [NM 615 254]. On the cliffs above Laggan the gabbro is easily discerned and, further uphill, the granite is also obvious, although the contact between the two lithologies is not visible. Bailey *et al*. (1924) allude to a contact above the cliffs at Laggan, but none was seen despite extensive fieldwork. There may, however, be a zone of what appears to be a "mixed rock" between the two lithologies, possibly hybridisation (Emeleus & Bell 2005); some samples collected from the contact zone show hybrid features, for example, a sample (no 384), taken from the cliff shows ophitic clinopyroxene and plagioclase with some interstitial silicic material.

Along the south side of Loch Uisg at [NM 637 249] a stream section reveals both the gabbro and the granite, although no contact is observable. The rock grades from gabbro to granite over a distance of 20m, with no evidence of xenoliths or back veining, and the rock has a distinct hybrid character over the middle part of this section (Figure 2.23). The mixed rock has an appearance different from the gabbro and the granite. In hand specimen it looks like a medium-grained dioritic intermediate rock. At no point in this section, even allowing for the limited exposure, does the rock type suddenly change from gabbro to granite. It appears to have this transitional type which has compositional affinities with both the main lithologies.

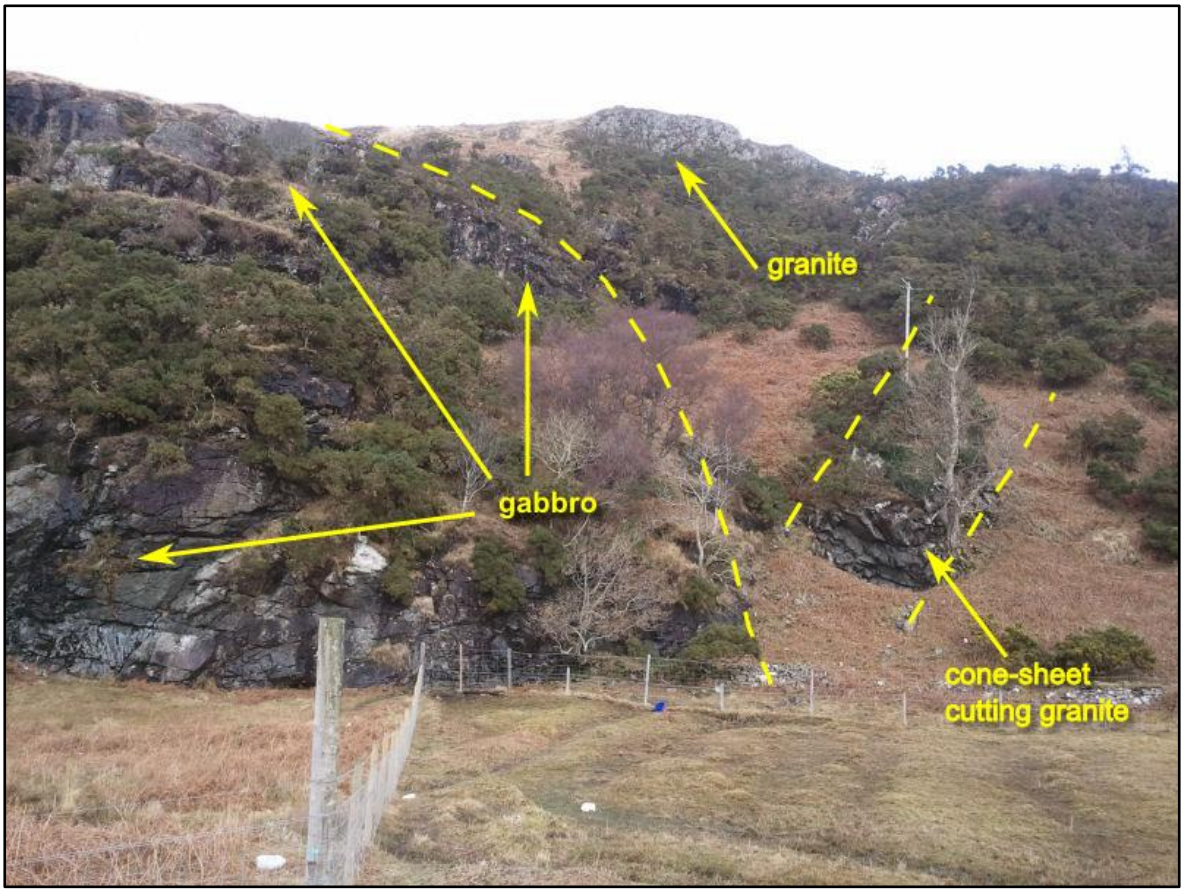

Figure 2.13: Part of the cliffs above Laggan Sands. Here, the Loch Uisg Gabbro forms the crags on the left-hand side and the granite occurs further uphill forming a prominent crag. A cone-sheet, one of many in the area, trends uphill. The boundary between the gabbro and the granite is not seen due to vegetation and is therefore inferred. Fence-post, for scale, is 2.5m long.

Much of the gabbro is massive, unlayered, commonly medium-grained, and, locally, texturally tends towards dolerite. In places, layering is present and psammitic xenoliths are also a prominent feature, for example, at [NM 623 245] on the Laggan shore (Figure 2.16). Poikilitic texture is common, leading to widespread knobbly weathering in many localities where the gabbro is exposed (Figure 2.14).

Figure 2:14 Loch Uisg Gabbro on the south shore of Loch Uisg, at [NM 644 247], near the eastern limit of the outcrop. Rock shows poikilitic texture-induced weathering pattern and is traversed by numerous thin, pale-green hydrothermal veins. Hammer for scale, shaft length 33cm.

Locally, the Loch Uisg Gabbro displays good sub-horizontal layering, especially at the western end of the main outcrop, near the Laggan shore where several prominent bands are noticeable. Thinner bands, up to 2 cm thick of more leucocratic gabbro, alternating with slightly thicker darker layers up to 15cm in thickness, stand slightly proud of the rock surface (Figure 2.15). However, the layering cannot be traced laterally further than a few metres. Above the road, at [NM 623 246], the gabbro contains a faint layering, but apart from these two examples, layering has not been observed anywhere else.

The Loch Uisg Gabbro is hydrothermally altered and has a distinctive greenish appearance on freshly broken surfaces. Epidotisation has taken place and can be clearly seen in hand specimens and on joint surfaces. Hydrothermal veins are common over the entire outcrop.

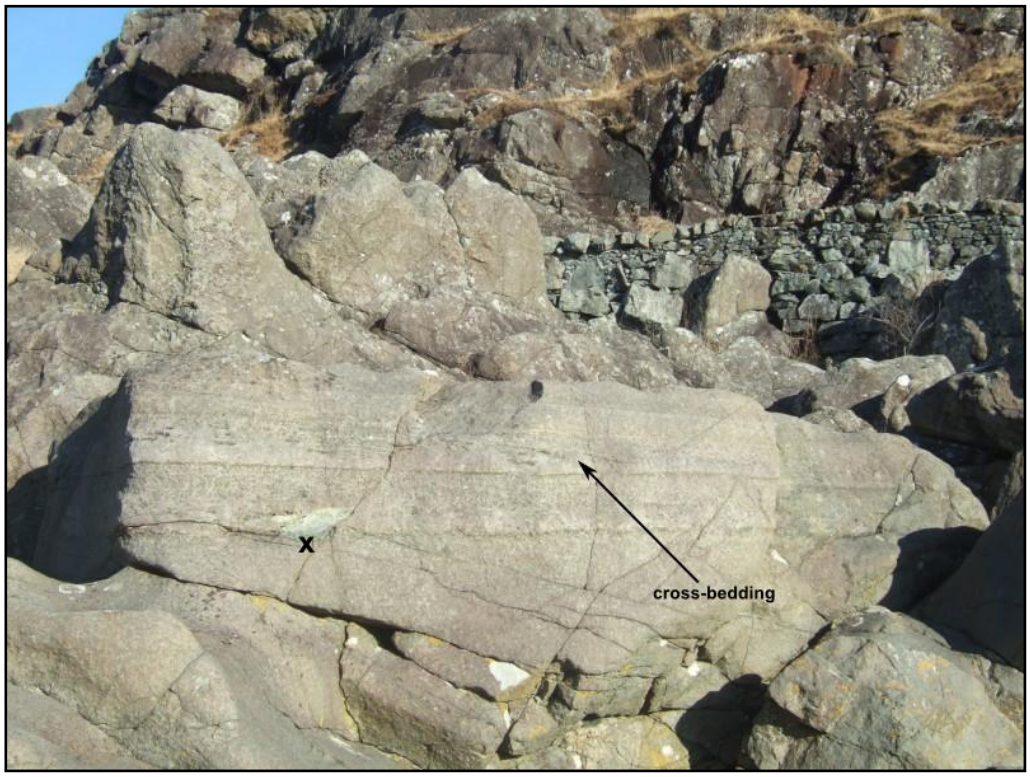

Figure 2:15 Layering in the Loch Uisg Gabbro at Laggan Sands (at [NM 643 246]). The layering is sub-horizontal and an obvious but oblique layering fabric (based on the geometry, analogous to cross bedding?) is present in the uppermost layers. The greenish tinge to the rock is the result of hydrothermal alteration. This is clearly seen at the "x" where the rock has been sampled in the recent past, leaving a freshly broken surface.

Xenoliths are also a prominent feature of the gabbro at Laggan Sands. These appear to be clustered at the lowest visible level of the intrusion, just above the beach sand and clearly extending to depth. The xenoliths are large, up to 1m across, rounded and have reaction rims dominated by anorthosite. These xenoliths were not observed at any other outcrop of the Loch Uisg Gabbro and appear to be confined to the Laggan Sands location.

Figure 2.16: Xenolith in the Loch Uisg Gabbro, Laggan Sands, at [NM 623 245]. A pale anorthosite rim is clearly visible. Ruler is 30cm long. The anorthositic nature of the rim is determined by thin section observation. It is not a weathering effect.

Close to the area where the xenoliths occur, the rock is traversed by numerous sheets, possibly related to the cone-sheets, of fine-grained basalt, up to 7cm across, which show flow banding and chilled margins.

Figure 2.17: Sheets of basalt cutting the Loch Uisg Gabbro at [NM 623 245]. Ruler is 30cm long. These probably represent basic cone sheets based on the rock type and the orientation.

Figure 2.18: Detail of sheets shown in Figure 2.17 showing the flow banding that is evident throughout the width of the sheets.

2.4.2 The Loch Uisg Gabbro - Glen Libidil

The Glen Libidil outcrop of the Loch Uisg Gabbro is indicated as Intrusion No. 2 in Figure 2.1 and crops out on the floor of Glen Libidil where it is best exposed in the Glenlibidil Burn. No contacts with the country-rock basaltic lavas are visible as the glen is covered in tussocky grass and heather. A typical view is given in Figure 2.19.

Figure 2.19: Looking west across Glen Libidil from [NM 668 232]. The rock in the foreground and in the stream bed is Loch Uisg Gabbro.

The country-rocks of the gabbro around Glen Libidil are mostly basaltic lavas. No actual contacts are exposed. However at the NW end of the outcrop, in the

upper reaches of Glen Libidil, the gabbro appears to be separated from the basalt lavas by overlying granite. Along the South Loch Uisg – Laggan section gabbro is nowhere seen in contact with the basaltic lavas. Granite is found in the steeper upper ground above the gabbro, which is seen in the river bed. According to Bailey *et al.* (1924), the gabbro underlies the Loch Uisg Granite in the upper part of Glen Libidil, although the nature of the contact is not discernible due to very poor exposure (Figure 2.19).

The rock is a medium-grained gabbro, locally poorly layered (Figure 2.20), but due to the poor exposure, internal features and structures are not particularly obvious. Poikilitic texture is common, manifest in the distinctive pock-marked weathering pattern that characterises the other main gabbro intrusions in the Loch Uisg area.

Figure 2.20: Indistinct layering in the Glen Libidil outcrop of the Loch Uisg Gabbro at [NM 668 225]. The dip of the layering is to the NW. Ruler is 30cm long.

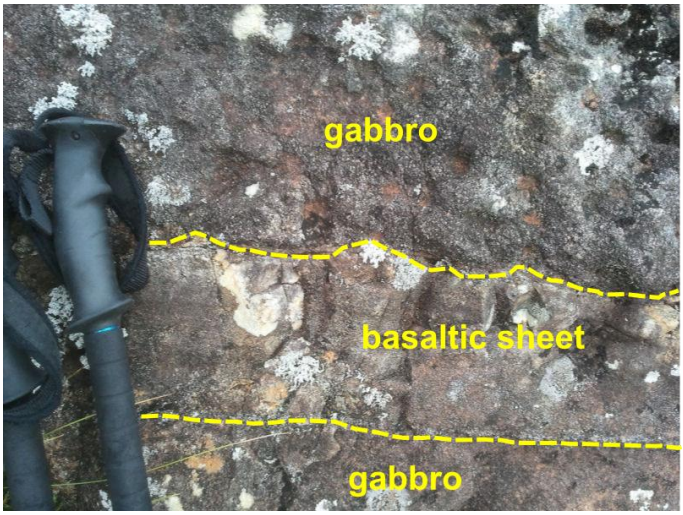

Figure 2.21: Close up detail of the Loch Uisg Gabbro at [NM 659233], showing rusty pock-marking characteristic of poikilitic texture and a finer grained basaltic sheet cutting the gabbro. The sheet dips to the east at 5-10°. This is in contrast to the dip of the layering in Figure 2.20. The handle of walking pole is approximately 15 cm in length.

2.4.3 Comparison of the two gabbro outcrops

Allowing for the limited exposure, the Glen Libidil outcrop of the LUG appears to be more homogenous than the Loch Uisg – Laggan outcrop. Apart from some limited indistinct layering (Figure 2.20) there is not much variation across the Glen Libidil outcrop either vertically or laterally. No obvious cumulate textures are seen and no xenoliths were recorded.

2.5 The Gabbro / Granite contact

There are very few locations where the contact between these two lithologies is clearly discernible. Over much of the area and especially where the contact would be expected, there is thick vegetation. According to Bailey *et al*. (1924), "*Contacts have been examined in the cliff above Loch Buie, and also in a tributary of the Glenlibidil Burn descending Coill' a' Bhealaich Mhoir. There is no chilling of the one intrusion against the other, but rather, near Loch Buie, a suggestion of local admixture without the development of a xenolithic structure. Altogether, the appearances noted are too ambiguous to be interpreted with certainty*".

Several localities are worth mentioning:

2.5.1 Loch Buie Cliffs: The cliffs above Loch Buie near the Laggan Beach were examined in detail as part of the fieldwork but no clear contact was seen. Although there are large areas of exposed rock, the contact zone between the gabbro and the granite is not well exposed due to vegetation. Instead, and in line with the 1924 citation above, there appears to be a narrow zone of mixing between the two rock types. The width of this zone can be no more than 10 metres, based on field observations. Several sections were examined, starting on the shore where the gabbro is obvious and moving uphill towards the granite. No sharp contacts are observable, no xenoliths are obvious and no veining of one lithology by the other can be discerned. The only noticeable feature is that the "local admixture" mentioned by Bailey *et al*. (1924) can be found along the length of the contact zone. This hybridisation is seen in two of the thin section samples (384 from location [NM 6249 2442] in the cliffs and 307 from [NM 6246

2443] from the hill slope above the cliffs) Figures 2.29, 2.34. These sample localities are shown in Figure 2.22.

Figure 2.22: The cliffs above Loch Buie seen from near the beach, looking north. The location of several of the Loch Uisg Gabbro samples referred to in Chapter 2 are indicated.

2.5.2 South Shore of Loch Uisg, Allt Bealach na Leitreach: This is the stream which runs into Loch Uisg at [NM 6373 2493] (Figure 2.23). The Loch Uisg Gabbro crops out on the shore and can be traced up the stream towards the granite. At approximately 50 metres from the loch shore, the character of the rock changes and it displays the "mixed rock" appearance similar to the rocks seen in the cliffs above Loch Buie. In hand specimen, the rock is less clearly gabbroic and instead displays a much more dioritic appearance. The overall colour is lighter. Ten metres further upstream, the rock is clearly granite and this is observable for a considerable distance up the hill, although the vegetation makes detailed mapping difficult.

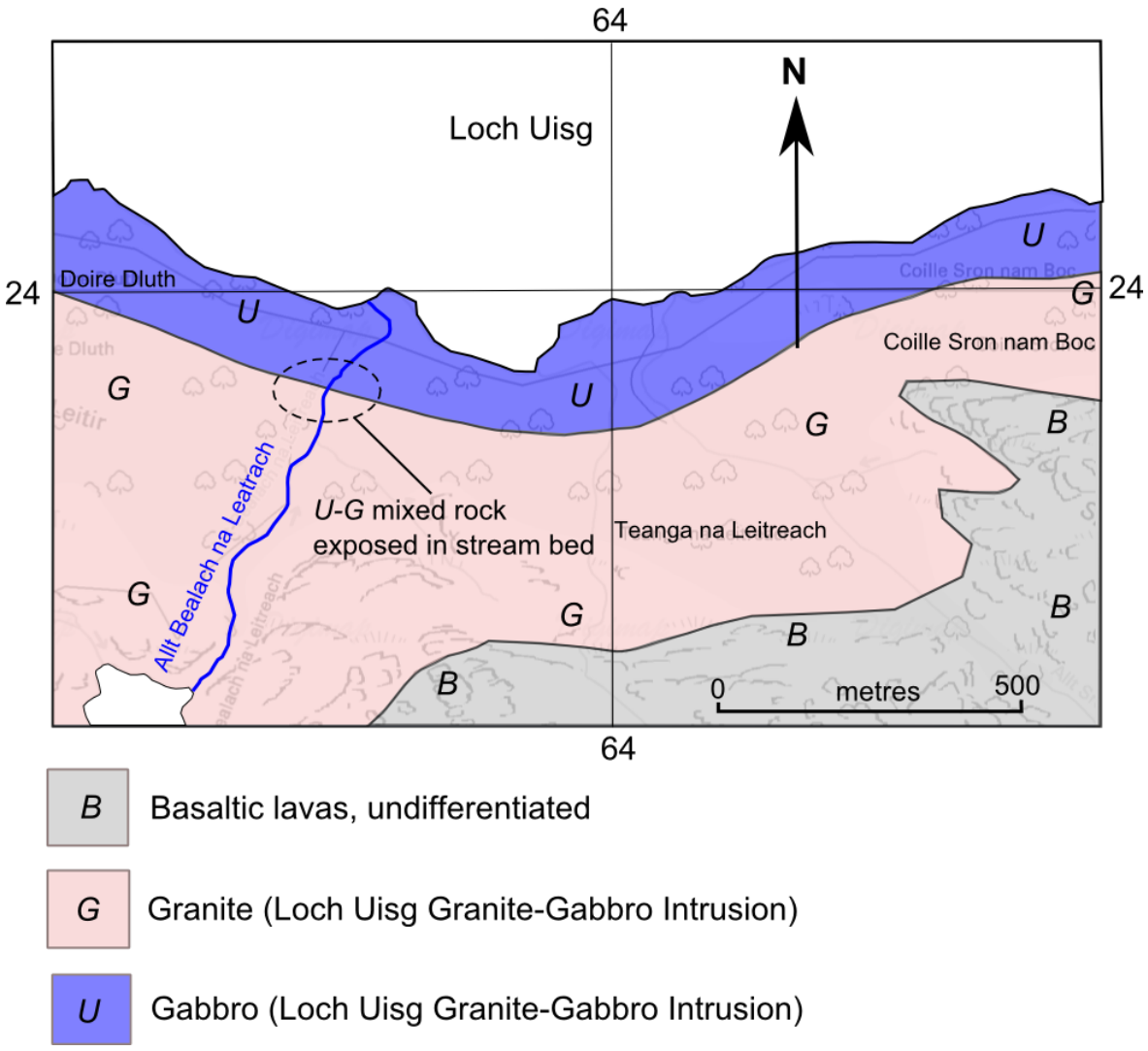

Figure 2.23: The location of Allt Bealach na Leitreach on the south shore of Loch Uisg. Contact of gabbro and granite shown where the zone of hybridised rock occurs.

2.5.3 Glen Libidil: Coille a' Bhealaich Mhoir:

At the wooded area known as Coille a'Bhealaich Mhoir in upper Glen Libidil, several small streams run in a south easterly direction into the Glen Libidil Burn. This area is indicated in the lower right hand side of the satellite image in Figure 2.2. The exposure, as in most of Glen Libidil, is poor, but the stream sections reveal some limited detail of the underlying rock types. As is the case with the Loch Uisg – Laggan outcrop of the Loch Uisg Gabbro, no well-defined contact is seen. Bailey *et al.* (1924) referred to the contact in Coille a'Bhealaich Mhoir, but no clear distinct boundary was found during the course of this study. Instead, in several of the stream beds, the granite was observed to a lower topographic level than the published map shows. At one location (Figure 2.25) [NM 6575 2263], approximately 20 m from the contact, the granite has abundant pink felsitic veins, 5–10 mm wide, running through it. At the location [NM 6563 2335] the felsite is white. Examination of freshly broken pieces of the veins indicates that the colour of the rock appears to be due to the presence of K-feldspar, rather than due to weathering.

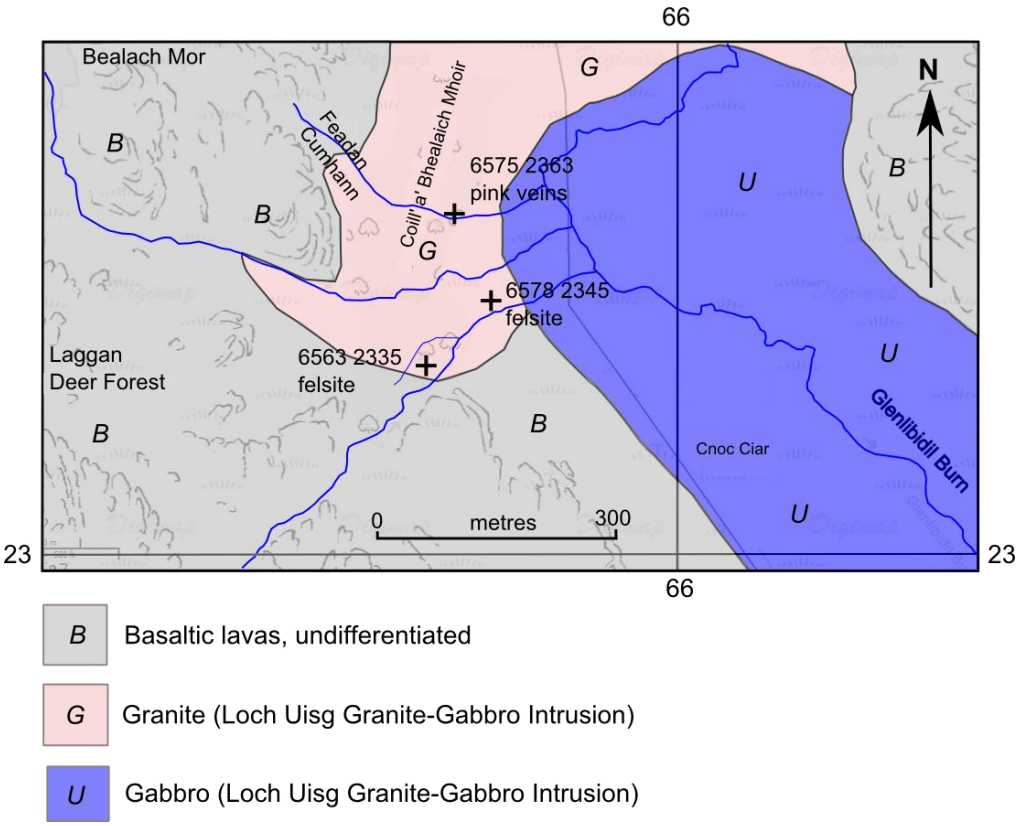

Figure 2.24: Map of the Coille a' Bhealaich Mhoir area showing outcrops of felsites referred to in the text.

2.6 Petrography and mineral chemistry of the LUGGI

2.6.1 Introduction

The field relationships of both outcrops of the Loch Uisg Gabbro and the granite with which it is associated have already been described in the first part of this chapter. The Glen Libidil outcrop (indicated by "2" on Figure 1.5 in Chapter 1) appears to be fairly homogeneous in the field, although exposure is poor. The Laggan outcrop (indicated "1" on Figure 1.5) exhibits a greater degree of heterogeneity, both vertically and horizontally, with layering being well developed, the presence of large xenoliths, hybridization with the granite and varying degrees of hydrothermal alteration.

In order to study the petrography and mineral chemistry, a number of samples were selected for sectioning and analysis. Samples were chosen from the localities that were likely to give the most useful information. Additional samples were sourced from the Hunterian Museum (Glasgow University) collections.

The original petrographic work undertaken on these intrusions (Bailey *et al*. 1924) appears to have been based on only three thin sections, two from the Loch Uisg area (BGS numbers 15067 and 17347) and one from Glen Libidil (BGS number 17366).

2.6.2 Sampling

Nine samples for optical and SEM analysis were collected from the Loch Uisg Gabbro – eight from the Laggan outcrop and one from the Glen Libidil outcrop. These are summarized in Table 2.1 and the locations are indicated on the maps in Figures 2.25 and 2.26.

Sample	Location	Grid Reference	Type
155	Laggan Bay, at lowest tide. Lowest possible sample from the intrusion	[NM 6184 2450]	Polished thin section
307	Cliffs above Laggan Beach	[NM 6246 2443]	Thin section
308	Cliffs above Laggan Beach	[NM 6246 2443]	Thin section
309	Cliffs above Laggan Beach	[NM 6242 2445]	Thin section
TS 22432	Laggan Beach, near a xenolith in the exposed rock at shore level. (Hunterian Museum sample)	[NM 623 245]	Thin section
TS 22448	Laggan Beach, near a xenolith in the exposed rock at shore level. (Hunterian Museum sample)	[NM 623 245]	Polished thin section
333	South Loch Uisg shore, near a small cave	[NM 6298 2508]	Polished thin section
384	Cliffs above Laggan Beach	[NM 6249 2442]	Polished thin section
396	Glen Libidil	[NM 6648 2276]	Polished thin section

Table 2.1: The locations and grid references of the samples, polished (for SEM work and optical examination) and ordinary thin sections (for purely optical work).

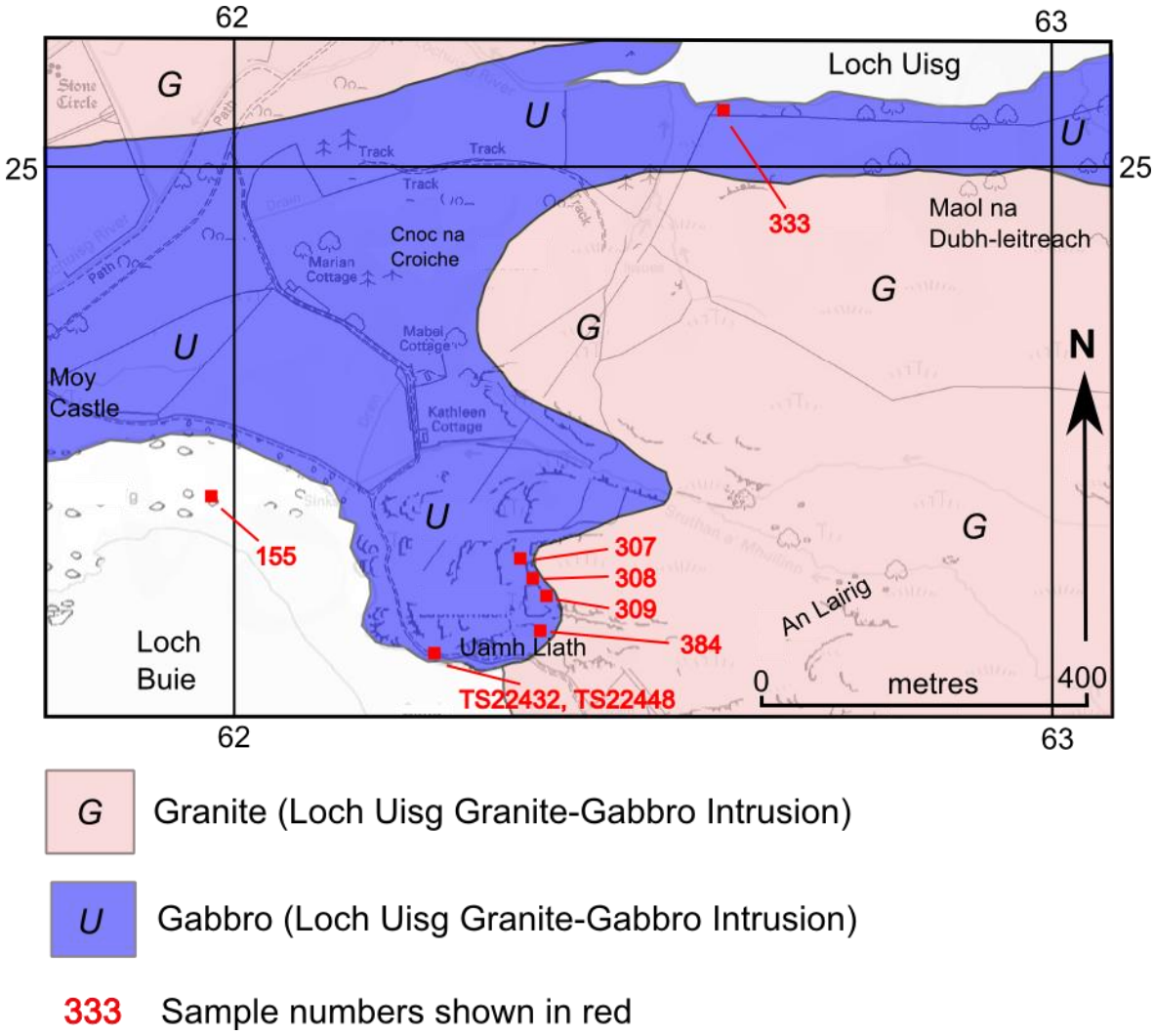

Figure 2.25: Map showing the locations where the South Loch Uisg - Laggan samples of the Loch Uisg Gabbro were obtained. As can be seen, several samples were taken from the contact zone of the gabbro and granite in order to assess any magma mixing along this zone.

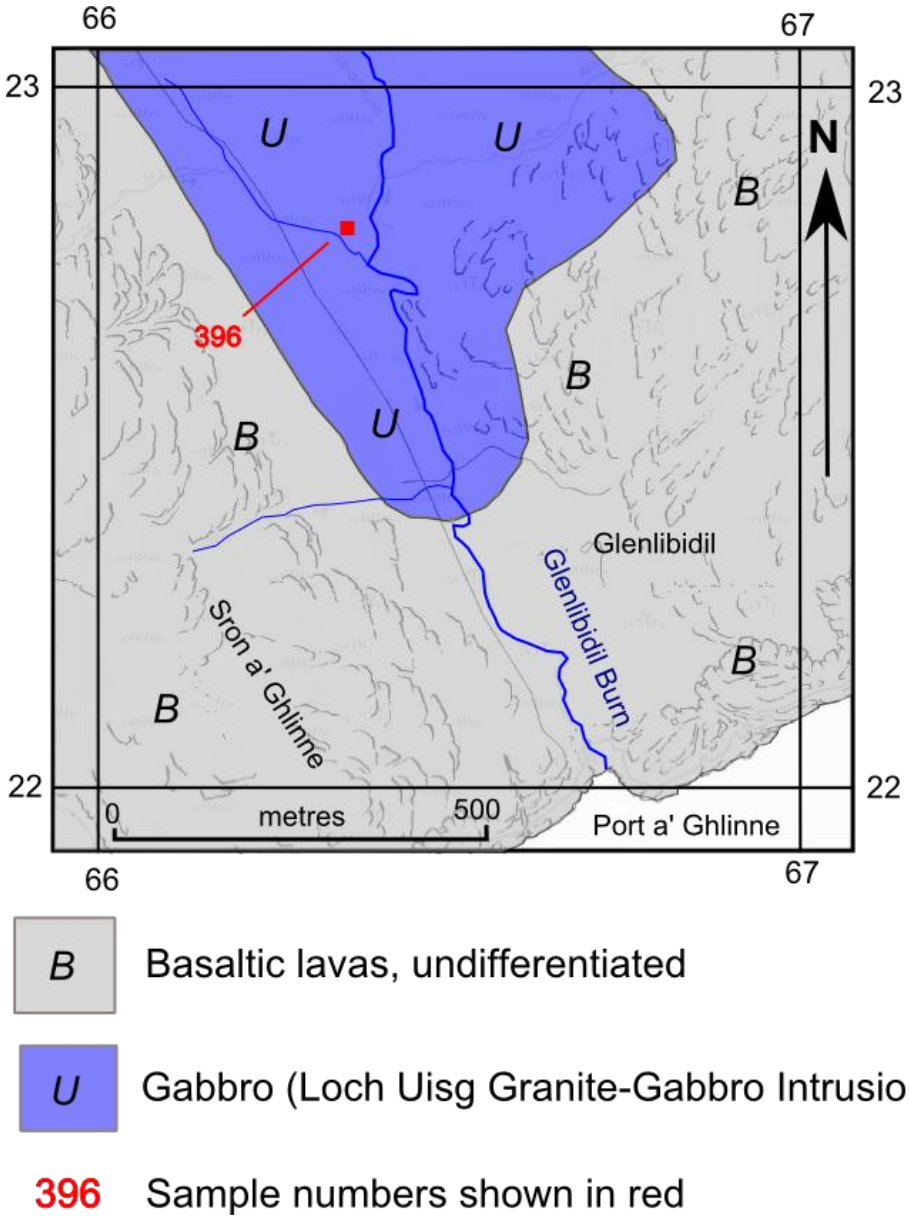

Figure 2.26: Map showing the location where the Glen Libidil sample of the Loch Uisg Gabbro was obtained. Sample 396 was the only sample chosen from this locality of thin section / SEM analysis due to time and resource constraints.

2.6.3 Petrography

Figures 2.27 – 2.35 show the Loch Uisg Gabbro samples in thin section under both plain polarized light and crossed polars. Each slide is a standard 2.5 cm wide, except Figure 2.35 (50 x 75 mm). Widths of rock slices are given in the descriptions.

Figure 2.27: Thin section view (PPL) of sample 155, from Laggan Bay at [NM 6184 2450]. Gabbro, obtained at low tide. Rock slice width is 40 mm.

Figure 2.28: Thin section view (PPL) of sample 307, cliffs above Laggan Beach at [NM 6246 2443]. Hybridized rock. Rock slice width is 40 mm.

Figure 2.29: Thin section view (PPL) of sample 308, cliffs above Laggan Beach at [NM 6246 2443]. Gabbro. Rock slice width is 40 mm.

Figure 2.30: Thin section view (PPL) of sample 309, cliffs above Laggan Beach at [NM 6242 2445] . Gabbro. Rock slice width is 40 mm.

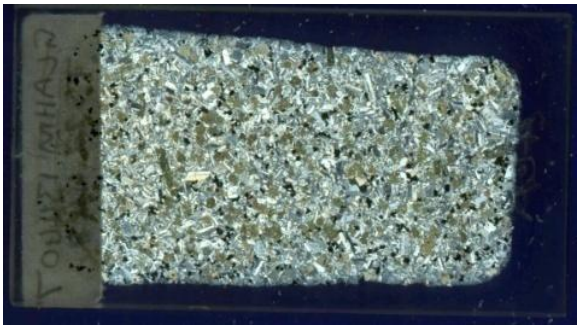

Figure 2.31: Thin section view (PPL) of sample TS 22448, from the shore at Laggan Beach at [NM 623 245]. Gabbro, near a large xenolith. Rock slice width is 40 mm.

Figure 2.32: Thin section view (PPL) of sample 333, from the south shore of Loch Uisg near the western end at [NM 6298 2508]. Gabbro. Rock slice width is 40 mm.

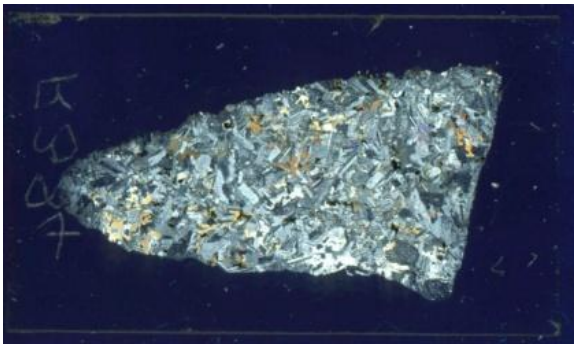

Figure 2.33: Thin section view (XPL) of sample 384, Laggan Cliffs at [NM 6249 2442]. Gabbro with felsitic material. Rock slice width is 35 mm.

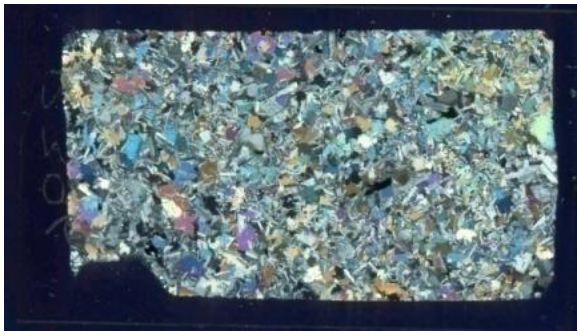

Figure 2.34: Thin section view (XPL) of sample 396 from Glen Libidil at [NM 6648 2276]. Gabbro. Rock slice width is 40 mm.

Figure 2.35: Thin section view (PPL) of sample TS 22432, Laggan Shore at [NM 623 245]. Gabbro. Rock slice width is 50 mm.

2.6.4 General observations on the samples

The dominant minerals are plagioclase and clinopyroxene, commonly displaying ophitic texture, which is also prominent in the field. Magnetite is a common opaque mineral in all of the thin sections, rarely displaying a strongly skeletal texture. However, the Glen Libidil sample, 396, has considerably less modal magnetite than the Laggan samples. Epidote is a common alteration mineral forming veins and crystal clusters. Olivine occurs only as rare pseudomorphs. Bailey *et al.* (1924) mention pseudomorphs after olivine in their Loch Uisg gabbro samples and imply that it is plentiful. However, their surprisingly detailed petrography is based on only three samples.

The rocks range from medium to coarse grained. Bailey *et al.* (1924) described the Loch Uisg Gabbro as a "gabbro or dolerite" without any specific elaboration on which parts are coarse or medium grained. The gabbro in the Laggan area is

very rich in plagioclase, which is the dominant phase; leuco-gabbro would be the correct descriptive term. The gabbro from the Glen Libidil outcrop has a greater modal percentage of clinopyroxene, giving the rock a darker appearance. The grain size of the feldspars varies depending on the textural qualities of the rock. In some of the coarser-grained varieties, such as the samples from near Laggan shore, the plagioclase crystals are up to 5 mm in length.

In some samples, which are highly ophitic, the clinopyroxene oikocrysts are up to 2 cm in length. Sample 309 displays this well (Figure 2.44). Poikilitic (ophitic) texture is well developed throughout the Loch Uisg Gabbro, and is visible in the field, where it produces a distinctive weathering pattern and an obvious "sheen" in bright sunlight, and under the microscope where large clinopyroxene crystals are obvious. The opaque minerals, mainly magnetite, occur as small grains up to 1 mm in length, commonly in clusters and chains (Figure 2.36).

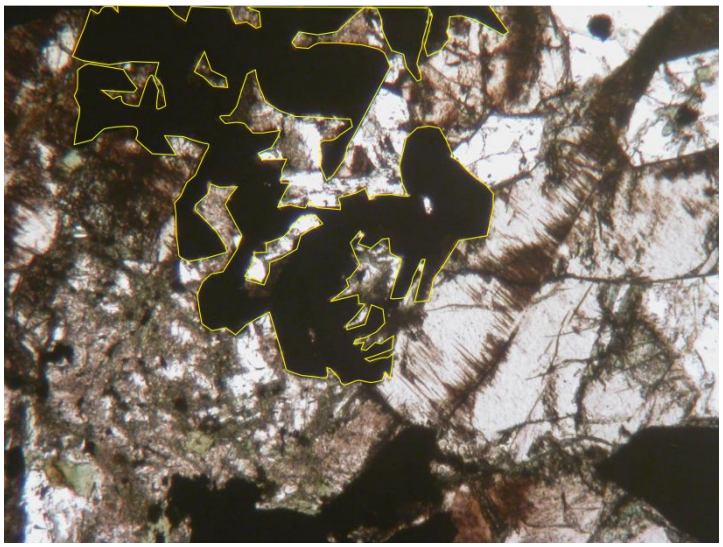

Figure 2.36: Thin section view (PPL) of sample 155 from Loch Buie at NM 6184 2450], showing a cluster of skeletal magnetite crystals, outlined in yellow. Horizontal Field of View (HFOV): 2 mm.

Variations in mineralogy are clearly seen on the shore at Laggan, where layering is well developed. Cumulus plagioclase, determined by thin section inspection, is present in distinct layers in the rock (Figure 2.5). Nearby, running through massive gabbro, veins and pods of gabbroic pegmatite are visible (Figure 2.37).

Figure 2.37: Gabbroic pegmatite, part of a network of veins running through the Loch Uisg Gabbro on the shore at Laggan Sands at [NM 623 245]. Ruler for scale marked in cm.

2.6.5 Mineral phases

Figures 2.38 to 2.49 are photomicrographs of several of the Loch Uisg Gabbro samples. The salient features of the individual mineral phases are described below.

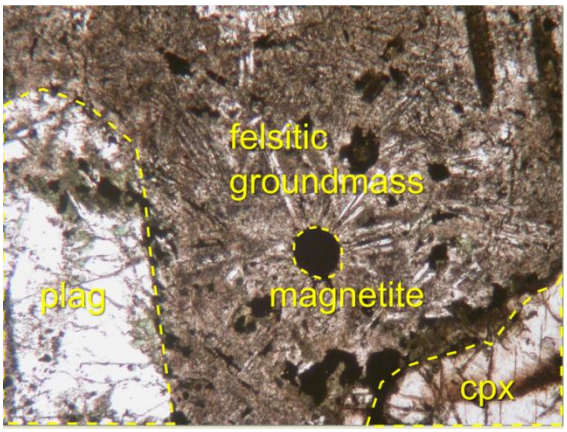

Figure 2.38: Thin section view (PPL) of sample 155 from Loch Buie at [NM 6184 2450] showing radiating plagioclase crystals from magnetite in a large felsitic patch. Plagioclase crystal on the LHS. Cpx crystal on the lower RHS. HFoV: 2 mm.

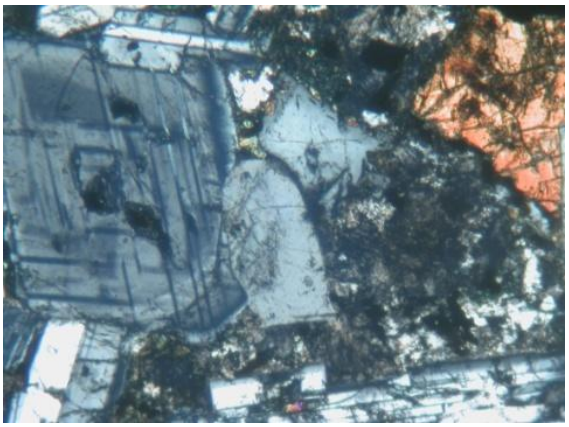

Figure 2.39: Thin section view (XPL) of sample 155 from Loch Buie at [NM 6184 2450] Zoned plagioclase. HFoV: 2 mm.

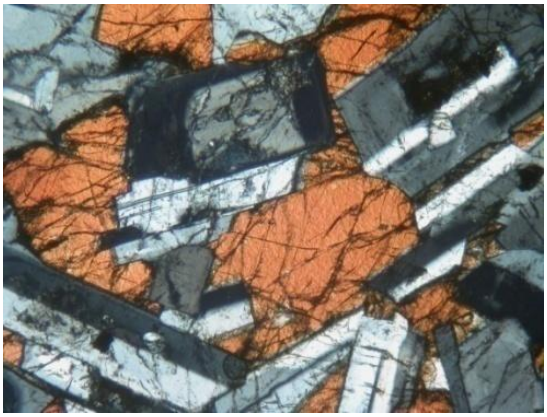

Figure 2.40: Thin section view (XPL) of sample 333 from the Loch Uisg Shore at [NM 6298 2508] showing ophitic texture, of zoned plagioclase and clinopyroxene. Very fresh. HFoV: 2 mm.

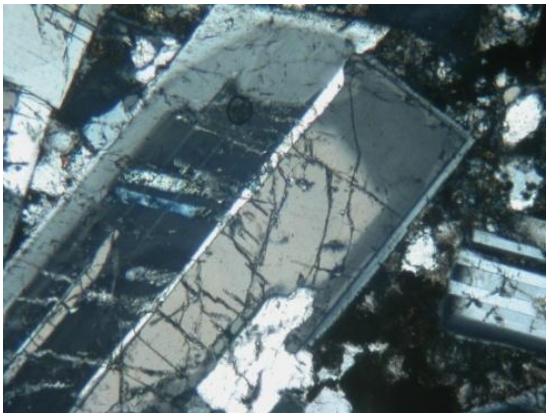

Figure 2.41: Thin section view (XPL) of sample 333 from the Loch Uisg Shore at [NM 6298 2508] showing a large plagioclase crystal with obvious zoning. HFoV: 2 mm.

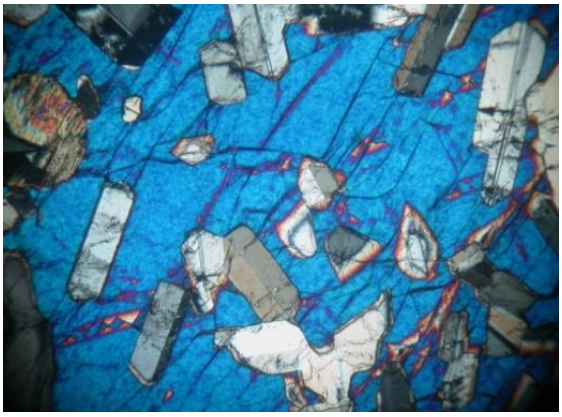

Figure 2.42: Thin section view (XPL) of sample TS 22432 from Laggan Beach at [NM 623 245] showing a large clinopyroxene oikocryst with enclosed plagioclase. HFoV: 2 mm.

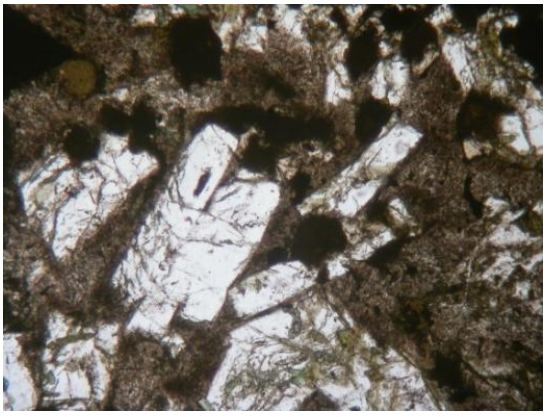

Figure 2.43: Thin section view (PPL) of sample 307 from near the contact zone above the Laggan Cliffs at [NM 6246 2443] showing altered plagioclase and felsic mesostasis. HFoV: 2 mm.

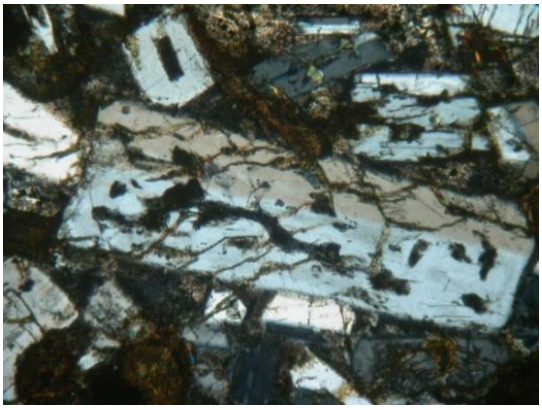

Figure 2.44: Thin section view (XPL) **of s**ample 308 from Laggan Cliffs at [NM 6246 2443] showing plagioclase with a well developed sieve texture. HFoV: 2 mm.

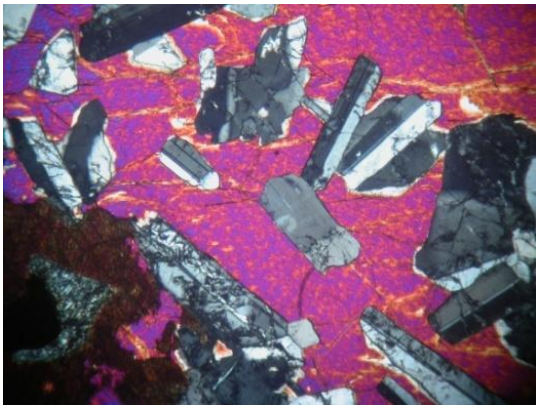

Figure 2.45: Thin section view (XPL) of sample 309 from Laggan Cliffs at [NM 6242 2445] showing ophitic texture of plagioclase and clinopyroxene. HFoV: 2 mm.

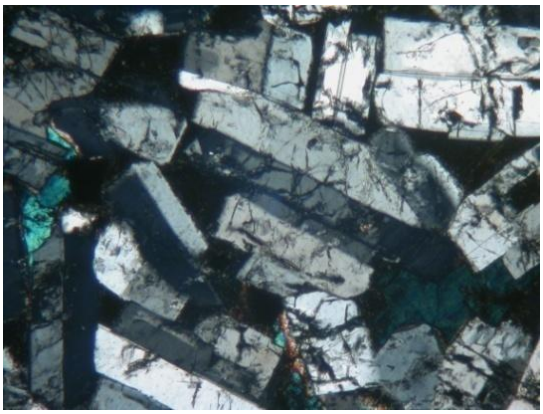

Figure 2.46: Thin section view (XPL) of sample 309 from Laggan Cliffs at [NM 6246 2443], showing the cumulus texture of plagioclase. Alignment of the plagioclase crystals is obvious. HFoV: 2 mm.

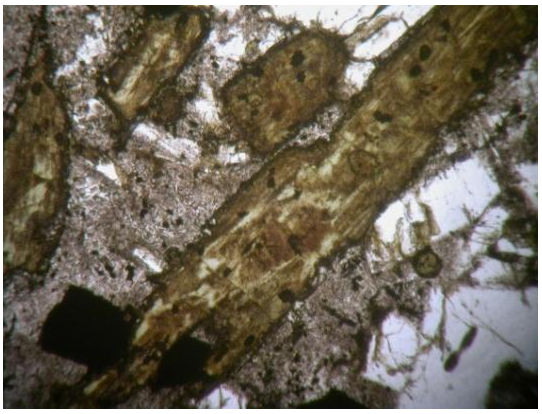

Figure 2.47: Thin section view (PPL) of sample 308 from Laggan Cliffs at[NM 6246 2443] showing fibrous and greenish brown pseudomorph after opx. HFoV: 2 mm.

Figure 2.48: Thin section (XPL) view of sample 384 from Laggan Cliffs at [NM 6249 2442] showing hybridized rock from the contact zone. Felsitic material (cream coloured on LHS of image) is mixed with gabbro. FoV: 5 mm.

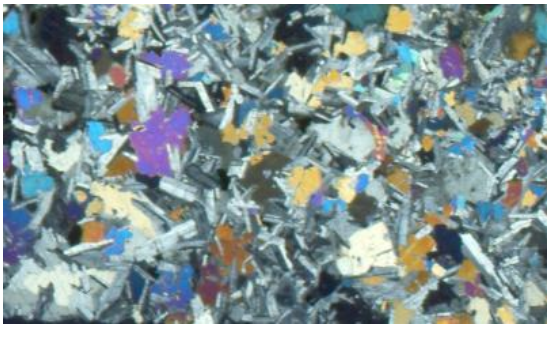

Figure 2.49: Thin section view (XPL) of sample 396 from Glen Libidil at [NM 6648 2276] showing a general view of the rock texture. Phenocrysts of clino-pyroxene in a groundmass of acicular plagioclase and small cpx crystals. FoV: 5 mm.

2.6.5.1 Plagioclase

Considerable variation is seen in the form and habit of the plagioclase in the Loch Uisg Gabbro, most of which appears to be a cumulus phase. Sample 155 (which at low tide, is from the lowest level of the intrusion) shown in Figures 2.36 and 2.38 displays varying degrees of alteration as well as acicular crystals forming radiating masses around magnetite crystals, although this is only seen in this particular sample.

Ophitic texture is clearly seen in many of the samples (Figures 2.40, 2.42 and 2.45). In all these samples the plagioclase and clinopyroxene are remarkably fresh, given the manifest hydrothermal alteration throughout much of the intrusion. There is a hint of mineral alignment of the plagioclase crystals within some of the clinopyroxene oikocrysts. In Figure 2.46, the plagioclase crystals are oriented in two main directions, normal to each other.

Sieve texture development of plagioclase can be well seen in samples 307 and 308 and to a lesser extent in sample 309. These samples are all from near the contact with the granite. Sieve-textured plagioclase is also seen in sample 155. However, no sieve texturing is observed in sample 333, which was taken from a location much further from the contact with the granite.

The plagioclase crystals display normal zoning, the interiors being more Ca rich. SEM analyses confirm the optical evidence although in some instances the zoning is clearly discontinuous. Sample 333 (Figure 2.41) shows an abrupt change within a plagioclase crystal, going from the rim to the core.

2.6.5.2 Clinopyroxene

The most obvious feature of the clinopyroxene is its texture. A poikilitic (ophitic) texture is clearly visible in several of the sectionss, especially the samples from the South Loch uisg – Laggan outcrop. In some cases, such as sample 309 in Figure 2.43, the oikocrysts are up to 2 cm across. The poikilitic texture of the rock is responsible for the distinctive weathering pattern, characterized by pock marks where the oikocryst has been weathered out. Clinopyroxene also occurs as an interstitial groundmass phase in most of the samples. Sample 155 shows no ophitic texture, only groundmass clinopyroxene. The condition of the mineral itself varies from very fresh (sample TS 22432 in

Figure 2.42) to considerably altered (sample 155 in Figure 2.38). In sample 396 from Glen Libidil, the clinopyroxene is more granular and much less ophitic. The mineral is commonly polycrystalline and triple junctions between sintered crystal boundaries are common (Figures 2.50 to 2.51).

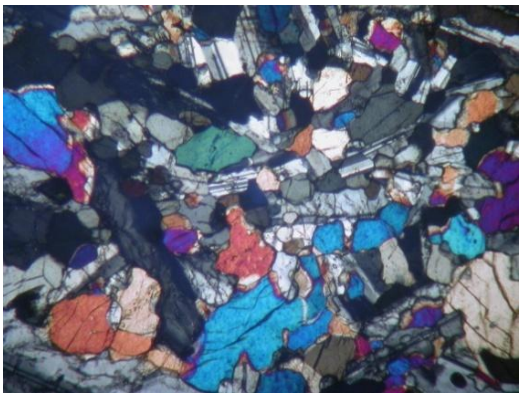

Figure 2.50: Thin section view (XPL) of sample 396 from Glen Libidil at at [NM 6648 2276] showing the granular nature of much of the clinopyroxene in the gabbro. HFoV: 2 mm.

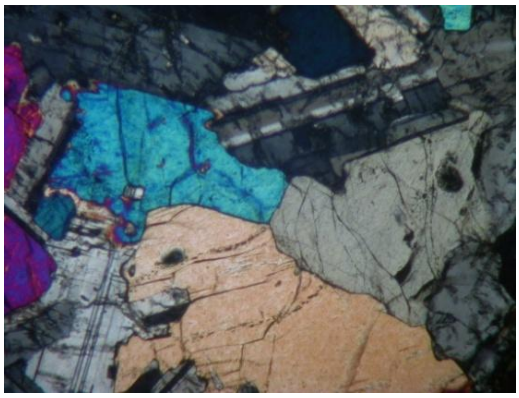

Figure 2.51: Thin section view (XPL) of sample 396 from Glen Libidil at at [NM 6648 2276] showing a triple point crystal boundary in polycrystalline clinopyroxene. HFoV: 2 mm.

2.6.5.3 Orthopyroxene

Pseudomorphs after orthopyroxene are seen in several of the slides as fibrous, greenish brown aggregates, sometimes distinctly laminated e.g. sample 308 (Figure 2.47). It is also found as an overgrowth on olivine pseudomorphs, for example in sample 309 in Figure 2.52. The orthopyroxene appears to be more common among the samples taken from close to the contact zone with the granite.

2.6.5.4 Olivine

Olivine does not occur as fresh crystals, but instead is rarely seen as pseudomorphs. The morphology of the original olivine is preserved. The shapes of the crystals and the distinctive curving cracks are clearly visible e.g. sample 309 (Figure 2.52) and sample 396 Figure 253).

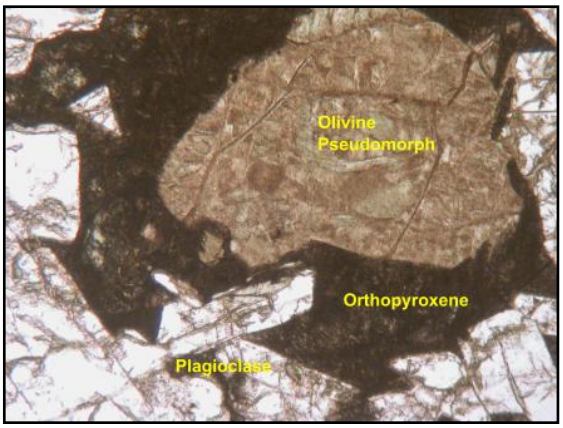

Figure 2.52: Thin section view (PPL) of sample 309 from near the contact with the granite in the cliffs above Loch Buie at Laggan at [NM 6246 2443] showing an olivine pseudomorph. Relict typical olivine morphology is surrounded by an overgrowth of what appears to be orthopyroxene. HFoV: 2mm.

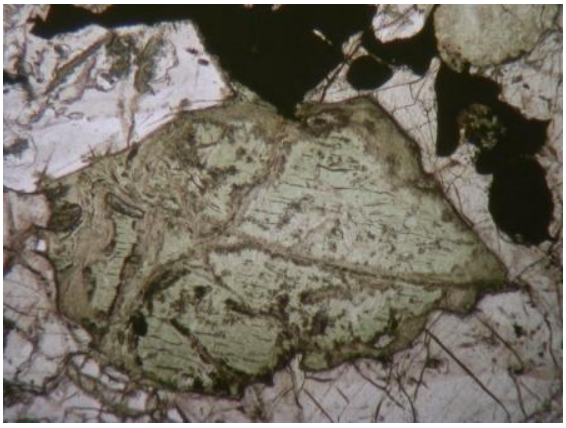

Figure 2.53: Thin section view (PPL) of sample 396 from the Glen Libidil gabbro at [NM 6648 2276] showing an olivine pseudomorph displaying euhedral form and curving cracks. HFoV: 2 mm.

2.6.5.5 Opaque minerals (Oxides)

The oxide minerals that show up as opaques in the thin sections are mainly magnetite. A single crystal of chrome spinel, (identified by the SEM), possibly a xenocryst, was found in one sample (sample 384 from the Laggan Cliffs). This is in complete contrast to the rocks of the Loch Uisg Picrite Suite, where this type of spinel is ubiquitous. Distribution of the oxides varies considerably: a regular scattering of individual crystals is common, as are knots, clusters and chains of grains. Many of the crystals show skeletal textures. Rarely, as in Sample TS 22432 from the Laggan Shore area, the oxides are clearly interstitial to the plagioclase (Figure 254).

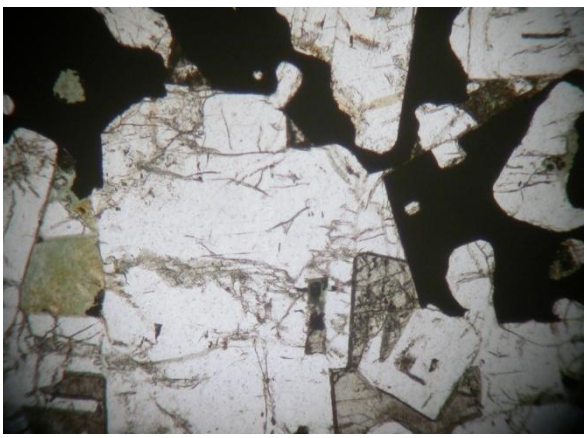

Figure 2.54: Thin section view (PPL) of sample TS 22432 from Laggan Beach at [NM 623 245] showing cumulus plagioclase with intercumulus oxides. HFoV: 2mm.

2.6.5.6 Interstitial felsite

Two of the slides, (Sample 155 in Figures 2.36 and 2.38 and Sample 384 in Figure 2.48) show interstitial felsitic material between the main mineral phases (clinopyroxene and plagioclase). In Figure 2.48 it appears as a cream coloured amorphous material in XPL. In Figure 2.38 it appears as a dirty coloured mass of altered material between the plagioclase and clinopyroxene. This effect is also noted in a loose (not *in situ)* boulder sample obtained by Dr John Faithfull where the interstitial felsite is visible at hand-specimen scale.

Sample 384 was obtained from the cliffs above Loch Buie, very close to the contact with the granite. Sample 155 is the "low-tide sample" from Loch Buie, apparently much further away from the contact. It may well be that the contact with the granite is indeed much closer at this location, below sea level.

This interstitial material may represent silicic material from the Loch Uisg Granite that has interacted with the gabbro, or it may be some form of mesostatis in a much more evolved rock. It may also be derived from some late-stage peritectic liquids from the gabbro itself. However, it does not appear to be present in gabbro samples taken much further away from the contact with the granite.

2.6.5.7 Secondary minerals

Hydrothermal alteration and the production of secondary minerals such as zeolites and epidote are common in the Loch Uisg Gabbro. This is clearly visible in the field, with veins and knots of epidote commonplace as well as an overall green tinge to the rocks. Sample TS 22432 (Figure 2.55) shows the bright interference colours of the epidote.

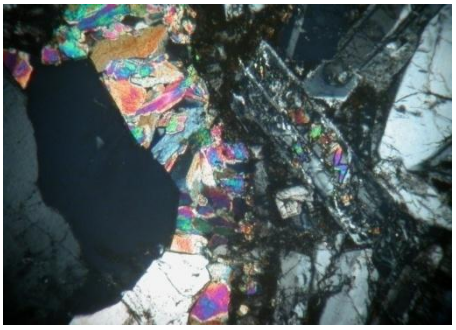

Figure 2.55: Thin section view (XPL) of sample TS 22432 from the Laggan Beach outcrop of the Loch Uisg Gabbro at [NM 623 245] showing the bright interference colours of secondary epidote. Also visible is possible epidote after plagioclase (the lath like crystal immediately to the right of the large epidote patch). HFoV: 2mm.

2.6.6 Felsite (Loch Uisg Granite)

The Loch Uisg Granite is the main country rock for both outcrops of the gabbro. Two sections of the granite from the Hunterian Museum's collection were examined and the petrography is described below. The samples were obtained from Glen Libidil. Representative images from sample JF2010-6 [NM 6563 2335] are shown in Figures 2.56 and 2.57.

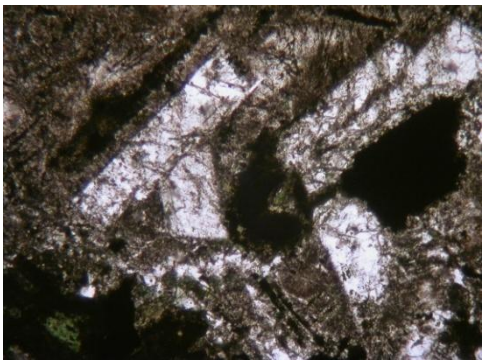

Figure 2.56: Thin section view (PPL) of sample JF2010-6 from the Loch Uisg granite in Glen Libidil at [NM 6563 2335] showing a cluster of feldspar and oxides in a fine grained groundmass. Alteration of both phenocryts and groundmass is evident. HFoV: 2mm.

Figure 2.57: Thin section view of sample JF2010-6 from the Loch Uisg granite in Glen Libidil at [NM 6563 2335] showing sieve textured plagioclase crystals. HFoV: 2mm.

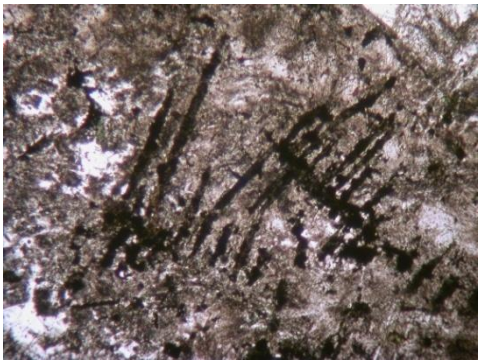

Figure 2.58: Thin section view (PPL) of sample JF2010-6 from the Loch Uisg Granite in Glen Libidil at [NM 6563 2335] showing dendritic quench structure in altered ferromagnesian silicates. FoV: 2mm.

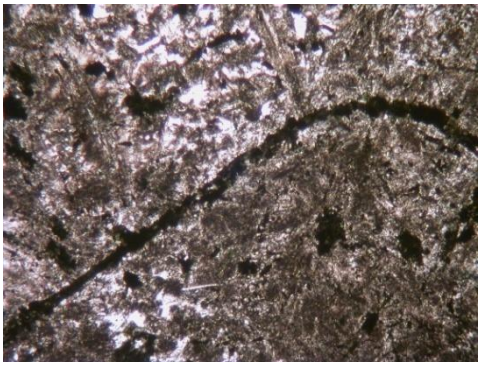

Figure 2.59: Thin section view (PPL) of sample JF2010-6. from the Loch Uisg Granite in Glen Libidil at [NM 6563 2335] showing curving chain of oxides / mafic minerals. FoV: 2mm.

Generally, the rock is highly altered, with few fresh minerals present. The texture is commonly porphyritic with a very fine grained groundmass – the term "microgranite" is more appropriate than "granite" or "granophyre". Throughout

the extent of the intrusion, the felsitic appearance dominates. No granophyric texture was observed in the samples studied. The plagioclase is commonly sieve textured, in the form of large phenocrysts, (Figure 2.57). It rarely forms distinct crystal clusters together with magnetite (Figure 2.56). The oxides are commonly found with altered mafic minerals forming curving chains of crystals (Figure 2.59).

The skeletal nature of the feldspars and the quench structures noted in the dendritic and curving crystal groups of oxides and mafic minerals possibly implies a rapid degree of growth under supersaturated conditions (Donaldson 1976; Lofgren 1983).

2.6.7 Mineral chemistry:

The polished thin sections noted in Table 2.1 were analysed using the SEM at Glasgow University. Samples were chosen to be as representative as possible of the Loch Uisg Gabbro. Energy-dispersive X-ray spectroscopy (EDS) was used for the main elements. Wavelength-dispersive X-ray Spectroscopy (WDS) was used to analyse for nickel due to the smaller quantities preent. A 20 kV, 4.5nA beam current was employed using a 120 μM aperture at a working distance of 8.5 mm. The phases that were analysed were plagioclase, clinopyroxene and oxide minerals. For the plagioclase analyses, the beam was rasterised by defocusing. Electron back scatter images were obtained as well as mineral chemistry analyses. Full results are given in Appendix 1 and the salient details are outlined below.

2.6.7.1 Plagioclase

The samples examined and analysed by SEM were: 155 (Low Tide), 396 (Glen Libidil), 384 (Laggan Cliff), TS 22448 (Laggan Shore). Results are graphically shown on the plots below (Figures 2.60 to 2.63).

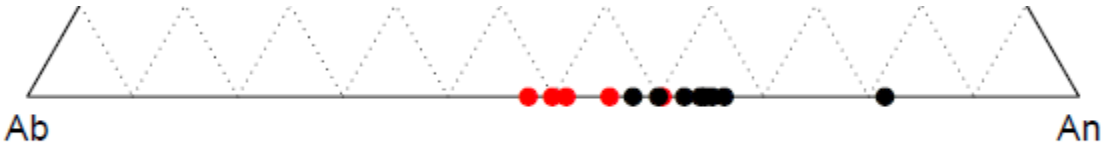

Figure 2.60: Sample 155: Low Tide: (Black Core, Red Rim)
Cores: Max An: 81.55 Min An: 57.60 Average An: 65.18
Rims: Max An: 60.41 Min An: 47.64 Average An: 52.92

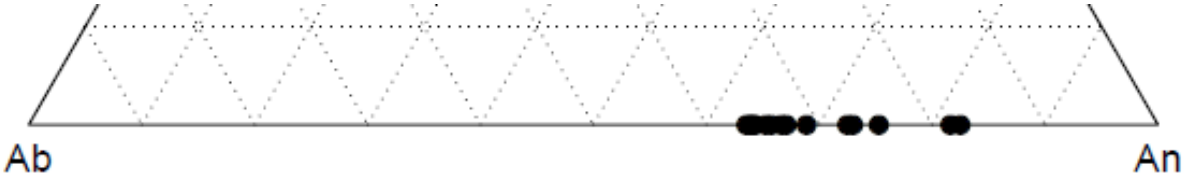

Figure 2.61: Sample 384: Laggan Cliff: (Black Core) No rim readings taken
Cores: Max An: 82.48 Min An: 63.56 Average An: 69.59

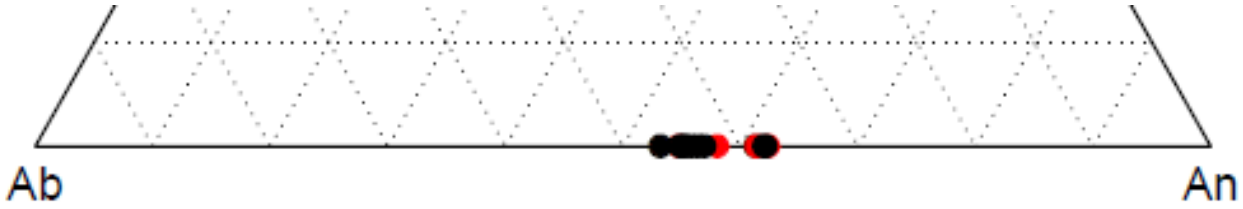

Figure 2.62: Sample TS 22448: Laggan Shore: (Black Core, Red Rim)
Cores: Max An: 62.12 Min An: 53.14 Average An: 57.28
RIms: Max An: 62.32 Min An: 54.77 Average An: 59.12

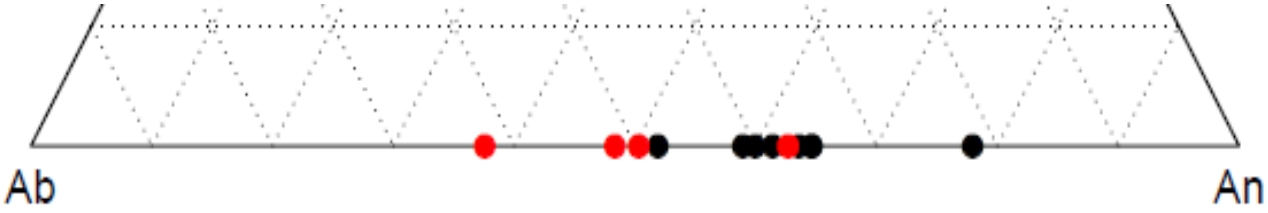

Figure 2.63: Sample 396: Glen Libidil: (Black Core Red Rim)

Cores: Max An: 77.91 Min An: 51.86 Average An: 62.86
Rims: Max An: 62.68 Min An: 37.55 Average An: 49.73

The range of plagioclase compositions for the Loch Uisg Gabbro is typical of other gabbros from the British Palaeogene Igneous Province:

1) Normal zoning is observed, with the rims being noticeably more sodic than the cores. Sample TS 22448 shows less of a spread but this may be due to the fact that this is a plagioclase-rich cumulus sample with less interstitial melt.

2) The two samples from lower levels of the intrusion (155 and TS 22448) in the Laggan area show lower average core values for anorthite than the sample (384) taken much higher up the cliff.

2.6.7.2 Clinopyroxene

The mineral chemistry values for clinopyroxene are shown on the pyroxene quadrilateral (Di-He-En-Fs) based on the ternary diagram. Samples 155, 384, TS 22448 and 396 were analysed (Figure 2.64).

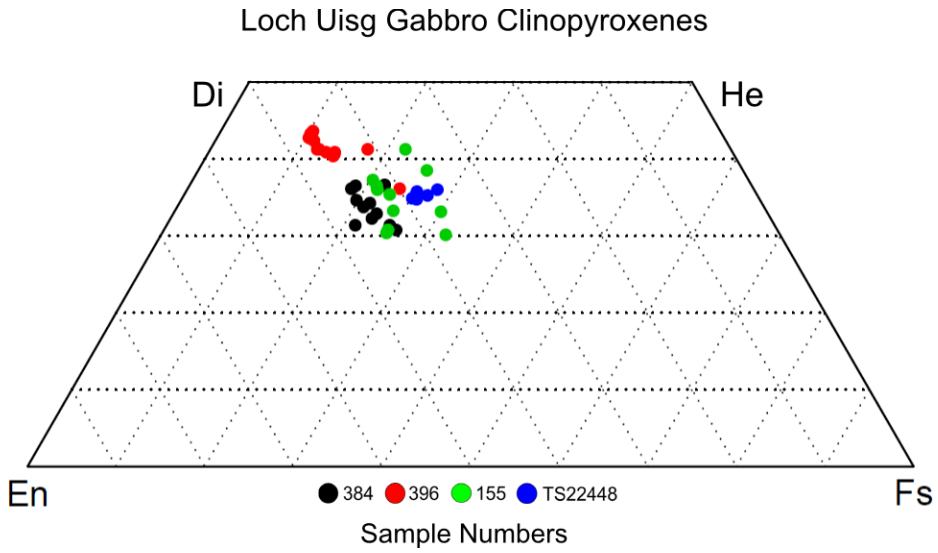

Figure 2.64: Clinopyroxene plot of the Loch Uisg Gabbro samples.

The compositions of the Loch Uisg Gabbro clinopyroxenes are very similar to other clinopyroxenes from other suites in the BPIP. Kerr (1998) analysed a variety of lavas from the Mull and Morvern areas and the results plot in the same diopside-augite region of the chart. An interesting comparison may be drawn

with the work done by Preston *et al.* (unpublished) on the Ben Buie Gabbro, which, like the Loch Uisg Gabbro, is a "Centre 1" intrusion and lies geographically very closeby to the north. These results, which lie in a very similar part of the plot are shown in Figure 2.65.

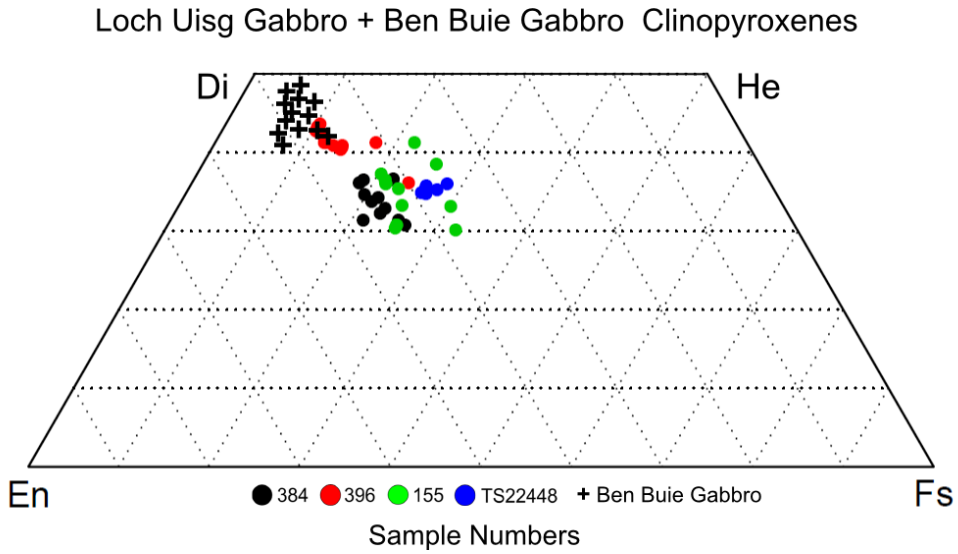

Figure 2.65: LUG Clinopyroxenes compared with a selection of clinopyroxenes from the Ben Buie Gabbro (Preston, *et al,* unpublished work).

Several points are evident from Figure 2.65:

1) There is a bigger and wider spread of compositions for clinopyroxene from the Loch Uisg Gabbro compared to the Ben Buie Gabbro.

2) The Loch Uisg Gabbro, on average, is poorer in Ca and richer in Fe when compared to the Ben Buie samples. The values for Ben Buie Gabbro plot between 40 and 50% wollastonite, whereas the Loch Uisg Gabbro figures fall between 30 and 45% wollastonite.

3) The Laggan outcrop of the Loch Uisg Gabbro shows a much wider range than the other three groups of clinopyroxenes. This may be a statistical effect due to the greater number of samples analysed.

4) The Laggan samples seem to be slightly more Fe rich and Ca poor than the Glen Libidil sample, but given the limited dataset, it is difficult to assess the significance of this.

2.6.7.3 Oxides

One of the distinguishing characteristics of the Loch Uisg Gabbro oxides under the SEM is the degree of skeletal development seen in some of the crystals (Figure 2.66).

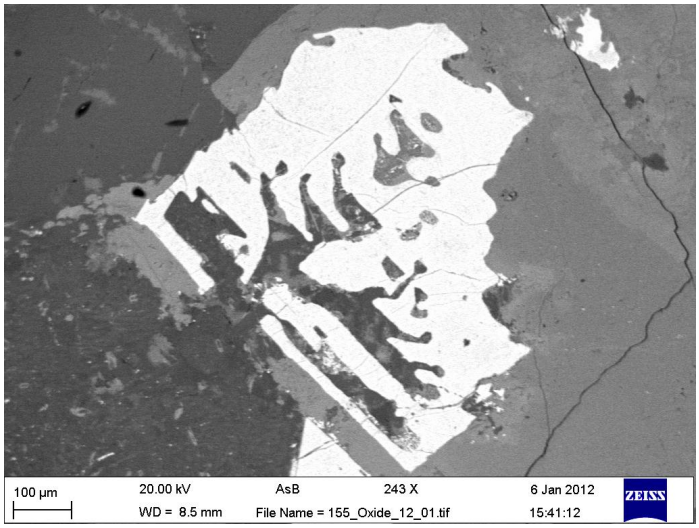

Figure 2.66: Electron back scatter image of a skeletal magnetite crystal in Sample 155.

Mineral chemistry was determined by SEM / EDAX (Appendix 2) and the results processed to give cations per formula unit. Plots for MnO, Al2O3, Cr2O3 and TiO2 vs FeO in Wt % are given in Figures 2.67 – 2.70. All iron has been recorded as FeO.

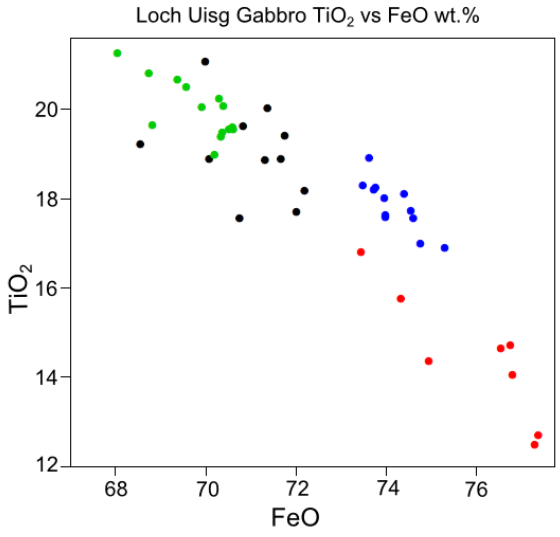

Figure 2.67: TiO_2 vs FeO (in wt.%) for oxides in the Loch Uisg Gabbro.

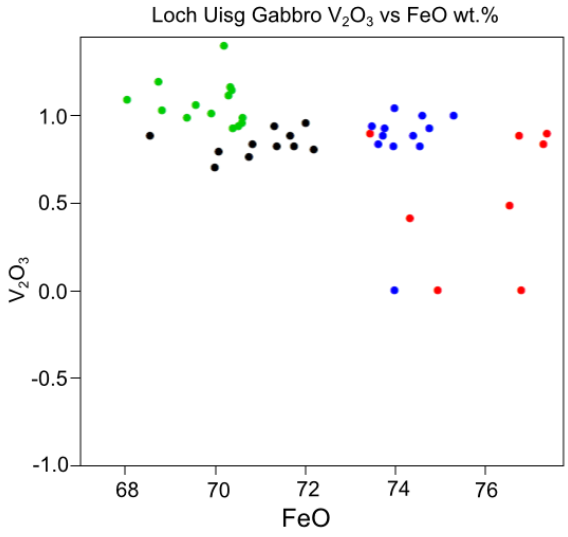

Figure 2.68: V_2O_3 vs FeO (in wt.%) for oxides in the Loch Uisg Gabbro.

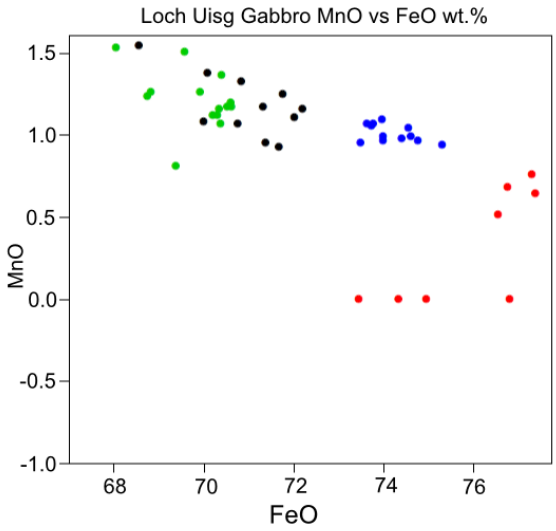

Figure 2.69: MnO vs FeO (in wt.%) for oxides in the Loch Uisg Gabbro.

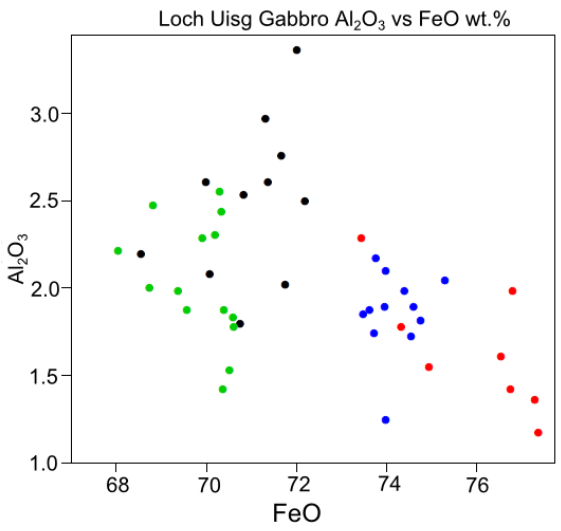

Figure 2.70: Al_2O_3 vs FeO (in wt.%) for oxides in the Loch Uisg Gabbro.

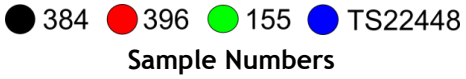

Figure 2.67 shows a clear negative correlation between TiO_2 and FeO, with the Glen Libidil sample (396) being the least Ti-rich. This particular trend is common in gabbroic rocks. Another negative correlation is seen in Figure 2.69 where MnO decreases with increasing FeO content and again,the Glen Libidil sample shows the least MnO wrt FeO. The plot in figure 2.68 for V_2O_3 shows a slight negative correlation with FeO content, although there is a considerable amount of scatter. The plot for Al_2O_3 (Figure 2.70) does not show any strongly discernible trend, due to the scatter of the data, other than perhaps a slight negative correlation.

2.7 Discussion

2.7.1 Form and shape of the intrusions

In the Mull Memoir (Bailey *et al*, 1924), a cross section is given (on page 231) showing the authors interpretation of the shape and extent of the gabbro and "granophyre" intrusions (Figure 2.71).

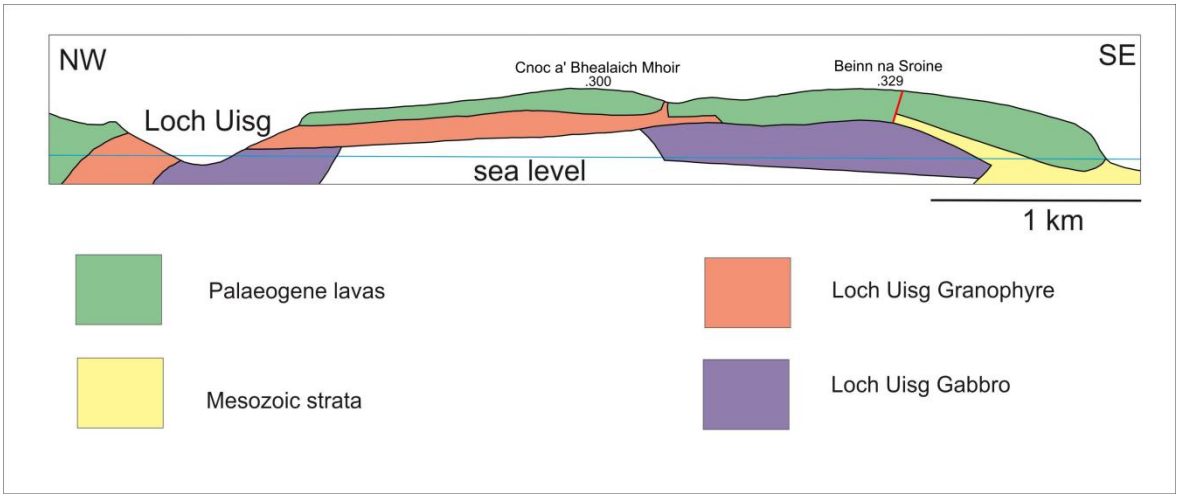

Figure 2.71: Schematic cross-section across the Loch Uisg gabbro and granophyre units (redrawn with extra detail after Bailey *et al*. 1924).

Field evidence gathered for this project supports the view that the granitic part of the intrusion is, largely, sill-like. Field observations of the contacts with the basalt lava country rock confirm that the northern contact is steeply dipping in a northerly direction and that the other contacts are horizontal to sub-horizontal. (Figures 2.4, 2.5 and 2.6). In the Memoir (Bailey *et al,* 1924), the authors noted that the granite dips steeply at its southern contact on Cnoc a'Chronain at [NM 623 232]. Examination of this contact in the field reveals that it is simply a localized steepening in the contact over a short distance near the top of the hill. The overall average dip of the contact with the basalt lava country rocks is sub-horizontal, as is the case elsewhere along the SE contact of the granite with the basalt lava country rocks.

However, it is less clear from the field evidence that the gabbro is also sheet-like in its form. In their paper on edifice and substrata deformation by intrusion on Mull, Mathieu & van Wyk de Vries (2009) propose intrusion of the gabbro and granite along a thrust plane at the base of the lava pile. The authors propose that the thrust was active due to the uplift and emplacement of the Centre1 intrusions However, as they state in the paper, although they provide evidence for thrust planes in the Loch Don area which lies to the north of the Loch Uisg area their evidence for these thrust planes in the Loch Buie and Glen Libidil areas is based on limited field observations (Figure 2.72).

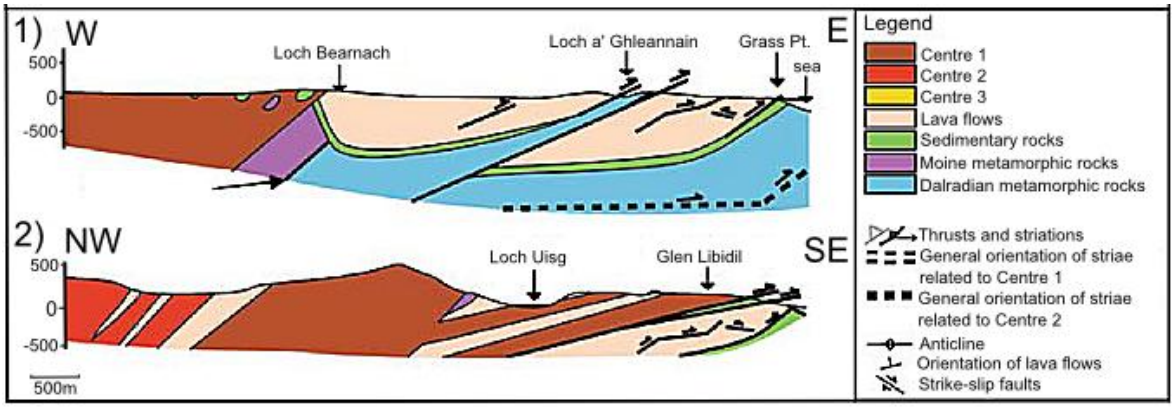

Figure 2.72: The lower diagram is a cross section of the Loch Uisg - Glen Libidil area showing the Centre 1 intrusions of SE Mull, (undifferentiated) and the structural geology of the country rocks into which they are intruded. (Mathieu & van Wyk de Vries 2009).

One of the biggest problems in assessing the extent and nature of the contact of the gabbro and the granite is the lack of good exposed sections. From the east end of Loch Uisg to the Laggan area, the contact with the granite can only be inferred, and the contact dip angle is difficult to estimate. However, at the Laggan Sands, the contact appears to dip steeply. If the intrusion were in the form of a gently dipping sheet, the gabbro / granite contact would extend much further in a southerly direction (towards the RHS of the view in Figure 2.73).

Figure 2.73: Panorama of the Laggan area showing the Loch Uisg Gabbro / Granite contact as a dashed yellow line. The occurrence of granite *in situ* at the points shown on the view demonstrates that the contact must be steeper than would be the case if it were a sill-like intrusion.

The steeper dip on the gabbro / granite contact implies that the intrusion is perhaps more dome-like in profile, as opposed to a sill. There are also implications for the order of intrusion if this is the case. If the gabbro is like a small pluton rather than a sill, then it may well be later than the granite. However, the steepening of the contact at Laggan Sands may just be a local effect and not representative of the whole intrusion. No contacts with the granite are visible on the northern edge of the gabbro, so the profile there

cannot be estimated with any accuracy. The gabbro is seen *in situ* at the east end of Loch Uisg on the shore, but the exact nature of the contact with the granite cannot be ascertained due to poor exposure.

In the Glen Libidil area, the exposure is also very poor and the form of the gabbro outcrop, which is approximately rectangular, is very difficult to assess. Figure 1.3 shows the Glen Libidil outcrop, as given on the BGS Map (BGS,1923, 1992). The NW contact of the gabbro closely follows the 150 m contour. The lowest extent of the SE contact occurs about the 40 m contour. Thus, the total thickness of the intrusion, as exposed, is about 110 m. At no point is the actual dip of the contact observable, so it is impossible to state with certainty the form and shape of the intrusion.

At both locations, South Loch Uisg to Laggan and in Glen Libidil, the gabbro appears to be at a lower topographical level than the granite. Nowhere is the gabbro seen above the level of the granite. This is in agreement with the work of the original Memoir authors (Bailey *et al*. 1924).

2.7.2 One gabbro or two?

The authors of the Mull Memoir (Bailey *et al*. 1924) state that "The unity of the Loch Uisg Gabbro" ... "is perhaps more open to question", but go on to justify a correlation with the following points:

1) The interval between the northern and southern exposure is only 1.5 km.
2) Both localities show extensive, and sufficiently similar, basic masses at the base of the Loch Uisg Granophyre.
3) There are no exposures of the base of the Loch Uisg Granophyre where dolerite, or gabbro, does not occur in mass.

The first point is debatable – proximity does not imply contiguity. The third point is confirmed by the field evidence from this study. The second point is perhaps the most important one and has been expanded upon by the study of the petrography and mineral chemistry.

There are both similarities and differences between the two outcrops of the Loch Uisg Gabbro. However, these may represent subtle changes laterally rather than evidence for two separate intrusions. The heterogeneity of the South Loch Uisg to Laggan outcrop of the gabbro is most marked at the Laggan Sands location, where distinctive features such as the localised layering and xenoliths are clearly seen. In addition there are grain size and rock colour differences over the extent of the outcrop. It varies from a leuco-gabbro at Laggan Sands to a dark grey dolerite at the east end of Loch Uisg. The Glen Libidil outcrop of the gabbro displays little variation apart from some localised layering, over its exposed outcrop. Grain size and colour appears to be uniform over the extent of the outcrop. The field evidence, therefore, suggests that the degree of heterogeneity of the Glen Libidil outcrop is less than that displayed by the South Loch Uisg – Laggan outcrop

Of the two outcrops, the Glen Libidil one appears to be more sill-like, intruded between the basalt and the granite. The morphology of the South Loch Uisg – Laggan outcrop is less clear. The steep dip of the contact at Laggan may only be a local effect. Elsewhere, the dip of the contact with the granite is not seen. It may also be sill-like, in which case, the two outcrops may well be two exposures of the same body of rock. This is the model that the Memoir authors used (Bailey *et al*. 1924). The paucity of samples (only one from Glen Libidil and only eight from the Laggan section of the other outcrop) means that only an indication of petrographic differences can be established. The mineral chemistry (discussed separately below) also hints at differences between the two outcrops, although the differences are not major. Due to the heterogeneity of the South Loch Uisg – Laggan outcrop, it is difficult to say with certainty, that the Glen Libidil outcrop does not simply represent a lateral extension of the former.

2.7.3 Field evidence

The two gabbro outcrops bear certain similarities in the field. Both are relatively fine grained; both locally show well developed poikilitic weathering. However, there are several significant differences:

The South Loch Uisg – Laggan outcrop is generally richer in plagioclase. Its appearance is typically paler than the Glen Libidil Gabbro, which is darker due to the larger percentage of clinopyroxene in the rock.

There is greater heterogeneity within the South Loch Uisg – Laggan outcrop. It varies from massive to layered, locally displaying large xenoliths with anorthosite rims, as confirmed by optical and SEM analysis. At Laggan shore it is quite pale. At the east end of the outcrop it is darker. The rock, near the contact with the granite shows evidence of hybridization. This is not seen in the field in Glen Libidil. The Glen Libidil outcrop is much more uniform. In a few places there are hints of layering but it is not as pronounced as in the South Loch Uisg - Laggan outcrop.

The two outcrops weather differently. The Glen Libidil outcrop has a much rougher appearance and the weathered-out pits have a rusty appearance (Figure 2.21). The South Loch Uisg – Laggan outcrop displays much smoother weathering surfaces (Figure 2.14). These particular weathering patterns are consistent across both outcrops of the gabbro. This difference in weathering is not unexpected considering the difference in the mineralogy, the Glen Libidil outcrop being richer in clinopyroxene. It could be argued that the weathering style at Laggan Sands is influenced by proximity of the outcrop to the sea. However, at the east end of Loch Uisg, well away from the influence of the sea, the weathering is similar. It is proposed that the maritime influence is minor.

2.7.4 Petrographic evidence

The most obvious difference between samples from the two outcrops when examined under the microscope is in the relative amounts of clinopyroxene and plagioclase. In addition, pseudomorphs after orthopyroxene are found in the Laggan samples but not in the Glen Libidil sample (Figure 2.47). Only one Glen Libidil sample was available for this study: a greater number of samples taken from a spread of locations over the outcrop would yield a better overall picture of the petrography. The Laggan samples in particular are very rich in plagioclase, which occurs as a cumulus phase. Clinopyroxene is of lesser importance but occurs as very distinctive oikocrysts (Figure 2.45). In the Glen

Libidil sample (no 396 in figures 2.49, 2.50 and 2.51) the ophitic texture is less well developed and the clinopyroxene is much more granular. There is also a difference in the amount of opaque oxide minerals. There are noticably fewer oxides in the Glen Libidil sample compared to any of the samples from the South Loch Uisg – Laggan outcrop. The clinopyroxene in the Glen Libidil gabbro may represent disturbed cumulus material, the crystals having been transported from elsewhere.

2.7.5 Mineral chemistry

The average values for plagioclase composition do not show any significant variation between the two outcrops of the Loch Uisg Gabbro. Ca-contents for rims for the Glen Libidil sample show lower values when compared to the Laggan samples, although this difference is based on only one sample. Clinopyroxene compositions show a more distinct spread. The Laggan samples are more Fe-rich compared to the Glen Libidil sample, which shows a cluster of values similar to the Loch Uisg Picrite Suite (Chapter 3). Figures 2.64 and 2.65 show this clearly.

Magnetite compositions show distinct trends, as is indicated in figures 2.67 to 2.70. For each element measured, (Ti,Al, Mn and V), the Glen Libidil sample displays a slightly greater negative correlation with increasing Fe compared with the samples from the other outcrop. Again, these data are based on only one Glen Libidil sample (396). From the limited data available it would appear that there is a small difference between the two outcrops. More samples would be required to establish whether these differences point to two separate intrusions rather than a local lateral variation within one contiguous body of rock. It is possible that, with an intrusion of this areal extent, there will be lateral variations in mineral chemistry and petrography. Although there are some minor differences in the mineral chemistry, these are not major and it seems likely, from the evidence gathered in this study that the two outcrops are one and the same intrusion. More extensive sampling of the Glen Libidil outcrop would be required to determine if the differences were significant.

2.7.6 Comparison with other Mull Gabbros

The Loch Uisg Gabbro differs in many respects from the other gabbros found in the MCC. It is finer grained, almost doleritic in places, compared with the Ben Buie Gabbro which is much coarser. It is also olivine-poor in comparison with the other gabbros. As has been shown (Figures 2.52, 2.53) the olivine is found as pseudomorphs. No fresh olivine was found at the level of the intrusion observed in the field. The clinopyroxene is typical of the Mull gabbros, occupying the augite field on the pyroxene quadrilateral (Di-He-En-Fs) (Figure 2.65). Plagioclase compositions are typical for Palaeogene gabbros, varying from bytownite to labradorite, with no extreme compositions recorded.

2.7.7 Relationship of Loch Uisg Gabbro to the Loch Uisg Granite

Both outcrops of the Loch Uisg Gabbro are overlain by the Loch Uisg Granite, but there are very few locations where the contact can actually be seen. It can be inferred to within a few metres, but actual visible contacts have proved elusive. What is observed, however, is a degree of gabbro / granite hybridisation at most of the localities where there is an inferred contact. As the authors of the Mull Memoir (Bailey *et* al. 1924) stated: *"If, eventually, it can be shown that the mixed zone at Loch Uisg has resulted from assimilation of granophyre by gabbro, its interest will be heightened ; but at present it is uncertain as to whether the gabbro was acidified by later granophyre, or vice versa."*

Pankhurst *et al*. (1978) state that the granite overlies a later gabbro, but offer no references or evidence for this statement.

The following points are worthy of note:

1) The gabbro always appears to be topographically lower than the granite.

2) Gabbro taken from close to the contact shows interstitial felsitic material. Samples much further from the contact do not.

3) Skeletal structure in magnetite is best developed in the gabbro samples closest to the contact zone. This is not seen in sample 333, which was taken at a distance of 300 metres from the contact.

4) No "mixed zone", as Bailey *et al*. (1924) refer to, was detected at the Glen Libidil outcrop. However, the exposure is particularly poor in this area.

5) Sieve textures are seen in many of the plagioclase crystals both from the granite and the gabbro (Figures 2.44, 2.57).

Although the results of this study have given greater insight into the mineral chemistry and the field relations of the Loch Uisg Granite-Gabbro Intrusion, certain key questions still remain unanswered:

1) The contact between the granite and the gabbro is elusive. There are specific locations, such as the hill-slope above Laggan Sands [NM624244] where excavation of the surface might reveal the contact. Similarly, there is a location in Glen Libidil where the granite/gabbro contact may also be determined with some excavation [NM 662 237].

2) Whether the granite came before the gabbro or *vice versa* is still not resolved. There is evidence which points to either scenario being the correct one. Quench textures found in both the gabbro and the granite make for ambiguity. More extensive sampling over both gabbro bodies and the granite would be required to provide more conclusive evidence. The current study has only looked at a limited range of samples, which although shedding more light on the subject, still leave unanswered questions.

2.7.8 Emplacement

Historically, the Loch Uisg Granite-Gabbro intrusions have been considered as part of the Centre 1 activity in the Mull Central Complex at approximately 58 Ma, based on the work of Mussett using the ^{40}Ar-^{39}Ar step-heating method (1986). However revised data, since then, using U/Pb dating, suggests that the majority

of the Mull igneous activity took place between 60.5 Ma for the Staffa Lava Formation and 58.5 Ma for the Centre 3 Loch Ba Felsite (Emeleus & Bell, 2005). Current data for the Loch Uisg Granite is not available, but these recent figures imply that it is closer to 60 Ma. Kerr *et al.* (1999) list the main Centre 1 intrusive sequence, starting with the oldest, as:

1) Glas Bheinn-Derrynaculen Granophyre;
2) Explosive acid volcanism (vents formed);
3) Loch Uisg Granite-Gabbro Intrusion;
4) Ben Buie layered gabbro.

These intrusions are shown on the following map (Figure 2.74).

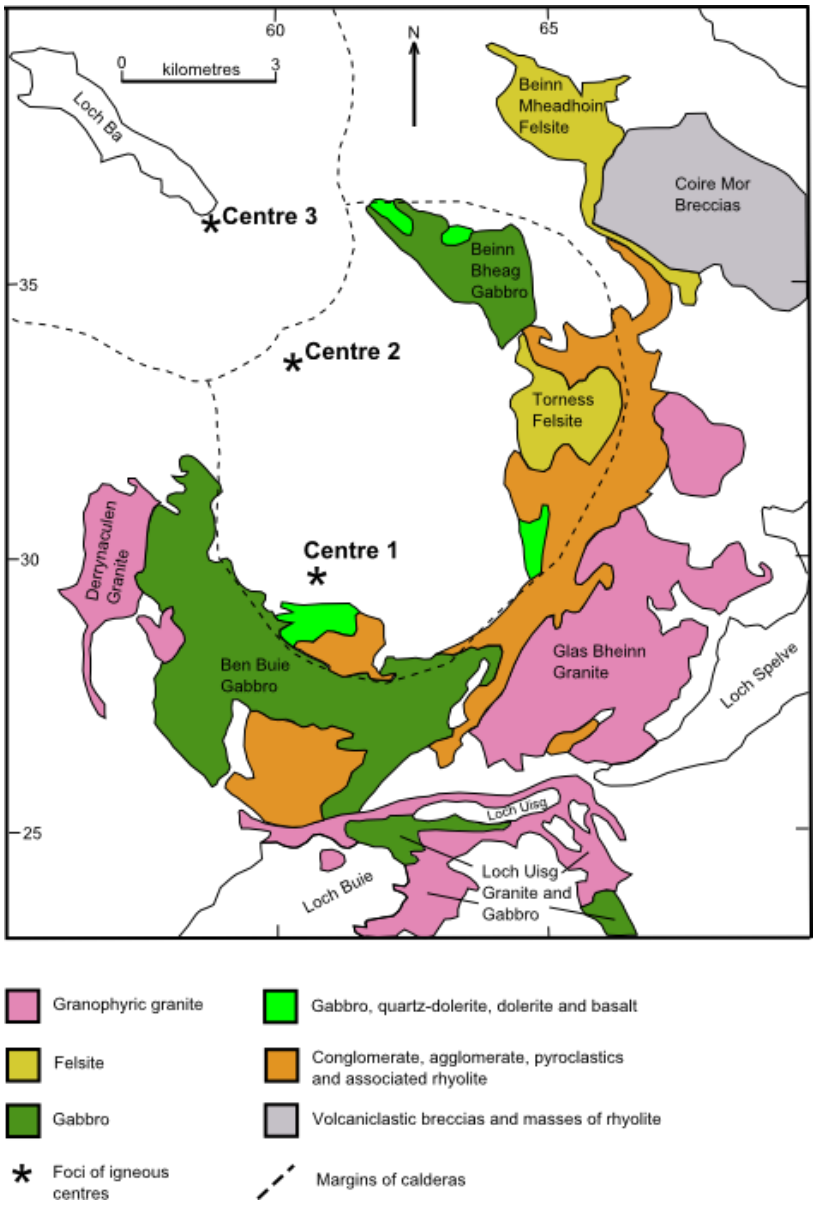

Figure 2.74: The main intrusions associated with Centre 1 of the MCC. Cone sheets ommited for clarity.

The final major intrusive phase in Centre 1 was the emplacement of the Ben Buie Gabbro. At a later stage, possibly after Centre 3 activity had ended, the area was further affected by magmatic activity which gave rise to the rocks of the LUPS. The LUPS intrusions, although only observed in the field cutting the Loch Uisg Granite, almost certainly cut through the Loch Uisg Gabbro below the surface.

The whole area was then subsequently cut by dykes of the Mull Dyke Swarm and cone-sheets of varying ages. Hydrothermal activity and the development of secondary minerals such as epidote and zeolite continued until the end of the igneous activity on Mull.

Chapter 3: The Loch Uisg Picrite Suite (LUPS)

3.1 Introduction

In addition to the Loch Uisg Gabbro-Granite Intrusion, there are other significant coarse-grained basic and ultrabasic intrusions, that crop out in the Laggan - Loch Uisg district and in Glen Libidil (see Chapter 2), especially towards the eastern end of Loch Uisg. These are conveniently split into two suites, based on their appearance in the field: (i) the Loch Uisg Picrite Suite (LUPS), described in this chapter; and, (ii) the Miscellaneous Minor Intrusions described in Chapter 4.

There are three intrusions that belong to the LUPS (Figures 3.1 and 3.2):

1) A thin intrusion to the west of Loch Uisg Cottage, referred to as the Loch Uisg Cottage Sheet (#4 in Figure 3.1);

2) A similar thin intrusion on the south side of Loch Uisg in the woods of Coille Sron nam Boc, referred to as the Coille Sron Nam Boc Sheet (#9 in Figure 3.1);

3) An irregular intrusion in the Gleann Beag – Creag nam Fitheach area, referred to here as the Gleann Beag Intrusion (Figure 3.2 and #10 in Figure 2.1).

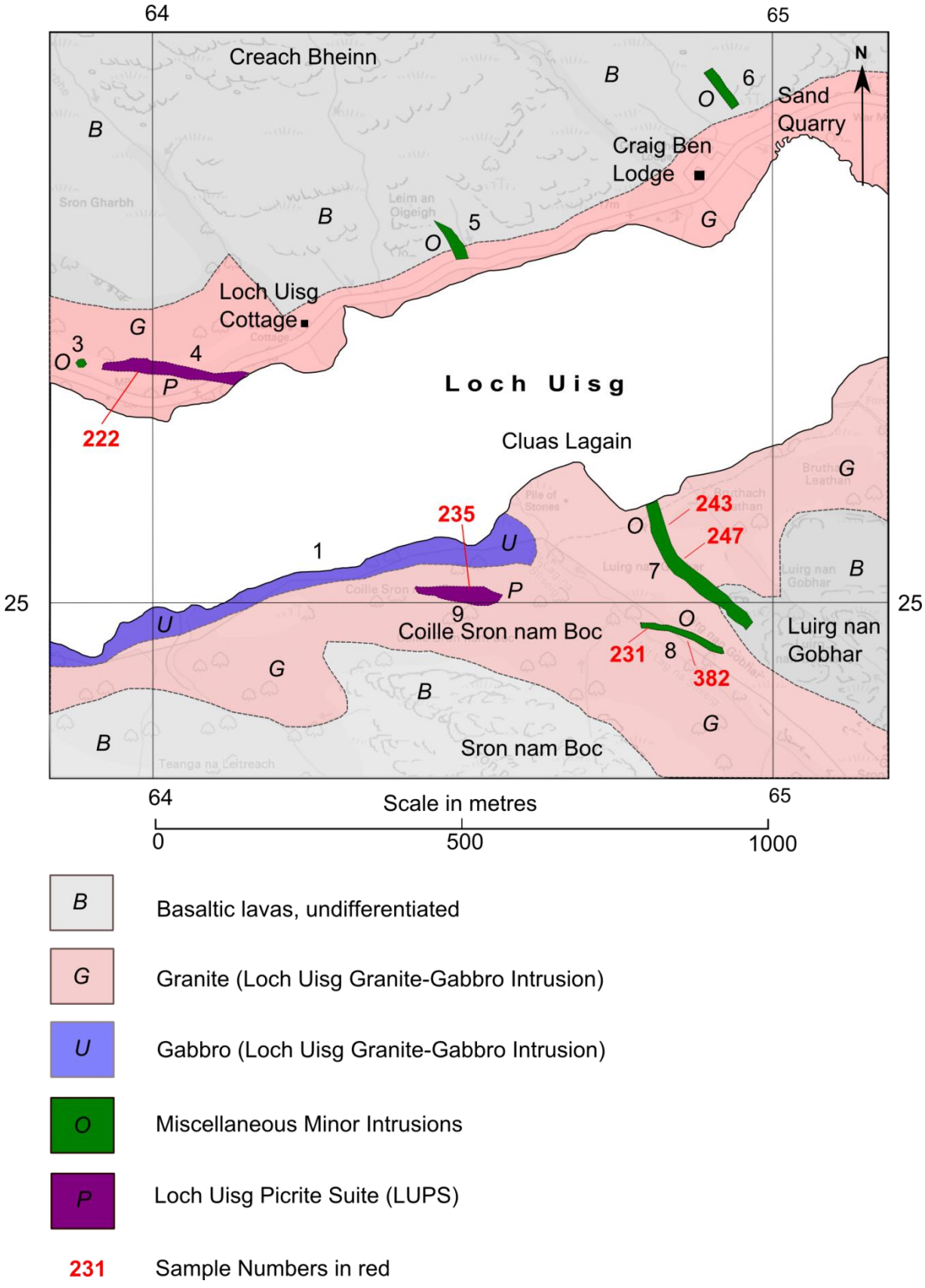

Figure 3.1: Gabbroic intrusions in the East Loch Uisg area. The Loch Uisg Cottage Sheet is indicated by the #4 on the map, above. The Coille Sron nam Boc Sheet is #9. LUPS samples collected for analysis indicated in red. (222 & 235).

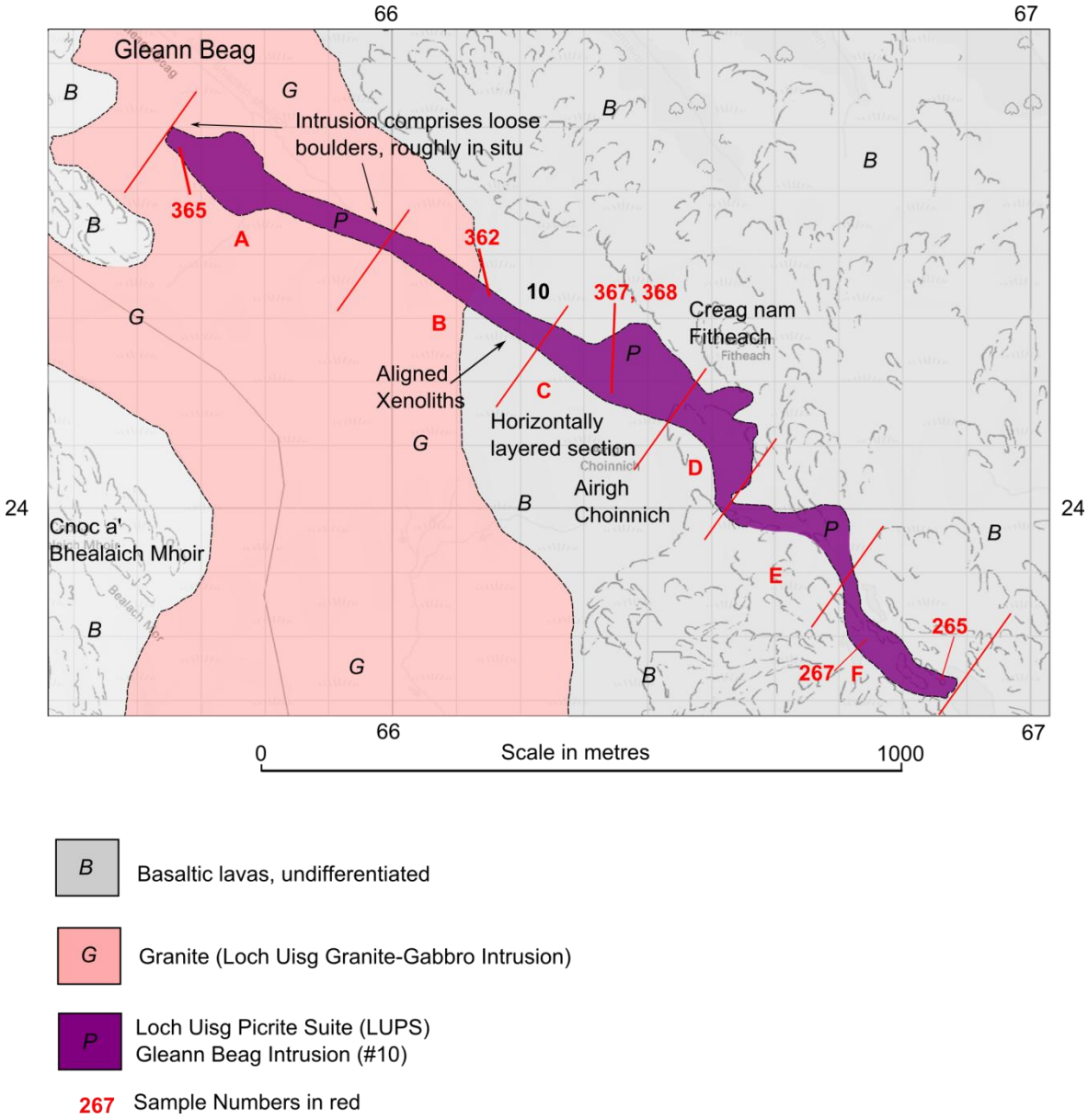

Figure 3.2: Location of the Gleann Beag Intrusion, #10, showing the main areas of interest. Samples taken for analysis indicated in red (265, 267, 362, 365, 367 & 368).

The three intrusions are almost identical in hand specimen. The only other ultramafic bodies in Mull to which they are similar are certain peridotites from the Ben Buie Gabbro:

1) They are all extremely fresh, showing very little hydrothermal alteration. In this respect they differ from both the Loch Uisg Gabbro (Chapter 2) and the "Miscellaneous Minor Intrusions" (Chapter 4);

2) They are very rich in olivine. Fresh olivine is clearly visible on broken surfaces as small honey-yellow crystals that weather to a rusty brown;

3) Layering is well developed in all three intrusions, especially in the Gleann Beag Intrusion;

4) All show distinctive pock-marked weathering, reminiscent of the peridotites of Rum and Skye (Emeleus & Bell, 2005).

The existing literature contains no direct reference to these intrusions (Bailey *et al*. 1924). The Loch Uisg Cottage Sheet is indicated on the BGS map (1923, 1992) as an "other gabbro", whereas the Coille Sron nam Boc Sheet is not shown. On the same map, the Gleann Beag Intrusion is portrayed as a member of the Mull Dyke Swarm, although it is clearly very different from most of the other dykes. The Memoir (Bailey *et al*. 1924) makes no mention of the LUPS intrusions: the Loch Uisg Cottage Sheet is not described, nor is the Coille Sron nam Boc Sheet, although it may have been originally mapped as part of the Loch Uisg Gabbro. None of the noteworthy features of the Gleann Beag Intrusion are mentioned in the Memoir.

3.2 The Coille Sron nam Boc Sheet

Coille Sron nam Boc is the natural woodland below the crags of Sron nam Boc on the south side of Loch Uisg (Figure 3.1). The intrusion comprises an east-west - trending outcrop, approx. 200 m long, is relatively coarse-grained, dominated by plagioclase and olivine, and is intruded into the Loch Uisg Granite.

This olivine-rich sheet is quite distinct from the relatively finer-grained Loch Uisg Gabbro, dominated by plagioclase and clinopyroxene, that crops out a few tens of metres to the north on the southern shore of Loch Uisg (Figure 3.1). No contacts are seen due to the thick vegetation, but the sheet may be up to 20 m thick.

Figure 3.3: The location of the main outcrop of the Coille Sron nam Boc Sheet at [NM 645 250], looking west from near the head of Loch Uisg. The intrusion is hidden by the trees growing on the lower slopes of Sron nam Boc.

No contacts with the country-rock are visible as the exposure in this area is relatively poor. The sheet appears to jut out from the hillside, between the 30m and 40 m contours, and although the morphology is not obvious, "sheet-like" best describes it. It is diffusely layered, with near horizontal layering. (Figures 3.4 and 3.5). No xenoliths have been observed.

Figure 3.4: General view of part of the Coille Sron nam Boc Sheet at [NM 645 250], showing the layering.

Figure 3.5: Close-up of the layered section of the Coille Sron nam Boc Sheet, depicted in Figure 3.4 showing horizontal to sub-horizontal layering and pock-marked weathering. Hammer for scale.

Epidote-rich hydrothermal veins are common in the Loch Uisg Gabbro, but this sheet, and the other LUPS bodies, is remarkably fresh and free of such alteration features. The absence of such veins implies a relatively late intrusion of the sheet, relative to the period of hydrothermal fluid circulation that occurred during the main intrusive phase. There is no evidence of felsic back veining of the granite into the sheet or offshoots of the sheet into the granite.

3.3 The Loch Uisg Cottage Sheet

This sheet is indicated on the BGS map (1924, 1992) as "eD: miscellaneous gabbros and dolerites" (#4 in Figure 2.1). Apart from this one reference to it, it does not appear to be mentioned elsewhere (specifically in Bailey *et al.* 1924). It forms a distinctive rocky exposure on the hill slope just above the main road east of Loch Uisg Cottage, at [NM 639 254] (Figure 3.6), and beside the road at [NM 641 253] (Figure 3.7). The total length of the exposure is *ca.* 250 m between the 30 m and 40 m contours.

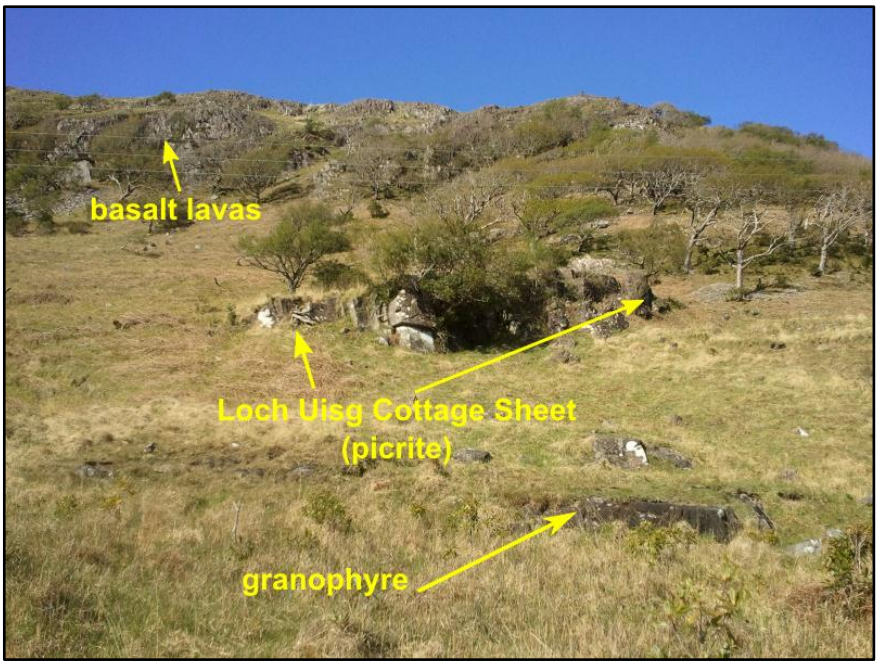

Figure 3.6: The Loch Uisg Cottage Sheet. Foreground is granite and cliffs are basaltic lavas.

Figure 3.7: Part of the Loch Uisg Cottage Sheet beside the road, looking westwards.

The exposure is sheet-like in appearance and, near its western end, has a gently inclined (*ca.* 5°), upper surface towards the north. This reflects the sheet's layering (Figure 3.8). Despite being undescribed in the literature, this unusual rock has been quarried here: there is clear evidence of "plug and feather" holes bored into it for splitting into blocks, although it is not currently known where the extracted material was used.

Figure 3.8: The Loch Uisg Cottage Sheet at [NM 639 254], showing layering and distinctive pock-marked weathering. Hammer for scale.

In terms of intrusive relationships, the sheet is not cut by any other intrusions and appears only to cut the granite. Actual contacts are inferred, not seen. No xenoliths were observed.

3.4 The Gleann Beag Intrusion (GBI)

The BGS map (1923, 1992) features a rather large irregular dyke, marked as a member of the Mull Dyke Swarm, and designated "M: Dolerite, Basalt or Teschenite" (#10 in Figures 2.1 and 3.2). In reality, it is a layered ultrabasic intrusion rich in fresh olivine. This intrusion is clearly later than both the basaltic lava country-rock and the Loch Uisg Granite, both of which it cuts (Figure 3.2). Exposure is relatively good for the most part, although contacts are seen in only a few places (Figures 3.17 - 3.20). The exposure of the intrusion, traceable for *ca.* 1.4 km, is discernible between [NM 656 245] at its NW end and [NM 668 237] at its SE end, where it terminates at a small (unnamed) loch. It is not seen on the other side of the loch.

The width of the intrusion is variable, from approximately 10 m in the NW section to 150 m at its widest point (between [NM 663 242 and [NM 664 242]). The width of the upper, SE section is *ca.* 30 m.

The Intrusion roughly follows the regional NW-SE trend that is characteristic of the Mull Dyke Swarm. No other dykes appear to cut it and it does not seem to be tectonically affected: there is no evidence of faults disrupting the intrusion. Figure 3.9 shows the Gleann Beag Intrusion viewed from near the hill, Creag nam Fitheach.

Figure 3.9: The sinuous, irregular form of the Gleann Beag Intrusion (GBI) seen from Creag nam Fitheach [NM 664 242], looking towards the NW.

3.5 Detailed description of Gleann Beag Intrusion

The intrusion is described below, under six sections, A to F, between the red lines in Figure 3.2, from NW to SE.

3.5.1 A: [NM 656 245] to [NM 660 244]. The lowest section is characterised by only a few *in situ* exposures, but also by many large blocks, up to 3m in size, suspected to be close to being *in situ*, which lie along the trend of the outcrop. The *in situ* material and the boulders all show strong, mostly horizontal, layering. Figure 3.10 illustrates the typical appearance of the *in situ* intrusion at its NW extremity.

The layering in the blocks is spectacular (Figures 3.11 to 3.14), including deformation or trough structures and erosive surfaces.

At [NM 659 244], a small felsitic dykelet cuts the picrite. This may represent back-veining of the granite into the intrusion (Figure 3.15).

3.5.2 B: [NM 660 244] to [NM 662 242]. Over the course of this section of the intrusion it is easy to follow, with good *in situ* exposures. The width is fairly consistent at around 10 m, although contacts with the country-rock are rarely seen. The exact shape and orientation of the intrusion is, locally, difficult to ascertain.

Within this section of the intrusion, the layering is not so pronounced and the rock has a more homogenous texture. One of the most distinctive features of this section is the development of pock marks, many of which are up to 10 cm across (Figure 3.16). There is also a zone of what appear to be xenoliths in this section at [NM 6692 2405] (Figure 3.17). Nowhere else along the course of the intrusion are xenoliths observed. However, microscopic examination of the mineralogy reveals that these are autoliths rather than xenoliths. The autoliths are dark grey, fine–grained and pod-shaped, up to 10 cm in length and 5 cm wide, occupying a zone approx 5 m long and are aligned with the intrusion margins. In thin section, they appear to be similar to the intrusion picrite but lack the large olivine crystals which are described in detail below.

3.5.3 C: [NM 662 242] to [NM 664 241]. In this section of the intrusion, immediately NW of where the intrusion opens out and becomes more irregular in shape, there is a very strongly layered zone (Figures 3.18 and 3.19). Most of the layering is approximately horizontal. The darker bands stand slightly proud of the surface and are finer grained than the coarser, more olivine-rich layers.

In places, *e.g.* at [NM 663 241], steep (50°) layering cuts across earlier low angle layers, but is itself overprinted by later low angle layering. Truncation of one layer by another is clearly seen, indicating a dynamic magmatic environment (Figures 3.20 and 3.21).

3.5.4 D: [NM 664 241] to [NM 665 240]. This part of the intrusion is characterised by its irregular shape, where it opens out into a wider section, before narrowing towards the SE (Figures 3.9 and 3.22). The layering present in Section C continues in this structurally higher section, although it is more subtle and more akin to the style of layering seen in the boulders at the NW end of the intrusion,

described in Section A, above. Several contacts with the country-rock basaltic lavas are visible in this section on both sides of the intrusion. On the NE and SW sides of the intrusion, near the cliff of Creag nam Fitheach, the contacts are relatively obvious (Figures 3.23 and 3.24, respectively).

Near the structurally highest point of this section, the contacts are also seen. On the NE side, at [NM 669 240] (Figure 3.21), the intrusion is clearly finer-grained adjacent to the country-rock basaltic lavas. On the other side of the intrusion, the SW contact is also well exposed (Figure 3.22). Both contacts dip to the NE at a similar angle of *ca.* 45°, implying that the intrusion is a steeply inclined sheet. Between the two contacts, the picrite has a sub-horizontal layering and is characterised by its pock-marked appearance, with deep curved cracks. The layering is therefore, not parallel to the contacts in this part of the intrusion where the contacts and morphology of the intrusion are clearly observable. In several places, irregular grey veins or dykelets up to 5 cm wide, cut the picrite. These are gabbroic in character displaying very fresh plagioclase and clinopyroxene (Figure 3.29).

3.5.5 E: [NM 665 240] to [NM 667 238]. Here, the intrusion is narrower and has a more typical dyke-like appearance. The pock marking of the weathered surface is particularly obvious (Figure 3.27). Layering is less obvious and the rock is much more homogenous in appearance. No contacts are seen.

3.5.6 F: [NM 667 238] to [NM 668 237]. The most south-easterly section of the intrusion runs to a small unnamed lochan at [NM 668 237] where it appears to terminate. The picrite is unlayered, appears to be fairly homogenous, and pock-marked surfaces are rare. The most noticeable feature is the presence of grooves in the rock running parallel to the margins (Figure 3.28). No contacts are seen.

Figure 3.10: The most north westerly exposure of the intrusion at [NM 656 245], showing weathered surface pock marks. [Section A].

Figure 3.11: One of the loose blocks lying along the line of the NW section of the intrusion at [NM 657 244], showing very pronounced layering [Section A]

Figure 3.12: Prominent curving layers cutting across folds in the GBI at [NM 659 244]. [Section A].

Figure 3.13: Close up detail of layers cutting folds shown in Figure 3.12. [NM 659 244]. [Section A].

Figure 3.14: Pronounced layering in the GBI, here dipping at a shallow angle towards the intrusion centre at [NM 663 242]. [Section A].

Figure 3.15: Felsitic dykelet cutting across the GBI at [NM 659 244].[Section A].

Figure 3.16: *In situ* intrusion with deep curving cracks and pock marks clearly visible at [NM 661 244]. [Section B].

Figure 3.17: Aligned picritic autoliths in the Gleann Beag Intrusion at [NM 662 242]. [Section B].

Figure 3.18: Pronounced layering in the Gleann Beag Intrusion at [NM 663 242]. [Section C].

Figure 3.19: Prominent layers standing proud of the rock surface at [NM 663 242]. [Section C].

Figure 3.20: Cross cutting layers in the GBI. Low angle layers truncated by overlying layers at [NM 663 242]. [Section C].

Figure 3.21: Erosion surface: sub-horizontal layers truncated by 40° dipping layers at [NM 663 241]. [Section C].

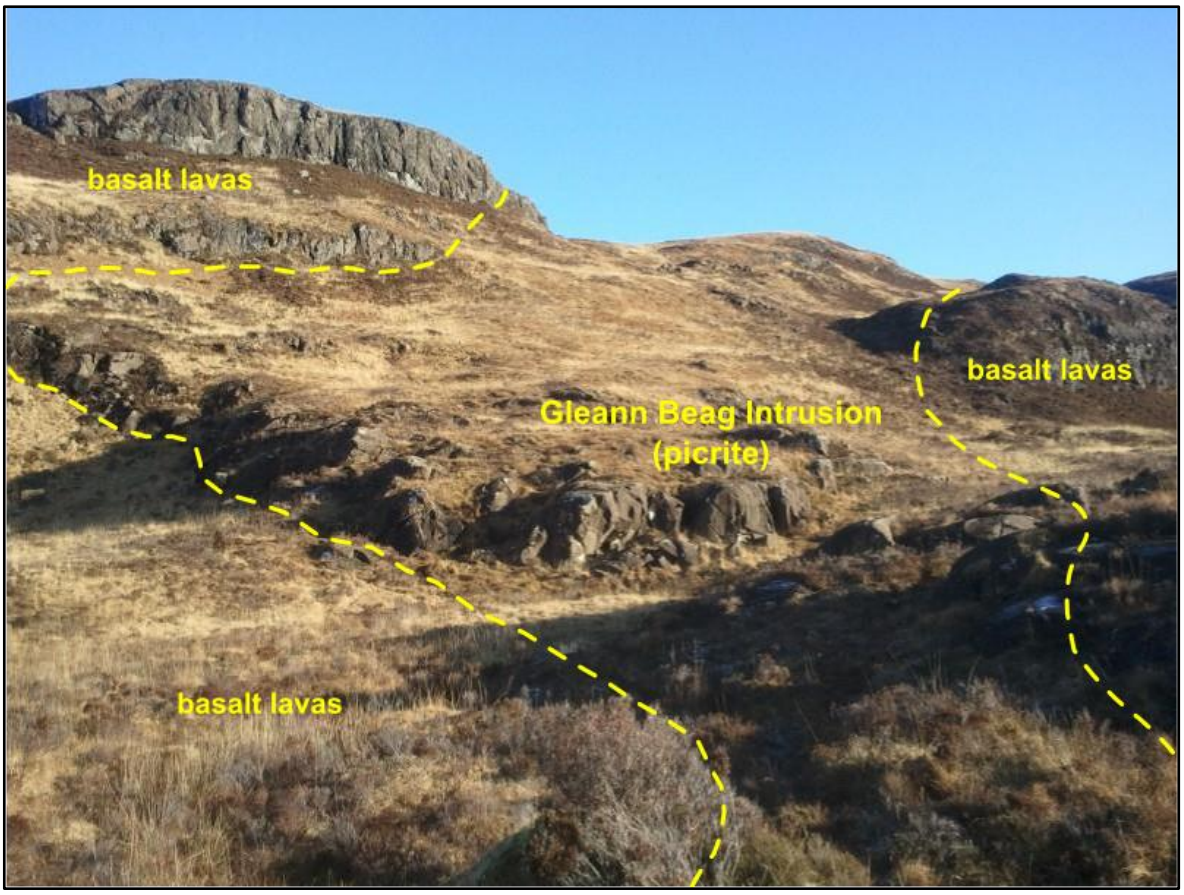

Figure 3.22: Trace of the Gleann Beag Intrusion in section D looking towards the SE. View is from [NM 663 242], the strongly layered section, looking up the hill slope in a SE direction.

Figure 3.23: Contact of GBI and basalt lava country rock. Dip of contact is *ca*. 60º due north at [NM 665 241]. [Section D].

Figure 3.24: Contact of GBI and basalt lava country rock. Dip of contact is 50º; direction of dip is 80º at [NM 665 240]. [Section D].

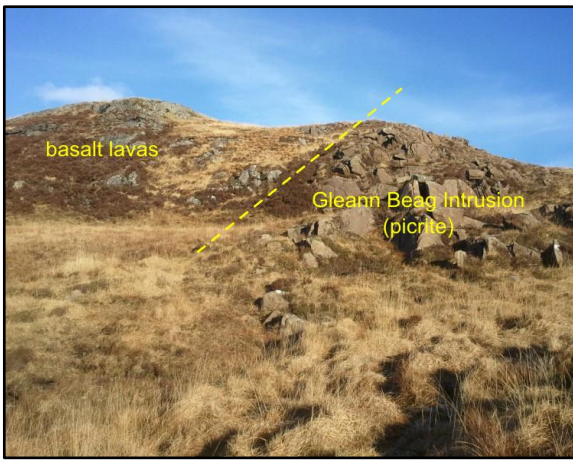

Figure 3.25: Contact between the GBI and the country-rock basaltic lavas. Dip is 40º - 50º; direction of dip is 45º at [NM 666 240].[Section D].

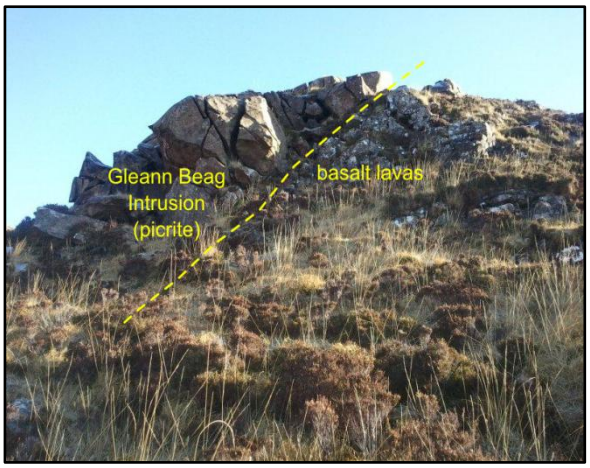

Figure 3.26: Contact of GBI and country-rock basaltic lavas on the SW side of the intrusion. Dip is 55º; direction of dip is 45º at [NM 665 239]. [Section D].

Figure 3.27: GBI showing typical weathered appearance of the upper section at [NM 667 238]. [Section E].

Figure 3.28: Upper part of GBI near its SE termination showing distinctive grooves in the rock at [NM 668 237]. [Section F].

3.6 Post-intrusion events

There is no evidence of major dykes or sheets cutting the LUPS intrusions, apart from the veins / dykelets described in Section D (Figure 3.29). The Gleann Beag Intrusion runs along the same general line as the Mull Dyke Swarm (NW – SE), thereby minimizing the likelihood of being cut by one of these dykes. None of the suites of cone-sheets which cut many of the intrusions of the Mull Central Complex appears to have intruded the GBI.

Figure 3.29: Small veins / dykelets cutting the Gleann Beag Intrusion at [NM 665 240]. [Section D].

3.7 Summary of the layering

The layering in the LUPS rocks is an extremely obvious and important feature of these intrusions, especially the Gleann Beag Intrusion in which it is most pronounced. It can be summarized thus:

1) The layering is ubiquitous. It is found in both the sheets and the Glean Beag Intrusion (GBI).

2) The layering in the sheets is similar in many respects to that found in most of the GBI, being low angle, on a 1 cm – 0.5 m scale.

3) Most of the layering is sub-horizontal to horizontal. Where the layering is inclined, on the GBI, the dip, which varies considerably, is generally along the line of the intrusion, in a SE – NW direction.

4) Layering is found over the entire length of the GBI, from the lowest topographic level in the NW to the highest level in the SE.

5) The layering is very obvious on weathered surfaces, where the finer grained layers appear darker and stand proud of the rock surface. On fresh surfaces, the layering is less obvious.

6) Steep layering, up to 40° is conspicuous at several points along the GBI where erosion and truncation of layers is visible. Folding, curved layers and trough structures can be seen and deformation of these has occurred.

These features are further covered in Section 3.9 (Discussion of magmatic conditions) at the end of this chapter.

3.8 Loch Uisg Picrite Suite petrography and mineral chemistry

3.8.1 Introduction

The three LUPS intrusions, the Loch Uisg Cottage Sheet, the Coille Sron nam Boc Sheet and the Gleann Beag Intrusion are similar in many respects. Key features are picritic compositions with abundant fresh olivine, sub-horizontal layering, (although the Gleann Beag Intrusion also has layering inclined at up to 40º) and near-identical lithologies at outcrop, hand-specimen and thin-section scales.

Despite the presence of mineral layering, there does not appear to be any systematic variation in petrology or mineral chemistry, either within any given intrusion or between the intrusions. The outcrops of the two sheets (Loch Uisg Cottage and Coille Sron nam Boc) are relatively small, up to 250 m in length and no more than 10 m thick. Both are uniformly olivine-rich (picritic) in character over their entire outcrop. The Gleann Beag Intrusion, in contrast, has a substantial outcrop length of *ca*. 1.4 km (see Figures 3.2, 3.11 – 3.21), with diverse layering styles.

3.8.2 Definition of the term *picrite*

The term *picrite* as a rock type is used in several older papers (e.g. Harker 1904, Walker 1929) to loosely describe a rock that is merely rich in olivine. Drever and Johnston (1958) discuss the use of the term *picrite* in their paper on minor intrusions in Skye. They use the definition *picrite* to describe a rock that contains between 25% and 60% olivine. Similarly, 15% to 25% is “olivine-rich” and values above 60% are considered rare.

The BGS definition of *picrite* (Gillespie and Styles, 1999), uses whole rock data where MgO > 18 wt.%. However, the IUGS reclassification of high-Mg and picritic volcanic rocks sets the limit at MgO > 12 wt.% (Le Bas, 2000). Whole rock analyses were not available for the rocks in this study; however, based on modal percentages, assuming average MgO in olivine of 47 wt.% (Appendix 1) and 45 %

average modal abundance, whole rock MgO would give 21 wt.% MgO (ignoring Mg in other phases such as spinel and clinopyroxene). On the same basis, rocks with higher contents of more Mg-rich olivine would contain 25 wt.% MgO, or more. These rocks clearly satisfy the conditions for the definition *picrite*. It is important to note, however, that these values do not imply that these figures represent melt compositions: all these rocks are likely to be enriched in cumulus olivine (see below).

Based on these percentages, the three intrusions which comprise the LUPS can be accurately classified as *picrites*, both according to the historical definition and the modern classification.

3.8.3 Previously described picritic minor intrusions in the Palaeogene lava fields and central complexes of the Inner Hebrides

Having defined the LUPS rocks as a picritic suite, several previously described picritic minor intrusions in the BPIP are introduced here and briefly described, thereby allowing comparison with the LUPS in terms of intrusion morphology, petrography and mineral chemistry, the data for which is given in detail below.

Picritic minor intrusions have been recorded from several localities throughout the British Palaeogene Igneous Province (BPIP), especially on the Isle of Skye. (Harker 1904; Walker 1929, Drever and Johnston 1957, 1958; Gibb 1968, 1970; Donaldson 1975; Parslow 1976). However, ultrabasic and picritic rocks, the former term used in earlier literature, are barely mentioned in the Mull Memoir (Bailey *et al.* 1924). The picritic intrusions described in this study are classified in the Memoir and the associated map either as *Miscellaneous Minor Intrusions* or included with the members of the Mull Dyke Swarm. In contrast with many of these previously described intrusions, the LUPS intrusions are entirely picritic, without associated evolved components (e.g. the so-called crinanites of the North Skye - Shiant Isles Sill Complex (Walker 1929; Gibson 1990)). The picritic minor intrusions that share compositional affinities with the LUPS include dykes and sheets intruded into the Cuillin Centre of the Skye Central Complex described in detail by Drever and Johnston (1957, 1958) and the dykes in Rum described by Upton *et al.*(2002).

In addition to the earlier studies, more recent work over the past 50 years includes:

Wyllie and Drever (1962): The authors examined the petrology of a 2 m thick picritic sill on the island of Soay, near Skye. The distribution, size, quantity and habit of the olivines are described in detail. The authors proposed that this material, based on the olivine composition, was derived from a deep ultrabasic source rather than being the ultrabasic facies of a typical Palaeogene plutonic mass, supporting the conclusions of Drever and Johnston (1958).

Gibb (1968): In this paper, the author studied a suite of dykes referred to as the "Ben Cleat" type, after the type locality on the Strathaird Peninsula, SE of the Cuillin Hills in the Isle of Skye. These dykes show variations in olivine content across the width of the intrusions. This distribution is attributed to flow differentiation of a magmatic suspension of crystals during emplacement.

Donaldson (1975): Several dykes in NW Skye were studied in this work. These dykes are rich in megacrysts of Ca-rich plagioclase and olivine, together with plagioclase-rich xenoliths in a groundmass of high-Ca olivine-tholeiite. The dykes are interpreted as volcanic plugs; feeder systems for nearby lava flows which bear considerable compositional similarities.

Parslow (1976): This study concerns an unusual coarse-grained layered picritic dyke at Suisnish in the Strath district of Skye. The section of the dyke that is visible on the shore has up to 20 gently dipping rhythmically layered units each comprising an olivine rich layer and an overlying plagioclase rich layer. Figure 3.30.

Figure 3.30: The Suisnish Dyke in Skye showing the layering in the picrite. Hammer for scale.

The chilled margin and contact metamorphism of the country rock show that it is an *in situ* dyke and not part of a faulted block. The presence of layering and coarse grain size in what should be a rapidly cooled body of rock raises several questions.

Andersen *et al*. (2002): In a paper which is concerned with Platinum-group elements within the Ben Buie Gabbro, the authors state that "only the Ben Buie intrusion contains ultramfic lithologies". The paper describes small bodies of troctolite and peridotite within the main gabbroic intrusion and that it is within these bodies that PGE-rich chromitite layers occur.

Prout et al. (2002): In a paper which deals with PGE within the Ben Buie Gabbro, the authors describe the intrusion in detail. The ultramafic bodies (troctolite and peridotite) are described as small and laterally discontinuous bodies, up to 100 m in length, of olivine-rich cumulates. An extensive cross-section through the intrusion shows the variation with height of the olivine and plagioclase mineral chemistry.

Upton *et al*. (2002): The authors studied three picritic dykes from Rum, one of which (M9) shows "very primitive characteristics" in that it has olivines showing very high Mg contents (Fo_{93}) and very aluminous spinels. A highly magnesian magma (18 – 20 wt.% MgO) must have been involved in the production of such a Forsterite-rich cumulus phase. Intrusions with this olivine composition are extremely rare in Phanerozoic magmatic rocks. Similar rocks are found in Namibia (Thompson & Gibson 2000), but the authors consider the M9 dyke to be unique within the BPIP. A small fraction melt from a depleted mantle source is proposed as the source of the magma, caused by unusual conditions (possibly movement of the Long Loch Fault that cuts the layered peridotites on Rum), affecting mantle lithosphere.

Holness *et al*. (2012): The authors examined several peridotite plugs associated with the Rum Igneous Complex. It is proposed by the authors that these ultramafic bodies represent conduits through which olivine-rich magma flowed to surface levels. The morphology of the plugs varies from circular to elongate,

inclined at various angles to the vertical. Modal olivine content is seen to increase from the margins to the centres of the intrusion. This is attributed by the authors to overgrowth and mechanical re-arrangement. Olivine from the plugs gives values up to Fo_{89}. The authors suggest that, although the plugs are less forsteritic than the dykes described by Upton *et al*. (2002), they may well have contained a similar type of magma. A magma temperature of 1400° C is proposed.

3.8.4 Sampling of the LUPS rocks

Eight representative samples of the LUPS rocks were sectioned (polished thin sections) for both optical and SEM analysis. One sample was taken from each of the sheets and six samples were taken from the Gleann Beag Intrusion (GBI). Their locations are shown on the maps in Figures 3.1 and 3.2.

Sample	Location	Grid Ref.
222	Loch Uisg Cottage Sheet, above the road	[NM 639 254
235	Coille Sron nam Boc Sheet, south shore of Loch Uisg	[NM 645 250]
265	Gleann Beag Intrusion, (GBI) SE extremity of the intrusion	[NM 668 237]
267	GBI, small cliff near SE end of the intrusion	[NM 668 238]
362	GBI, middle section of the intrusion	[NM 661 244]
365	GBI, NW extremity of the intrusion	[NM 656 245]
367	GBI, strongly layered section, coarse grained layer	[NM 663 242]
368	GBI, strongly layered section, fine grained layer	[NM 663 242]

Table 3.1: The LUPS samples chosen for analysis.

Samples of all three intrusions look very similar in hand-specimen. On a macroscopic scale, weathered surfaces are easily recognized by the presence of small near-circular depressions caused by the differential weathering and erosion of material comprising macro-poikilitic developments of clinopyroxene

and plagioclase (Figure 3.31) (see below). Weathered surfaces are typically pale rusty brown and pitted where olivines have been substantially oxidized. By comparison, fresh broken surfaces are dark grey.

Figure 3.31: LUPS picrite showing the typical weathering pattern (GBI at [NM 6697 2399]).

Under the hand lens, on fresh surfaces, green to honey-coloured olivines are abundant in a groundmass of near-black clinopyroxene and very pale brown plagioclase. Some of the larger olivines are up to 1 cm across. Layering is not usually obvious at the hand specimen scale. Samples taken from the most strongly layered part of the Gleann Beag Intrusion (Figures 3.18 to 3.21) show obvious crystal size variations - the more prominent bands, which stand slightly proud of the rock face, are finer grained. Overall, the rocks look very fresh, with remarkably little hydrothermal alteration visible. This is in stark contrast with other intrusions associated with Centre 1, where hydrothermal alteration is significant. Minerals such as epidote, found in the Loch Uisg Gabbro (Chapter 2) and the "Miscellaneous Minor Intrusions" (Chapter 4) were not recorded. Chromite is an abundant mineral in thin section, but no chromitite seams were noted at outcrop.

3.8.5 Petrography

The eight thin sections used for optical and SEM analysis are shown in figures 3.32 to 3.38. In thin section the samples from the two sheets and the Gleann Beag Intrusion look very similar. Two populations of olivine are present in all of the samples, referred to here as "large" and "small":

1) Large: Blocky, commonly euhedral olvines, interpreted as cumulus grains, either phenocrysts or xenocrysts). Many of these form glomerocrysts, up to 1 cm in size;

2) Small: Smaller, granular, rounded groundmass olivines and skeletal olivines, up to 2 mm in size, probably grown in situ during emplacement.

The groundmass also contains common clinopyroxene, rare orthopyroxene, plagioclase and Cr-spinel. In contrast to all the other minor, and most of the large, intrusions in SE Mull, the rocks are extremely fresh.

The polished thin sections used for SEM analysis were scanned between two sheets of polarizing material. The images are presented below (Figures 3.32 to 3.39).

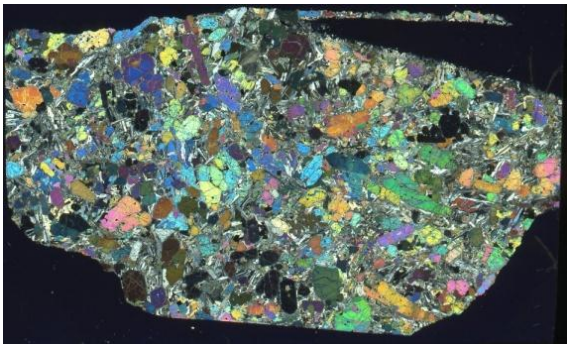

Figure 3.32: Thin section view (XPL) of sample 222 from the Loch Uisg Cottage sheet at [NM 639 254] showing abundant large blocky and euhedral olivines in a groundmass of plagioclase, clinopyroxene and small granular and skeletal olivines. Rock slice width: 42 mm.

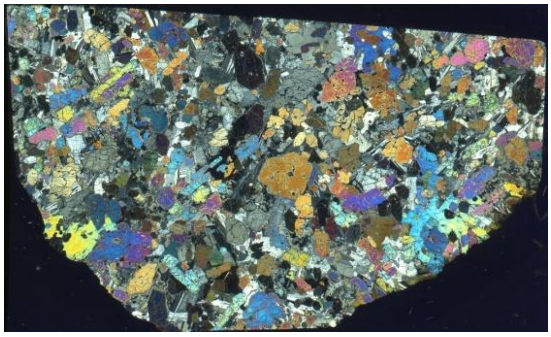

Figure 3.33: Thin section view (XPL) of sample 235 from the Coille Sron nam Boc Sheet at [NM 645 250] showing abundant large blocky and euhedral olivines in a groundmass of plagioclase, clinopyroxene and small olivines, some of which show slight alteration. Rock slice width: 45 mm.

Figure 3.34: Thin section view (XPL) of sample 265 from the GBI at [NM 668 237] showing abundant large blocky and euhedral olivines in a groundmass of plagioclase, clinopyroxene and small granular and skeletal olivines. Rock slice width: 40 mm.

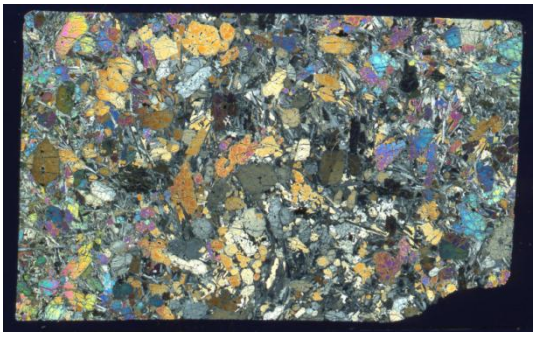

Figure 3.35: Thin section view (XPL) of sample 267 from the GBI at [NM 668 238] showing large, commonly euhedral olivines in a groundmass of plagioclase, clinopyroxene and small olivines. Rock slice width: 40 mm.

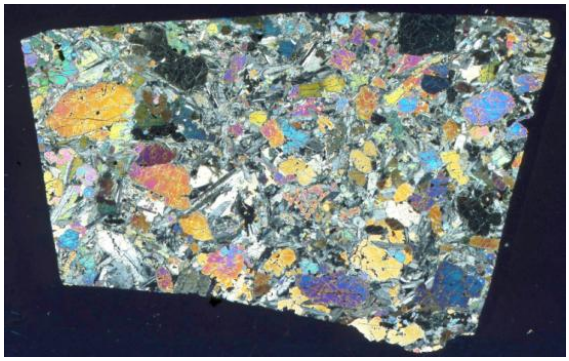

Figure 3.36: Thin section view (XPL) of sample 362 from the GBI at [NM 661 244] showing abundant large olivine phenocrysts in a groundmass of small olivine, ophitic plagioclase, clinopyroxene and Cr-spinel. Rock slice width: 35 mm.

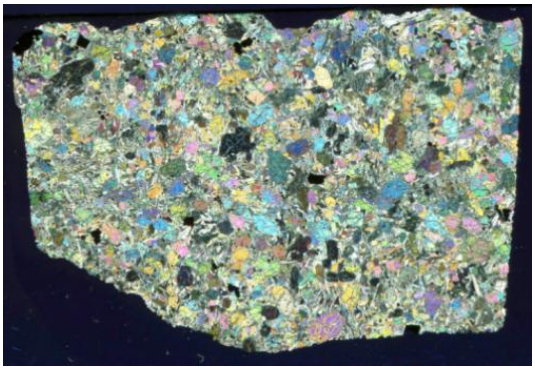

Figure 3.37: Thin section view (XPL) of sample 365 from the GBI at [NM 656 245] showing large euhedral and blocky crystals of olivine in a finer groundmass. Rock slice width: 35 mm.

Figure 3.38: Thin section view (XPL) of sample 367 from the GBI at [NM 663 242] illustrating the coarse, lighter coloured part of the intrusion from the strongly layered section. Rock slice width: 40 mm.

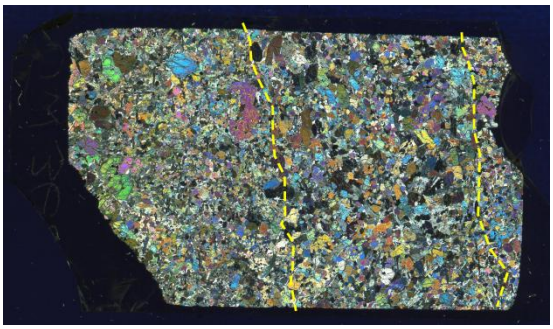

Figure 3.39: Thin section view (XPL) of sample 368 from the GBI at [NM 663 242] showing one of the darker bands in the intrusion. Much finer grained than sample 367. Large euhedral phenocrysts are seen in a much finer groundmass. Section between the dashed yellow lines is coarser than the rest of the slide. Rock slice width: 40 mm.

Sample 365 (Figure 3.37) appears slightly washed out due to the thickness of the section being slightly less than the standard 30 microns. The individual mineral phases are now described in detail in subsequent sections.

3.8.6 Mineral phases

3.8.6.1 Olivine

The rocks are extremely rich in olivine, up to 40% modal, both as phenocrysts, and as a groundmass mineral where it occurs as smaller equant crystals and as skeletal crystals. The olivine is remarkably fresh, compared with most olivine-

gabbros in SE Mull. Figures 3.39 to 3.42 show examples of the typical appearance of the olivine.

i) Large: cumulus olivines

The large olivines, which can be up to 1 cm in length, display either an irregular blocky form or a euhedral habit, the latter displaying the classic textbook shape, relief and curving cracks that are so obvious under the microscope (Figures 3.40 and 3.42). Glomerocrysts composed of large olivines are common. Alteration along the cracks is commonly observed, but the crystals are otherwise generally very fresh. The olivines enclose Cr-spinels, either as clusters or as individual crystals (Figure 3.40, 3.44). Rarely, strain lamellae can be seen in some of the blocky and euhedral olivines (Figure 3.42). The glomerocrysts and strain lamellae are reminiscent of the olivines seen in some Hawaiian magmas (Vinet & Higgins, 2010).

ii) Small: groundmass olivines (granular)

These tend to be small, equant, rounded crystals, up to 1mm in length, within the groundmass. Several samples show reaction rims. Together with commonly ophitic-texture plagioclase and clinopyroxene, they form the major part of the groundmass in most of the samples (Figure 3.43). Enclosed Cr-spinels are rare.

iii) Small: groundmass olivines (skeletal)

Skeletal olivine is found in the groundmass of many of the samples, the best examples being in the Loch Uisg Cottage Sheet (Figure 3.41). The crystals tend to be elongated with an embayed appearance. Alteration along the rims is common but not extensive.

iv) Zoning in the olivines

None of these olivine types displays zoning that can be readily detected optically, unlike the plagioclase which can be conspicuously zoned. However, normal zoning is readily detectable by SEM analysis, where the rims are considerably more Fe-rich than the cores. The rims of the large olivines have a similar Mg content to the smaller, granular and skeletal olivines. The cores of the large olivines however are much richer in Mg than any of the smaller olivines. This suggests that the large olivines grew from a much hotter, Mg rich

magma and were transported by a less Mg-rich liquid which crystallized to give the smaller olivines during emplacement.

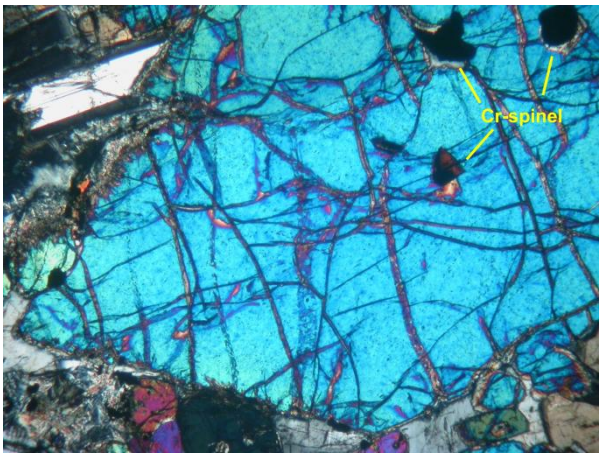

Figure 3.40: Thin section view (XPL) of sample 222 from the Loch Uisg Cottage sheet at [NM 639 254] showing a large euhedral olivine. Slight alteration to the rim.Several Cr-spinels are enclosed within the phenocryst. FoV: 2 mm.

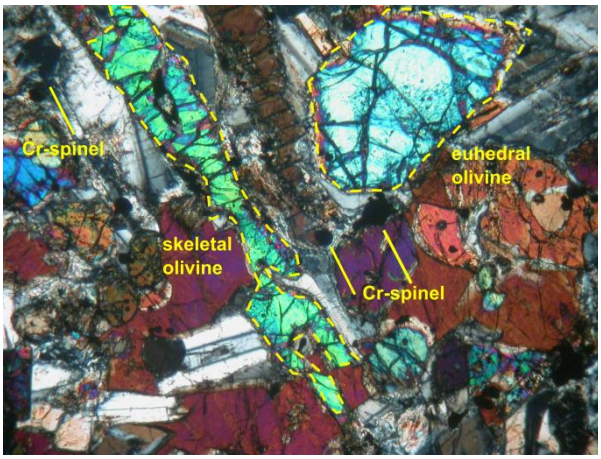

Figure 3.41: Thin section view (XPL) of sample 222 from the Loch Uisg Cottage sheet at [NM 639 254] showing long skeletal olivine and a smaller euhedral groundmass olivine (indicated by yellow dashed lines). Alteration on the rims is visible. Several small Cr-spinels are also indicated. FoV: 2 mm.

Figure 3.42: Thin section view (XPL) of sample 267 (GBI) at [NM 668 238] showing a large, very fresh, strained euhedral olivine crystal in a plagioclase and clinopyroxene- dominated groundmass. FoV: 2 mm.

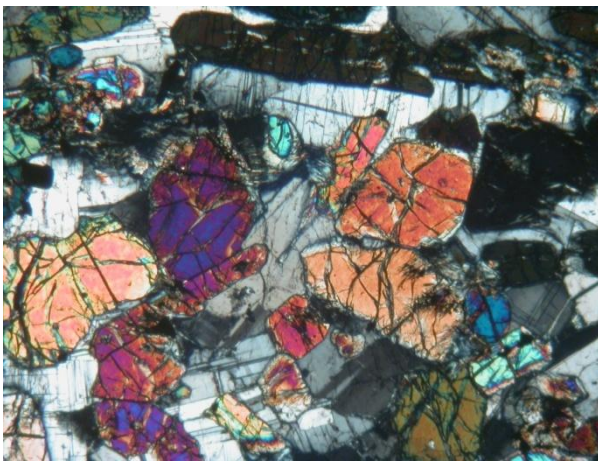

Figure 3.43: Thin section view (XPL) of sample 368 (GBI) at [NM 663 242], the strongly layered section. Smaller olivines and plagioclase in the groundmass. Some of the olivines are euhedral, others show skeletal textures. FoV: 2 mm.

3.8.6.2 Cr-Spinel

Cr-rich spinels are common in all the LUPS rocks; other oxide minerals are rare. Figures 3.44 to 3.47 show the typical appearance of Cr-spinels in both PPL, XPL and as electron back-scatter images. Rarely, a cluster of Cr-spinels occurs within an olivine, as in Figures 3.44 and 3.47, where the Cr-spinels often have brown aluminium-rich centres. Most of the Cr-spinels, however, appear black in both PPL and XPL. The Al-rich Cr-spinels appear to be associated with the large olivines. Cr-spinels can also be found throughout the groundmass, as in several of the samples, either as isolated crystals or as clusters and strings (Figure 3.46). Sieve texture is common in many of the Cr-spinels. This characteristic is well seen in the electron back-scatter images (Figure 3.45), where the crystals appear embayed and perforated, especially near rims. This texture implies a degree of resorption has occurred. The rims of the Cr-spinels analysed show Fe-enrichment.

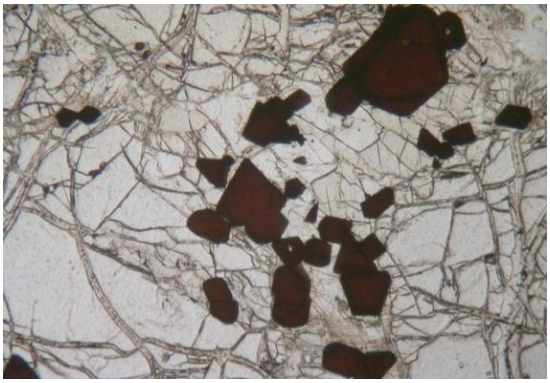

Figure 3.44: Thin section view (PPL) of sample 267 (GBI) at [NM 668 238], showing a cluster of Al-rich Cr-spinels contained within a large olivine crystal. Al_2O_3 values are up to 26.85 wt.% in this sample.FoV: 2mm.

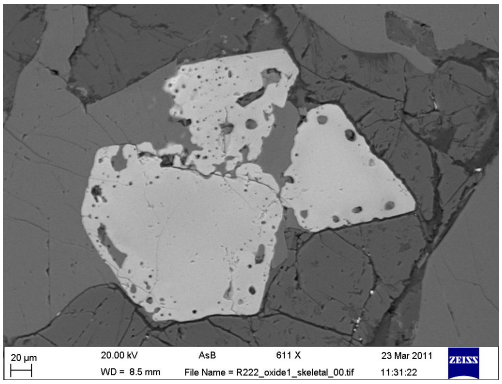

Figure 3.45: Sample 222. SEM Electron backscatter image of Cr-spinels from the Loch Uisg Cottage Sheet at [NM 639 254] showing sieve textures, especially round the rims.

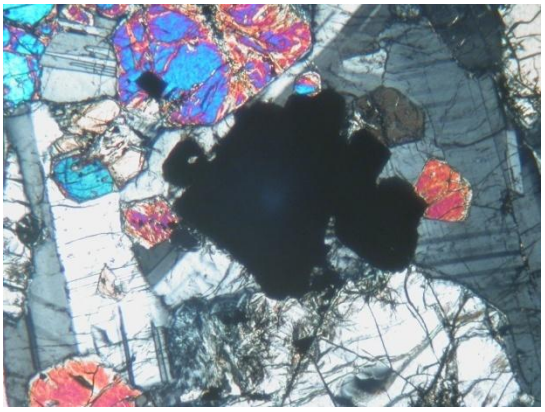

Figure 3.46: Thin section view (XPL) of sample 367 (GBI) at [NM 663 242] showing a large cluster of Cr-spinels in the groundmass with olivine, plagioclase and clinopyroxene. FoV: 2 mm.

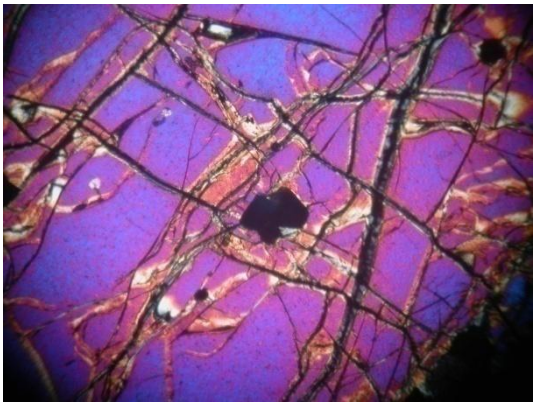

Figure 3.47: Thin section view (XPL) of sample 362 (GBI) at [NM 661 244] showing a very large olivine phenocryst containing brown tinged (Al-rich) Cr-spinels. Alteration of the olivine can be seen in the cracks. FoV: 2 mm.

3.8.6.3 Clinopyroxene

Clinopyroxene, for the most part, is typically fresh and unaltered and displays both a sub-ophitic and granular texture with the plagioclase in the groundmass. It does not occur as a cumulus phase, unlike the olivine and Cr-spinel (Figure 3.48).

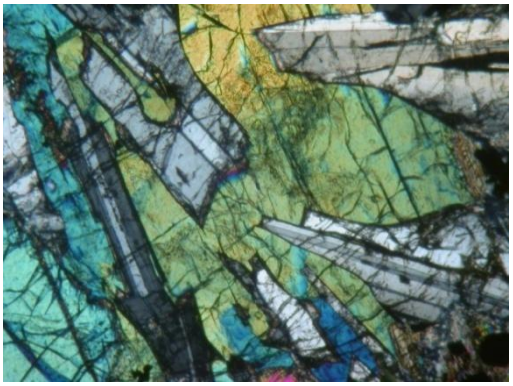

Fig 3.48: Thin section view (XPL) of sample 222 from the Loch Uisg Cottage Sheet at [NM 639 254]. Clino-pyroxene (yellow-green) and plagioclase in the groundmass displaying ophitic texture. FoV: 2 mm.

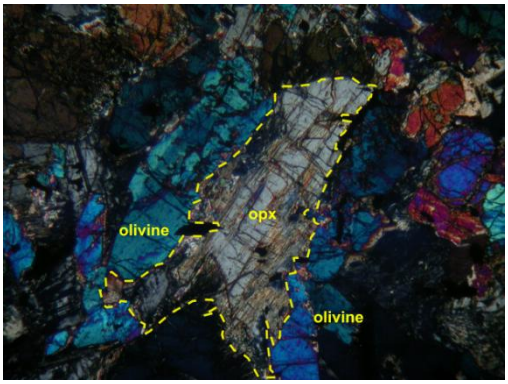

Fig 3.49: Thin section view (XPL) of sample 235 from the Coille Sron nam Boc Sheet at [NM 645 250] showing ?orthopyroxene (light grey, labeled opx in the image) between olivine grains (blue). FoV: 2 mm.

3.8.6.4 Orthopyroxene

Orthopyroxene is normally absent from the LUPS rocks, but what appears to be orthopyroxene is seen in sample 235 from the Coille Sron nam Boc Sheet (Figure 3.5). This sample was obtained from close to the contact with the Loch Uisg

Granite country rocks and the orthopyroxene may have resulted from assimilation of the granite by the picrite (Figure 3.49).

3.8.6.5 Plagioclase

Like clinopyroxene, plagioclase occurs as a groundmass phase and is very fresh, with little obvious alteration (Figures 3.50 to 3.51). Normal, continuous zoning is present. Rarely crystals are sub-ophitically enclosed in clinopyroxene (Figure 3.48).

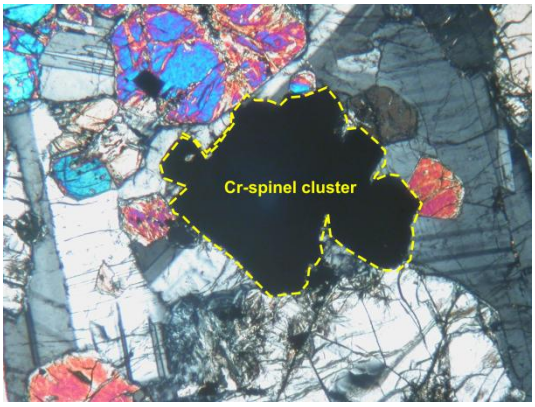

Figure 3.50: Thin section view (XPL) of sample 367 (GBI) at [NM 663 242]. A glomerocryst of Cr-spinels in a predominantly plagioclase and olivine groundmass. FoV: 2 mm.

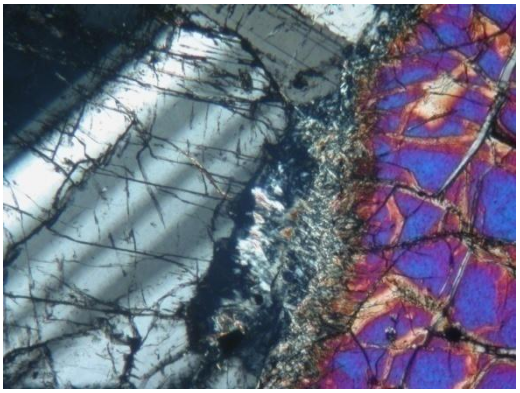

Figure 3.51: Thin section view (XPL) of sample 235 (Coille Sron nam Boc Sheet) at [NM 645 250]. LHS: Large plagioclase crystal showing distinctive twinning. RHS: Olivine showing alteration along rims. FoV: 2 mm.

3.8.7 Summary of general petrographic observations

1) Many of the olivine phenocrysts are large, typically euhedral or blocky in form. Many of these large olivines contain Cr-spinel clusters. Some of these olivines show strain lamellae. Rarely, what appear to be large single olivines in hand specimen are actually glomerocrysts. This group of olivines is referred to as “large”.

2) The groundmass also contains olivine, ranging between small and granular crystals to elongated skeletal crystals. These types comprise the “small” olivines.

3) The groundmass clinopyroxene and plagioclase show ophitic textures.

4) Cr-spinels are abundant, varying in distribution from clusters of crystals to individual crystals, commonly enclosed within olivine.

5) The Cr-spinels are commonly zoned with brown cores and darker margins.

6) No glassy non-crystalline material (representing quickly cooled liquid)was oibserved in the groundmass.

3.8.8 Mineral chemistry

Polished thin sections were analysed using the Scanning Electron Microscope at the University of Glasgow. The analyses were carried out over two separate sessions, in March 2011 and January 2012. The samples were analyzed for **Mg, Si, Ca, Mn, Fe and Ni.** Analytical procedures are described in Appendix 2. The eight samples are listed in Table 3.1. In total, 236 individual analyses were carried out on both the cores and the rims of the crystals. The data are given in Appendix 1. Recalculation methods are given in Appendix 3.

3.8.8.1 Olivine data

i) Mg and Fo content

Not only are the rocks rich in olivine, but many of the olivine phenocrysts are extremely Mg rich. Analyses obtained from the SEM on the Loch Uisg Cottage sheet sample show values of up to Fo_{92}. Assessment of the olivine present gives an average figure of 45% modal abundance, based on five representative samples. This is similar to the values for the M9 dyke in Rum (Upton *et* al, 2002). High Mg content is one of the most distinctive features of these rocks.

SEM analysis of the mineral chemistry of these two distinct populations reveals that not only is there a bimodal distribution in terms of size of the crystals, there is also a bimodal distribution in terms of the mineral chemistry, although there is a small overlap between the two populations. Figure 3.52 shows the range of values for Fo within the two olivine populations as green bars on the plot.

The olivines are very Mg-rich. The average core value for MgO is 49 wt.%, with a highest recorded value of almost 52 wt.%. These values are among the highest

recorded from the BPIP, exceeded in Fo content only by some ultramafic rocks from Rum, in particular, the M9 dyke (Upton *et al*. 2002).

Compared directly with rocks from Rum (Upton *et al*. 2002), the LUPS olivines show very similar compositions to the olivines from the M9 dyke. They are also significantly more Mg-rich than the olivines from the neighbouring Ben Buie Gabbro in SE Mull (Preston *et al*. unpublished data, Prout *et al*. 2002). The LUPS rocks are also more Mg-rich than the Rum plugs (Holness *et al*. 2012). Figure 3.52 shows the relative forsterite contents of these sets of olivines.

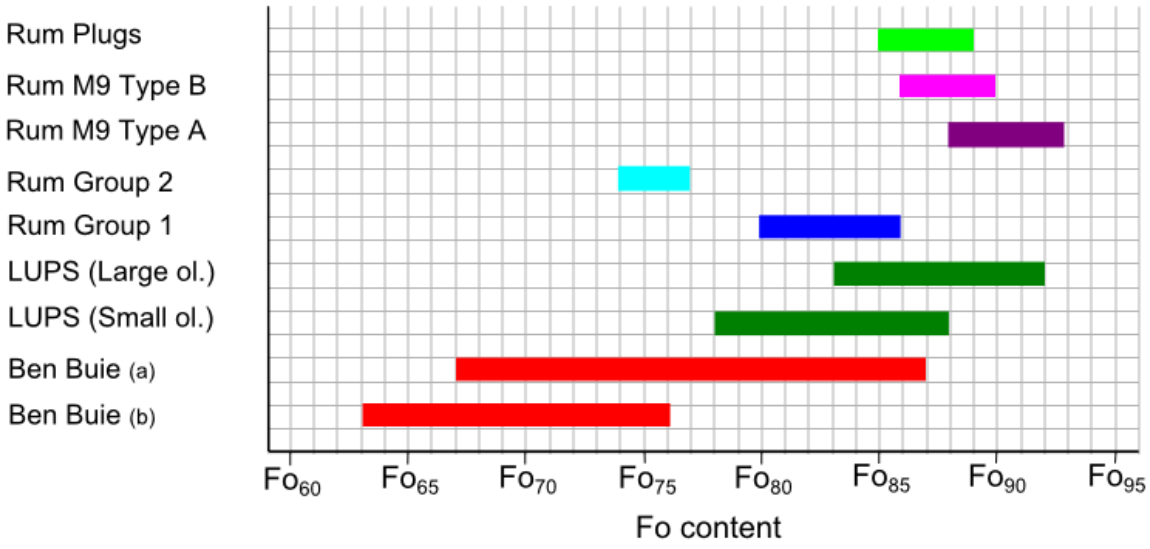

Figure 3.52: Forsterite percentages for the LUPS olivines compared to figures obtained from the Ben Buie Gabbro ((a) Prout *et al*. 2002), the Ben Buie Gabbro ((b)Preston *et al*. unpublished data), the Rum Plugs (Holness *et al*. 2012) and the Rum picritic dykes (Upton *et al*. 2002). The LUPS data are segregated by crystal type.

Both sets of crystals show typical Fe/Mg distribution patterns, the cores being more Mg rich than the rims. No samples were recorded where this was not the case.

The large olivines show higher levels of Mg in the cores but the rims overlap both the cores and the rims of the small olivines. The highest core forsterite value approaches Fo_{92}. The average difference between core and rim for both the large and small crystal sets is 4.58 wt.%.

The large olivines do not appear to have a bimodal distribution between euhedral and non-euhedral forms. The range for Mg# is similar across all the

large phenocrysts. This is in contrast with similar intrusions such as the M9 Dyke in Rum (Upton *et al,* 2002) and the Horingbaai Dykes in Namibia (Thompson and Gibson, 2000), where a clear bimodal distribution can be detected among large phenocrysts. The only bimodality observable among the LUPS rocks is between the phenocrysts and the groundmass olivines, but even between these two populations there is an overlap in terms of MgO content.

Thompson and Gibson (2000) studied the Horingbaai dykes in Namibia, which are also extremely Mg-rich. As part of that research, they compared the Fo content values for olivine in the dykes with similar data from other igneous provinces. The results, together with the corresponding LUPS data, are reproduced in Figure 3.53.

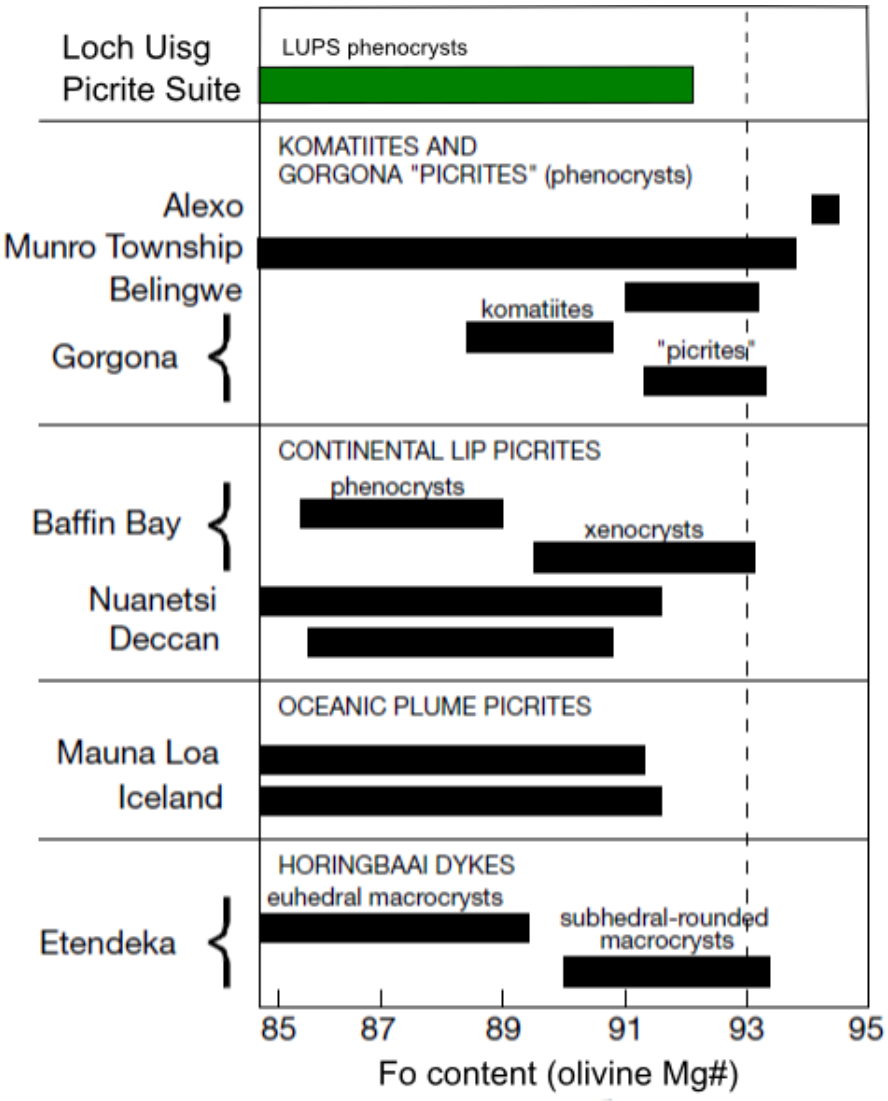

Figure 3.53: The range of Fo content for the olivines from a selection of igneous rocks from other provinces. LUPS data added for comparison (after Thompson and Gibson, 2000).

The MgO and Fo content data demonstrate that the LUPS rocks are amongst the most Mg-rich intrusions recorded worldwide, with values approaching the maximum recorded from magmatic rocks.

ii) Ni Content

Nickel values were measured using WDS (see Appendix 2 for details). In the large crystal set, a clear trend of increasing Ni content as a function of Fo content is apparent. The cores of the large olivines form a distinct cluster on the RHS of the "Large Olivines" plot in Figure 3.54. The trend, although discernible in the set of "Small Olivines", the groundmass and skeletal crystals, shows less of a separation between rims and cores. There is greater overlap.

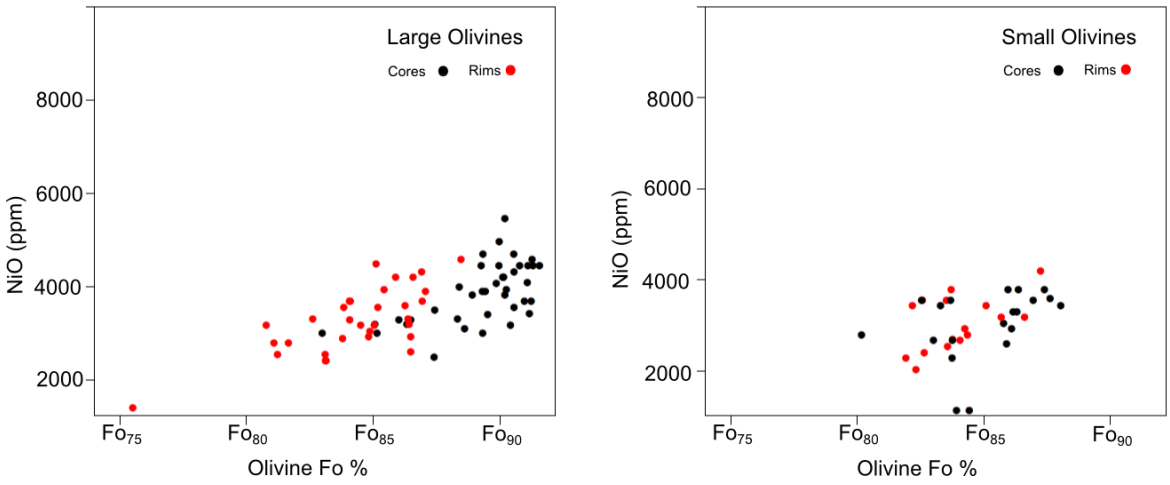

Figure 3.54: Plots of NiO ppm against Fo content for the LUPS olivines.

Ni values vary from about 1500 ppm up to a maximum of almost 4000 ppm. These values are higher than average for MORB (Herzberg *et al.* 2013) and are closer to the results for Alexo komatiites or West Greenland and Baffin Island Palaeocene picrites, where nickel values up to 3800 ppm have been recorded (Herzberg *et al.*, 2013). The Baffin Island picrites, like the LUPS have high values for Mg# achieving values just over 93 for some of the xenocrysts (Figure 3.53). The authors attribute the high Ni values in these highly magnesian rocks to the presence of a Ni-enriched source due to core-mantle interaction which is periodically sampled by mantle plumes.

iii) Ca content

The data for CaO vs Fo content are presented in Figure 3.55.

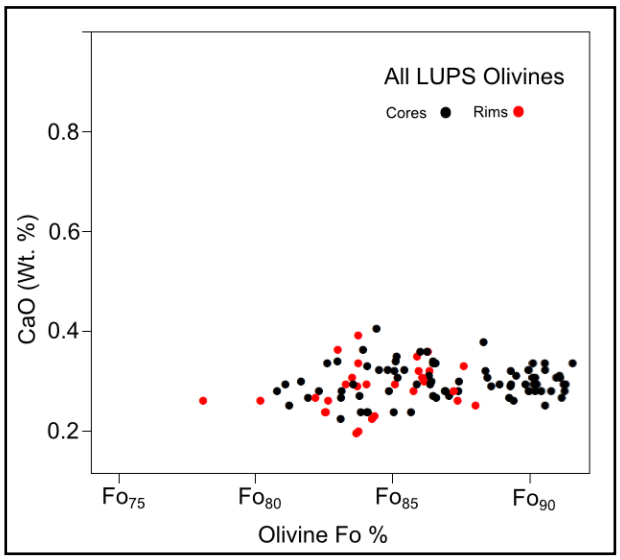

Figure 3.55: CaO plotted against Fo content for all the LUPS olivines.

The compositional values for CaO are above the typical 0.1 wt.% level for mantle xenocrystic olivines (Thompson and Gibson, 2000), implying that the olivines are magmatic and not derived from a mantle source. There does not appear to be any correlation between Fo content and CaO content. This flat line contrasts with the experimental model of Libourel (1999) on Ca-partitioning, where a correlation between Mg# and CaO content was established.

3.8.8.2 Clinopyroxene data

The clinopyroxenes all occupy a small area on the Diopside – Hedenbergite – Enstatite – Ferrosilite quadrilateral, (Figure 3.56). The maximum, minimum and average values are summarised in Table 3.2.

Statistic	Wo (Wt. %)	En (Wt. %)	Fs (Wt. %)
Max.	45.27	51.07	14.59
Min.	39.27	44.27	6.84
Avg.	42.91	47.55	9.53

Table 3.2: Clinopyroxene data for the LUPS rocks.

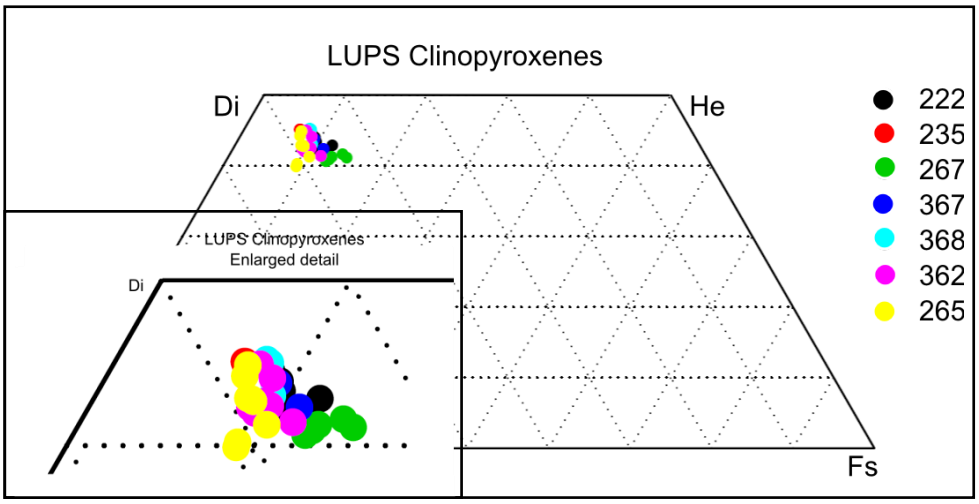

Figure 3.56: Plot of clinopyroxene data for the LUPS samples, showing a small cluster in the top LHS of the quadrilateral. Sample numbers and colour symbols on the RHS. Insert shows an enlargement of the area where the samples are plotted.

When compared to the clinopyroxenes from the other rocks in this study, the following trends are apparent (Figure 3.57):

1) The clinopyroxenes of the LUPS rocks do not show much compositional variation.

2) The clinopyroxenes of the Loch Uisg Gabbro (see Chapter 2) and the Miscellaneous Minor Intrusions (see Chapter 4) show a trend towards higher Fe and lower Ca relative to the LUPS, in line with a normal tholeiitic trend.

3) The Laggan outcrop of the Loch Uisg Gabbro shows slightly lower levels of Ca in the clinopyroxene than the LUPS rocks, which is discussed in Chapter 2.

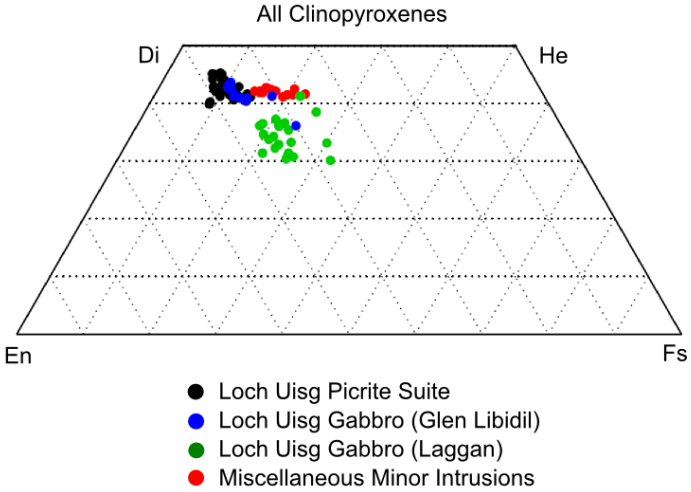

Figure 3.57: Clinopyroxenes from the LUPS, the "Miscellaneous Minor Intrusions", and both outcrops of the Loch Uisg Gabbro.

Using the plot of Nisbet and Pearce (1977) for SiO_2 vs. Al_2O_3, the LUPS rocks can be compared with various other sub-alkaline, alkaline and peralkaline rocks. The LUPS data fit comfortably within the "Ocean Floor Basalt" field, and within the subalkaline field of Le Bas (1962) (Figure 3.58).

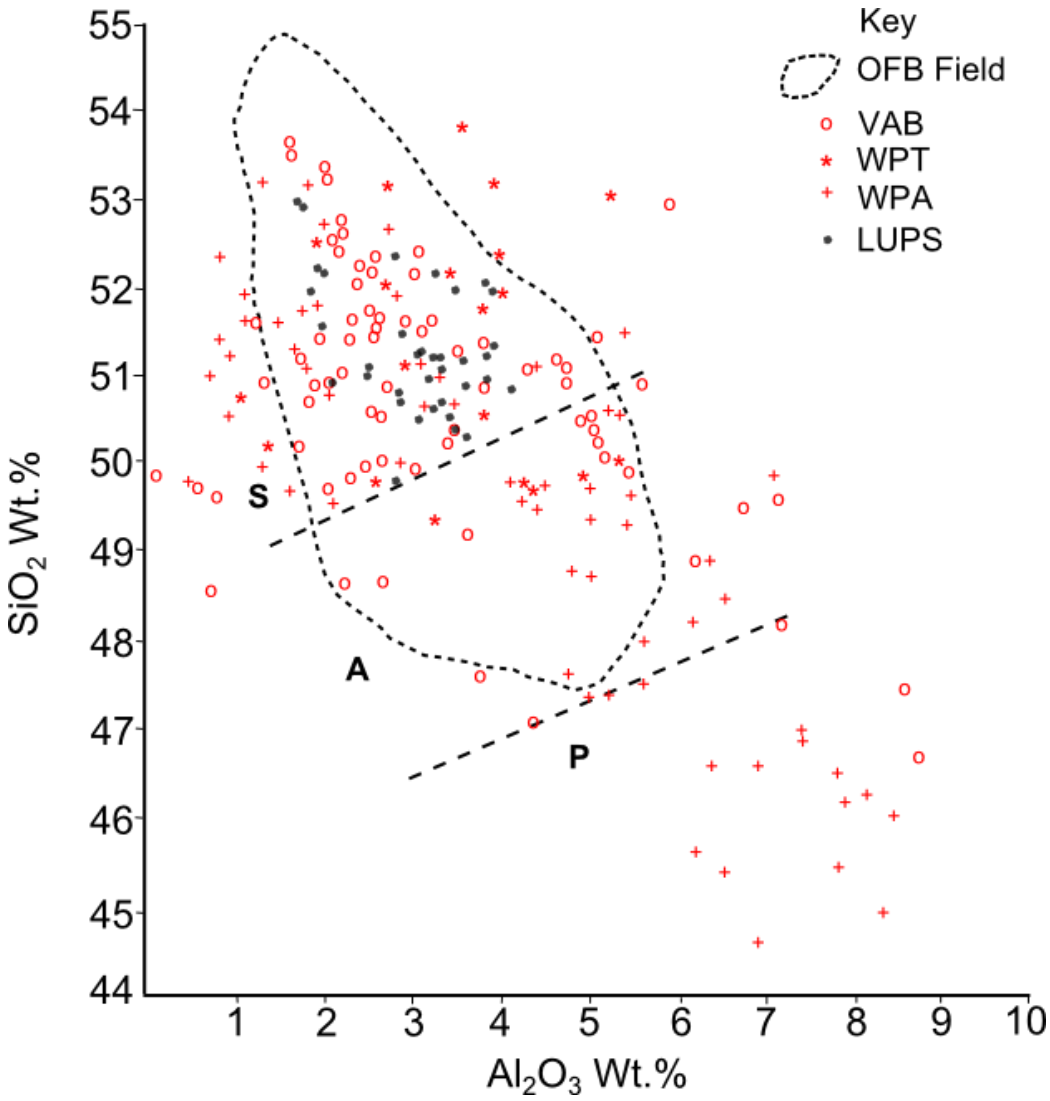

Figure 3.58: SiO_2 vs. Al_2O_3 variation diagram for clinopyroxene for various magma types. VAB = Volcanic Arc Basalt. WPT = Within Plate Tholeiite. WPA = Within Plate Alkaline Basalt. LUPS clinopyroxene shown as black dots. OFB = Ocean Floor Basalt Field. After Nisbet and Pearce (1977). S = Subalkaline. A = Alkaline. P = Peralkaline

On the basis of this SiO_2 vs Al_2O_3 plot for clinopyroxene data, The LUPS magmas are likely to have sub-alkaline tholeiitic affinities.

3.8.8.3 Plagioclase data

Plagioclase data are given in Figure 3.59. Values were obtained from SEM data (see Appendix 2 for details of the SEM technique used) and evaluated using the Gabbrosoft.org spreadsheets (Appendix 3). All the plagioclase analysed is intercumulus.

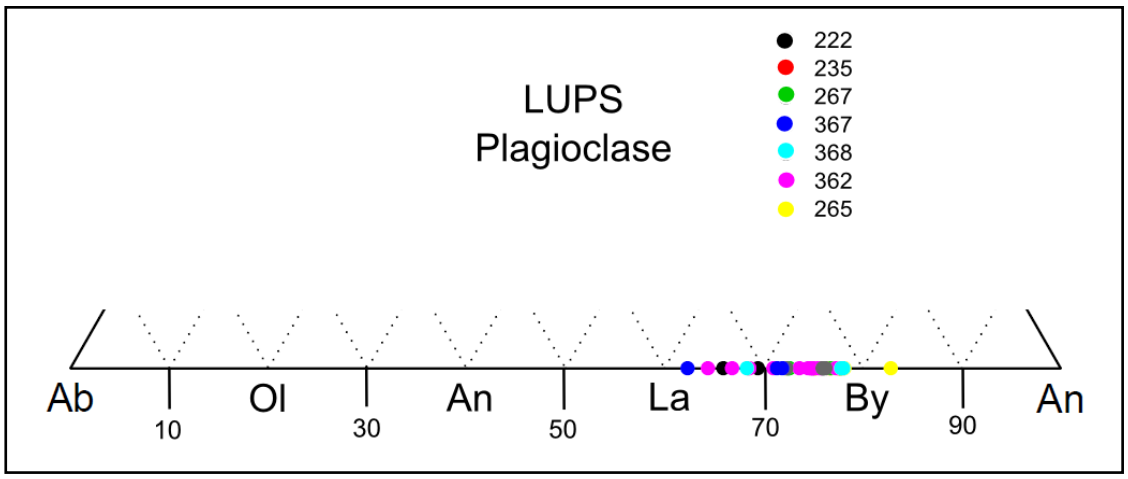

Figure 3.59: LUPS Plagioclase compositional data, from SEM analysis.

Figure 3.60 is an enlargement of part of the graph in Figure 3.59 to show more clearly the individual samples making up the suite.

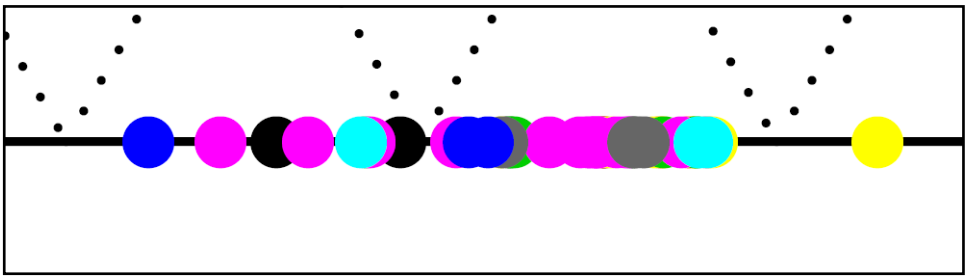

Figure 3.60: Enlarged portion of Figure 3.59 showing the compositional ranges of individual samples. Legend as in Fig 3.59.

As can be seen from the results, the compositions form a fairly tight group straddling the labradorite / bytownite compositional border. The data is summarized in Table 3.3.

Average value for An:	$An_{74.24}$ (bytownite)
Lowest recorded value for An:	$An_{62.32}$ (labradorite) Sample 367 (GBI)
Highest recorded value for An:	$An_{78.06}$ (bytownite) Sample 365 (GBI)

Table 3.3: Highest, lowest and average plagioclase compositions for the LUPS rocks.

3.8.8.4 Cr-Spinel data

The Cr-spinel data are given in Appendix 1 and summarized in Table 3.4. Compositional values from the raw data were recalculated using the Gabbrosoft.org spreadsheet, SPINCALC, (see Appendix 3)

Element (wt.%)	MgO	Al_2O_3	TiO_2	Cr_2O_3	Fe (total)
Highest Comp.	16.62	26.85	7.19	42.18	51.83
Lowest Comp.	7.15	5.73	0.00	24.35	14.68
Average Comp.	12.44	19.89	1.84	37.27	26.69

Table 3.4: Cr-spinel data from the LUPS intrusions. All values in wt. %.

Upton et al. (2002) plotted various Cr-spinel data for the Rum M9 dyke and other dykes against a variety of Cr-spinel data from differing igneous provinces. The LUPS data, when compared with these data are displayed in the plots in Figures 3.61 and 3.62. A very close correlation is noted between the LUPS Cr-spinel compositional data and that for the Rum M9 Dyke.

.

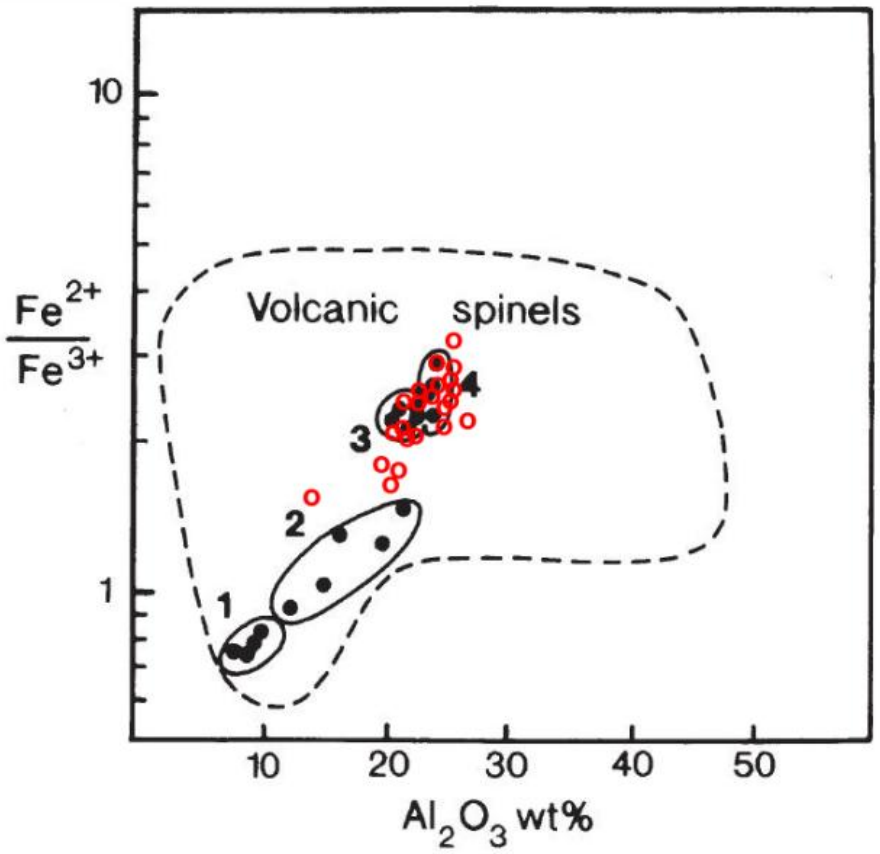

Figure 3.61: Al_2O_3 vs Fe^{2+}/Fe^{3+} ratio. 1,2,3 and 4 are Rum dyke spinels (after Upton *et al*. 2002). The Group 4 Cr-spinels are from the Rum M9 dyke. The LUPS spinels are represented by the red circles. The "Field of Volcanic spinels" is indicated by the dashed line and is after Kamenetsky, Crawford and Meffre (2001).

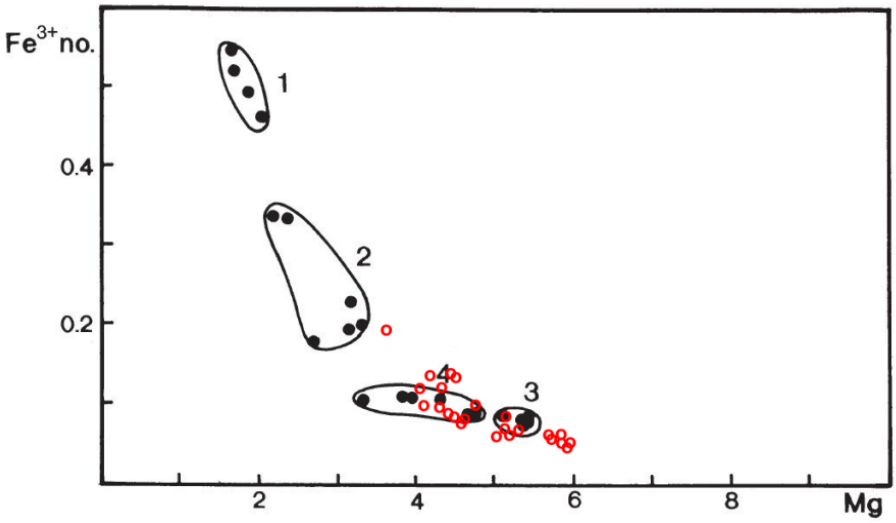

Figure 3.62: Plot of Fe^{3+}no. vs Mg (cations per formula unit) for the Rum dyke Cr-spinels (after Upton *et al*. 2002) with LUPS data added as red circles. Fe^{3+}no = Fe^{3+} / (Fe^{3+} +Al +Cr) based on cations per formula unit.

3.9 Discussion of magmatic conditions

In terms of intrusion morphology, petrography and mineral chemistry, the LUPS represents a locally and globally unusual suite of highly magnesian igneous rocks. The olivine compositions approach the "ultramagnesian olivines" of Keiding *et al*. (2011). Their emplacement and preservation at high levels in the Mull volcano must therefore reflect unusual conditions.

3.9.1 Olivines and parental magma compositions

Previous research has shown that there is typically a strong correlation between the forsterite content of olivine in basic igneous rocks and the MgO content and temperature of the parental magma. (Roeder and Emslie 1970; Ulmer 1989; Matzen *et al*. 2011).

Roeder and Emslie (1970) examined the olivine-liquid exchange coefficient, K_D and established the relationship:

$$K_D = (FeO/MgO)^{ol} / (FeO/MgO)^{liq}$$

where FeO and MgO refer to concentrations by weight and "ol" refers to crystalised olivine and "liq" refers to the melt. They proposed a value of 0.30 ± 0.03 for K_D, independent of liquid composition or temperature. This coefficient has been widely used to demonstrate equilibrium (or not) between phenocrysts and their host groundmass or bulk rock composition (Ulmer,1989). There is a strong correlation between the Mg/Fe ratio, the Mg#, in the olivines for any given basalt, and from this information the original melt MgO content can be estimated, as long as various other parameters can be accounted for.

Matzen *et al*. (2011) worked with synthetic Hawaiian picrites and suggested a revised value for the olivine-liquid exchange coefficient:

$$K_D = (FeO/MgO)^{ol} / (FeO/MgO)^{liq} = 0.345 \pm 0.009$$ (FeO and MgO values in Wt.%)

A number of factors may affect the applicability of this coefficient:

1) Alkali content of the parental liquid has an effect on K_D. It can reach as low as 0.18 for highly nepheline- and leucite-normative bulk compositions. For

normal basaltic rocks, the effect can be ignored as insignificant. (Matzen *et al*. 2011).

2) Low silica and high-Ti melts can also generate lower values for the K_D, (Longhi et al., 1987), but such melts are commonly also alkali-rich.
3) Oxidised melts tend to produce more magnesian olivines, but for melts along the QFM or NNO buffers, the above coefficient is applicable.

In terms of alkalis, silica saturation and oxygen fugacity, the LUPS rocks are likely to be similar to the Hawaiian picrites studied by Matzen *et al*. (2011).The constraining factors are discussed blow:

1) Magma Ti, Na and Si contents can be broadly constrained by pyroxene compositions (e.g. Nisbet and Pearce, 1977; Leterrier *et al*. 1982). The LUPS clinopyroxenes have a neutral colour, rather than the violet-brown tint of Ti-rich compositions, and analysis shows no more than 0.9 wt.% TiO_2, and 0.5 wt.% Na_2O, typical of "normal" basalts. Plots of SiO_2 vs. TiO_2 and SiO_2 vs. Al_2O_3 show a spread of values coincident with those expected for sub-alkaline MORB (Le Bas 1962). SiO_2 is between 49 and 53 wt.%, Al_2O_3 is between 2 and 4.5 wt.% and TiO_2 is between 0.35 and 2.5 wt.% (Nisbet and Pearce 1977).

2) The oxide minerals in the LUPS Cr-spinels, are similar to those in the Hawaiian picrites, having Cr# in the range 0.50 – 0.74, where Cr# is defined as Cr/Cr+Al atomic. Oxygen fugacities are therefore probably similar to the Hawaiian picrites (Matzen et al. 2011).

3) Orthopyroxene is present in a few rocks, most likely the result of contamination by melted silicic country rocks, but its scarcity suggests that the LUPS melts may have had a transitional / mildly alkaline basalt chemistry (*cf*. the Rum picrites; Upton *et al*. 2002).

3.9.2 Estimate of parental magma MgO content

There is an approximately linear relationship between olivine Mg# and parental magma MgO content in Hawaiian basalts and picrites. (Matzen *et al*.2011) (Figure 3.63).

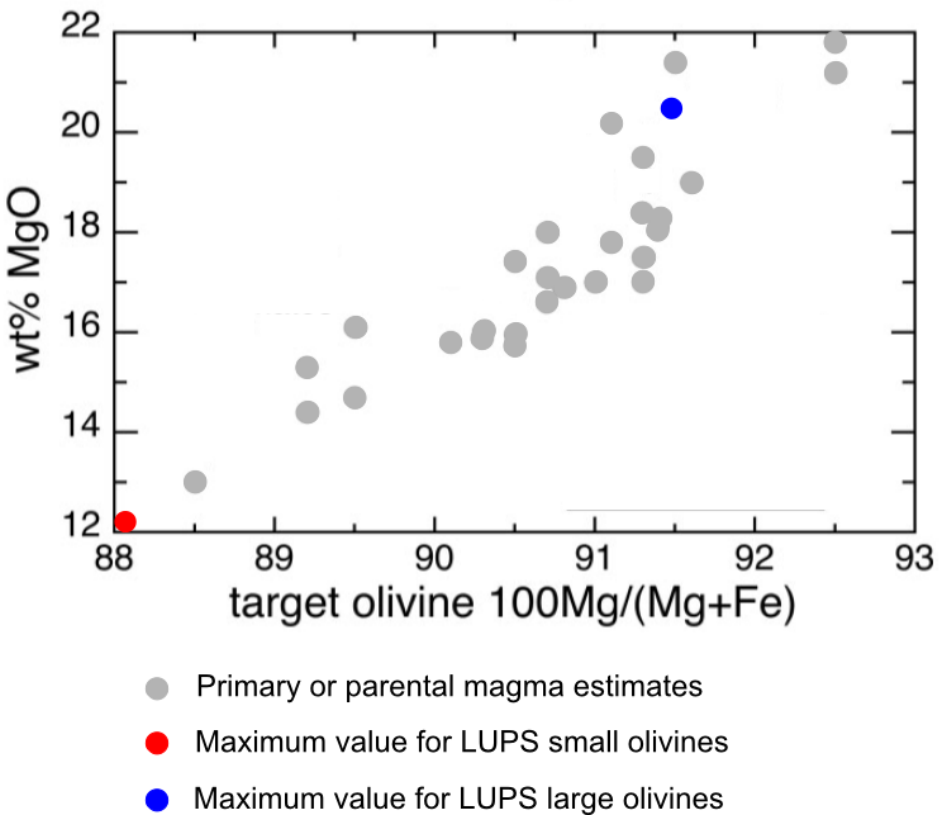

Figure 3.63: The approximately linear relationship between Mg# and parental magma MgO content in Hawaiian basalts and picrites. (Modified plot based on Matzen *et al*.2011)

Matzen *et al*. (2011) suggest a value of 0.34 for the olivine-liquid Mg exchange coefficient, using experimental synthetic picrite and published data. This coefficient can be affected by several factors, such as oxidation state, alkali content and low levels of Si and Ti. A graphical estimate of melt MgO contents associated with the olivine composition can be made from the data of Matzen *et al*. (2011). This assumes that the LUPS rocks are not affected by the factors noted above. Using the highest values for LUPS large and small olivines, the following values for MgO are produced from the plot in Figure 3.63:

Large Olivines, Fo_{92} 20.5 wt.% MgO

Small Olivines, Fo_{88} 12% wt.% MgO

The large olivines are likely to be xenocrystal, from a disrupted high temperature cumulate transported by a liquid rich in the smaller crystals.

3.9.3 Temperature of parental magma

The relationships between olivine composition, parental magma MgO content, parental magma temperature and mantle temperature have been extensively researched. Although there are many references in the published literature (*e.g.* Sobolev *et al.*2005; Putirka *et al.*2007; Falloon *et al.*2007; Keiding *et al.* 2011), precise relationships are complex and are influenced by other factors such as pressure, H_2O content and alkali content (*e.g.* Matzen *et al.* 2011). The melting regime and dynamics of melt extraction can also have a significant effect on calculated mantle temperatures (Keiding *et al.* 2011).

In the LUPS magmas, like most of the magmas in the BPIP, crystallization of olivine ± spinel is followed by olivine and plagioclase. Olivine-pyroxene saturated liquids have been used in some studies (*e.g.* Sugawara, 2000) but these are not found in the BPIP and are thus unlikely to be relevant here.

While most workers assume a peridotite source for basalts and picrites, even this has been questioned. Sobolev *et al.* (2005), have suggested, on the basis of high NiO and SiO_2 contents of Hawaiian shield basalts, that the source material may be a secondary pyroxenite source produced by mantle peridotite mixing with recycled oceanic crust (eclogite). A mixed source is therefore proposed for these Hawaiian basalts. The olivines in the LUPS rocks are also high in nickel, up to 4000 ppm as shown in Figure 3.54.

Given the paucity of analytical data, other than olivine compositions for the LUPS rocks, detailed assessments of mantle conditions are unlikely to be robust. Magma MgO can be used to estimate the mantle source potential temperature (***T*p**). Several methods exist for estimating this temperature. Herzberg *et al.*(2007) and Herzberg and Gazel (2009) used the empirically derived equation: ***T*p = 1463+12.7 MgO − 2924 / MgO.** Trumbull *et al.* (2002) used a graphical method, involving an approximately linear relationship between melt MgO

content and mantle source potential temperature (***T*p**) but this gives very high figures with the LUPS data (over 1800°C), so is not considered here. It is highly unlikely that a liquid with a temperature of over 1800°C would be found at such high levels in the crust.

Using the above equation, a mantle source potential temperature (*T*p) of **1580°C** was obtained for the magma which crystallized the large olivines.

Using the same method, a mantle source potential temperature (*T*p) of **1371°C** was obtained for the entraining liquid represented by the small olivines.

3.9.4 Ultramagnesian olivine

The olivines in the LUPS rocks are unusually Mg-rich, having Fo values up to Fo_{92}. Keiding *et al*. (2011) define ultramagnesian olivine as "*Magmatic rocks having a forsterite proportion [Fo = Mg/(Mg + Fe) in molar percent] greater than the maximum* $Fo_{91.5}$ *known from Earth's mid-ocean ridge systems*". Olivine of this composition is common among Archaen komatiites, but rare among Phanerozoic rocks. Examples can be found in Baffin Island (Francis, 1985), West Greenland (Larsen *et al*. 2000), Gorgona, Colombia, which is the only known location for a Phanerozoic komatiite (Révillon *et al*. 2000), the Etendeka province, Namibia (Thompson and Gibson, 2000) and Rum (Upton *et al*. 2002). Ultramagnesian olivines are also found among Siberian meimechites (Arndt *et al*.1995).

While ultramagnesian olivines require hot magmas with high Mg/Fe ratios, the exact circumstances of melt generation are unclear. Keiding *et al*. (2011) suggest that "dynamic melting" involving separation of small melt increments can produce such melts without extreme mantle temperatures. This process also leaves a distinctive depletion in incompatible trace elements. Trace element data was not available for this study, so it is not possible to state with certainty that "dynamic melting" was involved.

3.9.5 Mg-rich melts within the North Atlantic Igneous Province

Mg-rich basalt and picrite are significant components of lava piles and central complexes developed across the North Atlantic Igneous Province (NAIP) (Larsen and Pedersen, 2009). Picrites with ultramagnesian olivines are particularly well developed in Baffin Island and West Greenland (e.g. Kent *et al*, 2004, Larsen and Pedersen, 2009), but are also recorded from Rum (Upton *et al* (2002).

Within the British area of the NAIP, igneous activity is developed around a number of centres and tends to follow a similar pattern:

1) Early flood basalt activity (and dykes);

2) Local uplift of basement and development of intrusive / extrusive centres (and dykes);

3) Locally developed sill complexes;

4) Late dykes.

Rocks derived from Mg-rich basalts and picrites are found in all these settings, (e.g. Emeleus and Bell, 2005), although olivine compositions are typically not quite as Mg-rich as those in the LUPS.

Ultrabasic rocks are particularly well developed in the Rum Central Complex (e.g. Emeleus 1997) and include a wide range of dunitic to peridotitic cumulates. It is generally accepted that highly magnesian parental magmas must have been involved in the generation of these rocks.

The picritic dykes of Rum, described by J.McClurg, (unpub. Ph.D. thesis, Univ. Edinburgh, 1982) and Upton *et al*. (2002) are among the most MgO-rich intrusions in the BPIP, with olivines having a composition up to Fo_{93} (Upton *et al*. 2002). Peridotite plugs, which have a dyke-like form, radiating from the Central Complex, have also been described (Holness *et al*. 2012) and contain olivine

with very high Fo contents, in the range Fo_{85-89}. It is suggested that the plugs are the remains of deep-level conduits through which olivine-rich magma flowed, giving rise to Hawaiian-style fire fountains. The picritic dykes are also considered to be conduits, bringing highly magnesian magma to near-surface levels. Similar rocks are well developed in the Cuillin Centre in Skye (Emeleus and Bell, 2005) and almost certainly represent the products of similar magmas. The Rum M9 Dyke is perhaps the intrusion in the BPIP that matches most closely the LUPS intrusions in terms of mineral chemistry, especially olivine and spinel. The petrogenetic conditions that gave rise to the LUPS rocks are likely to be similar to those that produced the M9 Dyke. However, in terms of texture, morphology and size, the two sets of intrusions are quite unlike each other and represent different crystallisation and emplacement histories.

The Gleann Beag Intrusion may represent a major conduit which was open for a long time with multiple pulses of magma moving through it. However, any potential lavas produced from such a conduit late in the Palaeogene history of the Mull Central Complex are no longer preserved in the existing lava pile due to erosion.

3.9.6 Mg-rich rocks in Mull

Basalts with over 14% MgO have been described from the Mull Plateau Lava Formation by Kerr (1995, 1998) and Peate (2012). These are typically transitional to mildly alkaline basalts.

The Mull Central Complex includes one large ultrabasic / basic intrusion, the Ben Buie Gabbro (Bailey *et al*. 1924; Lobjoit,1959; Skelhorn *et al*. 1969). Apart from platinum group elements (PGE) mineralogy (Pirrie *et al*. 2000, Prout 2002) there is little modern published work on the Ben Buie Gabbro in SE Mull, but it includes large bodies of layered peridotites (with chromitite layers) and skeletal olivine rocks, which may be analogous to the harrisitic crescumulates of Rum. The range of lithologies is similar to that seen in Skye and Rum, although layering tends to be highly disrupted and xenoliths are abundant, suggesting tectonically dynamic conditions during crystallisation (J. Faithfull, *pers. comm*.).

Prout (2002) records olivine compositions from Ben Buie of up to Fo_{87}. The Ben Buie Gabbro is a much larger intrusion than any of the LUPS members so it is not directly analogous. The Ben Buie Gabbro is the largest gabbroic body in the Mull Central Complex and displays many of the features of a large magma chamber. The LUPS are minor intrusions of limited areal extent.

3.10 Morphology of the LUPS

The LUPS rocks comprise three distinct bodies which, although morphologically different, are petrographically identical. The Gleann Beag Intrusion, (GBI) is an irregular sinuous intrusion that although dyke–like in appearance over part of its outcrop, also shows transgressive sill-like characteristics, especially in its upper section where the dipping / inclined attitude is discernible. The Loch Uisg Cottage Sheet is a gently dipping sill-like body but the Coille Sron nam Boc Sheet has a less discernible morphology. It may be sill-like but the poor exposure prevents proper assessment of the overall form and orientation.

3.10.1 Layering in the GBI

Layering is visible in all three intrusions, although best developed in the Gleann Beag Intrusion, where diverse styles of layering are developed along its course. Figures 3.11 to 3.21 illustrate the diversity of the layering in the GBI. The type of layering can range considerably over a relatively short distance; parallel sub-horizontal banding can be found a few metres away from disrupted surfaces where the layers dip steeply. Horizontal to sub-horizontal layering is obvious in the middle section of the GBI (Section C) at [NM 663 242]. Here, the darker, thinner, melanocratic layers appear to stand out from the rock surface and microscopic examination reveals that they are finer grained and poorer in phenocrystic olivine when compared to the lighter coloured layers from the same locality. Up to seven of the darker layers can be identified at this locality, between 2 and 10 cm thick. The layers are parallel, with no truncation or erosional surfaces to be seen (Figure 3.18).

About 10 m to the east of this zone of prominent layering, the darker bands appear to be thicker (Figure 3.19), but there is no easy way, due to vegetation, to correlate the layering between the two locations. In this section, all the layering is subhorizontal, suggesting fairly quiet, consistent conditions of accumulation.

In the same general area however, layers can be seen to truncate other layers at a gentle gradient of up to 10° (Figure 3.20). On the other side of the dyke, about 10 m to the NE, the truncation angle is much steeper, dipping at about 40° (Figure 3.21). Over a short distance, of 10 to 20 m, the dynamic environment appears to have changed considerably, with magma emplacement apparently being a more energtic process.

Most of the layers appear to dip along the strike of the intrusion and not across its width. This type of layering could arise if the conduit was being replenished by regular pulses of magma, followed by periods of crystal settling.

In Section D, the middle to upper part of the GB, (Figures 3.23 – 3.26), where the form of the intrusion is more akin to a transgressive sill, dipping at 45°, the layering is approximately horizontal, and does not display the truncation and erosion surface features that are so obvious in the lower parts of the intrusion. The implication is that, in this upper, dipping section, the emplacement of magma pulses was less dynamic, and that the observed layering is due to crystal settling alone. The GBI bears certain similarities to the Rum plugs described by Holness *et al* (2012). The authors suggest that the settling of crystals, due to the large load involved, took place during the waning phase of the flow.

3.10.2 Autoliths

At [NM 662 242], there is a zone of autoliths (Figure 3.17). This is the only location along the course of the intrusion where autoliths or xenoliths are found. Optical analysis reveals that the autolith rock is a fine-grained variant, without the large olivine phenocrysts, but containing abundant skeletal olivine and

plagioclase, together with small granular olivines. They are not country-rock xenoliths. These autoliths may represent remnants of a chilled marginal facies of the main intrusion.

3.10.3 Orientation

The approximate orientation of the GBI is NW-SE. The BGS map (BGS 1923,1992) has mapped it as a member of the Mull Dyke Swarm which mostly follow this trend. Although clearly not a normal member of the dyke swarm, it has almost certainly been intruded in a similar manner, following the same NW-SE regional trend.

The two smaller sheets of the LUPS complex (the Loch Uisg Cottage Sheet and the Coille Sron nam Boc Sheet) may be lateral offshoots from the GBI, but they outcrop at a lower level. The lowest point of the GBI is 170 m and its highest point is near 310 m, but the two sheets are found between the 30 m and 4 0m contours. The sheets may be lateral offshoots from another intrusion similar to the GBI, or indeed part of the GBI itself, as shown in the cross-section in Figure 3.64.

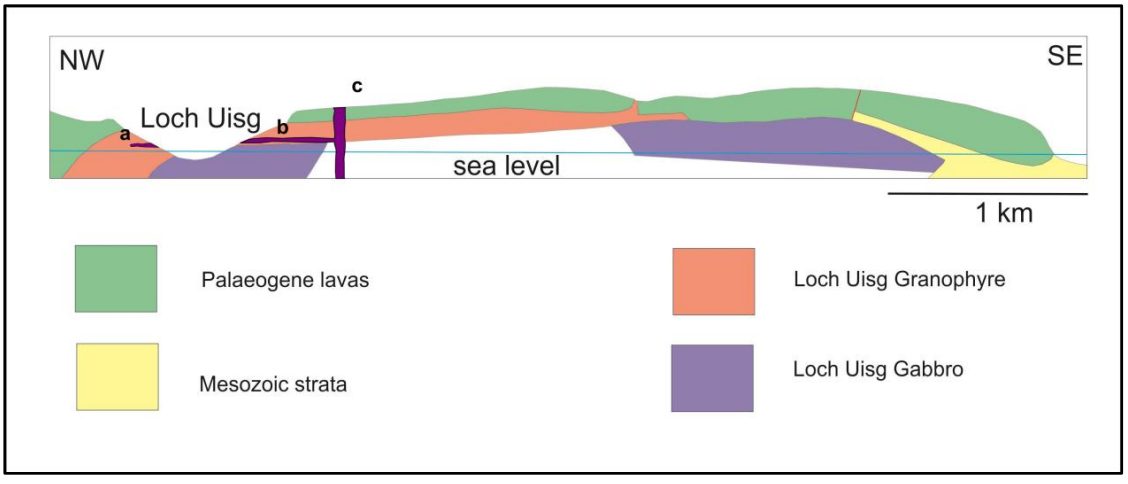

Figure 3.64: Based on the original by Bailey *et al* (1924), the LUPS intrusions are indicated in purple. a: Loch Uisg Cottage Sheet. b: Coille Sron nam Boc Sheet. c: Gleann Beag Intrusion.

3.11 Geometry and emplacement of the LUPS

3.11.1 Source material

The LUPS intrusions, although apparently morphologically different, are petrographically similar. Rhythmic layering is a feature of all three intrusions, but is especially pronounced in the GBI. Multiple pulses of magma injection are proposed as the reason for this feature. No cryptic layering (a change in mineral chemistry within the layering, not visible in the field) is detected; from the lowest to the highest exposed parts of the GBI, the samples all have very similar compositional values for olivine, clinopyroxene and plagioclase. The material being intruded appears to have been of a constant composition over the duration of the emplacement event.

All three intrusions display evidence of multi-stage olivine crystallization. There are clearly two main populations of olivine in the intrusions: a groundmass of small, granular and skeletal olivines (the "small olivines") and the larger, euhedral and blocky olivines, which form a distinct population (the "large olivines", which are very Fo-rich). Unlike the M9 Dyke in Rum (Upton *et al*. 2002) or the Horingbaai Dykes in Namibia (Thompson and Gibson, 2000), where there is clear bimodality within the phenocrysts, the large olivines of the LUPS intrusions, whether euhedral, blocky or irregular in form, comprise one population.

The large olivine crystals display a variety of forms – many are blocky and irregular shaped, whereas others display a classic euhedral form. Whatever the form, they commonly occur as glomerocrysts. The large olivines appear to be xenocrystic, most likely derived from a partially crystallised deep ultramafic cumulate that has been disrupted. The strain-related features seen in many of the large olivines attests to this scenario. The very high Fo content of some of these crystals (up to Fo_{92}) implies that they are derived from a very hot parental magma. In their paper on Hawaiian (Kilauea) basalt lavas, Vient and Higgens (2010) describe strained, deformed olivines very similar to those seen in the LUPS. The authors use the term "antecryst" to describe these olivines, and state:

"These antecrysts are interpreted to have started as cumulates from earlier Kilauea magmas, which were subsequently disrupted and incorporated into the later magmas." (Vient and Higgens, 2010).

The small olivine crystals are commonly granular, rarely euhedral, and form a major part of the groundmass. Skeletal crystals are common and the presence of these suggests a rapidly cooling environment, which would not be unusual in a minor intrusion.

The large crystals most likely represent disrupted cumulates that were entrained by melt in equilibrium with the small olivines, and subsequently brought up to higher crustal levels where the skeletal olivines grew, with periodic crystal settling and solidification taking place. Although the entraining liquid was less magnesian and cooler than that which produced the cumulate, it would still have been very hot and rich in magnesium, as the groundmass olivines can have compositional values approaching Fo_{88}. (*e.g.* Larsen & Pedersen, 2000).

3.11.2 Geometry

The actual morphologies of the Loch Uisg Cottage Sheet and the Coille Sron nam Boc Sheet are difficult to determine due to poor exposure of the contacts with the country rock (Loch Uisg Granite) at the two locations. The sheets only display horizontal to sub-horizontal layering, with none of the dynamic features seen in the GBI. The layering is also fairly subtle and not as nearly pronounced as it is in the GBI. No slumping or truncation features are visible and no xenoliths were recorded.

The morphology and geometry of the GBI is more obvious due to its better exposure. It is most dyke-like at each end, especially the SE end where the planar sub-vertical form is clearly seen (Sections E and F). In the middle part of the BGI, the form is much more irregular (Sections C and D) and appears almost sill like. Sections A and B at the NW end of the intrusion are poorly exposed so no firm conclusions as to geometry can be made. Layering is however very well developed in this section.

The type country rock does not appear to have had any obvious effect on the shape of the intrusion. The most dyke-like parts of the GBI are intruded into

both the granite and the basalt lava country rocks. The irregular sill-like middle to upper section is entirely within the basalt lava but this does not appear to have exerted any constraints on the morphology of the GBI. The dip of the contacts does not appear to be related to any structural features within the lavas.

The GBI is, in some respects, similar to the Rum plugs (Holness *et al*. 2012). In addition to the petrography and mineral chemistry, many of the surface features such as the eroded layering and jointing are very similar. The Rum plugs are described as open system conduits and it may be that the GBI is a similar intrusion, but with a more oblique orientation, certainly in its middle section.

3.11.3 Emplacement

The emplacement process appears to have comprised multiple pulses of olivine xenocryst-rich magma. In the case of the GBI, this must have been a fairly dynamic process, as there are numerous features such as erosion surfaces, truncated layering and slump folds that could only develop in a high-energy environment. Such features are found in large scale magma bodies such as Skaergaard (McBirney *et al*. 2007, Irvine *et al*. 2009) and Rum (Emeleus 1997). The presence of such features implies that the emplacement process involved lateral as well as vertical flow. The orientation of the cross-cut erosion surfaces implies that the lateral flow was from the SE towards the NW. A large volume of olivine xenocrysts was transported and questions arise as to how this volume of material could be present in an active conduit. The case of the Rum plugs (Holness *et al*. 2012) may be similar. The authors conclude that the accumulation took place when a given flow was waning and the crystals settled out.

The cross-cutting truncation features are likely to have arisen via various processes, including:

1. Downward / lateral density currents eroding unlithified cumulates. This could happen during periods of low flow rates when cumulates could fall from the walls of the intrusion. The degree of truncation would be

dependent on the energy associated with this current. A high-energy pulse would cause greater disturbance, erosion and truncation.

2. A vertically driven pulse of crystal-laden magma being intruded upwards through cumulates causing erosion and redistribution of unconsolidated cumulate. This could also account for the occurrence of autoliths of already consolidated material.
3. Lateral movement of magma along the intrusion due to non-uniform supply of magma from below.

In their paper on the Rum M9 Dyke, Upton *et al.* (2002) speculate that the Long Loch Fault (LLF) in Rum overlay a zone of weakness that facilitated the intrusion of magma and that it may have extended to the base of the lithosphere. This would have caused decompression of the underlying plume-head and caused melting as well as providing a conduit for the ascent of picritic magmas.

A similar scenario could be suggested for SE Mull. The GGF, as can be seen in Figure 1.4, runs through the Loch Uisg area. If the GGF also extended to the base of the lithosphere, it may well have behaved in exactly the same way as the LLF, as proposed by Upton *et al.* (2002). Early Palaeocene movement of the GGF has been demonstrated (Holgate, 1969). Decompression melting of the plume-head would have provided the picritic material for the LUPS intrusions.

The illustrations in Figures 3.65 to 3.70 show graphically a possible emplacement mechanism for the LUPS.

Stage 1: Continuing crustal tension, at a late stage in the Palaeogene igneous activity on Mull results in a conduit opening up, aligned in a NW-SE direction. This conduit bisects both the lava pile and the Loch Uisg Granite country rocks (it may also cut the Loch Uisg Gabbro at depth, but there is no field evidence for this). The conduit is not simply a planar dyke-like feature, but is irregular in shape and almost sheet-like in places, the orientation and morphology revealed by the presence of the Gleann Beag Intrusion at today's erosion level. The intrusion possibly started off with a more dyke-like morphology but has become irregular in form due to thermal erosion of the country rock. The filling process involves lateral as well as vertical flow as evidenced by the layering and truncation features (Figure 3.65).

Stage 2: Into this conduit, further hot, highly magnesian magma entraining even more Mg-rich xenocrysts is intruded as a series of pulses. The xenocrysts are most likely derived from an underlying crustal magma chamber. This is a high energy, dynamic process, repeated several times, which creates the many structures within the intrusion. Mixing with cooler residual magma in the intrusion causes the rapid crystalisation of skeletal olivines. Xenocrysts settle out (Figure 3.66).

Stage 3: A layer of cumulate material is deposited. This is characterized by large olivine xenocrysts, up to Fo_{92} in some samples, and Al-rich chromite. Some of the olivine xenocrysts show strain lamellae, indicating disturbed cumulate from elsewhere. The entraining liquid is rich in smaller olivines, commonly skeletal, which form a non-cumulate layer together with plagioclase and clinopyroxene. The layered material is found in the centre of the intrusion. At the margins, chilling takes place against the country-rock lavas. No chilling is observed against the Loch Uisg Granite due to poor exposure of the picrite / granite contact. Some back-veining of the granite into the picrite takes place, suggesting melting and possibly thermal erosion of the granite. The basalt does not appear to have been melted by the picrite (Figure 3.67).

Stage 4: Later pulses of similar magma are intruded into the conduit. This disrupts the existing layers, which are not completely solidified, producing erosion surfaces, many of which are steeply inclined (Figure 3.68).

Stage 5: Deposition of crystals takes place on top of these erosion surfaces, as well as on undisturbed cumulate, and successive layers are built up (Figure 3.69).

Stage 6: Successive pulses of magma continue to be intruded along the length of the conduit, building up a complex layered intrusion. There may be a high-Mg basalt magma extruded as a surface manifestation of this intrusive activity, but no evidence of this is preserved at the present surface level. Such a basalt would be very olivine-rich (Figure 3.70).

A variety of structures can be seen in the dyke. 1) Simple horizontal layering; 2) Truncation surfaces with steeply inclined layering; 3) Slump and fold structures;

4) Curved layers, commonly truncating others; 5) Broad, prominent banding, always horizontal to sub-horizontal (Figures 3.71, 3.72).

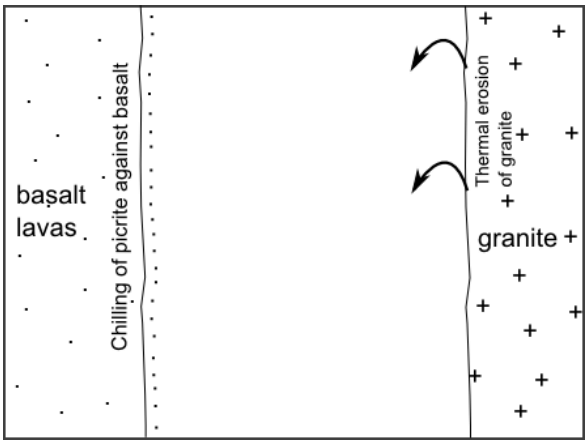

Figure 3.65: Crustal tension causes a conduit to open up in the lava pile and Loch Uisg Granite country rocks. Into this conduit, a highly magnesian magma entraining very magnesian xenocrysts is intruded. The emplacement occurs as a series of pulses of magma. The composition of these pulses is consistently high in Mg-rich Fo over the period of intrusion. Chilling of the picrite occurs against the (basalt) lavas and thermal erosion of the granite occurs.

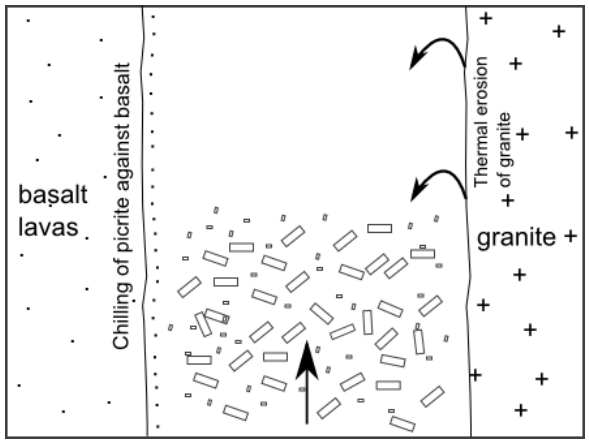

Figure 3.66: The initial pulse of crystal-rich magma is intruded into the conduit. The liquid has entrained highly magnesian olivine crystals (the large olivines) from a cumulate source. These are carried up into the conduit. The liquid carrying the xenocrysts is, itself, rich in highly magnesian olivine and starts to crystallize out small olivines, many of which are skeletal.

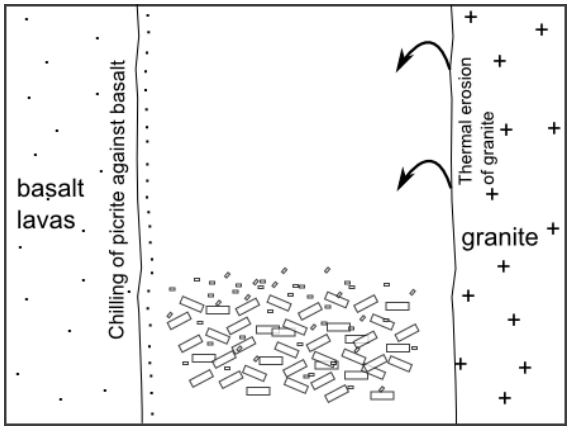

Figure 3.67: The first phase of crystal settling has taken place and a cumulate layer of high-Fo olivine builds up in the middle of the intrusion. The entraining liquid crystallizes as a finer-grained layer. Flow has stopped at this point.

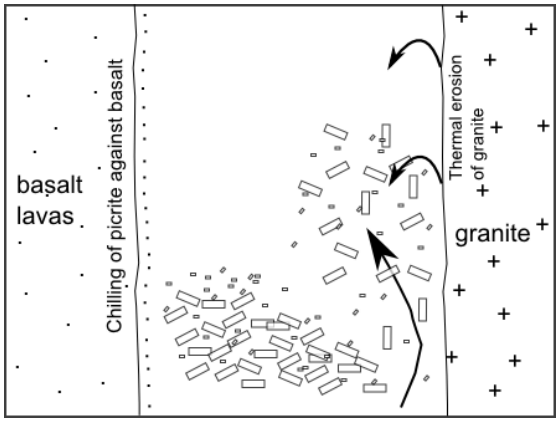

Figure 3.68: A second pulse of magma is injected into the conduit. This causes erosion of the existing layers resulting in a sloping erosion surface. The cumulate is disrupted and crystals are re-distributed, together with fresh material to produce another layer.

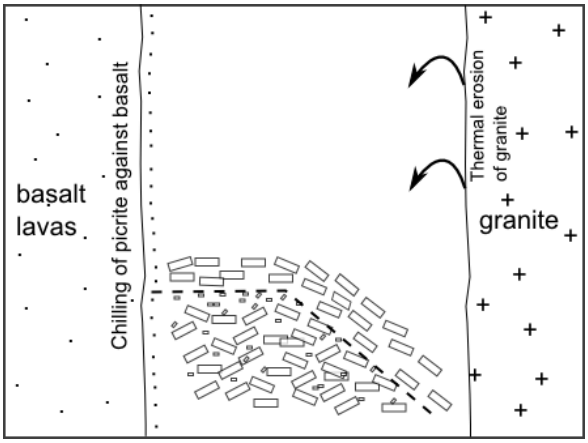

Figure 3.69: The second pulse of magma deposits a layer of olivine crystals over the eroded surface of the first layer, indicated by the dashed line. Settling occurs and the layer solidifies. Gradually, a complex layered sequence is built up.

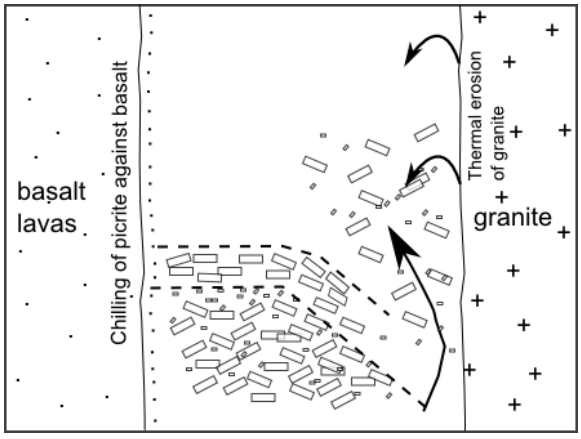

Figure 3.70: Further pulses of magma are intruded into the conduit, resulting in disruption of existing layers and the deposition of newer ones, using both fresh transported olivines as well as disrupted cumulate.

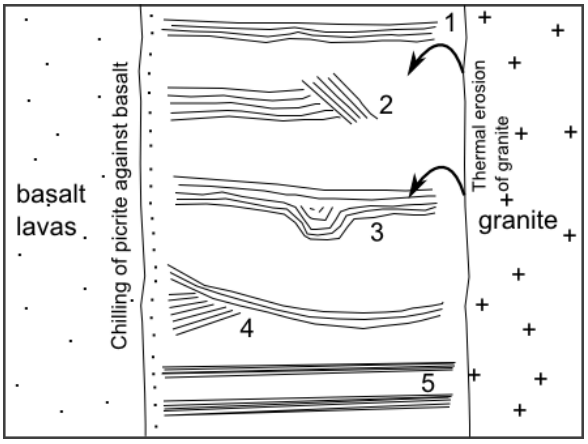

Figure 3.71: Typical layering, folding and slump structures seen in the Gleann Beag Intrusion. See text for details.

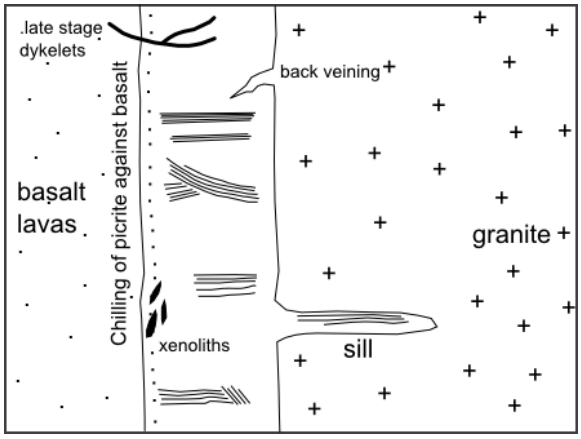

Figure 3.72: The overall scenario showing the intrusion, the sheets (Loch Uisg Cottage Sheet and Coille Sron nam Boc Sheet) and the relationships to the country rocks.

3.12 Occurrence of layered dykes and sills

Layered sills are globally abundant and several Hebridean examples of varying sizes, with similar compositions to the LUPS, have already been noted and described (*e.g.* Walker 1929; Drever and Johnston 1957, 1958, Upton *et al.* 2002, Andersen 2002). However, layered dykes are very uncommon, with only a few examples having been recorded, (*e.g.* the "Great Dyke" in Zimbabwe (Wilson

1982, 1996 Mushayandebvu *et al*. 1994 and the "Giant Dykes" of Southern Greenland, including the Eqaloqarfia layered dyke from Nunarssuit (Pulvertaft, 1965)). The only layered dyke of note in the BPIP is the Suisnish Dyke on Skye (Parslow 1976).

The Great Dyke in Zimbabwe (Wilson, 1982, 1996; Mushayandebvu *et al*. 1994) is a massive structure running for 550 km across the Zimbabwe craton. The Great Dyke seems not to be a true dyke *per se* but a series of near-contiguous layered igneous bodies emplaced along a line of weakness in the crust (Mushayandebvu *et al*. 1994). The 1.4 km long Gleann Beag Intrusion appears to be a contiguous body, with no internal contacts, and is several orders of magnitude smaller than the Great Dyke.

In the Gardar Province of southern Greenland, there is a suite of composite basic "Giant Dykes" (Upton *et al*. 2003). These range between 200 m and 800 m in width and can be traced over 140 km. These dykes display internally, synformally layered structures analogous to those of the Zimbabwe Great Dyke (Upton and Thomas 1978). Again, these dykes, although displaying layering and cumulus structures, are on a much greater scale than the Gleann Beag Intrusion.

The dyke which is most similar to the Gleann Beag Intrusion, in terms of morphology and extent, is the Suisnish Dyke in Skye (Parslow, 1976). It displays similarities in form and appearance to the Gleann Beag Intrusion: both belong to the BPIP; both dykes are picritic; both show horizontal to sub-horizontal layering and both are roughly of the same size. The Suisnish Dyke is traceable over 600 m, with an average width of 40 m. However, closer examination reveals differences between them:

The Suisnish Dyke is a simple parallel-sided planar, vertical body of rock that fits the description of a "dyke" perfectly.

The Gleann Beag Intrusion is a much more variable body, with an irregular, sinuous shape for much of its outcrop. Only at its NW and SE ends is it "dyke-like" in form. The middle section has a very irregular shape. In the upper section, the Gleann Beag Intrusion is clearly sheet-like in form, dipping at approximately 40 – 50°to the NE (Figures 3.25 and 3.26).

The Susinish Dyke displays distinct rhythmic layering normal to the contacts, consisting of alternating plagioclase-rich leucocratic and olivine-rich melanocratic layers. This regular, repeated pattern is not seen in the Gleann Beag Intrusion, where the layering shows a greater range of forms and structures.

The layers in the Suisnish Dyke are generally parallel to sub-parallel, dipping gently at 18° due west. In the Gleann Beag Intrusion, the layering, as described in Seection 3.11 above, is much more complex: truncation and slump structures are seen. The layering suggests a much more dynamic environment, with movement of melts, crystal mushes and erosion of cumulates.

Parslow (1976) suggests that a slower than normal cooling rate is required for the layering to develop and the mechanism proposed by the author is of an elevated local geothermal gradient. Emplacement at depth is discounted as the British Palaeogene Igneous Province has involved emplacement at high crustal levels (Thompson *et al*. 1972, Carmichael *et al*. 1974).

Modal values for the olivine agree with the picrite definition given by Drever and Johnston (1958) and Fo_{83} is common, determined by both chemical and optical means.

The shape and crystal boundary relationships of the olivine and plagioclase crystals are typical of cumulus rocks. The layering is parallel to sub-parallel with no cross-cutting relationships. Rhythmic layering without associated cryptic layering implies that gravity settling alone was not the only agent responsible for the dyke's development. The model proposed is of pulses of magma with flow differentiation taking place, then gravity settling taking over. The system was probably "open" and possibly a feeder conduit.

There appears to be very little in the way of subsequent research on the Suisnish Dyke and the drill core samples cannot currently be traced (J. Fathfull, *pers comm*.). Parslow (1976) is the main source of information but much of that particular work is quite limited in its scope. Mineral chemistry data for olivine and Cr-spinel were obtained using optical and wet chemical means. However, no SEM data were obtained.

In summary, the Gleann Beag Intrusion appears to be distinctly different. The few other rare examples of layered dykes are much larger bodies of rock, whose length and width are several orders of magnitude greater. The closest example in terms of general morphology, appearance and size is the Suisnish Dyke in Skye, but factors such as its modal olivine, MgO content and temperature of parental magma mean that its proposed mode of emplacement and petrogenesis is very different. The highly magnesian dykes of Rum (Upton *et al*. 2002) and the Horingbaai Dykes of Namibia (Thompson and Gibson, 2000) more closely represent the products of magmas similar to the LUPS. However, both these suites of dykes lack the cross-cutting layers and truncation features of the GBI.

3.13 Timing of emplacement

In order to estimate the timing of emplacement of the LUPS intrusions and where they occur within the timeframe of the Mull Palaeogene igneous history, several factors need to be considered:

1) Freshness of the rock, especially the olivine;
2) Relationship of the LUPS rocks to the country rocks;
3) Relationship of the LUPS rocks to the suites of cone-sheets;
4) Late veins cutting the LUPS intrusions.

3.13.1 Freshness of the rock

One of the most distinctive features of the LUPS intrusions is the freshness of the rock. All three intrusions display very fresh olivine. Alteration, where present, is minor and accounts for a very small percentage of any given olivine crystal. This is in stark contrast to the other mafic rocks in the area: the gabbro of the Loch Uisg Granite-Gabbro Intrusion shows pronounced alteration, imparting a greenish tinge to the rock and the dykes that make up the "Miscellaneous Minor Intrusions" suite display high levels of alteration. The Ben Buie Gabbro complex does include fresh olivine (Preston *et al*. unpublished data, Prout *et al*. 2002). This has been attributed to its size and low permeability. However, the smaller basic bodies in SE Mull are much more altered.

Although the LUPS intrusions are found in the vicinity of Centre 1 of the Mull Central Complex, it may well be that the lack of alteration indicates that they are of a much later date, possibly quite late in the igneous intrusive sequence. Rocks associated with Centre 3 display hydrothermal alteration, which continued for some time after the intrusive activity was over, so the freshness of the LUPS material suggests that they may even be later than the Centre 3 intrusions. Radiometric and / or palaeomagnetic analysis could possibly confirm this age relationship.

3.13.2 Relationship of the LUPS rocks to the country rocks

The LUPS intrusions cut the Loch Uisg Granite (although none are seen to cut the Loch Uisg Gabbro) and the basaltic country rocks, so they are clearly younger than these Centre 1 intrusions. The presence of orthopyroxene, although limited (Figure 3.49) suggests that the granite has, locally, been partially melted by the Gleann Beag Intrusion. There is also the possibility of back-veining, where, locally, felsitic dykelets are rarely seen cutting the picrite (Figure 3.15).

3.13.3 Relationship of the LUPS rocks to the suites of cone-sheets

None of the "early basic cone-sheets" indicated by "*bl*" on the BGS map (1992) are seen to cut the Gleann Beag Intrusion. These cone sheets strike almost at right angles to the trend of the dyke, but none appear to cut it. Therefore, the GBI appears to be younger than this particular suite of cone-sheets.

3.13.4 Late veins cutting the LUPS intrusions

Small dykelets can be seen cutting the Gleann Beag Intrusion at [NM 665 240] (Figure 3.29). The material is similar to the fine grained picrite although free of olivine and may represent the last remaining liquid to crystallise.

3.13.5 Implications

If the LUPS intrusions are indeed a late feature of the Mull igneous activity, then the implication is that there must have existed, at that time, beneath Mull, a hot Mg-rich body of picritic magma capable of entraining and transporting material from an even more Mg-rich cumulate. The location of the LUPS activity, in the SE of the island, implies that, although the focus of activity had moved NW from Centre 1 (Glen More) through Centre 2 (Beinn Chaisgidle) to Centre 3 (Loch Bà) (Emeleus and Bell, 2005), there must still have been some intrusive activity in the SE of the island, where hot, high-level magma chambers were still active. Although there was a "progression" of major intrusive activity from SE to NW, it seems likely, given the freshness and hence possible late age of the LUPS that this progression was in the form of a continuum rather than a series of discrete centres. It is also possible that intrusions similar to the LUPS might exist in the vicinity of Centres 2 and 3, although at the time of writing, none have been recorded as picritic intrusions. The Gleann Beag Intrusion was mapped by the Survey officers (BGS 1923, 1992) as an ordinary member of the Mull Dyke Swarm. It is possible that other dykes associated with the Mull Central Complex are also of a similar character. Extensive fieldwork would be required to establish if this is indeed the case.

Chapter 4: Miscellaneous Minor Intrusions

4.1 Introduction and state of knowledge prior to this study

In addition to the "Loch Uisg Gabbro" described in the Mull Memoir (Bailey *et al*,1924), now referred to as the Loch Uisg Granite-Gabbro Intrusion (BGS, 2012) and described in Chapter 2, and the Loch Uisg Picrite Suite described in Chapter 3, there are several other minor gabbroic intrusions that crop out around the eastern half of Loch Uisg. These are shown on Figure 4.1.

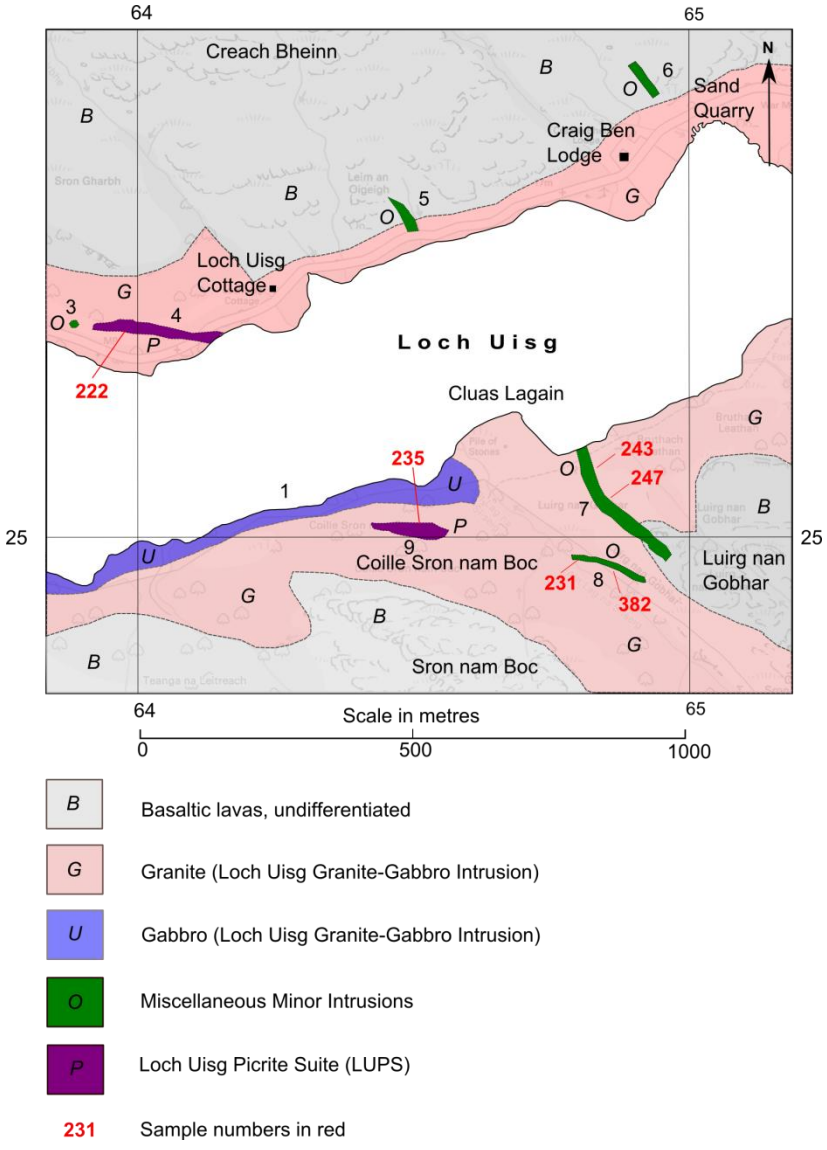

Figure 4.1: Simplified geological map of the eastern end of Loch Uisg, showing the main lithologies (Loch Uisg Granite-Gabbro intrusion) and the various gabbroic intrusions described in Chapter 4.

The "Miscellaneous Minor intrusions" (MMI) are (numbers in brackets from Figure 4.1):

- #3 A small unnamed intrusion *ca*. 100 m west of Loch Uisg Cottage on the north side of Loch Uisg [NM 6392 2539];
- #5 A small dyke that forms a prominent exposure beside the road between Craig Ben Lodge and Loch Uisg Cottage on the north side of Loch Uisg;
- #6 A dyke *ca*. 100 m west of the sand quarry at the eastern end of Loch Uisg;
- #7 A dyke that runs up the hill from the south shore of Loch Uisg, *ca*. 200m east of Cluas Lagain;
- #8 A small dyke, that runs up the hill from the south shore of Loch Uisg, *ca*. 300 m SE of Cluas Lagain.

All of these intrusions have dyke-like outcrops, apart possibly from #3, and trend approximately NW, parallel to the Mull Dyke Swarm (Emeleus and Bell, 2005). Much of the ground is covered in vegetation and these dykes are traceable for short distances only. Exposed contacts are rare. None of these intrusions are considered in any detail in the Mull Memoir by Bailey *et al*. (1924), although #5 is indicated on the BGS (1992) map as a member of the "*miscellaneous gabbros and dolerites*" and #6 and #7 are depicted on it in the category "*dolerite, basalt and teschenite*".

4.2 Field relationships

4.2.1 Intrusion #3 [NM 6392 2539] (Figure 4.2): A small exposure of gabbro intruded into the Loch Uisg Granite, although no contacts are visible. It is a coarse-grained, medium to dark grey, homogenous mass of gabbro, with abundant secondary epidote, in complete contrast to the fresh, olivine-rich (picritic) Loch Uisg Cottage Sheet (Chapter 3) that crops out *ca*. 10 m to the east.

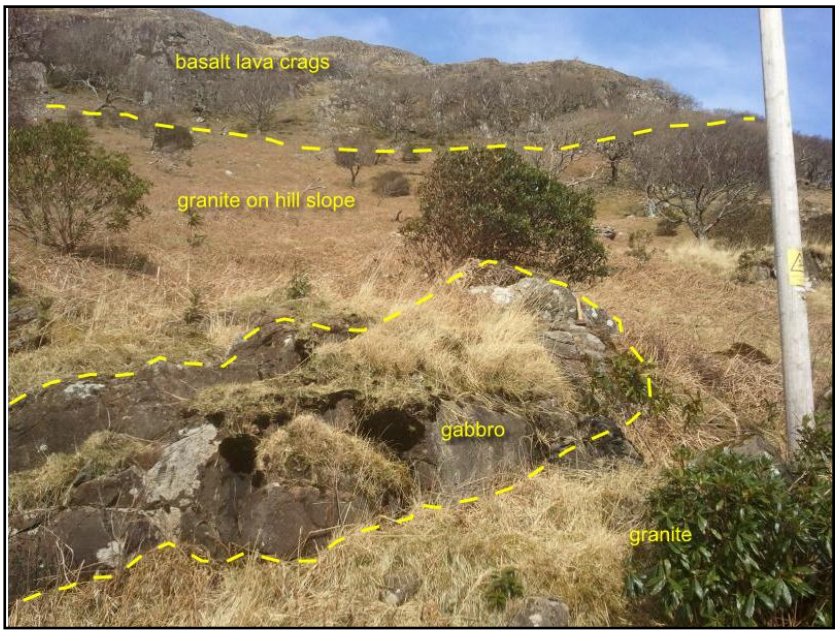

Figure 4.2: View of Intrusion #3, looking north. Hammer at right-hand end of exposure for scale (45cm long). The exposure is relatively featureless and is composed of a coarse-grained gabbro.

4.2.2 Intrusion #5: [NM 6454 2553] (Figures 4.3 and 4.4): This intrusion forms a very prominent exposure beside the road, between Craig Ben Lodge and Loch Uisg Cottage, on the north side of Loch Uisg. No contacts are visible. It is approximately 10 m wide, can be traced for *ca*. 50 m, and trends at *ca*. 140°. The exposure continues to the lochside but is largely inaccessible. Its exposure pattern suggests that it is a short, wide dyke. It intrudes both the granite and the country-rock basaltic lavas (Figure 4.1). The rock is a homogenous medium to dark grey gabbro. It is highly hydrothermally altered with abundant epidote (Walker 1971; Emeleus and Bell 2005).

Figure 4.3: View of Intrusion #5, looking east on the road on the north side of Loch Uisg. Gabbro crag is *ca*. 10m high just beyond the obvious evergreen shrubs in the left-hand part of the view. The exposure is relatively featureless and is composed of a coarse-grained gabbro; at the far end of the exposure the paler tinge is a fresher surface where the rock has been removed during construction of the road.

Figure 4.4: View of Intrusion #5, looking NW from the uppermost part of the crag shown in Figure 4.3. The dyke-like outcrop pattern is obvious, although no contacts with the country-rocks are seen.

4.2.3 Intrusion #6: (Sand Quarry Dyke) [NM 6490 2588] (Figure 4.5): This intrusion shows a much more dyke-like structure and intrudes the basaltic lavas. It is located 100 m west of the prominent sand quarry at the eastern end of Loch Uisg, where it forms a 10 m wide outcrop trending 325°, where it can be traced for *ca*. 60 m. Contacts are not visible, but can be confidently inferred. The intrusion is obviously finer-grained towards its inferred margins, elsewhere it is relatively coarse-grained. If its outcrop continues to the SE it should cut the Loch Uisg Granite, typical of the other gabbroic intrusions described in this chapter; however, exposure is very poor. The rock is, like the other intrusions of this grouping, a coarse-grained gabbro showing significant hydrothermal alteration.

Figure 4.5: View of Intrusion #6, looking NW. At this location, the intrusion is *ca*. 4 m wide (hammer for scale; *ca*. 45 cm long). The smooth-weathering surfaces are ice-moulded and contrast with the more hackly surfaces where ice plucking (?) has occurred.

4.2.4 Intrusion #7: [NM 6483 2517] (Figure 4.6): This intrusion is shown on the BGS map (1992) as a member of the Mull Dyke Swarm. It is a medium to coarse grained gabbro, very altered and composed mainly of pyroxene and plagioclase. It has been mapped as a dyke-like body, but there are significant differences in texture and mineralogy between samples taken from the lower and upper sections. It has a tapering outcrop trending 150° from the south shore of Loch Uisg where it forms a prominent headland. It intrudes both the Loch Uisg Granite

and the basaltic lavas. The dyke eventually disappears at the point shown in Figure 4.6. At [NM 6488 2503], where the dyke is 2 m wide, another basaltic dyke appears to cut it, although exposure is poor and the field relationships are difficult to determine. No xenoliths are observed.

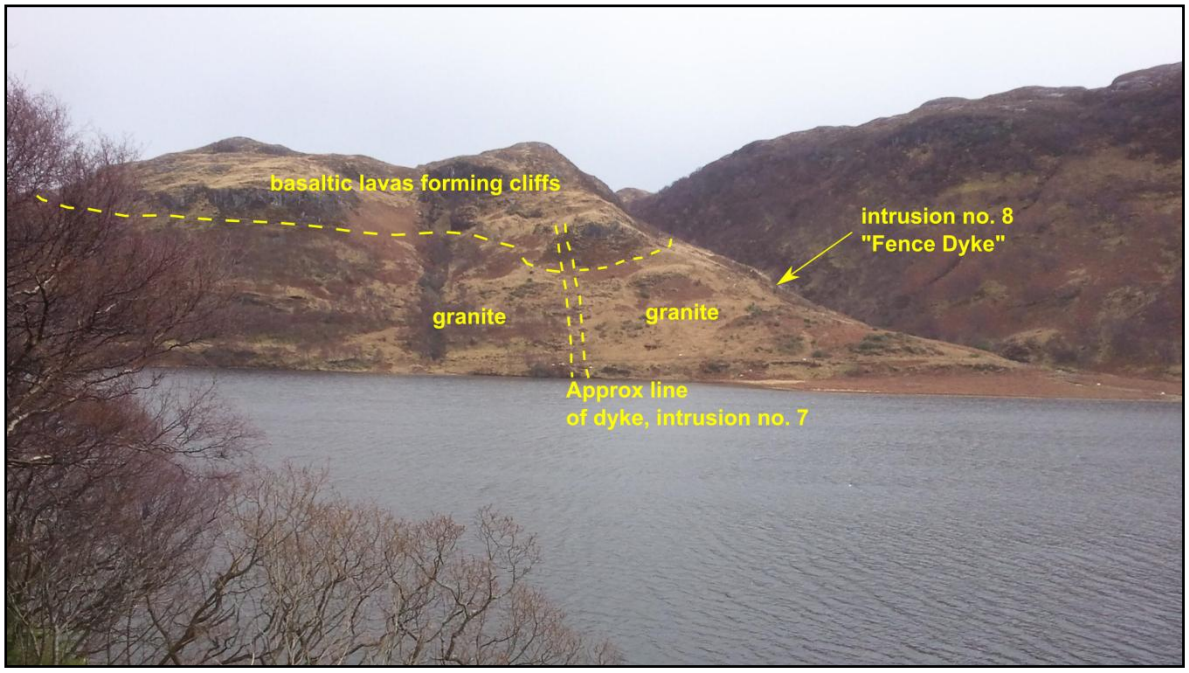

Figure 4.6: View of Intrusion #7, looking SE from the north side of Loch Uisg. Its contacts with the Loch Uisg Granite and the basaltic lavas are indicated. Intrusion #8 is also shown.

4.2.5 Intrusion #8: [NM 64832497] (Figure 4.7): This intrusion forms a small outcrop close to a very prominent fence which runs right across the Laggan Peninsula. It forms an obvious structure running up the hill, again roughly following the NW-SE regional trend. Figure 4.6 shows the location relative to Intrusion #7. No contacts are discernable in the field so it is impossible to determine the attitude of its contacts. The rock is a coarse gabbro, dominated by pyroxene and plagioclase and heavily altered. It has a distinctive appearance in the field in that the rock displays the curved joint fractures that make it appear more like a member of the Loch Uisg Picrite Suite. The rock is relatively homogenous, with no visible layering, xenoliths or any other internal structures. It appears to cut only the granite as it is not traceable as far as the contact with the country rock basalt lavas.

Fig 4.7: Intrusion #8, the "Fence Dyke" seen looking in a NW direction towards Loch Uisg.

4.3 Petrography and mineral chemistry of the Miscellaneous Minor Intrusions

4.3.1 Sampling

In hand specimen, the rocks show considerable differences in appearance across the five intrusions that make up the suite. They are typically dark grey, medium-grained with a greenish tinge due to post-intrusive hydrothermal alteration. Intrusion # 5 (Figures 4.3 and 4.5) contains plagioclase phenocrysts up to 2 mm in a medium grained groundmass; the others do not display this porphyritic character.

Four samples were selected for petrographic analysis: two from intrusion #7 and two from intrusion #8. These samples were chosen because of the proximity of the intrusions to both the LUPS and the Loch Uisg Gabbro (Table 4.1).

Sample No	Location	Grid Reference
243	Intrusion #7, south shore of Loch Uisg, near the loch shore	[NM 6483 2517]
247	Intrusion #7, south shore of Loch Uisg, approx. half way along the outcrop	[NM 6483 2505]
231	Intrusion #8, "Fence Dyke", south Loch Uisg, lower end of dyke	[NM 6483 2497]
382	Intrusion #8, "Fence Dyke", south Loch Uisg, half way along the outcrop	[NM 6480 2499]

Table 4.1: The Miscellaneous Minor Intrusions samples chosen for analysis.

4.3.2 Petrography

Two of the intrusions were sampled for optical and SEM analysis. Sample 382, from which a polished thin section was made, was taken from Intrusion #8, the "Fence Dyke" (Figure 4.7). Samples 243 and 247 (ordinary optical thin sections) were taken from the dyke which runs uphill in a SE direction from the shore of Loch Uisg, shown in Figure 4.6 as intrusion number 7. Sections from both intrusions are shown in Figures 4.8 to 4.11.

Fig 4.8:. Thin section view (PPL) of sample 382, intrusion #8 the "Fence Dyke" from about the middle of the dyke. Rock slice width: 40 mm

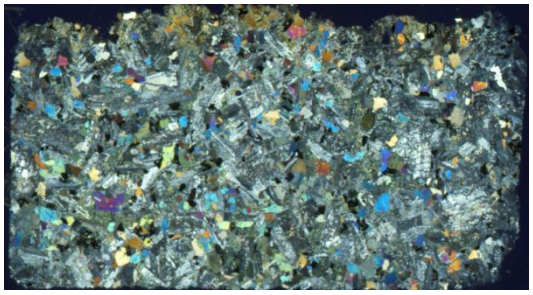

Fig 4.9: Thin section view (XPL) of sample 382, intrusion #8 the "Fence Dyke" from about the middle of the dyke. Rock slice width: 40 mm

Fig 4.10: Thin section view (PPL) of sample 243, Intrusion #7. Rock slice width: 40 mm.

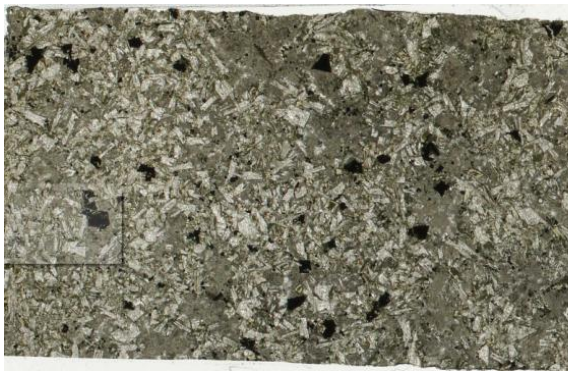

Fig 4.11: Thin section view (PPL) of sample 247, Intrusion #7. Rock slice width: 40 mm.

Fig 4.12: Thin section view (PPL) of sample 231, Intrusion #8, the "Fence Dyke". Rock slice width: 40 mm.

As can be seen in Figures 4.10 and 4.11, although samples 243 and 247 are taken from what appears to be the one continuous intrusion, and which has been mapped as such on the BGS map (1924,1992), the samples look very different. Although both samples were taken from apparently central positions in the dyke, 247 may represent a chilled margin.

4.3.3 Mineral Phases

The individual mineral phases are now described in detail. Considerable variation in the habit of the individual minerals is seen, and the degree of alteration is highly variable.

4.3.3.1 Olivine

Olivine is rarely seen in sample 243, (Intrusion #7), either as fresh sub-hedral crystals or as pseudomorphs. Figures 4.13 and 4.14 show the two habits of the olivine. No olivine was observed in sample 251, which is also from intrusion #7, but at a higher elevation up the hillside. Sample 382, from Intrusion 8, the Fence Dyke, rarely contains olivine pseudomorphs (Figure 4.15)

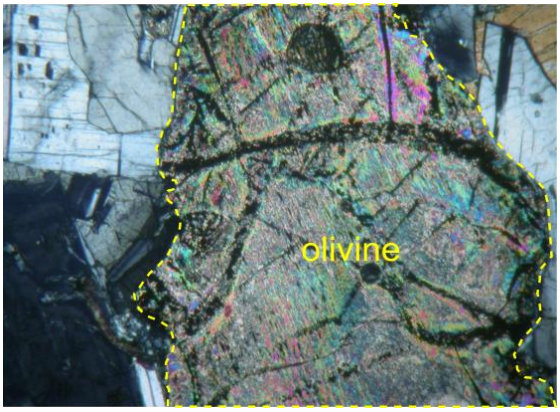

Fig 4.13: Thin section view (XPL) of sample 243, Intrusion #7 showing an olivine pseudomorph in a groundmass of mainly plagioclase. Some clinopyroxene is visible in the top RH corner. HFoV: 2 mm.

Fig 4.14: Thin section view (XPL) of sample 243, Intrusion #7 showing a fresh olivine crystal. HFoV: 2 mm.

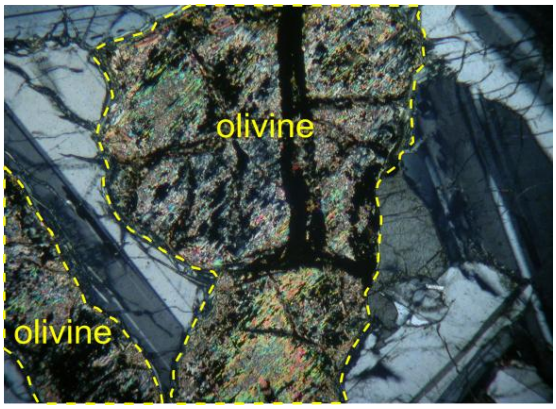

Fig 4.15: Thin section view (XPL) of sample 231, Intrusion #8, showing olivine pseudomorphs in a groundmass of mainly plagioclase. HFoV: 2 mm.

4.3.3.2 Plagioclase

The plagioclase in this sundry suite of intrusions varies considerably in appearance. It is typically fresh and unaltered, but one of the samples, 382 from Intrusion #8 shows considerable alteration. In some of the samples it appears to form almost a cumulate texture. In others it is clearly in an ophitic relationship with clinopyroxene (Figures 4.16 to 4.19).

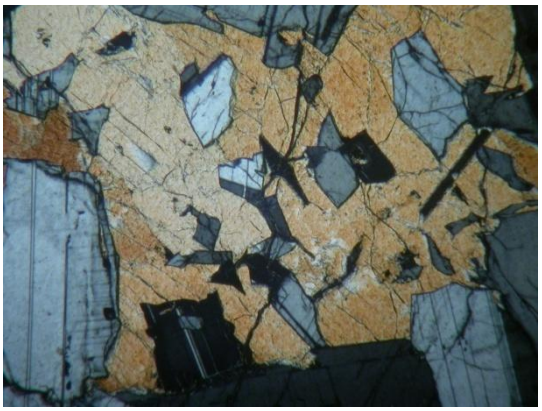

Fig 4.16: Thin section view (XPL) of sample 231, Intrusion #8 showing a large clinopyroxene oikocryst enclosing plagioclase crystals. HFoV: 2 mm.

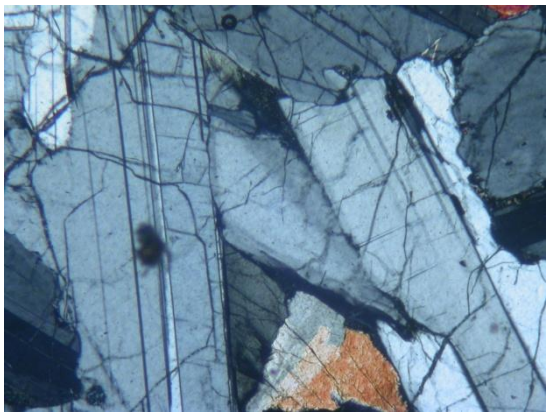

Fig 4.17: Thin section view (XPL) of sample 231, Intrusion #8, showing large crystals of plagioclase forming a cumulate-like mass. HFoV: 2 mm.

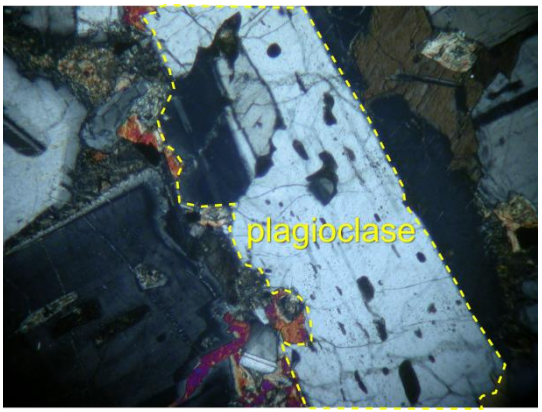

Fig 4.18: Thin section view (XPL) of sample 243, Intrusion #7, showing a large plagioclase crystal containing melt inclusions. HFoV: 2 mm.

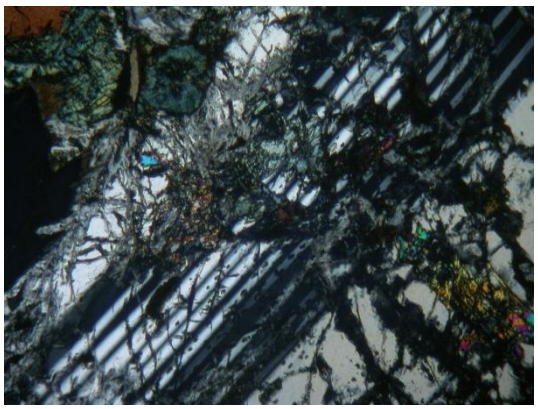

Fig 4.19: Thin section view (XPL) of sample 382, Intrusion #8, showing a large highly altered plagioclase crystal. HFoV: 2 mm.

4.3.3.3 Clinopyroxene

Clinopyroxene appears to be reasonably fresh in most of the samples. It displays a variety of textures, from single crystals in a predominantly plagioclase groundmass (Figure 4.20) to ophitic texture crystals with enclosed plagioclase (Figures 4.16 and 4.21).

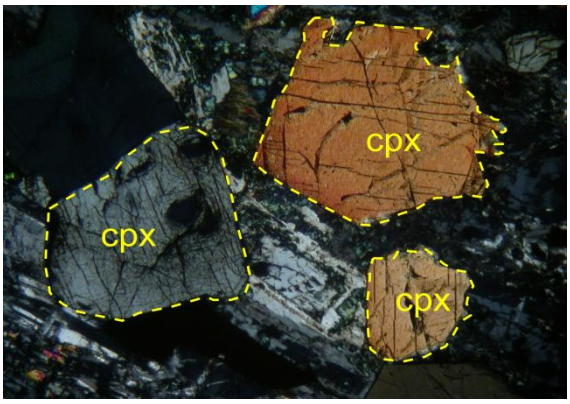

Fig 4.20: Thin section view (XPL) of sample 382, Intrusion #8, showing clinopyroxene crystals (cpx) in a groundmass of altered plagioclase. HFoV: 2 mm.

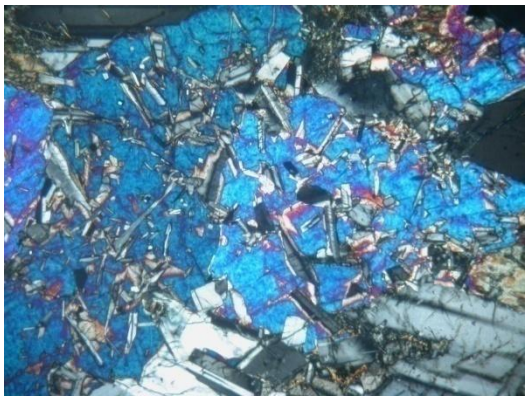

Fig 4.21: Thin section view (XPL) of sample 243, Intrusion #7, showing a large clinopyroxene oikocryst enclosing very small, thin plagioclase crystals. HFoV: 2 mm.

4.3.3.4 Oxides

The main oxide mineral present is magnetite. In samples 243 and 251, from Intrusion #7, magnetite is relatively rare. However, the Fence Dyke, Intrusion #8, represented by samples 231 and 382, contains a lot more magnetite. This difference between the two intrusions is clearly seen in the full-slide images in Figures 4.8 to 4.12.

Figures 4.19 to 4.20 show SEM electron back-scatter images of the magnetite found in sample 382. Skeletal development of magnetite is illustrated in Figures 4.22 and 4.23.

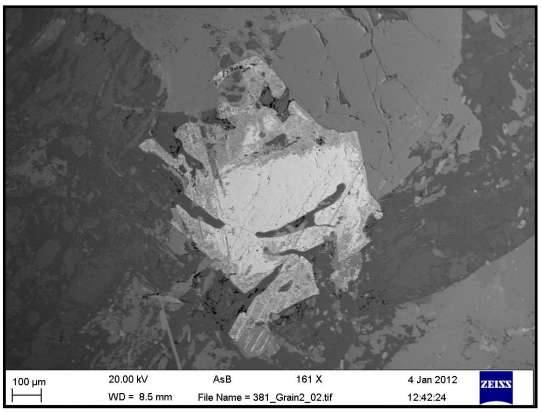

Figure 4.22: SEM electron backscatter image of sample 382, Intrusion #8, showing a magnetite crystal displaying skeletal texture. HFoV: 1.8 mm.

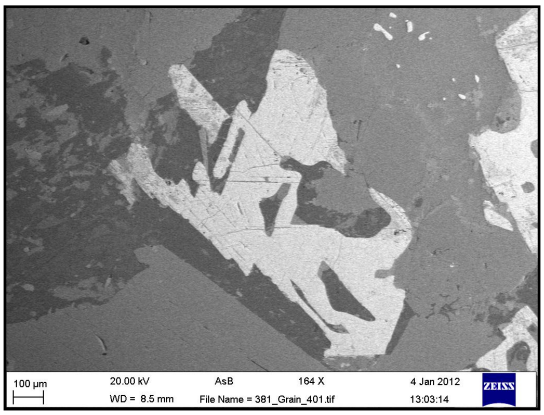

Figure 4.23: SEM electron backscatter image of sample 382, Intrusion #8, showing the embayed and lobate appearance of a skeletal magnetite crystal. HFoV: 1.8 mm.

Skeletal development of magnetite is illustrated in Figures 4.22 and 4.23.

4.3.3.5 General observations on the sections

In both of the sampled dykes, Intrusion #7 and Intrusion #8, there appears to be considerable variation in the mineralogy, especially Intrusion #8, the Fence Dyke. Sample 231 taken low down from Intrusion #8, near the stream bed, appears to be much fresher than sample 382 taken from about half way up the same dyke, which displays considerable alteration to the plagioclase.

Considerable variation in the minerals can also be seen within individual thin sections. The olivine in sample 243 from Intrusion #7 appears as fresh crystals as well as pseudomorphs. It also appears as small granular crystals as well as larger phenocrysts. In sample 247, taken from the same intrusion but higher up the hillside, no olivine is seen.

In sample 231 from Intrusion #8, the plagioclase appears to have a cumulate-like texture similar to the Loch Uisg Gabbro at Laggan, as well as displaying strong ophitic and sub-ophitic textures (Figures 4.16 and 4.17). Figures 4.16 and 4.19 both show ophitic texture involving a large clinopyroxene crystal but the enclosed plagioclase chadacrysts vary considerably in size. Some of the plagioclase from sample 243 displays melt inclusions in fairly fresh crystals. Figure 4.18.

Intrusion #8, the Fence Dyke, is the MMI intrusion which, in external appearance most closely resembles the rocks of the LUPS. However, examination of the mineralogy by both optical and SEM techniques reveals that it is quite different and clearly a separate intrusion.

4.3.4 Mineral chemistry

Sample 382, from the Fence Dyke, Intrusion #8, was prepared as a polished thin section for SEM analysis. Mineral phases analysed include clinopyroxene and magnetite. Plagioclase was not analysed due to its severe alteration.

4.3.4.1 Clinopyroxene

The data for clinopyroxene are plotted on the Diopside – Hedenbergite – Enstatite – Ferrosilite quadrilateral in Figure 4.24. The data plot in a cluster similar to the LUPS rocks and the Glen Libidil outcrop of the Loch Uisg Gabbro. The plot is based on sample 382 from the MMI suite.

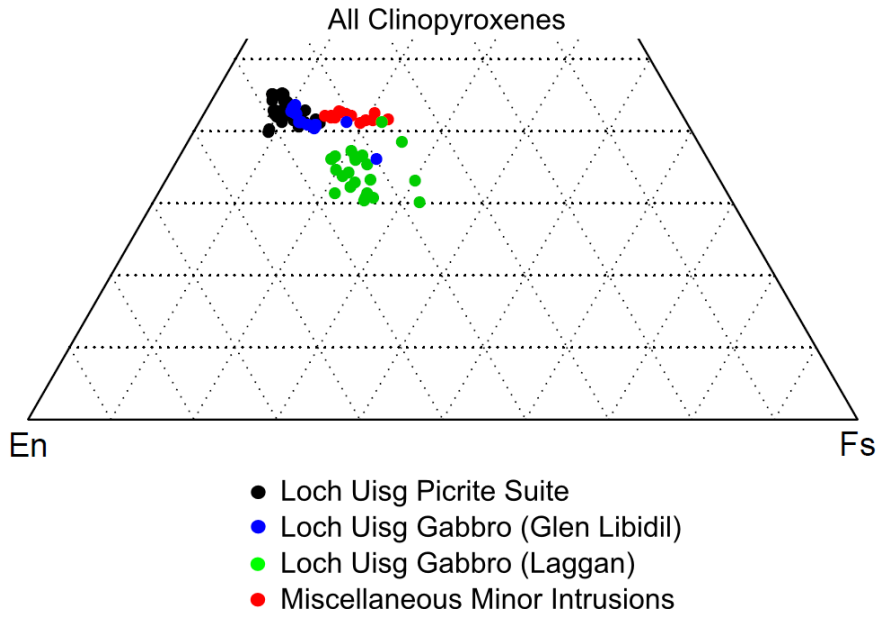

Figure 4.24: Plot showing the clinopyroxene data for all the rocks in this study, the MMI sample (382) shown in red.

4.3.4.2 Magnetite

The magnetite in sample 384, from Intrusion 8, was analysed using the SEM. Figures 4.25 to 4.28 show various elements plotted against FeO in wt.%.

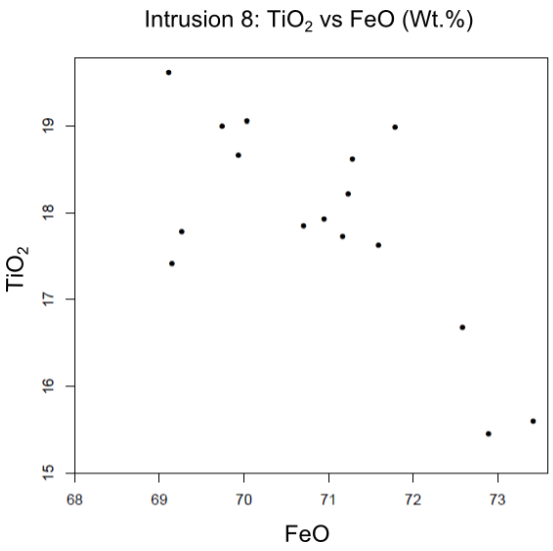

Figure 4.25: TiO_2 plotted against FeO.

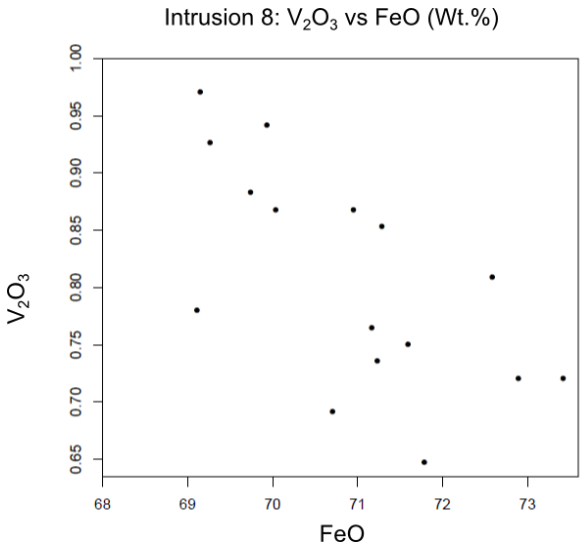

Figure 4.26: V_2O_3 plotted against FeO.

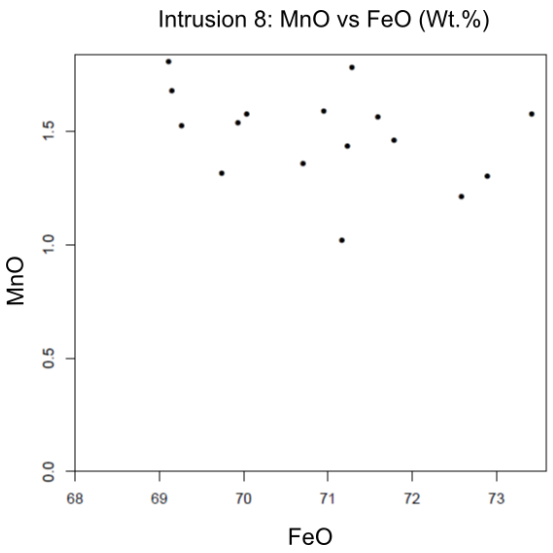

Figure 4.27: MnO plotted against FeO.

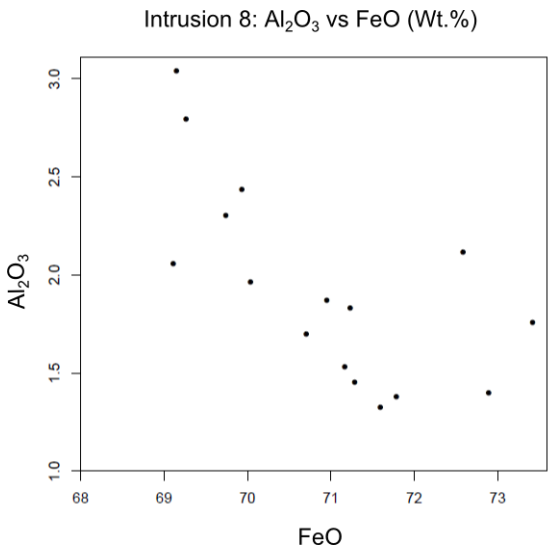

Figure 4.28: Al_2O_3 plotted against FeO.

Figures 4.25 to 4.28: Plots of TiO_2, V_2O_3, MnO and Al_2O_3 against FeO for magnetite in sample 384 from Intrusion #8, the "Fence Dyke". A fairly wide scatter of data points is observed, but the overall trend is for a decrease in each of the elements plotted with increasing FeO, which is the expected pattern.

Overall, given the limited amount of data available, there does not appear to be anything exceptional about the mineral chemistry of the MMI rocks. Given the wide variation in mineralogy observed in the thin sections and the variation seen in the field in hand specimen for some of the intrusions, extensive sampling would be required to establish any particular patterns.

4.4 Discussion

4.4.1 Classification as a "suite"

For the purposes of this study the "Miscellaneous Minor Intrusions" are grouped together as a suite for the following reasons:

1) They are all gabbroic in character, unlike most of the other typical members of the Mull Dyke Swarm, which texturally tend to be basaltic or doleritic.

2) They are clearly dyke-like in form, running for the most part, in a NW-SE direction. Intrusion #4 is a possible exception to this trend.

3) They are quite unlike the rocks of the LUPS or the gabbroic units of the Loch Uisg Granite-Gabbro intrusion. In this respect, they represent an "everything else" group.

In the published literature (Bailey *et al*. 1924; BGS 1923, 1992), the MMI are either not mapped, or are classified as "eD – Miscellaneous gabbros and dolerites" or as "M – dolerite, basalt and teschenite" members of the Mull Dyke Swarm.

4.4.2 Field evidence

The MMI have many field characteristics in common. They nearly all run on a NW-SE trend, in keeping with the regional trend of the Mull Dyke Swarm. Only one of the dykes, Intrusion #7, is traceable over any significant distance, but as can be seen from the images in Figures 4.10 and 4.11, there are question marks over whether it is indeed one continuous intrusion. Most of the dykes can only be

traced over short distances. Contacts with the country rocks are not observed in the field, so it is not possible to establish with any certainty the nature of the contacts with the surrounding granite and basalt lavas. However, at places where the contact can be inferred to within a few centimetres, such as Intrusion #6 (Figure 4.5), the rock is noticeably finer grained, implying a degree of chilling at the margins.

4.4.3 Relationship to country rocks

The dykes of the MMI suite nearly all appear to cut the Loch Uisg Granite. The exception is Intrusion #6 which is only observed cutting the basalt lavas but this may be due to poor exposure in the area. Intrusions #5 and #7 are clearly seen to intrude both the basalt lavas and the granite.

None of the dykes appears to cut the Loch Uisg Gabbro. Intrusion #8 which is closest to the easternmost outcrop of the LUG ends in the stream bed 300 m from the inferred contact of the LUG and the granite.

4.4.4 Relationship to the Loch Uisg Gabbro

An obvious question is “Are the MMI simply apophyses of the Loch Uisg Gabbro?” There are several factors which make this unlikely:

1) The rocks are of totally different character. Even allowing for lateral heterogeneity within the LUG, the MMI are generally coarser and show greater alteration. The LUG at the eastern end of Loch Uisg, where the MMI are found is medium grained and almost doleritic in character. It is also less altered.
2) Although poikilitic texture is recorded in some of the thin sections, it is not observed in the field. This is in strong contrast with the LUG, where poikilitic texture is clearly visible.
3) Based on the limited number of samples available, the mineral chemistry appears to be slightly different. The plot for clinopyroxene displays a clear gap between the LUG values and those for the MMI. The MMI are more Ca-rich (Figure 4.24).

From the limited evidence available, it therefore appears that the MMI and the LUG are separate intrusions.

4.4.5 Emplacement

The orientation of these intrusions matches the regional trend for the Mull Dyke Swarm. It appears that intrusion occurred in the same stress field associated with the crustal tension and dilation associated with the opening up of the Atlantic Ocean. The source material is probably the same mafic / ultramafic material which appears to form a large body underlying Mull (Bott & Tantrigoda, 1987). Like the dykes of the Mull Dyke Swarm, the dykes described here may well have been conduits feeding material to higher levels, which have now been removed by erosion.

4.4.6 Age

The intrusions all lie within the "zone of pneumatolysis" (Bailey *et al*. 1924) where hydrothermal alteration has affected the rocks, resulting in abundant secondary epidote. With the exception of Intrusion #6, they all intrude the granite. Two of the dykes are also seen cutting the basalt lava country rocks. One of the dykes, Intrusion #7, is clearly cut by a dyke of the Mull Dyke Swarm. From this evidence, they probably post-date the granite of the Loch Uisg Granite-Gabbro Intrusion, but it is not possible in this study to state with any certainty a more accurate estimate of age.

Chapter 5: Summary

There are three distinct suites of mafic and ultramfic rocks in the south-eastern area of the Isle of Mull. This study has classified them as:

1. The Loch Uisg Granite-Gabbro Intrusion
2. The Loch Uisg Picrite Suite
3. Miscellaneous Minor Intrusions

5.1 The Loch Uisg Granite-Gabbro Intrusion

This intrusion, originally described in the Memoir (Bailey *et al.* 1924) as two intrusions - the Loch Uisg Gabbro and the Loch Uisg Granophyre still remains enigmatic. The field relations and topography of the intrusion have been described in more detail but the exact relationship between the two components of the intrusion remains unclear. It has not been possible to describe with certainty the order of emplacement of the two lithologies. Further evidence for magma mixing along a hybridized zone is presented but more extensive sampling and analysis would be required to ascertain the exact nature of this phenomenon. The new petrographic and mineral chemistry data from Loch Uisg gabbro, although limited, indicate that its surface exposures are much more evolved than most of the other exposed gabbro intrusions in Mull and the other Scottish Palaeogene centres. Its relationship with the overlying granite remains uncertain, although localities have been identified where small-scale digging/excavation is likely to reveal critical contacts, which might resolve the current uncertainty.

5.2 The Loch Uisg Picrite Suite

The LUPS intrusions represent a style of magmatism not previously recognised on Mull. They bear a strong resemblance to certain picritic rocks of Rum, especially the M9 dyke described by Upton *et al.* (2002), the peridotite plugs of Rum

(Holness *et al*. 2012) and other picritic rocks from the Isle of Skye (Drever & Johnston 1957, 1958, 1962) and Gibb (1968). However, the LUPS appears to be fresher, displaying little alteration and occurs as larger intrusions compared to the M9 and associated dykes of Rum. They are similar in many respects to the Rum plugs (Holness *et al*. (2012) both in terms of field appearance, layering and mineral chemistry. These rocks, the LUPS from Mull and the picrites and peridotites from Rum, with extremely magnesian olvine compositions, confirm the role of hot picritic magmas in the Scottish Palaeogene central complexes, and offer new opportunities to examine their genesis, and role in high level magmatic systems.

The M9 picrite and related rocks have been the subject of much study (J. McLurg, unpub PhD thesis, Univ. Edinburgh, 1983; Upton et al. 2002; Holness et al. 2012). The LUPS intrusions imply that these apparently rare highly magnesian intrusions may actually be a more common component in the development of the central complexes within the British Palaeogene Igneous Province.

The presence of the LUPS rocks, and especially the largest body, the Gleann Beag Intrusion indicates that extremely hot, highly magnesian magma was available at high crustal levels in SE Mull, late in the evolution of the Mull Central Complex. The evolution of the Central Complex is therefore not a simple story of migration from Centre 1 in the SE to Centre 3 (Loch Bà) in the NW. Given that the Centre 3 intrusions show significant hydrothermal alteration, it is even possible that the near-pristine LUPS rocks in SE Mull may be among the youngest intrusions in Mull. Confirmation of this would require radiometric and/or palaeomagnetic dating.

One of the most distinctive features of the LUPS intrusions, and especially the Gleann Beag Intrusion, is the presence of extensive layering. Much of this layering displays features such as erosion surfaces, cross cutting and slump structures that are common in large magma chambers such as those found in Rum and Skaergaard. These features in such a relatively small intrusion are almost certainly due to the vertical and lateral emplacement of crystal-laden magma in an open conduit-type system. The presence of such structures in a minor ultramafic body like the Gleann Beag Intrusion is very unusual.

5.3 Miscellaneous Minor Intrusions

A range of other gabbroic rocks occurs in the Loch Uisg are of SE Mull which occur as small dyke-like and plug-like bodies. Although they appear to follow the same NW-SE trend, these intrusions appear to be significantly different from the Mull Swarm Dykes. Although morphologically distinct from the main Loch Uisg gabbro, they appear similar in their mineral chemistry, and probably share a similar early Centre 1 (Glen More) age, with extensive hydrothermal alteration.

References

ANDERSEN, J.C.Ø., POWER, M.R. & MOMME, P. 2002. *Platinum-group elements in the Palaeogene North-Atlantic igneous province*. Cabri L J (ed.). The Geology, Geochemistry, Mineralogy and Mineral Beneficiation of Platinum-Group Elements. Canadian Institute of Mining and Metallurgy, Special Volume 54, p. 637–667

ARNDT, N.T., LEHNERT, K. & VASIL'EV, Y. 1995. *Meimechites: highly magnesian alkaline magmas from the subcontinental lithosphere?* Lithos **34**, 41–59.

BAILEY, E.B., CLOUGH, C.T., WRIGHT, W.B., RICHEY, J.E.& WILSON, G.V. 1924. *Tertiary and Post-Tertiary Geology of Mull, Loch Aline and Oban*. Memoir of the Geological Survey of Great Britain, HMSO, Edinburgh.

BOTT, M.H.P & TANTRIGODA, D.A., *Interpretation of the gravity and magnetic anomalies over the Mull Tertiary intrusive complex, NW Scotland.* Journal of the Geological Society 1987; v. 144; p. 17-28.

CARMICHAEL,I.S., TURNER, F.J., VERHOOGEN, I. *Igneous Petrology*. McGraw-Hill, New York, 1974.

BGS, 123,1992. *Eastern Mull*, S44W.

BOWEN,N.L, *The Evolution of Igneous Rocks*, 1928.

DONALDSON, C. H., 1975. *Petrology of Anorthite-bearing Gabbroic Anorthosite Dykes in northwest Skye*. Journal of Petrology, 18, **(4)**, 595 -620.

DREVER, H, & JOHNSTON, R, 1957. *Crystal growth of forsteritic olivine in magmas and melts*. Transactions of the Royal Society of Edinburgh,**63**, 289 – 315.

DREVER, H, & JOHNSTON, R, 1958. *The Petrology of Picritic Rocks in Minor Intrusions – A Hebridean Group*.Transactions of the Royal Society of Edinburgh, LXIII, Part III, 459 – 499.

EMELEUS, C.H. & BELL, B.R. 2005. *British Regional Geology: The Palaeogene volcanic districts of Scotland* (4th edn). British Geological Survey, Nottingham.

FALLOON, TREVOR J., DANYUSHEVSKY, LEONID V., ARISKIN, ALEXEI.,GREEN, DAVID H., FORD, CLIFFORD E., 2007. *The application of geothermometry to infer crystallisation temperatures of parental liquids: Implications for the temperature of MORB magmas*. Chemical Geology, 2007. Volume 241, Issues 3–4, Pages 149-374.

FRANCIS, D. 1985. *The Baffin Bay lavas and the value of picrites as analogues of primary magmas*. Contributions to Mineralogy and Petrology **89**, 144–54.

GIBB, F.G.F. 1968. *Flow Differentiation in Xenolithic Ultrabasic Dykes of the Cuillins and the Strath aird Peninsula, Isle of Skye, Scotland.* Journal of Petrology, 9, (**3**), 411 – 443.

GIBB, F.G.F. 1971.*Crystal-Liquid Relationships in Some Ultrabasic Dykes and Their Petrological Significance.* Contributions to Mineralogy and Petrology, **30**, 103 – 118.

GIBSON, S.A. 1990. *The geochemistry of the Trotternish sills, Isle of Skye: crustal contamination in the British Tertiary Volcanic Province*. Journal of the Geological Society 1990, v.147; p1071-1081.

GILLESPIE, M.R. & STYLES, M.T. 1999. *BGS Rock Classification Scheme, Vol 1, Classification of Igneous Rocks.*British Geological Survey Research Report, (2nd Edition). RR 99-06.

GILLESPIE, M.R., CAMPBELL,S.D.G., STEPHENSON, D. 2012. *BGS classification of lithodemic units: a classification of onshore Phanerozoic intrusions in the UK* . BGS Research Report RR/12/01.

HANSEN, J.,JERRAM, D.A., McCAFFREY, K.,PASSEY, S.R., *The onset of the North Atlantic Igneous Province in a rifting perspective*. Geological Magazine, **146** (3), 2009; 309 – 325.

HARKER, A. 1904. *The Tertiary Igneous Rocks of Skye*. Memoir of the Geological Survey of Great Britain, HMSO, Edinburgh.

HERZBERG, C. & GAZEL, E. 2009. *Petrological evidence for secular cooling in mantle plumes.* Nature, **458**, 619-622 (2 April 2009).

HERZBERG,C.,ASIMOW,P.D.,ARNDT,N.,NIU,Y.,LESHER,C.M.,FITTON,J.G.,CHEADLE M.J.,SAUNDERS,A.D. 2007. *Temperatures in ambient mantle and plumes: Constraints from basalts, picrites, and komatiites.* Geochemistry Geophysics Geosystems. Vol 8, number 2.

HERZBERG, C. 2011. *Basalt as temperature probes of Earth's mantle*. Geology, December 2011; v.39; no.12; pp 1179-1180.

HERZBERG,C., ASIMOW, P. D., IONOV, D.A., VIDITO, C., JACKSON, M. G., GEIST, D. 2013. *Nickel and helium evidence for melt above the core-mantle boundary.* Nature, 493, 393 -397.

HOLGATE, N. 1969. *Palaeozoic and Tertiary transcurrent movements on the Great Glen Fault.* Scottish Journal of Geology. 1969; **(5)**;. 97-139.

HOLNESS, M.B., SIDES, R., PRIOR, D.J., CHEADLE, M.J., UPTON, B.G.J. 2012. *The peridotite plugs of Rum: Crystal settling and fabric development in magma conduits.* Lithos, 134-135 (2012) 23–40.

KAMENETSKY, V.S., CRAWFORD, A.J.,MEFFRE S. 2001.*Factors Controlling Chemistry of Magmatic Spinel: an Empirical Study of Associated Olivine, Cr-spinel and Melt Inclusions from Primitive Rocks.*Journal of Petrology, **42** (4), 655 – 671.

KEIDING, J.K.,TRUMBULL, R.B.,VEKSLER, I.V.,JERRAM, D.A.,2011. *On the significance of ultra-magnesian olivines in basaltic rocks*. Geology, December 2011; v.39; no 12; pp 1095-1098.

KENT, A.J.R.,STOLPER,E.M.,FRANCIS,D.,WOODHEAD,J.,FREI,R.,EILER,J. 2004. *Mantle heterogeneity during the formation of the North Atlantic Igneous Province: Constraints from trace element and Sr-Nd-Os-O isotope systematics of Baffin Island picrites*. Geochemistry Geophysics Geosystems. Vol.5, number 11.

KERR, A.C. 1995. *The geochemistry of the Mull-Morvern Tertiary lava succession, NW Scotland: an assessment of mantle sources during plume-related volcanism.*Chemical Geology Volume 122.

KERR, A.C. 1998. *Mineral chemistry of the Mull-Morvern Tertiary lava succession, western Scotland.* Mineralogical magazine. Volume 62, Number 3.

KERR, A. C., KENT, R.W., THOMSON, B.A., SEEDHOUSE, J. K. & DONALDSON, C. H., 1999. *Geochemical Evolution of the Tertiary Mull Volcano, Western Scotland.* Journal of Petrology Vol 40 Issue 61.

LARSEN, L. M. & PEDERSEN, A. K. 2000. *Processes in high-Mg, high-T magmas: evidence from olivine, chromite and glass in Palaeogene picrites from West Greenland*. Journal of Petrology **41**, 1071–98.

LARSEN, L. M. & PEDERSEN, A. K. 2009. *Petrology of the Paleocene Picrites and Flood Basalts on Disko and Nuussuaq, West Greenland.* Journal of Petrology (2009) **50** (9): 1667-1711.

LE BAS, M.J., 1962. *The role of aluminum in igneous clinopyroxenes with relation to their parentage*. American journal of Science, April 1962, Vol 260 no. 4 . 267 – 288.

LETERRIER,J.,MAURY,R.C.,THONON,P.,GIRARD,D.,MARCHAI,M. 1982. *Clinopyroxene composition as a method of identification of the magmatic affinities of palaeo-volcanic series*. Earth and Planetary Science Letters. Volume 59, Issue 1.

LIBOUREL, G. 1999. *Systematics of calcium partitioning between olivine and silicate melt: implications for melt structure and calcium content of magmatic olivines.* Contributions to Mineralogy and Petrology, (1999) 136: 63 – 80.

LOBJOIT, W.M. 1959. *On the form and mode of emplacement of the Ben Buie Intrusion, Isle of Mull, Argyllshire*. Geological Magazine. Volume 96, Issue 05.

LONGHI, J.,WALKER, D., HAYS, J.F. 1978. *The distribution of Fe and Mg between olivine and lunar basaltic liquids*. Geochimica et Cosmichimica Acta, **42,** 1545-1558.

MATHIEU, L. & DE VRIES, VAN WYK, 2009.*Edifice and substrata deformation induced by intrusive complexes and gravitational loading in the Mull volcano (Scotland)*. Bulletin of Volcanology. December 2009, Volume 71, Issue 10, pp 1133-1148.

MATZEN, ANDREW K, BAKER, MICHAEL B, BECKETT, JOHN R. & STOLPER, EDWARD M., 2011. *Fe-Mg partitioning between Olivine and High-magnesian Melts and the nature of Hawaiian Parental Liquids.*Journal of Petrology, **52** (7 & 8), 1243 - 1263.

McLURG, J. 1982. Unpublished PhD thesis, University of Edinburgh.

MUSHAYANDEBVU, M.F.,JONES, D.L., BRIDEN, J.C. 1994. *A palaeomagnetic study of the Umvimeela Dyke, Zimbabwe: evidence for a mesoproterozoic overprint*. Precambrian Research, Volume 69, Issues 1-4, October 1994.

MUSSETT, A.E., 1986. *40Ar-39Ar step-heating ages of the Tertiary igneous rocks of Mull, Scotland*. Journal of Geological Society, 1986; v. 143; 887-896.

NISBET, E.G. & PEARCE, J.A. 1977. *Clinopyroxene Composition in Mafic Lavas from Different Tectonic Settings.* Contributions to Mineralogy and Petrology, 63, 149-160 (1977).

PANKHURST, R., WALSH,J.N.,BECKINSALE, R.D., SKELHORN,R.R., 1978. *Isotopic and other geochemical evidence for the origin of the Loch Uisg granophyre, Isle of Mull, Scotland* .Earth and Planetary Science Letters**, 38**, 355 – 363.

PARSLOW, G.R. 1976. *The Suisnish Layered Dyke*. Mineralogical Magazine, Sept 1976, Vol 40, 683 – 693.

PRESTON, J. *Unpublished Data on the Ben Buie Gabbro*, formerly on the AUMING website, Aberdeen University.

PROUT, S.J., ANDERSEN, J.C. Ø., BARNES, S-J, & POWER, M.R., 2002. *Platinum-Group Element Mineralisation Within Two Mafic/Ultramafic Intrusions of the British Palaeogene Igneous Province*. Proceedings of the 9th International Platinum Symposium, 2002.

PULVERTAFT, T.C.R., 1965. *The The Eqaloqarfia layered dyke, Nunarssuit, South Greenland.* (Meddelelser om Grønland)

PUTIRKA, KEITH, D., PERFIT, MICHAEL, RYERSON, F.J. & JACKSON, MATTHEW G., 2007, *Ambient and excess mantle temperatures, olivine thermometry, and active vs. passive upwelling*. Science, Volume 241, Issues 3–4, 15 July 2007, Pages 177–206.

RÉVILLON, N. T.,ARNDT, N. T., CHAUVEL, C. & HALLOT, E. 2000. *Geochemical study of ultramafic volcanic and plutonic rocks from Gorgona Island, Columbia: the plumbing system of an oceanic plateau*. Journal of Petrology **41**, 1127–53.

RICHEY, J.E., MACGREGOR, A.G., ANDERSON, F.W. 1961. *British Regional Geology:Scotland, the Tertiary Volcanic Districts.* 3rd edition, HMSO, Edinburgh.

ROEDER, P.L. & EMSLIE R.F. 1970. Olivine – Liquid Equilibrium. Contributions to Mineralogy and Petrology, 30. XII. 1970, Volume 29, Issue 4, pp 275-289.

SAUNDERS, A.D., FITTON, J.G., KERR, A.C., NORRY, M.J., KENT, R.W. 1997. *The North Atlantic Igneous Province. (Large Igneous Provinces: Continental, Oceanic and Planetary Flood Volcanism).* Geophysical monograph 100, American Geophysical Union.

SKELHORN, R. R., MacDOUGALL, J. D. S. & LONGLAND,P. J. N. 1969.*The Tertiary Igneous Geology of the Isle of Mull*. Geologists Association, London, Guide No. **20**, 35.

SOBOLEV, ALEXANDER V.,HOFMANN, ALBRECHT W., SOBOLEV, STEPHAN V. & NIKOGOSIAN, IGOR K. 2005. *An olivine-free mantle source of Hawaiian shield basalts.*Nature, Vol 434, March 2005.

STEPHENSON, D. 2011. *Mull and Iona A Landscape Fashioned by Geology*. SNH Publications.

SUGAWARA, T. 2000. *Empirical relationships between temperature, pressure, and MgO content in olivine and pyroxene saturated liquid*. Journal of Geophysical Research, Volume 105, Issue B4, pages 8457–8472, 10 April 2000.

THOMPSON, R.N., ESSON, J. & DUNHAM, A.C., 1972, *Major Element Chemical Variation in the Eocene Lavas of the Isle of Skye, Scotland*. Journal of Petrology, Vol. 13, Part 2, pp. 219-53, 1972.

THOMPSON, R.N. & GIBSON, S.A., 2000, *Transient high temperatures in mantle plume heads inferred from magnesian olivines in Phanerozoic picrites.* Nature, Vol 407, 2000.

TRUMBELL, R.B., SOBOLEV, S.V., BAUER, K. 2002. *Petrophysical modelling of high seismic velocity crust at the Namibian volcanic margin.* GSA Special Papers 362 – Volcanic Rifted margins.

ULMER, P. 1989. *The dependence of the Fe^{2+} - Mg cation-partitioning between olivine and basaltic liquid on pressure, temperature and composition. An experimental study to 30 kbars.* Contributions to mineralogy and Petrology,(1989) 101:261 – 273

UPTON, B.G.J. & THOMAS, J.E. 1978. *The Tugtotoq Younger Giant Dyke Complex, South Greenland: Fractional Crystallisation of Transitional Olivine Basalt Magma*. Journal of Petrology, Volume 21, Issue 1. pp 167 – 198.

UPTON, B. G. J., SKOVGAARD, A. C., McCLURG, J., KIRSTEIN, L. , CHEADLE, M., EMELEUS, C. H ., WADSWORTH, W. J. A., FALLICK, E. (2002). *Picritic magmas and the Rum ultramafic complex, Scotland.* Geological Magazine,139, pp 437 – 452.

UPTON, B.G.J., EMELEUS, C.H., HEAMAN, L.M., GOODENOUGH, K.M., FINCH, A.A. 2003. *Magmatism of the mid-Proterozoic Gardar Province, South Greenland: chronology, petrogenesis and geological setting.* Lithos, Volume 68, Issues 1 – 2, May 2003.

VINET, N. & HIGGINS, M.D. 2010 *Magma Solidification Processes beneath Kilauea Volcano, Hawaii: a Quantitative Textural and Geochemical Study of the 1969-1974 Mauna Ulu Lavas.* Journal of Petrology,Volume 51 Issue 6. pp 1293 – 1332.

WALKER, F. 1929. The Geology of the Shiant Isles (HEBRIDES). http://www.shiantisles.net/geology/g04_1.htm

WALSH,J.N., BECKINSALE, R.D., SKELHORN,R.R., & THORPE, R.S. 1979. *Geochemistry and petrogenesis of tertiary granitic rocks from the Island of Mull, Northwest Scotland.* Contributions to Mineralogy and Petrology Volume 71, Number 2, 99-116 1979.

WILSON, A.H. 1982. *The geology of the Great "Dyke" Zimbabwe: the Ultramafic Rocks.* Journal of Petrology, Volume 23, Issue 2. Pp. 240 – 292.

WILSON, A.H. 1996. *The Great Dyke of Zimbabwe*. Developments in Petrology, Volume 15, 1996.

WYLLIE, P.J. & DREVER, H.I. 1962. *The Petrology of Picritic Rocks in Minor Intrusions – a Picrite Sill on the Island of Soay (Hebrides).* Transactions of the Royal Society of Edinburgh, Volume 65, Issue 08, January 1962.

Appendix 1a: Olivine Data

Grain Information		Weight Per Cent						
Sample	Grain	MgO	SiO2	CaO	MnO	FeO	NiO	Sum
R222	Grain 1 Rim	46.44	40.69	0.34	0.19	12.99	0.45	101.10
R222	Grain 1 Core 2	49.15	41.34	0.29	0.17	9.32	0.00	100.28
R222	Grain 1 Core 3	49.39	41.49	0.32	0.15	9.33	0.30	100.99
R222	Grain 1 Core 3	49.15	41.37	0.26	0.16	9.27	0.39	100.59
R222	Grain 1 Rim 2	45.40	40.23	0.27	0.22	14.14	0.29	100.54
R222	Grain 2 Core 1	50.94	42.15	0.31	0.15	7.81	0.41	101.77
R222	Grain 2 Rim 2	47.72	40.99	0.27	0.20	11.33	0.39	100.91
R222	Grain 3 Core 1	43.24	40.02	0.26	0.31	17.26	0.28	101.37
R222	Grain 3 Rim 1	41.33	39.32	0.26	0.31	18.79	0.23	100.24
R235	Grain 1 Core 1	48.50	41.48	0.30	0.29	11.10	0.00	101.66
R235	Grain 1 Core 1	47.76	40.77	0.30	0.22	10.91	0.35	100.32
R235	Grain 1 Core 2	48.44	40.79	0.29	0.16	9.90	0.31	99.90
R235	Grain 1 Core 3	47.37	40.57	0.28	0.24	10.82	0.25	99.54
R235	Grain 1 Rim 1	44.90	40.19	0.34	0.24	14.76	0.30	100.73
R235	Grain 1 Rim 2	45.01	39.75	0.33	0.23	13.64	0.33	99.29
R235	Grain 1 Rim 4	45.91	40.24	0.35	0.16	12.83	0.30	99.79
R235	Grain 2 Core 1	47.05	40.73	0.32	0.20	11.87	0.38	100.54
R235	Grain 2 Core 2	46.95	40.76	0.30	0.23	12.04	0.33	100.61
R235	Grain 2 Rim 2	45.10	40.02	0.29	0.24	14.08	0.38	100.11
R235	Grain 3 Core 1	47.41	40.37	0.26	0.22	10.92	0.38	99.56
R235	Grain 3 Core 2	47.91	40.42	0.33	0.12	10.84	0.36	99.98
R235	Grain 3 Core 3	46.43	40.39	0.32	0.17	12.13	0.38	99.81
R235	Grain 3 Core 4	46.50	40.36	0.35	0.16	12.21	0.26	99.84
R235	Grain 3 Core 5	47.26	40.68	0.36	0.20	11.93	0.33	100.77
R235	Grain 3 Rim 1	45.57	40.55	0.20	0.24	14.30	0.27	101.12
R235	Grain 3 Rim 2	44.86	40.42	0.26	0.28	15.17	0.24	101.23
R235	Grain 3 Rim 3	47.96	41.23	0.28	0.16	11.25	0.42	101.29
R235	Grain 3 Rim 4	45.21	39.92	0.23	0.20	13.57	0.28	99.42
R235	Grain 4 Core 1	49.48	41.31	0.31	0.16	9.16	0.34	100.76
R235	Grain 4 Core 2	49.61	41.63	0.29	0.16	9.44	0.39	101.52
R235	Grain 4 Core 3	48.52	41.32	0.32	0.16	10.10	0.40	100.83
R235	Grain 4 Rim 3	44.40	40.22	0.30	0.32	16.03	0.28	101.54
R265	Grain 2 Core 1	48.49	41.03	0.29	0.28	11.83	0.00	101.93
R265	Grain 2 Core 1	47.11	40.62	0.34	0.15	11.76	0.33	100.31
R265	Grain 2 Core 2	47.10	40.74	0.31	0.22	11.88	0.32	100.56
R265	Grain 2 Rim 1	47.30	40.86	0.36	0.20	11.98	0.36	101.05
R265	Grain 2 Rim 2	47.88	41.34	0.30	0.23	12.00	0.32	102.07
R265	Grain 2 Rim 3	47.26	40.63	0.27	0.15	11.88	0.26	100.44
R265	Grain 3 Core 1	46.76	40.90	0.32	0.19	13.17	0.32	101.65
R265	Grain 3 Core 3	47.47	41.00	0.36	0.26	12.24	0.33	101.66
R267	Grain 1 Core 3	51.56	41.87	0.34	0.14	7.46	0.45	101.81
R267	Grain 1 Rim 1	46.14	40.59	0.24	0.21	14.24	0.37	101.78
R267	Grain 1 Rim 2	46.68	40.29	0.24	0.12	13.43	0.32	101.07

Sample	Grain	MgO	SiO2	CaO	MnO	FeO	NiO	Sum
R267	Grain 2 Core 2	51.33	41.55	0.28	0.15	7.77	0.46	101.55
R267	Grain 2 Core 3	51.23	41.81	0.31	0.12	7.93	0.45	101.84
R267	Grain 2 Core 4	51.20	41.64	0.29	0.05	7.80	0.45	101.42
R267	Grain 2 Rim 2	47.98	41.06	0.34	0.19	12.04	0.29	101.90
R267	Grain 2 Rim 3	43.97	39.73	0.25	0.28	16.54	0.25	101.03
R267	Grain 2 Rim 4	48.58	41.49	0.28	0.17	11.79	0.37	102.67
R267	Grain 2 Rim 5	44.23	39.88	0.29	0.30	16.74	0.28	101.72
R267	Grain 4 Core 1 RHS	49.12	41.14	0.29	0.19	9.78	0.38	100.91
R267	Grain 4 Core 1 LHS	49.19	41.38	0.38	0.13	10.36	0.33	101.77
R267	Grain 4 Rim 1	40.57	38.90	0.15	0.40	21.59	0.14	101.75
R362	Grain 1 Core 1	49.32	40.42	0.29	0.08	8.64	0.42	99.17
R362	Grain 1 Core 2	49.37	40.70	0.28	0.13	8.79	0.50	99.77
R362	Grain 1 Core 3	49.47	40.82	0.29	0.15	8.90	0.41	100.05
R362	Grain 1 Rim 1	45.41	39.78	0.24	0.22	14.24	0.36	100.23
R362	Grain 1 RIm1 repeat	45.36	39.67	0.24	0.18	13.98	0.37	99.79
R362	Grain 2 Core 1	49.42	40.93	0.29	0.19	9.40	0.47	100.71
R362	Grain 2 Core 2	49.52	41.36	0.27	0.14	9.57	0.45	101.30
R362	Grain 2 Rim 1	43.25	39.20	0.28	0.32	16.68	0.32	100.05
R362	Grain 2 Rim 4	47.46	40.35	0.34	0.14	11.86	0.42	100.57
R362	Grain 3 Core1	46.49	39.88	0.28	0.21	12.44	0.31	99.60
R362	Grain 3 Rim 1	46.09	40.44	0.22	0.17	14.08	0.29	101.29
R362	Grain 3 Rim 3	45.04	39.50	0.31	0.27	14.33	0.36	99.80
R362	Grain 4 Core 1	44.86	39.82	0.29	0.26	14.55	0.34	100.13
R362	Grain 4 Core 2	45.82	40.65	0.20	0.25	14.58	0.36	101.85
R365	Grain 1 Core !	49.62	40.72	0.28	0.17	8.35	0.32	99.45
R365	Grain 1 Core 2	49.52	40.84	0.31	0.12	8.57	0.38	99.74
R365	Grain 1 Rim 1	45.41	40.35	0.27	0.23	14.98	0.24	101.48
R365	Grain 1 Rim 2	44.73	39.65	0.28	0.27	14.67	0.24	99.84
R365	Grain 2 Core 1	50.10	41.42	0.32	0.17	8.86	0.45	101.32
R365	Grain 2 Core 2	49.97	41.12	0.34	0.14	8.69	0.42	100.68
R365	Grain 2 Rim 2	45.51	40.52	0.22	0.25	15.07	0.25	101.83
R365	Grain 2 Rim 3	44.25	39.37	0.34	0.27	15.01	0.33	99.56
R365	Grain 3 Core 2	47.50	40.50	0.31	0.22	12.34	0.29	101.16
R365	Grain 3 Rim 1	45.04	40.29	0.24	0.27	15.47	0.36	101.66
R367	Grain 1 Core 1	50.00	40.78	0.31	0.14	8.74	0.38	100.36
R367	Grain 1 Rim 1	47.15	40.35	0.27	0.25	11.72	0.32	100.06
R367	Grain 1 Rim 2	47.15	40.59	0.24	0.15	12.84	0.32	101.29
R367	Grain2 Core 1	45.56	40.10	0.36	0.27	14.00	0.11	100.40
R367	Grain 2 Core 2	45.77	39.99	0.41	0.23	13.52	0.11	100.03
R367	Grain 2 Rim 1	44.98	39.69	0.29	0.21	14.34	0.25	99.76
R367	Grain 2 Rim 2	43.87	39.28	0.28	0.23	15.31	0.20	99.18
R367	Grain 2 Rim 3	43.58	39.22	0.27	0.28	15.61	0.23	99.19
R367	Grain 3 Core 1	49.99	40.70	0.27	0.10	7.73	0.34	99.13
R367	Grain 3 Core 2	49.24	40.40	0.28	0.15	8.52	0.55	99.14
R367	Grain 3 Core 3	49.85	40.67	0.31	0.18	7.79	0.37	99.17

Sample	Grain	MgO	SiO2	CaO	MnO	FeO	NiO	Sum
R367	Grain 4 Core 1	48.24	40.82	0.25	0.18	10.56	0.34	100.40
R367	Grain 4 Core 2	47.68	40.42	0.13	0.23	11.69	0.36	100.50
R367	Grain 4 Rim 1	45.69	40.10	0.29	0.21	14.04	0.27	100.59
R367	Grain 4 Rim2	46.59	40.33	0.29	0.18	13.22	0.34	100.95
R368	Grain 1 Core 1	50.22	41.40	0.25	0.10	8.41	0.43	100.82
R368	Grain 1 Core 2	50.68	41.47	0.34	0.13	8.37	0.47	101.46
R368	Grain 1 Rim 1	47.23	40.20	0.29	0.21	12.51	0.42	100.87
R368	Grain 1 Rim2	48.96	40.95	0.31	0.19	10.18	0.46	101.05
R368	Grain 1 Rim 3	46.77	40.16	0.32	0.26	12.80	0.39	100.70
R368	Grain 2 Core 1	50.52	41.02	0.28	0.14	8.17	0.45	100.56
R368	Grain 2 Core 2	50.02	41.32	0.29	0.13	8.61	0.39	100.76
R368	Grain 2 Rim 1	45.54	39.39	0.32	0.23	13.45	0.32	99.26
R368	Grain 2 Rim2	46.77	39.80	0.28	0.23	11.29	0.43	98.80
R368	Grain 3 Core 3	49.77	40.55	0.32	0.04	8.31	0.36	99.34
R368	Grain 3 Rim 1	45.61	39.43	0.31	0.22	12.77	0.36	98.70
R368	Grain 3 Rim 2	45.81	39.75	0.28	0.19	13.23	0.31	99.57
R368	Grain 4 Core 1	45.44	40.22	0.36	0.26	14.98	0.27	101.54
R368	Grain 4 Core 2	45.26	39.88	0.34	0.23	14.16	0.27	100.14
R368	Grain 4 Rim 2	43.70	38.94	0.27	0.27	15.38	0.34	98.90
R368	Grain 5 Core 1	45.36	39.95	0.39	0.28	14.08	0.23	100.29
R368	Grain 5 Core 2	44.43	39.56	0.24	0.22	15.34	0.36	100.14

Grain Information		Formulae recast to 4 oxygens						
Sample	Grain	Mg 4 O	Si 4 O	Ca 4O	Mn 4 O	Fe 4 O	Ni 4 O	Sum Cat
R222	Grain 1 Rim	1.71	1.00	0.01	0.00	0.27	0.01	2.00
R222	Grain 1 Core 2	1.79	1.01	0.01	0.00	0.19	0.00	1.99
R222	Grain 1 Core 3	1.78	1.01	0.01	0.00	0.19	0.01	1.99
R222	Grain 1 Core 3	1.78	1.01	0.01	0.00	0.19	0.01	1.99
R222	Grain 1 Rim 2	1.69	1.00	0.01	0.00	0.29	0.01	2.00
R222	Grain 2 Core 1	1.81	1.01	0.01	0.00	0.16	0.01	1.99
R222	Grain 2 Rim 2	1.74	1.00	0.01	0.00	0.23	0.01	1.99
R222	Grain 3 Core 1	1.61	1.00	0.01	0.01	0.36	0.01	2.00
R222	Grain 3 Rim 1	1.57	1.00	0.01	0.01	0.40	0.00	1.99
R235	Grain 1 Core 1	1.75	1.00	0.01	0.01	0.22	0.00	1.99
R235	Grain 1 Core 1	1.75	1.00	0.01	0.00	0.22	0.01	1.99
R235	Grain 1 Core 2	1.77	1.00	0.01	0.00	0.20	0.01	2.00
R235	Grain 1 Core 3	1.75	1.00	0.01	0.01	0.22	0.00	1.99
R235	Grain 1 Rim 1	1.67	1.00	0.01	0.01	0.31	0.01	2.00
R235	Grain 1 Rim 2	1.69	1.00	0.01	0.00	0.29	0.01	2.00
R235	Grain 1 Rim 4	1.71	1.00	0.01	0.00	0.27	0.01	1.99
R235	Grain 2 Core 1	1.73	1.00	0.01	0.00	0.24	0.01	1.99
R235	Grain 2 Core 2	1.72	1.00	0.01	0.00	0.25	0.01	1.99
R235	Grain 2 Rim 2	1.68	1.00	0.01	0.01	0.29	0.01	2.00
R235	Grain 3 Core 1	1.75	1.00	0.01	0.00	0.23	0.01	2.00
R235	Grain 3 Core 2	1.76	1.00	0.01	0.00	0.22	0.01	2.00
R235	Grain 3 Core 3	1.72	1.00	0.01	0.00	0.25	0.01	1.99
R235	Grain 3 Core 4	1.72	1.00	0.01	0.00	0.25	0.01	1.99
R235	Grain 3 Core 5	1.73	1.00	0.01	0.00	0.25	0.01	2.00
R235	Grain 3 Rim 1	1.68	1.00	0.01	0.01	0.30	0.01	1.99
R235	Grain 3 Rim 2	1.66	1.00	0.01	0.01	0.31	0.00	1.99
R235	Grain 3 Rim 3	1.74	1.00	0.01	0.00	0.23	0.01	1.99
R235	Grain 3 Rim 4	1.69	1.00	0.01	0.00	0.29	0.01	1.99
R235	Grain 4 Core 1	1.79	1.00	0.01	0.00	0.19	0.01	1.99
R235	Grain 4 Core 2	1.78	1.00	0.01	0.00	0.19	0.01	1.99
R235	Grain 4 Core 3	1.76	1.01	0.01	0.00	0.21	0.01	1.99
R235	Grain 4 Rim 3	1.65	1.00	0.01	0.01	0.33	0.01	2.00
R265	Grain 2 Core 1	1.75	1.00	0.01	0.01	0.24	0.00	2.01
R265	Grain 2 Core 1	1.73	1.00	0.01	0.00	0.24	0.01	1.99
R265	Grain 2 Core 2	1.73	1.00	0.01	0.00	0.24	0.01	1.99
R265	Grain 2 Rim 1	1.73	1.00	0.01	0.00	0.25	0.01	2.00
R265	Grain 2 Rim 2	1.73	1.00	0.01	0.00	0.24	0.01	1.99
R265	Grain 2 Rim 3	1.74	1.00	0.01	0.00	0.24	0.01	2.00
R265	Grain 3 Core 1	1.71	1.00	0.01	0.00	0.27	0.01	2.00
R265	Grain 3 Core 3	1.73	1.00	0.01	0.01	0.25	0.01	2.00
R267	Grain 1 Core 3	1.83	1.00	0.01	0.00	0.15	0.01	2.00
R267	Grain 1 Rim 1	1.69	1.00	0.01	0.00	0.29	0.01	2.00
R267	Grain 1 Rim 2	1.72	0.99	0.01	0.00	0.28	0.01	2.01
R267	Grain 2 Core 1	1.83	1.00	0.01	0.00	0.16	0.01	2.00
R267	Grain 2 Core 2	1.83	1.00	0.01	0.00	0.16	0.01	2.01

Sample	Grain	Mg 4 O	Si 4 O	Ca 4O	Mn 4 O	Fe 4 O	Ni 4 O	Sum Cat
R267	Grain 2 Core 4	1.83	1.00	0.01	0.00	0.16	0.01	2.00
R267	Grain 2 Rim 2	1.74	1.00	0.01	0.00	0.24	0.01	2.00
R267	Grain 2 Rim 3	1.64	1.00	0.01	0.01	0.35	0.01	2.01
R267	Grain 2 Rim 4	1.75	1.00	0.01	0.00	0.24	0.01	2.00
R267	Grain 2 Rim 5	1.64	0.99	0.01	0.01	0.35	0.01	2.01
R267	Grain 4 Core 1 RHS	1.78	1.00	0.01	0.00	0.20	0.01	2.00
R267	Grain 4 Core 1 LHS	1.77	1.00	0.01	0.00	0.21	0.01	2.00
R267	Grain 4 Rim 1	1.54	0.99	0.00	0.01	0.46	0.00	2.02
R362	Grain 1 Core 1	1.81	1.00	0.01	0.00	0.18	0.01	2.01
R362	Grain 1 Core 2	1.80	1.00	0.01	0.00	0.18	0.01	2.00
R362	Grain 1 Core 3	1.80	1.00	0.01	0.00	0.18	0.01	2.00
R362	Grain 1 Rim 1	1.69	1.00	0.01	0.00	0.30	0.01	2.01
R362	Grain 1 RIm1 repeat	1.70	1.00	0.01	0.00	0.29	0.01	2.01
R362	Grain 2 Core 1	1.79	1.00	0.01	0.00	0.19	0.01	2.01
R362	Grain 2 Core 2	1.79	1.00	0.01	0.00	0.19	0.01	2.00
R362	Grain 2 Rim 1	1.64	0.99	0.01	0.01	0.35	0.01	2.01
R362	Grain 2 Rim 4	1.75	1.00	0.01	0.00	0.24	0.01	2.01
R362	Grain 3 Core1	1.73	1.00	0.01	0.00	0.26	0.01	2.01
R362	Grain 3 Rim 1	1.70	1.00	0.01	0.00	0.29	0.01	2.00
R362	Grain 3 Rim 3	1.69	0.99	0.01	0.01	0.30	0.01	2.01
R362	Grain 4 Core 1	1.68	1.00	0.01	0.01	0.31	0.01	2.00
R362	Grain 4 Core 2	1.68	1.00	0.01	0.01	0.30	0.01	2.00
R365	Grain 1 Core !	1.81	1.00	0.01	0.00	0.17	0.01	2.00
R365	Grain 1 Core 2	1.81	1.00	0.01	0.00	0.18	0.01	2.00
R365	Grain 1 Rim 1	1.68	1.00	0.01	0.00	0.31	0.00	2.00
R365	Grain 1 Rim 2	1.68	1.00	0.01	0.01	0.31	0.00	2.00
R365	Grain 2 Core 1	1.80	1.00	0.01	0.00	0.18	0.01	2.00
R365	Grain 2 Core 2	1.81	1.00	0.01	0.00	0.18	0.01	2.00
R365	Grain 2 Rim 2	1.67	1.00	0.01	0.01	0.31	0.01	2.00
R365	Grain 2 Rim 3	1.67	1.00	0.01	0.01	0.32	0.01	2.01
R365	Grain 3 Core 2	1.74	0.99	0.01	0.00	0.25	0.01	2.01
R365	Grain 3 Rim 1	1.66	1.00	0.01	0.01	0.32	0.01	2.00
R367	Grain 1 Core 1	1.82	0.99	0.01	0.00	0.18	0.01	2.01
R367	Grain 1 Rim 1	1.74	1.00	0.01	0.01	0.24	0.01	2.00
R367	Grain 1 Rim 2	1.73	1.00	0.01	0.00	0.26	0.01	2.01
R367	Grain2 Core 1	1.69	1.00	0.01	0.01	0.29	0.00	2.00
R367	Grain 2 Core 2	1.70	1.00	0.01	0.00	0.28	0.00	2.00
R367	Grain 2 Rim 1	1.69	1.00	0.01	0.00	0.30	0.01	2.00
R367	Grain 2 Rim 2	1.66	1.00	0.01	0.01	0.33	0.00	2.00
R367	Grain 2 Rim 3	1.65	1.00	0.01	0.01	0.33	0.00	2.00
R367	Grain 3 Core 1	1.83	1.00	0.01	0.00	0.16	0.01	2.00
R367	Grain 3 Core 2	1.81	1.00	0.01	0.00	0.18	0.01	2.01
R367	Grain 3 Core 3	1.82	1.00	0.01	0.00	0.16	0.01	2.00
R367	Grain 3 Rim 1	1.70	1.00	0.01	0.01	0.27	0.01	2.00
R367	Grain 3 Rim 1?	1.75	0.99	0.01	0.00	0.25	0.01	2.01
R367	Grain 4 Core 1	1.76	1.00	0.01	0.00	0.22	0.01	2.00
R367	Grain 4 Core 2	1.75	1.00	0.00	0.00	0.24	0.01	2.01

Sample	Grain	Mg 4 O	Si 4 O	Ca 4O	Mn 4 O	Fe 4 O	Ni 4 O	Sum Cat
R367	Grain 4 Rim2	1.72	1.00	0.01	0.00	0.27	0.01	2.01
R368	Grain 1 Core 1	1.81	1.00	0.01	0.00	0.17	0.01	2.00
R368	Grain 1 Core 2	1.82	1.00	0.01	0.00	0.17	0.01	2.01
R368	Grain 1 Rim 1	1.74	0.99	0.01	0.00	0.26	0.01	2.02
R368	Grain 1 Rim2	1.78	1.00	0.01	0.00	0.21	0.01	2.01
R368	Grain 1 Rim 3	1.73	0.99	0.01	0.01	0.26	0.01	2.01
R368	Grain 2 Core 1	1.83	0.99	0.01	0.00	0.17	0.01	2.01
R368	Grain 2 Core 2	1.81	1.00	0.01	0.00	0.17	0.01	2.00
R368	Grain 2 Rim 1	1.71	0.99	0.01	0.00	0.28	0.01	2.01
R368	Grain 2 Rim2	1.75	1.00	0.01	0.00	0.24	0.01	2.01
R368	Grain 3 Core 3	1.82	1.00	0.01	0.00	0.17	0.01	2.01
R368	Grain 3 Rim 1	1.72	1.00	0.01	0.00	0.27	0.01	2.01
R368	Grain 3 Rim 2	1.71	1.00	0.01	0.00	0.28	0.01	2.01
R368	Grain 4 Core 1	1.68	1.00	0.01	0.01	0.31	0.01	2.01
R368	Grain 4 Core 2	1.69	1.00	0.01	0.00	0.30	0.01	2.00
R368	Grain 4 Rim 2	1.66	0.99	0.01	0.01	0.33	0.01	2.01
R368	Grain 5 Core 1	1.69	1.00	0.01	0.01	0.29	0.00	2.00
R368	Grain 5 Core 2	1.67	1.00	0.01	0.00	0.32	0.01	2.01

Grain Information			Components				
Sample	Grain	Te	Fo	Fa	Ca-Ol	Ni	Mg No.
R222	Grain 1 Rim	0.20	**85.11**	**14.25**	0.44	**0.45**	86.44
R222	Grain 1 Core 2	0.17	**89.30**	**10.14**	0.38	**0.00**	90.39
R222	Grain 1 Core 3	0.16	**89.31**	**10.11**	0.42	**0.30**	90.42
R222	Grain 1 Core 3	0.16	**89.43**	**10.08**	0.33	**0.39**	90.43
R222	Grain 1 Rim 2	0.23	**83.79**	**15.63**	0.35	**0.29**	85.13
R222	Grain 2 Core 1	0.14	**91.09**	**8.37**	0.40	**0.40**	92.08
R222	Grain 2 Rim 2	0.21	**87.07**	**12.37**	0.35	**0.39**	88.25
R222	Grain 3 Core 1	0.33	**80.16**	**19.16**	0.35	**0.27**	81.71
R222	Grain 3 Rim 1	0.33	**78.07**	**21.25**	0.34	**0.23**	79.68
R235	Grain 1 Core 1	0.29	**87.37**	**11.96**	0.38	**0.00**	88.62
R235	Grain 1 Core 1	0.23	**87.43**	**11.95**	0.39	**0.35**	88.64
R235	Grain 1 Core 2	0.16	**88.60**	**10.85**	0.39	**0.32**	89.72
R235	Grain 1 Core 3	0.26	**87.41**	**11.97**	0.37	**0.26**	88.64
R235	Grain 1 Rim 1	0.24	**82.98**	**16.33**	0.45	**0.30**	84.43
R235	Grain 1 Rim 2	0.25	**84.07**	**15.25**	0.43	**0.33**	85.47
R235	Grain 1 Rim 4	0.16	**85.14**	**14.25**	0.45	**0.30**	86.45
R235	Grain 2 Core 1	0.20	**86.35**	**13.04**	0.41	**0.38**	87.60
R235	Grain 2 Core 2	0.24	**86.15**	**13.22**	0.39	**0.33**	87.43
R235	Grain 2 Rim 2	0.26	**83.71**	**15.64**	0.39	**0.38**	85.10
R235	Grain 3 Core 1	0.23	**87.38**	**12.05**	0.33	**0.38**	88.56
R235	Grain 3 Core 2	0.12	**87.60**	**11.85**	0.42	**0.37**	88.74
R235	Grain 3 Core 3	0.18	**85.95**	**13.45**	0.43	**0.38**	87.22
R235	Grain 3 Core 4	0.16	**85.89**	**13.50**	0.45	**0.25**	87.16
R235	Grain 3 Core 5	0.20	**86.30**	**13.04**	0.46	**0.34**	87.60
R235	Grain 3 Rim 1	0.26	**83.75**	**15.73**	0.26	**0.26**	85.03
R235	Grain 3 Rim 2	0.30	**82.64**	**16.73**	0.33	**0.24**	84.06
R235	Grain 3 Rim 3	0.16	**87.23**	**12.24**	0.37	**0.41**	88.37
R235	Grain 3 Rim 4	0.21	**84.34**	**15.16**	0.30	**0.28**	85.59
R235	Grain 4 Core 1	0.17	**89.51**	**9.91**	0.40	**0.34**	90.59
R235	Grain 4 Core 2	0.16	**89.30**	**10.18**	0.36	**0.39**	90.36
R235	Grain 4 Core 3	0.16	**88.40**	**11.02**	0.42	**0.40**	89.55
R235	Grain 4 Rim 3	0.32	**81.64**	**17.64**	0.39	**0.27**	83.16
R265	Grain 2 Core 1	0.29	**87.37**	**11.96**	0.38	**0.00**	87.96
R265	Grain 2 Core 1	0.16	**86.48**	**12.92**	0.44	**0.33**	87.72
R265	Grain 2 Core 2	0.23	**86.32**	**13.04**	0.41	**0.32**	87.61
R265	Grain 2 Rim 1	0.20	**86.25**	**13.09**	0.46	**0.36**	87.56
R265	Grain 2 Rim 2	0.24	**86.42**	**12.97**	0.38	**0.31**	87.68
R265	Grain 2 Rim 3	0.15	**86.48**	**13.02**	0.35	**0.27**	87.64
R265	Grain 3 Core 1	0.19	**85.07**	**14.34**	0.40	**0.32**	86.36
R265	Grain 3 Core 3	0.27	**86.01**	**13.27**	0.46	**0.34**	87.36
R267	Grain 1 Core 3	0.14	**91.56**	**7.87**	0.43	**0.44**	92.49
R267	Grain 1 Rim 1	0.21	**84.06**	**15.41**	0.31	**0.36**	85.25
R267	Grain 1 Rim 2	0.12	**85.04**	**14.53**	0.31	**0.31**	86.11
R267	Grain 2 Core 1	0.10	**91.24**	**8.28**	0.38	**0.36**	92.11
R267	Grain 2 Core 2	0.16	**91.27**	**8.21**	0.36	**0.45**	92.17

Sample	Grain	Te	Fo	Fa	Ca-Ol	Ni	Mg No.
R267	Grain 2 Core 4	0.05	**91.31**	**8.26**	0.38	**0.44**	92.13
R267	Grain 2 Rim 2	0.20	**86.48**	**12.89**	0.44	**0.29**	87.66
R267	Grain 2 Rim 3	0.30	**81.21**	**18.15**	0.33	**0.25**	82.58
R267	Grain 2 Rim 4	0.17	**86.93**	**12.54**	0.36	**0.36**	88.02
R267	Grain 2 Rim 5	0.31	**81.08**	**18.23**	0.39	**0.27**	82.49
R267	Grain 4 Core 1 RHS	0.20	**88.91**	**10.51**	0.38	**0.38**	89.96
R267	Grain 4 Core 1 LHS	0.13	**88.32**	**11.06**	0.49	**0.32**	89.43
R267	Grain 4 Rim 1	0.42	**75.50**	**23.87**	0.21	**0.14**	77.01
R362	Grain 1 Core 1	0.08	**90.15**	**9.38**	0.39	**0.42**	91.06
R362	Grain 1 Core 2	0.13	**89.98**	**9.52**	0.37	**0.49**	90.92
R362	Grain 1 Core 3	0.16	**89.85**	**9.60**	0.38	**0.40**	90.84
R362	Grain 1 Rim 1	0.23	**83.84**	**15.62**	0.32	**0.35**	85.04
R362	Grain 1 RIm1 repeat	0.19	**84.10**	**15.39**	0.32	**0.37**	85.26
R362	Grain 2 Core 1	0.20	**89.33**	**10.09**	0.38	**0.47**	90.36
R362	Grain 2 Core 2	0.15	**89.27**	**10.24**	0.34	**0.44**	90.22
R362	Grain 2 Rim 1	0.34	**80.77**	**18.51**	0.38	**0.31**	82.21
R362	Grain 2 Rim 4	0.15	**86.57**	**12.85**	0.44	**0.41**	87.71
R362	Grain 3 Core1	0.22	**85.77**	**13.64**	0.37	**0.30**	86.94
R362	Grain 3 Rim 1	0.17	**84.24**	**15.29**	0.29	**0.29**	85.37
R362	Grain 3 Rim 3	0.29	**83.52**	**15.78**	0.41	**0.35**	84.86
R362	Grain 4 Core 1	0.27	**83.29**	**16.05**	0.39	**0.34**	84.61
R362	Grain 4 Core 2	0.25	**83.67**	**15.81**	0.26	**0.35**	84.86
R365	Grain 1 Core !	0.17	**90.42**	**9.04**	0.37	**0.32**	91.38
R365	Grain 1 Core 2	0.12	**90.20**	**9.28**	0.40	**0.38**	91.15
R365	Grain 1 Rim 1	0.24	**83.11**	**16.29**	0.35	**0.24**	84.38
R365	Grain 1 Rim 2	0.29	**83.14**	**16.20**	0.37	**0.24**	84.46
R365	Grain 2 Core 1	0.17	**89.96**	**9.45**	0.42	**0.44**	90.98
R365	Grain 2 Core 2	0.15	**90.11**	**9.31**	0.44	**0.42**	91.11
R365	Grain 2 Rim 2	0.25	**83.10**	**16.35**	0.29	**0.25**	84.33
R365	Grain 2 Rim 3	0.29	**82.61**	**16.65**	0.45	**0.33**	84.01
R365	Grain 3 Core 2	0.23	**86.09**	**13.29**	0.40	**0.29**	87.28
R365	Grain 3 Rim 1	0.28	**82.56**	**16.84**	0.31	**0.35**	83.85
R367	Grain 1 Core 1	0.15	**90.10**	**9.36**	0.40	0.38	91.07
R367	Grain 1 Rim 1	0.26	**86.60**	**12.79**	0.35	0.32	87.76
R367	Grain 1 Rim 2	0.16	**85.67**	**13.86**	0.31	0.31	86.75
R367	Grain2 Core 1	0.28	**83.91**	**15.32**	0.48	0.11	85.30
R367	Grain 2 Core 2	0.24	**84.41**	**14.81**	0.54	0.11	85.79
R367	Grain 2 Rim 1	0.22	**83.56**	**15.83**	0.39	0.25	84.83
R367	Grain 2 Rim 2	0.25	**82.31**	**17.07**	0.38	0.20	83.63
R367	Grain 2 Rim 3	0.30	**81.91**	**17.43**	0.36	0.23	83.27
R367	Grain 3 Core 1	0.11	**91.16**	**8.38**	0.35	0.23	92.01
R367	Grain 3 Core 2	0.16	**90.20**	**9.27**	0.37	0.55	91.15
R367	Grain 3 Core 3	0.19	**90.97**	**8.44**	0.40	0.37	91.95
R367	Grain 3 Rim 1	0.28	**84.82**	**14.47**	0.42	0.29	86.13
R367	Grain 3 Rim 1?	0.19	**86.37**	**13.05**	0.39	0.33	87.52
R367	Grain 4 Core 1	0.19	**88.03**	**11.45**	0.33	0.34	89.07
R367	Grain 4 Core 2	0.24	**86.94**	**12.66**	0.17	0.35	87.91

Sample	Grain	Te	Fo	Fa	Ca-Ol	Ni	Mg No
R367	Grain 4 Rim2	0.19	**85.09**	**14.34**	0.39	0.34	86.27
R368	Grain 1 Core 1	0.11	**90.55**	**9.01**	0.33	0.43	91.41
R368	Grain 1 Core 2	0.13	**90.55**	**8.89**	0.43	0.46	91.52
R368	Grain 1 Rim 1	0.21	**85.89**	**13.52**	0.38	0.41	87.07
R368	Grain 1 Rim2	0.20	**88.47**	**10.93**	0.40	0.45	89.55
R368	Grain 1 Rim 3	0.27	**85.42**	**13.89**	0.42	0.39	86.69
R368	Grain 2 Core 1	0.15	**90.78**	**8.72**	0.36	0.44	91.69
R368	Grain 2 Core 2	0.13	**90.26**	**9.23**	0.38	0.39	91.19
R368	Grain 2 Rim 1	0.25	**84.50**	**14.83**	0.43	0.32	85.79
R368	Grain 2 Rim2	0.25	**86.91**	**12.47**	0.37	0.44	88.07
R368	Grain 3 Core 3	0.04	**90.56**	**8.98**	0.42	0.36	91.44
R368	Grain 3 Rim 1	0.23	**85.18**	**14.17**	0.41	0.36	86.43
R368	Grain 3 Rim 2	0.20	**84.86**	**14.56**	0.37	0.30	86.06
R368	Grain 4 Core 1	0.27	**83.00**	**16.26**	0.48	0.26	84.39
R368	Grain 4 Core 2	0.24	**83.74**	**15.57**	0.45	0.26	85.07
R368	Grain 4 Rim 2	0.29	**82.17**	**17.18**	0.36	0.34	83.52
R368	Grain 5 Core 1	0.30	**83.74**	**15.44**	0.52	0.23	85.17
R368	Grain 5 Core 2	0.23	**82.53**	**16.92**	0.32	0.35	83.78

Appendix 1b: Plagioclase Data

Grain Information		Oxide Wt %					
Sample	**Grain**	**Na2O**	**Al2O3**	**SiO2**	**CaO**	**FeO**	**Sum**
R222	Grain 1 Core	3.17	30.54	49.42	14.90	0.68	98.71
R222	Grain 2 Core	2.85	31.06	48.21	15.56	0.67	98.34
R222	Grain 3 Core 1	3.49	29.95	49.79	14.36	0.63	98.22
R222	Grain 3 Core 2	3.90	29.46	50.82	13.66	0.67	98.50
R235	Grain 1 Core	2.52	31.99	48.29	16.24	0.37	99.42
R235	Grain 2 Core	2.67	31.69	48.35	15.95	0.40	99.06
R235	Grain 3 Core	2.58	31.84	48.48	16.08	0.41	99.39
R235	Grain 4 Core	2.87	31.22	48.65	15.66	0.50	98.90
R265	Grain 1 Core	2.55	33.09	49.13	16.50	0.57	101.82
R265	Grain 2 Core	2.63	33.07	49.45	16.62	0.61	102.37
R265	Grain 3 Core	2.93	32.75	50.11	16.15	0.69	102.62
R265	Grain 4 Core	3.28	32.01	50.58	15.42	0.73	102.01
R265	Grain 5 Core	2.01	34.09	47.76	17.56	0.66	102.07
R265	Grain 6 Core	2.76	33.12	49.45	16.58	0.58	102.49
R265	Grain 7 Core	2.75	32.99	49.64	16.24	0.62	102.25
R265	Grain 8 Core	2.60	32.92	49.32	16.37	0.49	101.69
R267	Grain 1 Core	2.55	31.65	48.16	16.10	0.60	99.07
R267	Grain 2 Core	3.09	30.46	48.63	14.83	0.85	97.86
R267	Grain 3 Core	2.63	31.27	47.69	15.74	0.63	97.96
R267	Grain 4 Core	3.14	30.33	49.00	14.99	0.75	98.20
R267	Grain 5 Core	2.55	31.76	48.14	16.06	0.60	99.12
R267	Grain 6 Core	2.74	31.27	48.23	15.62	0.68	98.53
R267	Grain 7 Core	3.56	29.80	49.55	13.98	0.75	97.64
R362	Grain 1 Core	2.86	31.03	48.38	15.50	0.54	98.30
R362	Grain 1 Rim	3.61	30.40	49.83	14.24	0.64	98.73
R362	Grain 2 Core	2.93	31.10	48.03	15.43	0.55	98.05
R362	Grain 2 Rim	2.87	31.12	47.65	15.50	0.80	97.94
R362	Grain 3 Core	2.87	31.22	48.31	15.53	0.51	98.45
R362	Grain 3 Rim	2.76	31.61	47.93	15.71	0.76	98.78
R362	Grain 4 Core 1	3.02	31.22	49.00	15.25	0.57	99.05
R362	Grain 4 Core 2	2.60	31.76	48.18	16.02	0.62	99.19
R362	Grain 5 Core	2.79	31.10	48.38	15.60	0.57	98.44
R362	Grain 5 Rim	3.34	30.61	49.15	14.78	0.64	98.52
R362	Grain 6 Core 1	2.93	31.12	49.04	15.66	0.54	99.28
R362	Grain 6 Core 2	2.87	31.33	48.83	15.53	0.53	99.09
R362	Grain 6 Rim	3.80	30.08	50.82	13.85	0.71	99.26
R362	Grain 7 Core 1	2.79	31.67	48.59	15.78	0.54	99.37
R362	Grain 7 Core 2	4.17	29.82	50.82	13.61	0.62	99.03
R362	Grain 8 Core	2.90	31.61	48.89	15.52	0.51	99.43
R365	Grain 4 Core	2.68	30.95	48.59	15.57	0.75	98.54
R365	Grain 5 Core	2.48	31.31	47.50	15.95	0.69	97.94
R365	Grain 6 Core	2.71	30.57	48.01	15.57	0.64	97.51
R365	Grain 7 Core	2.74	31.18	48.68	15.67	0.64	98.91

R367	Grain 1 Core	4.25	28.48	51.69	12.70	0.67	97.79
R367	Grain 2 Core	3.21	30.37	49.38	14.83	0.62	98.41
R367	Grain 3 Core	3.22	30.08	49.38	14.50	0.64	97.83
R368	Grain 1 Core	2.51	31.31	47.95	15.95	0.72	98.44
R368	Grain 2 Core	3.59	29.48	49.77	13.98	0.60	97.41
R368	Grain 3 Core	2.51	31.57	47.95	16.13	0.60	98.77
R155	Grain 1 Core	4.25	28.42	51.61	12.80	0.90	97.98
R155	Grain 1 Rim	5.54	26.64	54.43	10.55	0.82	97.99
R155	Grain 2 Core	2.09	32.46	47.14	16.75	0.76	99.20
R155	Grain 2 Rim	4.52	28.38	52.42	12.47	0.98	98.76
R155	Grain 3 Core	4.09	29.14	51.78	13.40	0.94	99.34
R155	Grain 3 Rim	5.70	26.76	55.37	10.31	0.78	98.93
R155	Grain 4 Core	3.86	29.50	51.33	13.70	0.89	99.27
R155	Grain 4 Rim	5.11	27.47	54.02	11.47	0.94	99.02
R155	Grain 5 Core	4.87	28.08	53.81	11.98	0.90	99.64
R155	Grain 5 Rim	5.88	25.94	55.76	9.68	0.69	97.96
R155	Grain 6 Core	4.10	28.89	51.39	13.19	0.82	98.40
R155	Grain 7 Core	3.95	29.16	50.64	13.35	0.91	98.01
R155	Grain 8 Core	4.52	28.10	52.18	12.26	0.89	97.94
R384	Grain 1 Core 1	2.04	31.12	45.68	16.36	0.80	95.99
R384	Grain 2 Core 1	3.94	27.89	50.28	12.86	0.84	95.80
R384	Grain 3 Core 1	2.99	29.51	48.10	14.66	0.81	96.08
R384	Grain 4 Core 1	3.47	28.87	48.95	13.87	0.77	95.93
R384	Grain 1 Core 2	3.74	28.57	49.49	13.49	0.94	96.22
R384	Grain 2 Core 2	3.05	29.14	47.97	14.51	0.86	95.53
R384	Grain 3 Core 2	2.74	30.08	47.31	15.10	0.86	96.08
R384	Grain 4 Core 2	3.86	28.19	50.13	13.11	0.89	96.18
R384	Grain 5 Core	3.96	27.78	50.09	12.82	0.90	95.55
R384	Grain 6 Core	3.65	28.61	49.62	13.50	0.89	96.27
R384	Grain 7 Core	4.06	27.89	50.54	12.80	0.84	96.12
R384	Grain 8 Core	3.80	28.31	49.90	13.24	0.86	96.10
R384	Grain 9 Core	1.96	31.44	45.62	16.71	0.82	96.54
R384	Grain 10 Core	3.99	27.93	50.47	12.77	0.82	95.99
R396	Grain 1 Core	4.56	28.61	51.89	11.82	0.69	97.57
R396	Grain 2 Core	4.07	29.10	50.58	12.86	0.78	97.39
R396	Grain 3 Core	4.31	28.63	51.26	12.42	0.84	97.47
R396	Grain 4 Core	2.47	31.67	46.92	15.76	0.75	97.56
R396	Grain 5 Core	5.42	27.13	53.55	10.56	0.76	97.43
R396	Grain 5 Rim	5.53	26.85	53.81	10.13	0.66	96.98
R396	Grain 6 Core	3.96	29.34	50.39	13.12	0.82	97.64
R396	Grain 6 Rim	4.13	26.15	51.39	12.55	1.83	96.05
R396	Grain 7 Core	4.52	28.34	51.71	12.24	0.84	97.65
R396	Grain 7 Rim	6.98	24.81	57.85	7.60	0.68	97.93
R396	Grain 8 Core	3.95	29.51	50.58	13.08	0.72	97.85
R396	Grain 8 Rim	5.85	26.47	54.41	9.92	0.86	97.52
TS22448	Grain 1 Core	4.56	28.12	52.12	12.09	0.91	97.80
TS22448	Grain 1 Rim	5.04	27.23	53.38	11.05	0.89	97.60
TS22448	Grain 2 Core	5.02	27.30	53.40	11.14	0.90	97.76

TS22448	Grain 2 Rim	4.27	28.40	51.80	12.33	0.89	97.69
TS22448	Grain 3 Core	4.95	27.00	53.15	11.08	0.82	97.00
TS22448	Grain 3 Rim	4.18	28.61	51.35	12.52	0.87	97.54
TS22448	Grain 4 Core	4.96	27.04	53.58	10.90	0.84	97.31
TS22448	Grain 4 Rim	4.64	27.70	52.55	11.59	0.96	97.44
TS22448	Grain 5 Core	4.76	27.34	52.89	11.39	0.91	97.30
TS22448	Grain 6 Core	4.83	27.30	52.81	11.29	0.91	97.14
TS22448	Grain 7 Core	4.26	28.38	51.67	12.58	0.91	97.81
TS22448	Grain 8 Core	4.25	28.36	51.50	12.61	0.95	97.67
TS22448	Grain 9 Core	5.22	26.59	54.15	10.70	0.99	97.65
TS22448	Grain 10 Core	4.88	27.38	53.10	11.12	0.93	97.42

Grain Information		Components		
Sample	**Grain**	**An**	**Ab**	**Or**
R222	Grain 1 Core	72.47	27.53	0.00
R222	Grain 2 Core	75.15	24.84	0.00
R222	Grain 3 Core 1	69.41	30.59	0.00
R222	Grain 3 Core 2	65.92	34.08	0.00
R235	Grain 1 Core	78.04	21.95	0.00
R235	Grain 2 Core	76.72	23.28	0.00
R235	Grain 3 Core	77.54	22.46	0.00
R235	Grain 4 Core	75.11	24.88	0.00
R265	Grain 1 Core	78.17	21.83	0.00
R265	Grain 2 Core	77.74	22.26	0.00
R265	Grain 3 Core	75.32	24.68	0.00
R265	Grain 4 Core	72.23	27.77	0.00
R265	Grain 5 Core	82.83	17.17	0.00
R265	Grain 6 Core	76.81	23.19	0.00
R265	Grain 7 Core	76.55	23.45	0.00
R265	Grain 8 Core	77.66	22.34	0.00
R267	Grain 1 Core	77.76	22.24	0.00
R267	Grain 2 Core	72.61	27.39	0.00
R267	Grain 3 Core	76.82	23.18	0.00
R267	Grain 4 Core	72.49	27.51	0.00
R267	Grain 5 Core	77.71	22.29	0.00
R267	Grain 6 Core	75.91	24.09	0.00
R267	Grain 7 Core	68.43	31.56	0.00
R362	Grain 1 Core	74.97	25.03	0.00
R362	Grain 1 Rim	68.54	31.46	0.00
R362	Grain 2 Core	74.48	25.52	0.00
R362	Grain 2 Rim	74.91	25.09	0.00
R362	Grain 3 Core	74.91	25.09	0.00
R362	Grain 3 Rim	75.85	24.15	0.00
R362	Grain 4 Core 1	73.62	26.38	0.00
R362	Grain 4 Core 2	77.31	22.69	0.00
R362	Grain 5 Core	75.51	24.49	0.00
R362	Grain 5 Rim	70.97	29.03	0.00
R362	Grain 6 Core 1	74.71	25.29	0.00
R362	Grain 6 Core 2	74.91	25.09	0.00
R362	Grain 6 Rim	66.82	33.18	0.00
R362	Grain 7 Core 1	75.75	24.25	0.00
R362	Grain 7 Core 2	64.35	35.65	0.00
R362	Grain 8 Core	74.71	25.29	0.00
R365	Grain 4 Core	76.25	23.75	0.00
R365	Grain 5 Core	78.06	29.94	0.00
R365	Grain 6 Core	76.04	23.96	0.00
R365	Grain 7 Core	75.96	24.04	0.00
R367	Grain 1 Core	62.32	37.68	0.00
R367	Grain 2 Core	71.87	28.13	0.00

R367	Grain 3 Core	71.34	28.66	0.00
R368	Grain 1 Core	77.83	22.17	0.00
R368	Grain 2 Core	68.30	31.70	0.00
R368	Grain 3 Core	78.04	21.96	0.00
R155	Grain 1 Core	62.46	37.53	0.00
R155	Grain 1 Rim	51.25	48.74	0.00
R155	Grain 2 Core	81.55	18.44	0.00
R155	Grain 2 Rim	60.41	39.59	0.00
R155	Grain 3 Core	64.46	35.54	0.00
R155	Grain 3 Rim	49.94	50.05	0.00
R155	Grain 4 Core	66.28	33.72	0.00
R155	Grain 4 Rim	55.38	44.62	0.00
R155	Grain 5 Core	57.60	42.40	0.00
R155	Grain 5 Rim	47.64	52.35	0.00
R155	Grain 6 Core	64.00	36.00	0.00
R155	Grain 7 Core	65.12	34.87	0.00
R155	Grain 8 Core	60.00	40.00	0.00
R384	Grain 1 Core 1	81.60	18.40	0.00
R384	Grain 2 Core 1	64.34	35.66	0.00
R384	Grain 3 Core 1	73.00	27.00	0.00
R384	Grain 4 Core 1	68.86	31.13	0.00
R384	Grain 1 Core 2	66.63	33.37	0.00
R384	Grain 2 Core 2	72.46	27.54	0.00
R384	Grain 3 Core 2	75.28	24.71	0.00
R384	Grain 4 Core 2	65.26	34.74	0.00
R384	Grain 5 Core	64.10	35.90	0.00
R384	Grain 6 Core	67.10	32.90	0.00
R384	Grain 7 Core	63.56	36.44	0.00
R384	Grain 8 Core	65.77	34.23	0.00
R384	Grain 9 Core	82.48	17.51	0.00
R384	Grain 10 Core	63.87	36.13	0.00
R396	Grain 1 Core	58.92	41.08	0.00
R396	Grain 2 Core	63.57	36.43	0.00
R396	Grain 3 Core	61.39	38.60	0.00
R396	Grain 4 Core	77.91	22.08	0.00
R396	Grain 5 Core	51.86	48.14	0.00
R396	Grain 5 Rim	50.32	49.67	0.00
R396	Grain 6 Core	64.65	35.35	0.00
R396	Grain 6 Rim	62.68	37.32	0.00
R396	Grain 7 Core	59.95	40.05	0.00
R396	Grain 7 Rim	37.55	62.44	0.00
R396	Grain 8 Core	64.65	35.35	0.00
R396	Grain 8 Rim	48.36	51.64	0.00
TS22448	Grain 1 Core	61.30	38.70	0.00
TS22448	Grain 1 Rim	54.77	45.23	0.00
TS22448	Grain 2 Core	55.09	44.91	0.00
TS22448	Grain 2 Rim	61.42	38.58	0.00
TS22448	Grain 3 Core	55.30	44.70	0.00

TS22448	Grain 3 Rim	62.32	37.68	0.00
TS22448	Grain 4 Core	54.82	45.18	0.00
TS22448	Grain 4 Rim	57.99	42.01	0.00
TS22448	Grain 5 Core	56.96	43.04	0.00
TS22448	Grain 6 Core	56.37	43.63	0.00
TS22448	Grain 7 Core	61.97	38.03	0.00
TS22448	Grain 8 Core	62.12	37.88	0.00
TS22448	Grain 9 Core	53.14	46.85	0.00
TS22448	Grain 10 Core	55.74	44.25	0.00

Appendix 1c: Clinopyroxene Data

Grain Information		Weight Per Cent									
Sample	Grain	Si02	TiO2	Al203	Cr2O3	FeO	MnO	MgO	CaO	Na20	Sum
R222	Gr1 C 1	50.11	0.77	3.76	0.73	5.75	0.00	16.08	21.04	0.36	98.61
R222	Gr1 C 2	50.24	0.82	3.55	0.70	6.03	0.00	16.22	20.85	0.34	98.74
R222	Gr1 C 3	50.34	0.88	3.16	0.72	6.23	0.00	16.37	20.34	0.39	98.43
R222	Gr2 C 1	50.54	0.73	4.50	0.67	5.31	0.00	16.27	21.55	0.28	99.85
R222	Gr3 C 1	49.17	1.95	3.10	0.12	7.37	0.00	15.47	20.46	0.51	98.15
R222	Gr3 C 2	50.62	1.45	2.36	0.15	7.33	0.00	16.10	20.29	0.53	98.83
R235	Gr1 C 1	51.01	0.63	3.65	0.85	4.40	0.00	16.68	21.63	0.36	99.21
R235	Gr2 C 1	51.18	0.67	4.27	1.23	4.26	0.00	16.70	21.84	0.35	100.49
R235	Gr3 C 1	50.67	0.62	4.19	1.42	4.27	0.00	16.55	21.66	0.35	99.73
R267	Gr1 C 1	51.05	0.80	3.38	0.38	7.94	0.00	16.08	20.08	0.35	100.06
R267	Gr2 C 1	51.01	1.20	3.55	0.35	8.70	0.00	15.60	20.30	0.40	101.12
R267	Gr3 C 1	50.47	1.30	3.14	0.15	9.15	0.00	15.45	19.98	0.46	100.10
R267	Gr4 C 1	51.46	0.70	2.23	0.32	7.72	0.00	16.50	19.84	0.38	99.15
R267	Gr5 C 1	50.69	0.83	3.50	0.48	7.83	0.00	16.22	19.85	0.39	99.80
R367	Gr1 C 1	50.84	0.63	3.67	0.64	5.53	0.00	16.27	21.17	0.38	99.13
R367	Gr2 C 1	50.34	0.75	3.67	0.79	5.71	0.00	16.07	20.89	0.35	98.57
R367	Gr3 C 1	50.09	1.18	3.38	0.58	6.82	0.00	15.87	20.12	0.38	98.42
R367	Gr4 C 1	52.25	0.47	2.25	0.51	5.45	0.00	17.28	20.78	0.31	99.30
R368	Gr1 C 1	49.94	0.72	3.82	0.95	4.86	0.00	15.92	21.45	0.31	97.96
R368	Gr2 C 1	50.86	1.07	2.80	0.70	5.81	0.00	16.48	20.76	0.38	98.86
R368	Gr3 C 1	49.81	0.80	3.95	1.02	5.03	0.00	15.89	21.35	0.31	98.16
R381	Gr1 C 1	50.00	1.00	3.33	0.00	10.03	0.26	14.24	20.61	0.49	99.96
R381	Gr1 R 1	51.52	0.78	1.66	0.00	12.02	0.40	13.40	20.12	0.46	100.36
R381	Gr2 C 1	51.44	0.92	2.38	0.00	9.82	0.26	14.72	20.46	0.49	100.47
R381	Gr2 R 1	51.37	0.87	2.23	0.00	11.90	0.34	13.78	19.98	0.53	100.99
R381	Gr3 C 1	50.26	0.98	3.29	0.00	10.05	0.00	14.26	20.61	0.44	99.89
R381	Gr3 R 1	50.43	1.10	2.95	0.00	10.55	0.22	14.11	20.55	0.46	100.37
R381	Gr4 C 1	51.09	0.80	2.89	0.23	9.24	0.00	15.09	20.54	0.46	100.34
R381	Gr4 R 1	51.22	0.68	1.76	0.00	12.36	0.36	12.80	20.44	0.46	100.09
R381	Gr5 C 1	51.39	0.77	2.46	0.00	9.56	0.26	14.94	20.44	0.42	100.23
R381	Gr5 R 1	50.90	0.85	2.12	0.00	12.50	0.39	13.03	19.98	0.50	100.27
R381	Gr 6 C 1	51.26	0.80	2.72	0.00	9.60	0.19	14.92	20.60	0.46	100.56
R381	Gr 6 R 1	50.20	1.02	2.78	0.00	10.78	0.27	13.76	20.13	0.46	99.40
R381	Gr 7 C 1	50.79	0.80	2.51	0.00	9.92	0.21	14.76	20.43	0.40	99.82
R381	Gr 7 R 1	50.88	0.62	1.59	0.00	13.50	0.41	12.30	19.92	0.49	99.71
R384	Gr1 C 1	50.92	0.58	1.91	0.00	12.97	0.36	15.97	16.59	0.30	99.60
R384	Gr1 R 1	50.99	0.60	1.72	0.00	13.93	0.37	15.80	15.73	0.28	99.43
R384	Gr2 C 1	50.43	0.62	1.91	0.00	13.10	0.40	15.47	16.64	0.30	98.86
R384	Gr2 C 2	50.90	0.65	1.78	0.00	12.16	0.34	16.02	16.90	0.28	99.02
R384	Gr3 C 1	50.26	0.62	2.12	0.00	13.96	0.41	15.37	15.89	0.35	98.98
R384	Gr4 C 1	50.77	0.68	2.19	0.00	11.48	0.32	15.67	17.77	0.30	99.18
R384	Gr4 R 1	50.47	0.65	2.38	0.00	11.28	0.32	15.87	17.62	0.26	98.85
R384	Gr5 C 1	50.07	0.82	2.00	0.00	13.30	0.40	14.36	17.64	0.27	98.86

R384	Gr 6 C 1	50.28	0.72	1.81	0.00	15.28	0.44	15.11	15.21	0.32	99.17
R384	Gr 7 C 1	50.84	0.63	2.23	0.00	11.40	0.30	16.02	17.74	0.30	99.45
R384	Gr 8 C 1	50.24	0.73	1.68	0.00	15.86	0.49	14.96	14.86	0.28	99.11
R384	Gr 9 C 1	50.05	0.90	2.17	0.00	13.28	0.37	14.36	17.57	0.31	99.01
R384	Gr10 C 1	50.67	0.62	2.08	0.00	12.97	0.37	16.53	15.22	0.32	98.78
R362	Gr1 C 1	51.97	0.70	2.10	0.60	5.75	0.00	17.53	20.89	0.36	99.90
R362	Gr2 C 1	52.31	0.60	2.17	0.64	5.48	0.00	17.63	21.14	0.30	100.28
R362	Gr3 C 1	50.94	0.83	3.91	0.98	5.75	0.00	16.96	20.92	0.39	100.69
R362	Gr4 C 1	50.58	0.83	3.93	0.91	5.53	0.00	16.42	21.44	0.39	100.03
R362	Gr 6 C 1	50.73	1.78	2.76	0.31	6.95	0.21	16.73	20.40	0.49	100.35
R362	Gr 7 C 1	51.07	0.85	3.40	0.73	6.09	0.00	17.00	20.92	0.43	100.49
R362	Gr 8 C 1	51.03	0.63	4.19	0.85	4.88	0.00	16.60	21.98	0.31	100.47
R155	Gr1 C 1	50.32	0.78	1.91	0.00	14.82	0.49	14.59	16.03	0.30	99.25
R155	Gr1 R 1	50.11	0.55	1.78	0.00	15.18	0.56	12.14	18.20	0.32	98.84
R155	Gr1 C 2	50.32	0.82	2.31	0.00	13.02	0.36	14.76	17.41	0.40	99.40
R155	Gr2 C 1	50.75	0.72	1.87	0.00	15.40	0.43	15.40	14.68	0.53	99.77
R155	Gr3 C 1	50.71	0.87	2.34	0.00	12.34	0.35	14.74	18.06	0.43	99.84
R155	Gr4 C 1	50.17	0.72	1.42	0.00	19.12	0.61	12.93	14.34	0.32	99.63
R155	Gr5 C 1	50.43	0.80	2.27	0.00	12.90	0.25	14.67	17.63	0.34	99.29
R155	Gr 6 C 1	50.22	0.57	2.00	0.00	13.03	0.45	12.55	19.60	0.42	98.84
R155	Gr 7 C 1	49.70	0.85	1.63	0.00	17.97	0.50	12.60	15.76	0.30	99.31
R155	Gr 8 C 1	50.30	0.82	2.06	0.00	14.01	0.37	14.34	17.03	0.38	99.31
R155	Gr 9 C 1	51.03	0.63	1.70	0.00	15.33	0.45	15.32	14.94	0.38	99.79
R265	Gr1 C 1	53.32	1.47	1.95	0.34	5.88	0.00	18.59	20.22	0.49	102.24
R265	Gr2 C 1	52.51	1.38	3.10	0.83	5.51	0.00	17.56	21.42	0.42	102.73
R265	Gr3 C 1	51.37	2.44	3.17	0.00	6.41	0.00	17.49	20.61	0.55	102.05
R265	Gr4 C 1	52.10	0.68	4.18	0.96	4.71	0.00	17.38	22.09	0.35	102.45
R265	Gr5 C 1	51.99	0.72	4.27	0.80	4.59	0.00	17.18	22.39	0.31	102.25
R265	Gr 6 C 1	52.01	0.90	3.82	1.07	5.35	0.00	17.39	21.25	0.38	102.18
R265	Gr 7 C 1	53.23	1.35	2.00	0.47	5.81	0.00	18.46	20.33	0.43	102.09
R265	Gr 8 C 1	52.25	1.00	3.57	1.05	5.25	0.00	17.63	21.51	0.38	102.63
R396	Gr1 C 1	51.48	0.42	2.15	0.00	7.47	0.21	16.55	20.30	0.32	98.91
R396	Gr2 C 1	50.86	0.58	2.34	0.00	8.86	0.21	15.90	19.92	0.36	99.05
R396	Gr3 C 1	50.82	0.57	2.19	0.00	8.99	0.00	15.85	19.67	0.36	98.46
R396	Gr4 C 1	51.31	0.40	2.40	0.00	6.78	0.00	16.50	20.95	0.34	98.67
R396	Gr4 R 1	50.11	0.67	1.57	0.00	14.40	0.43	13.78	17.36	0.36	98.67
R396	Gr5 C 1	51.12	0.40	2.14	0.00	6.99	0.00	16.28	20.69	0.26	97.87
R396	Gr5 R 1	50.69	0.57	2.27	0.00	8.62	0.28	15.64	19.83	0.36	98.25
R396	Gr 6 C 1	51.01	0.42	2.32	0.00	6.51	0.00	16.37	20.74	0.28	97.64
R396	Gr 6 R 1	51.39	0.47	2.44	0.00	6.48	0.00	16.32	21.10	0.30	98.49
R396	Gr 7 C 1	51.37	0.37	2.23	0.00	6.59	0.00	16.22	21.41	0.26	98.44
R396	Gr 7 R 1	51.05	0.53	2.34	0.00	8.09	0.22	16.05	19.91	0.30	98.50
R396	Gr 8 C 1	51.05	0.47	2.27	0.00	7.65	0.00	16.17	19.98	0.31	97.90
R396	Gr 8 R 1	49.55	0.58	2.82	0.00	10.38	0.31	13.76	19.28	0.39	97.08
TS22448	Gr1 R 1	49.83	0.68	1.44	0.00	16.54	0.53	12.88	16.94	0.30	99.15
TS22448	Gr2 R 1	50.20	0.55	1.36	0.00	16.13	0.46	13.48	16.87	0.24	99.30
TS22448	Gr2 R 2	49.98	0.62	1.53	0.00	15.98	0.49	13.46	17.22	0.28	99.57
TS22448	Gr3 R 1	49.13	0.35	0.85	0.00	25.58	0.72	16.10	4.39	0.00	97.12

TS22448	Gr4R 1	48.61	0.33	0.87	0.00	27.41	0.77	15.45	4.00	0.00	97.46
TS22448	Gr5 R 1	48.93	0.63	1.38	0.00	15.51	0.45	13.38	16.59	0.30	97.19
TS22448	Gr 6 R 1	48.70	0.67	1.42	0.00	15.32	0.44	12.87	16.79	0.27	96.47
TS22448	Gr 6 R 2	48.38	0.65	1.27	0.00	16.49	0.53	11.99	16.76	0.24	96.31

Grain Information		Formula recast to 6 oxygens											
Sample	Grain	Si	Al	Al	Fe(iii)	Cr	Ti	Fe(ii)	Mn	Mg	Ca	Na	Sum
R222	Gr1 C 1	1.87	0.13	0.04	0.08	0.02	0.02	0.10	0.00	0.90	0.84	0.03	4.02
R222	Gr1 C 2	1.88	0.12	0.03	0.08	0.02	0.02	0.11	0.00	0.90	0.83	0.02	4.02
R222	Gr1 C 3	1.89	0.11	0.02	0.07	0.02	0.02	0.12	0.00	0.91	0.82	0.03	4.02
R222	Gr2 C 1	1.86	0.14	0.06	0.07	0.02	0.02	0.10	0.00	0.89	0.85	0.02	4.02
R222	Gr3 C 1	1.86	0.14	0.00	0.09	0.00	0.06	0.14	0.00	0.87	0.83	0.04	4.03
R222	Gr3 C 2	1.90	0.10	0.00	0.08	0.00	0.04	0.15	0.00	0.90	0.81	0.04	4.03
R235	Gr1 C 1	1.88	0.12	0.04	0.06	0.02	0.02	0.07	0.00	0.92	0.86	0.03	4.02
R235	Gr2 C 1	1.87	0.13	0.05	0.06	0.04	0.02	0.07	0.00	0.91	0.85	0.02	4.02
R235	Gr3 C 1	1.86	0.14	0.05	0.06	0.04	0.02	0.07	0.00	0.91	0.85	0.02	4.02
R267	Gr1 C 1	1.89	0.11	0.04	0.07	0.01	0.02	0.18	0.00	0.89	0.80	0.03	4.02
R267	Gr2 C 1	1.88	0.12	0.03	0.07	0.01	0.03	0.19	0.00	0.86	0.80	0.03	4.02
R267	Gr3 C 1	1.88	0.12	0.02	0.09	0.00	0.04	0.19	0.00	0.86	0.80	0.03	4.03
R267	Gr4 C 1	1.92	0.08	0.02	0.07	0.01	0.02	0.17	0.00	0.92	0.79	0.03	4.02
R267	Gr5 C 1	1.88	0.12	0.03	0.08	0.01	0.02	0.16	0.00	0.90	0.79	0.03	4.03
R367	Gr1 C 1	1.89	0.11	0.05	0.06	0.02	0.02	0.11	0.00	0.90	0.84	0.03	4.02
R367	Gr2 C 1	1.88	0.12	0.04	0.06	0.02	0.02	0.12	0.00	0.89	0.84	0.03	4.02
R367	Gr3 C 1	1.88	0.12	0.03	0.05	0.02	0.03	0.16	0.00	0.89	0.81	0.03	4.02
R367	Gr4 C 1	1.93	0.07	0.03	0.04	0.01	0.01	0.12	0.00	0.95	0.82	0.02	4.01
R368	Gr1 C 1	1.87	0.13	0.04	0.06	0.03	0.02	0.09	0.00	0.89	0.86	0.02	4.02
R368	Gr2 C 1	1.89	0.11	0.02	0.05	0.02	0.03	0.13	0.00	0.91	0.83	0.03	4.02
R368	Gr3 C 1	1.87	0.13	0.04	0.06	0.03	0.02	0.10	0.00	0.89	0.86	0.02	4.02
R381	Gr1 C 1	1.88	0.12	0.02	0.11	0.00	0.03	0.20	0.01	0.80	0.83	0.04	4.04
R381	Gr1 R 1	1.94	0.06	0.01	0.06	0.00	0.02	0.32	0.01	0.75	0.81	0.03	4.02
R381	Gr2 C 1	1.91	0.09	0.02	0.08	0.00	0.03	0.23	0.01	0.82	0.82	0.04	4.02
R381	Gr2 R 1	1.92	0.08	0.02	0.08	0.00	0.02	0.29	0.01	0.77	0.80	0.04	4.02
R381	Gr3 C 1	1.88	0.12	0.03	0.09	0.00	0.03	0.22	0.00	0.80	0.83	0.03	4.03
R381	Gr3 R 1	1.89	0.11	0.02	0.10	0.00	0.03	0.23	0.01	0.79	0.82	0.03	4.03
R381	Gr4 C 1	1.90	0.10	0.03	0.09	0.01	0.02	0.20	0.00	0.84	0.82	0.03	4.03
R381	Gr4 R 1	1.94	0.06	0.02	0.06	0.00	0.02	0.33	0.01	0.72	0.83	0.03	4.02
R381	Gr5 C 1	1.91	0.09	0.02	0.08	0.00	0.02	0.22	0.01	0.83	0.82	0.03	4.02
R381	Gr5 R 1	1.92	0.08	0.02	0.08	0.00	0.02	0.32	0.01	0.73	0.81	0.04	4.02
R381	Gr 6 C 1	1.90	0.10	0.02	0.09	0.00	0.02	0.21	0.01	0.83	0.82	0.03	4.03
R381	Gr 6 R 1	1.90	0.10	0.02	0.08	0.00	0.03	0.26	0.01	0.78	0.82	0.03	4.02
R381	Gr 7 C 1	1.90	0.10	0.02	0.09	0.00	0.02	0.21	0.01	0.83	0.82	0.03	4.03
R381	Gr 7 R 1	1.94	0.06	0.01	0.07	0.00	0.02	0.36	0.01	0.70	0.81	0.04	4.02
R384	Gr1 C 1	1.92	0.08	0.00	0.09	0.00	0.02	0.31	0.01	0.90	0.67	0.02	4.03
R384	Gr1 R 1	1.93	0.07	0.01	0.08	0.00	0.02	0.36	0.01	0.89	0.64	0.02	4.02
R384	Gr2 C 1	1.92	0.08	0.01	0.09	0.00	0.02	0.32	0.01	0.88	0.68	0.02	4.03
R384	Gr2 C 2	1.93	0.07	0.00	0.08	0.00	0.02	0.30	0.01	0.90	0.68	0.02	4.02
R384	Gr3 C 1	1.91	0.09	0.01	0.10	0.00	0.02	0.34	0.01	0.87	0.65	0.03	4.03
R384	Gr4 C 1	1.92	0.08	0.01	0.08	0.00	0.02	0.28	0.01	0.88	0.72	0.02	4.02
R384	Gr4 R 1	1.91	0.09	0.02	0.09	0.00	0.02	0.27	0.01	0.89	0.71	0.02	4.03
R384	Gr5 C 1	1.91	0.09	0.00	0.08	0.00	0.02	0.34	0.01	0.82	0.72	0.02	4.02
R384	Gr 6 C 1	1.92	0.08	0.00	0.09	0.00	0.02	0.39	0.01	0.86	0.62	0.02	4.03
R384	Gr 7 C 1	1.91	0.09	0.01	0.09	0.00	0.02	0.26	0.01	0.90	0.71	0.02	4.03

R384	Gr 8 C 1	1.92	0.08	0.00	0.08	0.00	0.02	0.42	0.02	0.85	0.61	0.02	4.02
R384	Gr 9 C 1	1.91	0.09	0.01	0.08	0.00	0.03	0.34	0.01	0.82	0.72	0.02	4.02
R384	Gr10 C 1	1.92	0.08	0.01	0.08	0.00	0.02	0.32	0.01	0.93	0.62	0.02	4.03
R362	Gr1 C 1	1.91	0.09	0.00	0.08	0.02	0.02	0.09	0.00	0.96	0.82	0.03	4.03
R362	Gr2 C 1	1.91	0.09	0.01	0.07	0.02	0.02	0.10	0.00	0.96	0.83	0.02	4.02
R362	Gr3 C 1	1.86	0.14	0.03	0.09	0.03	0.02	0.08	0.00	0.92	0.82	0.03	4.03
R362	Gr4 C 1	1.86	0.14	0.03	0.09	0.03	0.02	0.08	0.00	0.90	0.85	0.03	4.03
R362	Gr 6 C 1	1.87	0.12	0.00	0.10	0.01	0.05	0.12	0.01	0.92	0.81	0.03	4.03
R362	Gr 7 C 1	1.87	0.13	0.02	0.10	0.02	0.02	0.08	0.00	0.93	0.82	0.03	4.03
R362	Gr 8 C 1	1.87	0.13	0.05	0.08	0.02	0.02	0.07	0.00	0.90	0.86	0.02	4.02
R155	Gr1 C 1	1.92	0.08	0.01	0.08	0.00	0.02	0.39	0.02	0.83	0.66	0.02	4.02
R155	Gr1 R 1	1.94	0.06	0.02	0.06	0.00	0.02	0.43	0.02	0.70	0.75	0.02	4.02
R155	Gr1 C 2	1.91	0.09	0.01	0.09	0.00	0.02	0.32	0.01	0.83	0.71	0.03	4.03
R155	Gr2 C 1	1.92	0.08	0.01	0.10	0.00	0.02	0.38	0.01	0.87	0.60	0.04	4.03
R155	Gr3 C 1	1.91	0.09	0.01	0.08	0.00	0.02	0.30	0.01	0.83	0.73	0.03	4.03
R155	Gr4 C 1	1.94	0.06	0.00	0.06	0.00	0.02	0.55	0.02	0.74	0.59	0.02	4.02
R155	Gr5 C 1	1.91	0.09	0.01	0.08	0.00	0.02	0.33	0.01	0.83	0.72	0.02	4.02
R155	Gr 6 C 1	1.93	0.07	0.02	0.08	0.00	0.02	0.34	0.01	0.72	0.81	0.03	4.02
R155	Gr 7 C 1	1.92	0.07	0.00	0.07	0.00	0.02	0.50	0.02	0.73	0.65	0.02	4.02
R155	Gr 8 C 1	1.92	0.08	0.01	0.08	0.00	0.02	0.36	0.01	0.81	0.69	0.03	4.02
R155	Gr 9 C 1	1.93	0.07	0.01	0.08	0.00	0.02	0.41	0.01	0.86	0.61	0.03	4.02
R265	Gr1 C 1	1.91	0.08	0.00	0.06	0.01	0.04	0.11	0.00	0.99	0.78	0.03	4.02
R265	Gr2 C 1	1.88	0.12	0.01	0.06	0.02	0.04	0.10	0.00	0.94	0.82	0.03	4.02
R265	Gr3 C 1	1.86	0.14	0.00	0.09	0.00	0.07	0.10	0.00	0.94	0.80	0.04	4.03
R265	Gr4 C 1	1.87	0.13	0.04	0.08	0.03	0.02	0.06	0.00	0.93	0.85	0.02	4.03
R265	Gr5 C 1	1.86	0.14	0.05	0.08	0.02	0.02	0.06	0.00	0.92	0.86	0.02	4.02
R265	Gr 6 C 1	1.87	0.13	0.03	0.07	0.03	0.02	0.09	0.00	0.93	0.82	0.03	4.02
R265	Gr 7 C 1	1.91	0.08	0.00	0.06	0.01	0.04	0.12	0.00	0.99	0.78	0.03	4.02
R265	Gr 8 C 1	1.87	0.13	0.02	0.08	0.03	0.03	0.08	0.00	0.94	0.82	0.03	4.02
R396	Gr1 C 1	1.92	0.08	0.02	0.09	0.00	0.01	0.15	0.01	0.92	0.81	0.02	4.03
R396	Gr2 C 1	1.91	0.09	0.01	0.10	0.00	0.02	0.17	0.01	0.89	0.80	0.03	4.03
R396	Gr3 C 1	1.92	0.08	0.02	0.09	0.00	0.02	0.19	0.00	0.89	0.80	0.03	4.03
R396	Gr4 C 1	1.92	0.08	0.02	0.09	0.00	0.01	0.12	0.00	0.92	0.84	0.02	4.03
R396	Gr4 R 1	1.93	0.07	0.00	0.09	0.00	0.02	0.37	0.01	0.79	0.72	0.03	4.03
R396	Gr5 C 1	1.93	0.07	0.02	0.07	0.00	0.01	0.15	0.00	0.92	0.84	0.02	4.02
R396	Gr5 R 1	1.92	0.08	0.02	0.09	0.00	0.02	0.18	0.01	0.88	0.80	0.03	4.03
R396	Gr 6 C 1	1.92	0.08	0.03	0.07	0.00	0.01	0.14	0.00	0.92	0.84	0.02	4.02
R396	Gr 6 R 1	1.92	0.08	0.03	0.07	0.00	0.01	0.14	0.00	0.91	0.85	0.02	4.02
R396	Gr 7 C 1	1.93	0.07	0.02	0.07	0.00	0.01	0.13	0.00	0.91	0.86	0.02	4.02
R396	Gr 7 R 1	1.92	0.08	0.02	0.07	0.00	0.02	0.18	0.01	0.90	0.80	0.02	4.02
R396	Gr 8 C 1	1.93	0.07	0.03	0.06	0.00	0.01	0.18	0.00	0.91	0.81	0.02	4.02
R396	Gr 8 R 1	1.91	0.09	0.04	0.06	0.00	0.02	0.27	0.01	0.79	0.80	0.03	4.02
TS22448	Gr1 R 1	1.93	0.07	0.00	0.10	0.00	0.02	0.44	0.02	0.74	0.70	0.02	4.03
TS22448	Gr2 R 1	1.93	0.06	0.00	0.09	0.00	0.02	0.42	0.02	0.77	0.70	0.02	4.03
TS22448	Gr2 R 2	1.92	0.07	0.00	0.11	0.00	0.02	0.39	0.02	0.77	0.71	0.02	4.03
TS22448	Gr3 R 1	1.95	0.04	0.00	0.05	0.00	0.01	0.79	0.02	0.95	0.19	0.00	4.01
TS22448	Gr4R 1	1.94	0.04	0.00	0.08	0.00	0.01	0.83	0.03	0.92	0.17	0.00	4.02
TS22448	Gr5 R 1	1.92	0.06	0.00	0.11	0.00	0.02	0.39	0.02	0.78	0.70	0.02	4.03

TS22448	Gr 6 R 1	1.93	0.07	0.00	0.09	0.00	0.02	0.42	0.01	0.76	0.71	0.02	4.03
TS22448	Gr 6 R 2	1.93	0.06	0.00	0.09	0.00	0.02	0.46	0.02	0.71	0.72	0.02	4.03

Grain Information		Components		
Sample	**Grain**	**Wo**	**En**	**Fs**
R222	Gr1 C 1	43.95	46.74	9.31
R222	Gr1 C 2	43.35	46.92	9.73
R222	Gr1 C 3	42.43	47.50	10.07
R222	Gr2 C 1	44.61	46.86	8.54
R222	Gr3 C 1	42.89	45.14	11.97
R222	Gr3 C 2	41.94	46.31	11.75
R235	Gr1 C 1	44.82	48.10	7.08
R235	Gr2 C 1	45.14	48.02	6.84
R235	Gr3 C 1	45.12	47.97	6.91
R267	Gr1 C 1	41.30	46.03	12.67
R267	Gr2 C 1	41.63	44.53	13.84
R267	Gr3 C 1	41.14	44.28	14.59
R267	Gr4 C 1	40.66	47.06	12.28
R267	Gr5 C 1	40.94	46.53	12.52
R367	Gr1 C 1	44.01	47.06	8.93
R367	Gr2 C 1	43.81	46.89	9.30
R367	Gr3 C 1	42.36	46.49	11.15
R367	Gr4 C 1	42.35	49.00	8.65
R368	Gr1 C 1	45.27	46.75	7.97
R368	Gr2 C 1	43.06	47.57	9.37
R368	Gr3 C 1	45.08	46.67	8.25
R381	Gr1 C 1	42.59	40.96	16.45
R381	Gr1 R 1	41.56	38.51	19.93
R381	Gr2 C 1	41.95	42.02	16.03
R381	Gr2 R 1	41.07	39.42	19.51
R381	Gr3 C 1	42.73	41.14	16.13
R381	Gr3 R 1	42.35	40.46	17.19
R381	Gr4 C 1	42.18	43.12	14.70
R381	Gr4 R 1	42.46	37.00	20.53
R381	Gr5 C 1	41.85	42.56	15.59
R381	Gr5 R 1	41.52	37.69	20.79
R381	Gr 6 C 1	42.07	42.42	15.50
R381	Gr 6 R 1	42.07	40.02	17.91
R381	Gr 7 C 1	41.85	42.07	16.07
R381	Gr 7 R 1	41.65	35.79	22.57
R384	Gr1 C 1	33.77	45.22	21.02
R384	Gr1 R 1	32.22	45.04	22.74
R384	Gr2 C 1	34.21	44.27	21.51
R384	Gr2 C 2	34.58	45.60	19.82
R384	Gr3 C 1	32.83	44.18	22.99
R384	Gr4 C 1	36.47	44.75	18.78
R384	Gr4 R 1	36.17	45.35	18.48
R384	Gr5 C 1	36.56	41.41	22.03
R384	Gr 6 C 1	31.41	43.42	25.17
R384	Gr 7 C 1	36.14	45.40	18.46

R384	Gr 8 C 1	30.73	43.04	26.23
R384	Gr 9 C 1	36.50	41.50	21.99
R384	Gr10 C 1	31.34	47.36	21.30
R362	Gr1 C 1	42.00	49.04	8.96
R362	Gr2 C 1	42.35	49.13	8.52
R362	Gr3 C 1	42.71	48.20	9.10
R362	Gr4 C 1	44.14	47.04	8.83
R362	Gr 6 C 1	41.44	47.30	11.26
R362	Gr 7 C 1	42.45	48.00	9.56
R362	Gr 8 C 1	44.99	47.27	7.74
R155	Gr1 C 1	33.25	42.11	24.64
R155	Gr1 R 1	38.47	35.69	25.84
R155	Gr1 C 2	36.03	42.51	21.46
R155	Gr2 C 1	30.34	44.32	25.34
R155	Gr3 C 1	37.31	42.37	20.32
R155	Gr4 C 1	30.09	37.76	32.14
R155	Gr5 C 1	36.54	42.32	21.14
R155	Gr 6 C 1	41.24	36.75	22.02
R155	Gr 7 C 1	33.08	36.82	30.10
R155	Gr 8 C 1	35.37	41.46	23.17
R155	Gr 9 C 1	30.80	43.95	25.25
R265	Gr1 C 1	39.92	51.07	9.01
R265	Gr2 C 1	42.73	48.74	8.53
R265	Gr3 C 1	41.29	48.77	9.94
R265	Gr4 C 1	44.25	48.44	7.31
R265	Gr5 C 1	44.91	47.95	7.15
R265	Gr 6 C 1	42.84	48.79	8.37
R265	Gr 7 C 1	40.23	50.83	8.94
R265	Gr 8 C 1	42.92	48.95	8.12
R396	Gr1 C 1	41.19	46.72	12.08
R396	Gr2 C 1	40.60	45.09	14.31
R396	Gr3 C 1	40.40	45.30	14.30
R396	Gr4 C 1	42.61	46.71	10.68
R396	Gr4 R 1	36.15	39.92	23.92
R396	Gr5 C 1	42.43	46.46	11.11
R396	Gr5 R 1	40.89	44.87	14.24
R396	Gr 6 C 1	42.70	46.90	10.40
R396	Gr 6 R 1	43.20	46.49	10.31
R396	Gr 7 C 1	43.61	45.98	10.41
R396	Gr 7 R 1	40.89	45.87	13.25
R396	Gr 8 C 1	41.26	46.46	12.27
R396	Gr 8 R 1	41.25	40.98	17.77
TS22448	Gr1 R 1	35.23	37.27	27.50
TS22448	Gr2 R 1	34.80	38.68	26.52
TS22448	Gr2 R 2	35.37	38.47	26.16
TS22448	Gr3 R 1	9.30	47.43	43.27
TS22448	Gr4R 1	8.45	45.40	46.15
TS22448	Gr5 R 1	34.88	39.14	25.97

TS22448	Gr 6 R 1	35.79	38.17	26.04
TS22448	Gr 6 R 2	35.94	35.77	28.30

Appendix 1d: Oxide Data

Grain Information		Weight Per Cent											
Sample	Grain	Mg	Al	Si	Ca	Ti	V	Cr	Mn	Fe	Ni	Zn	Sum
R222	G 1 C 1	12.85	22.01	0.00	0.00	0.30	0.00	40.30	0.25	23.09	0.00	0.31	99.11
R222	G 1 C 2	14.15	25.02	0.00	0.00	0.27	0.00	38.46	0.00	20.94	0.00	0.15	98.98
R222	G 2 C 1	13.90	25.87	0.00	0.00	0.30	0.00	39.77	0.00	19.85	0.20	0.00	99.89
R222	G 2 R 1	13.48	22.09	0.00	0.00	0.50	0.00	40.05	0.00	24.46	0.00	0.42	101.00
R222	G 3 C 1	11.43	21.64	0.00	0.00	0.30	0.00	39.96	0.00	25.55	0.00	0.00	98.87
R222	G 3 R 2	9.50	11.89	0.00	0.00	5.57	0.66	31.23	0.00	40.04	0.00	0.00	98.89
R222	G 3 C 2	11.41	18.76	0.41	0.00	1.35	0.00	39.45	0.00	27.61	0.00	0.70	99.69
R222	G 3 R 2	8.19	10.35	0.00	0.36	5.07	0.51	31.40	0.75	41.00	0.00	0.41	98.05
R222	G 3 R 2a	8.33	11.05	0.00	0.00	5.72	0.60	29.89	0.00	41.78	0.00	0.00	97.38
R222	G 3 C 3	11.91	22.83	0.00	0.00	0.33	0.00	39.77	0.80	23.45	0.00	0.02	99.12
R222	G 3 R 3	8.13	13.09	0.00	0.00	3.87	0.49	33.15	0.79	38.49	0.00	0.00	98.01
R235	G 1 C 1	12.59	24.49	0.00	0.00	0.00	0.00	39.36	0.00	22.96	0.00	0.01	99.41
R235	G 1 R 1	9.01	9.37	0.00	0.00	6.77	0.78	28.95	0.70	43.46	0.00	0.00	99.04
R235	G 2 C 1	12.31	24.09	0.00	0.00	0.32	0.00	39.41	0.79	22.67	0.00	0.66	100.23
R235	G 2 R 1	8.16	7.95	0.00	0.00	6.01	0.63	31.29	0.72	42.69	0.00	0.00	97.45
R235	G 2 R 2	8.69	8.77	0.00	0.00	6.04	0.60	32.10	0.74	40.54	0.00	0.00	97.47
R235	G 2 C 2	11.49	21.30	0.00	0.00	0.38	0.00	39.45	0.00	26.31	0.00	0.29	99.22
R235	G 2 R 3	8.64	7.80	0.00	0.00	6.69	0.68	31.85	0.00	41.84	0.00	0.00	97.50
R235	G 3 C 1	11.03	22.75	0.00	0.00	0.00	0.00	39.70	0.00	25.90	0.00	0.73	100.11
R235	G 3 R 1	7.43	7.18	0.00	0.00	7.19	1.15	25.72	0.00	49.47	0.19	0.00	98.33
R235	G 3 R 2	7.15	5.73	0.00	0.00	6.64	1.34	24.35	0.00	51.83	0.00	0.00	97.03
R267	G 1 C 1	16.45	26.85	0.00	0.00	0.00	0.00	40.30	0.00	15.68	0.00	0.35	99.63
R267	G 1 R 1	16.12	26.36	0.00	0.00	0.33	0.00	40.27	0.00	17.14	0.00	0.15	100.37
R267	G 1 C 2	14.76	25.64	0.00	0.00	0.33	0.00	40.00	0.00	18.85	0.00	0.46	100.05
R267	G 1 R 2	14.66	24.05	0.00	0.00	0.73	0.00	39.64	0.00	21.55	0.00	0.07	100.71
R267	G 2 C 1	16.14	25.15	0.00	0.00	0.00	0.00	41.20	0.00	15.53	0.00	0.37	98.39
R267	G 2 C 2	15.89	25.13	0.00	0.00	0.32	0.00	41.09	0.00	16.18	0.00	0.00	98.61
R267	G 2 R 1	14.76	24.43	0.00	0.00	0.55	0.00	38.65	0.00	20.49	0.00	0.07	98.96
R267	G 2 R 2	15.52	24.85	0.41	0.00	0.00	0.00	39.79	0.00	16.85	0.00	0.40	97.81
R267	G 3 C 1	12.52	24.83	0.41	0.00	0.32	0.00	37.71	0.00	23.22	0.00	0.10	99.10
R267	G 3 R 1	10.76	15.99	0.00	0.00	3.77	0.49	32.35	0.00	35.43	0.00	0.31	99.09
R267	G 4 C 1	16.62	25.53	0.00	0.00	0.33	0.00	41.50	0.00	14.69	0.25	0.41	99.33
R267	G 4 C 2	16.62	25.85	0.00	0.00	0.30	0.00	41.95	0.00	14.68	0.00	0.07	99.47
R267	G 4 C 3	16.52	25.51	0.00	0.00	0.33	0.00	42.18	0.00	15.27	0.00	0.05	99.86
R267	G 4 R 1	15.95	24.75	0.00	0.00	0.30	0.00	41.31	0.00	14.90	0.00	0.34	97.55
R267	G 4 R 2	16.50	26.21	0.00	0.00	0.32	0.00	41.69	0.00	15.06	0.00	0.07	99.85
R267	G 4 R 3	16.39	25.38	0.47	0.00	0.30	0.00	41.42	0.00	15.00	0.00	0.11	99.07
R365	G 8 C 1	13.10	22.50	0.00	0.00	0.52	0.13	40.14	0.71	23.05	0.24	0.00	100.40
R365	G 9 C 1	14.36	24.85	0.00	0.00	0.28	0.10	40.90	0.61	18.44	0.15	0.00	99.69
R365	G 10 C 1	15.80	25.13	0.00	0.00	0.33	0.15	40.78	0.62	16.27	0.32	0.00	99.41
R367	G 1 C 1	11.71	20.56	0.00	0.00	0.68	0.10	37.26	0.65	27.57	0.27	0.00	98.79
R367	G 2 C 1	13.91	23.01	0.00	0.00	0.28	0.09	41.48	0.68	18.82	0.20	0.00	98.49
R367	G 3 C 1	9.20	14.13	0.00	0.00	1.77	0.31	37.80	0.68	34.30	0.17	0.00	98.36

R368	G 1 C 1	15.99	25.11	0.00	0.00	0.35	0.12	41.25	0.63	15.82	0.23	0.00	99.50
R368	G 2 C 1	11.86	21.22	0.00	0.00	1.28	0.41	35.28	0.59	27.26	0.17	0.00	98.08
R368	G 3 C 1	11.00	19.88	0.00	0.00	0.80	0.19	37.94	0.65	28.53	0.24	0.00	99.23
R368	G 4 C 1	8.49	9.03	0.00	0.00	5.40	0.78	31.53	0.67	41.10	0.28	0.00	97.29
R368	G 5 LHS	10.48	20.77	0.00	0.00	0.40	0.16	37.45	0.71	26.90	0.17	0.00	97.03
R368	G 5 RHS	7.48	7.99	0.00	0.00	6.26	1.06	27.60	0.56	45.27	0.23	0.00	96.44
R381	G 1 C 1	0.00	1.32	0.47	0.00	17.63	0.75	0.00	1.56	71.59	0.00	0.68	94.01
R381	G 1 R 1	0.56	4.80	18.91	11.05	13.24	0.63	0.00	0.00	45.08	0.00	0.00	94.29
R381	G 3 C 1	0.00	1.97	0.34	0.00	19.05	0.87	0.00	1.58	70.04	0.00	0.00	93.84
R381	G 2 C 1	0.00	1.40	1.73	0.97	15.45	0.72	0.00	1.30	72.89	0.00	0.00	94.46
R381	G 2 R 1	0.58	5.88	22.66	13.40	17.63	0.43	0.00	0.00	32.84	0.00	0.00	93.42
R381	G 4 C 1	0.00	2.06	0.41	0.00	19.62	0.78	0.00	1.81	69.11	0.00	0.00	93.78
R381	G 4 C 2	0.00	2.12	0.00	0.00	16.68	0.81	0.00	1.21	72.58	0.00	0.00	93.40
R381	G 5 C 1	0.00	1.87	0.41	0.00	17.93	0.87	0.00	1.59	70.95	0.00	0.00	93.61
R381	G 5 C 2	0.00	2.31	0.34	0.00	19.00	0.88	0.00	1.32	69.74	0.00	0.00	93.59
R381	G 6 C 1	0.00	2.44	0.00	0.00	18.67	0.94	0.00	1.54	69.93	0.00	0.00	93.51
R381	G 7 C 1	0.00	1.76	0.00	0.00	15.60	0.72	0.00	1.58	73.42	0.00	0.00	93.07
R381	G 8 C 1	0.00	1.83	0.00	0.00	18.22	0.74	0.00	1.43	71.23	0.00	0.00	93.45
R381	G 9 C 1	0.00	1.70	0.00	0.00	17.85	0.69	0.00	1.36	70.71	0.00	0.00	92.30
R381	G 9 C 2	0.00	1.53	0.00	0.00	17.73	0.76	0.00	1.02	71.17	0.00	0.00	92.22
R381	G 10 C 1	0.00	3.04	0.00	0.00	17.41	0.97	0.00	1.68	69.15	0.00	0.00	92.25
R381	G 10 C 2	0.00	2.80	0.00	0.00	17.78	0.93	0.00	1.52	69.26	0.00	0.77	93.06
R381	G 11 C 1	0.00	1.38	0.41	0.00	18.98	0.65	0.00	1.46	71.79	0.00	0.00	94.66
R381	G 12 C 1	0.00	1.45	0.00	0.00	18.62	0.85	0.00	1.78	71.28	0.00	0.00	93.99
R381	G 12 R 1	0.00	3.70	18.68	14.23	15.78	0.46	0.00	0.00	40.83	0.00	0.00	93.68
R384	G 1 C 1	0.00	1.95	4.41	3.13	17.85	0.87	0.00	0.96	66.79	0.00	0.00	95.95
R384	G 1 R 1	0.00	2.49	0.53	0.00	18.17	0.81	0.00	1.16	72.18	0.00	1.21	96.56
R384	G 2 C 1	0.00	2.08	1.75	1.18	18.88	0.79	0.00	1.38	70.07	0.00	0.00	96.14
R384	G 2 R 1	0.66	6.33	27.86	19.42	22.50	0.51	0.00	0.00	19.57	0.00	0.00	96.86
R384	G 3 C 1	0.00	2.61	0.49	0.00	20.02	0.82	0.00	0.96	71.36	0.00	0.00	96.26
R384	G 3 R 1	0.00	1.80	2.91	1.90	17.55	0.76	0.00	1.07	70.74	0.00	0.00	96.74
R384	G 4 C 1	0.00	2.61	0.51	0.00	21.05	0.71	0.00	1.08	69.98	0.00	0.00	95.95
R384	G 4 R 1	0.00	1.87	20.43	17.71	22.64	0.49	0.00	0.00	34.26	0.00	0.00	97.40
R384	G 5 C 1	0.00	2.19	1.95	1.64	19.22	0.88	0.00	1.55	68.54	0.00	1.02	96.99
R384	G 6 C 1	0.00	2.76	0.41	0.00	18.88	0.88	0.00	0.93	71.66	0.00	0.00	95.52
R384	G 7 C 1	0.00	2.97	0.43	0.00	18.85	0.94	0.00	1.18	71.31	0.00	0.00	95.67
R384	G 8 C 1	0.00	2.53	0.45	0.00	19.62	0.84	0.00	1.33	70.82	0.00	0.00	95.59
R384	G 9 C 1	0.00	2.02	0.60	0.31	19.40	0.82	0.00	1.25	71.75	0.00	0.00	96.15
R384	G 10 C 1	0.00	3.36	0.39	0.00	17.70	0.96	0.00	1.11	72.00	0.00	0.00	95.52
TS22448	G 1 C 1	0.00	2.17	0.00	0.00	18.25	0.93	0.00	1.07	73.75	0.00	0.00	96.17
TS22448	G 2 C 1	0.00	1.98	0.00	0.00	18.10	0.88	0.00	0.98	74.38	0.00	0.00	96.33
TS22448	G 2 C 2	0.00	1.87	0.00	0.00	18.90	0.84	0.00	1.07	73.61	0.00	0.00	96.29
TS22448	G 3 C 1	0.00	1.85	0.00	0.00	18.30	0.94	0.00	0.96	73.47	0.00	0.00	95.52
TS22448	G 4 C 1	0.00	1.81	0.00	0.00	17.00	0.93	0.00	0.97	74.74	0.00	0.00	95.45
TS22448	G 5 C 1	0.00	1.72	0.00	0.00	17.73	0.82	0.00	1.05	74.54	0.00	0.00	95.86
TS22448	G 6 C 1	0.00	2.10	0.00	0.00	17.61	1.04	0.00	0.97	73.97	0.00	0.00	95.70
TS22448	G 7 C 1	0.00	1.89	0.00	0.00	18.02	0.82	0.00	1.10	73.95	0.00	0.00	95.77
TS22448	G 8 C 1	0.00	1.89	0.00	0.00	17.56	1.00	0.00	0.99	74.59	0.00	0.00	96.04

TS22448	G 9 C 1	0.00	1.74	0.00	0.00	18.20	0.88	0.00	1.06	73.72	0.00	0.00	95.59
TS22448	G 10 C 1	0.00	2.04	0.00	0.00	16.88	1.00	0.00	0.94	75.28	0.00	0.00	96.15
TS22448	G 10 C 2	0.00	1.25	0.00	0.00	17.58	0.00	0.00	0.99	73.97	0.00	0.00	93.80
R396	G 1 C 1	0.00	2.29	0.45	0.00	16.80	0.90	0.00	0.00	73.43	0.00	0.00	93.86
R396	G 2 C 1	0.00	1.98	0.75	0.00	14.05	0.00	0.00	0.00	76.79	0.00	0.00	93.57
R396	G 3 C 1	0.00	1.42	0.43	0.00	14.71	0.88	0.00	0.68	76.74	0.00	0.00	94.86
R396	G 4 C 1	0.00	1.78	0.64	0.00	15.76	0.41	0.00	0.00	74.32	0.00	0.00	92.91
R396	G 5 C 1	0.00	1.61	0.00	0.00	14.65	0.49	0.00	0.52	76.53	0.00	0.00	93.79
R396	G 6 C 1	0.00	1.17	0.73	0.28	12.69	0.90	0.00	0.65	77.36	0.00	0.00	93.77
R396	G 7 C 1	0.00	1.36	0.77	0.00	12.49	0.84	0.00	0.76	77.28	0.00	0.00	93.50
R396	G 8 C 1	0.00	1.55	0.98	0.71	14.35	0.00	0.00	0.00	74.94	0.00	0.00	92.53
R155	G 1 C 1	0.00	2.44	0.41	0.00	19.38	1.16	0.00	1.16	70.33	0.00	0.00	94.88
R155	G 2 C 1	0.00	1.87	0.45	0.00	20.07	0.93	0.00	1.37	70.38	0.00	0.00	95.07
R155	G 3 C 1	0.00	1.78	0.51	0.00	19.55	0.99	0.00	1.18	70.60	0.00	0.00	94.60
R155	G 3 C 2	0.00	1.83	0.49	0.00	19.58	0.96	0.00	1.20	70.59	0.00	0.00	94.65
R155	G 4 C 1	0.00	2.21	0.68	0.00	21.25	1.09	0.00	1.54	68.04	0.00	0.00	94.81
R155	G 5 C 1	0.00	1.53	1.24	0.38	19.55	0.94	0.00	1.18	70.51	0.00	0.00	95.33
R155	G 6 C 1	0.00	2.48	0.45	0.00	19.65	1.03	0.00	1.27	68.81	0.00	0.00	93.68
R155	G 7 C 1	0.00	2.31	0.58	0.00	18.98	1.40	0.00	1.12	70.19	0.00	0.81	95.39
R155	G 8 C 1	0.00	2.55	0.41	0.00	20.23	1.12	0.00	1.12	70.29	0.00	0.00	95.73
R155	G 8 C 2	0.00	2.29	0.49	0.00	20.03	1.02	0.00	1.27	69.91	0.00	0.00	95.00
R155	G 9 C 1	0.00	1.87	0.00	0.00	20.50	1.06	0.00	1.51	69.56	0.00	0.00	94.50
R155	G 10 C 1	0.00	1.98	0.36	0.00	20.67	0.99	0.00	0.81	69.37	0.00	0.42	94.60
R155	G 11 C 1	0.00	2.00	0.00	0.00	20.80	1.19	0.00	1.24	68.74	0.00	0.00	93.97
R155	G 12 C 1	0.00	1.42	0.73	0.00	19.48	1.15	0.00	1.07	70.36	0.00	0.00	94.20
R384	G 1 C 1	0.73	7.10	0.36	0.00	6.51	0.65	16.49	0.97	63.42	0.00	0.00	96.23
R384	G 1 C 2	1.63	7.73	0.45	0.00	6.81	0.68	16.74	0.67	62.55	0.00	0.00	97.24
R384	G 1 R 1	9.19	10.69	26.00	4.77	2.59	0.40	8.70	0.71	39.19	0.00	0.00	102.23
R384	G 1 R 2	1.76	11.05	3.21	0.71	4.52	0.59	17.14	1.10	60.49	0.00	1.07	101.65

Appendix 2

Scanning Electron Microscope Information

The mineral chemistry analyses were carried out using the equipment at the Imaging Spectroscopy and Analysis Centre (ISAAC) at the University of Glasgow. The instrument used was the Carl Zeiss Sigma Variable Pressure Analytical SEM with Oxford Microanalysis.

The SEM and associated equipment.

The following techniques were used:

• Energy-dispersive X-ray analysis (EDX): 80 mm silicon-drift detector enables rapid determination of elemental compositions and acquisition of compositional maps.

• Wavelength-dispersive X-ray analysis (WDX): Detector facilitates high precision quantitative microanalysis

• Electron backscatter diffraction (EBSD): HKL system permits determination of the orientations of crystalline samples at high spatial resolution and can be integrated with EDX.

Parameters and standards used:

Electron Beam: 20 kV and 4.5 nA beam current

Aperture: 120 µm

Working Distance: 8.5 mm

The beam was defocused when analysing plagioclase.

Calibration Standards

The following calibration standards, provided by P&H Developments Ltd, were used to calibrate the instrument.

1	Andradite glass	A synthetic glass of andraditic composition
2	Zircon	Natural Zirconium Silicate, Peixe, Goias, Brazil
3	Periclase	Magnesium Oxide, synthetic, 99.999%
4	Caesium glass	P& H Developments special glass
5	Apatite	Natural Fluo-apatite, Durango, Mexico
6	Jadeite	Natural Jadeite, Hweka+Mamon, Burma
7	Rutile	Titanium oxide, synthetic, 99.999%, PI-KEM Ltd, UK
8	Baryte	Natural Barium Sulphate, Cow Green Mine, UK
9	Cobalt	Metal, 99.997% JM batch, 08784
10	Wollastonite	Natural Ca-pyroxenoid, Leeds University, UK
11	Haematite	Natural haematite, Elba, Italy
12	Orthoclase	Natural K-Feldspar, Lucerne, Switzerland
13	Vanadium	Metal, 99.5%, JM batch 31310
14	Pyrite	Natural pyrite, Silver Valley Mine, N.S.W, Australia
15	Halite	Natural Halite
16	Fluorite	Natural fluorite, County Durham, UK
17	Olivine	Natural peridot, Sumput, Kohisthan, Pakistan
18	Rubidium glass	P& H Developments special glass
19	Rhodonite	Natural Rhodonite, Broken Hill, N.S.W, Australia
20	Kyanite	Natural kyanite, Collinsville, Conn, USA
21	Sphalerite	Synthetic sphalerite, Earth Jewelry Co, Japan
22	Celestine	Natural Celestine, Yale, Bristol, UK
23	Nickel	Metal, 99.997%, JM batch W12918

24	Chromium Oxide	Synthetic chromium oxide, Earth Jewelry Co, Japan
25	Almandine	Natural almandine, Roxbury, Conn, USA
26	Copper	Metal, 99.999%, JM batch 854
27	Diopside	Natural diopside, Dog Lake, Ontario, Canada
28	Corundum	Synthetic corundum, 99.9999%
29	Calcite	Natural Calcite, Iceland Spar

Standard 1, the andradite glass, is used to calibrate the positions of the WDS. Standards 2 to 29 are used for quantitative microanalysis.

Appendix 3

Software used for mineral chemistry recalculation and other tasks

The following programs were used to recalculate the mineral chemistry, to process the data and to produce graphics. The author would like to acknowledge his gratitude to the original software authors for using these programs. Programs were run on a variety of PCs and laptops running Windows XP and Windows 7.

Microsoft Excel. This was the main spreadsheet application used for storing, representing and recalculating the data. Versions 2003 and 2007 were used.

Microsoft Word. This was the main word processing program used to create this work. Versions 2003 and 2007 were used.

Gabbrosoft. Several of the Gabbrosoft programs were used: SPINCALC, PLAGCALC, OLICALC and PLAGCALC for spinel, plagioclase, olivine and plagioclase respectively.

The spreadsheet **Normalisation.V15.xls** from SERC at Carlton College (serc.carlton.edu) was used extensively and proved to be very useful.

FORMULA, a mineral chemistry recalculation spreadsheet was used to recast cations to a given number of oxygens per formula unit.

GCDKit, together with the **R** statistical analysis program, was the main plotting tool used for preparing variation diagrams.

I**nkscape, GIMP, Paint.net** and **Paint Shop Pro** were used for refining the plots output from GCDKit. These programs were also used for the other graphs, diagrams, maps and charts used throughout this work.

Snappix video capture software was used on a laptop attached to the optical microscope to capture the images of slides.

Syncback. For backup purposes, the open source utility Syncback was used. This is an excellent tool and arguably the most important piece of software employed during this project.

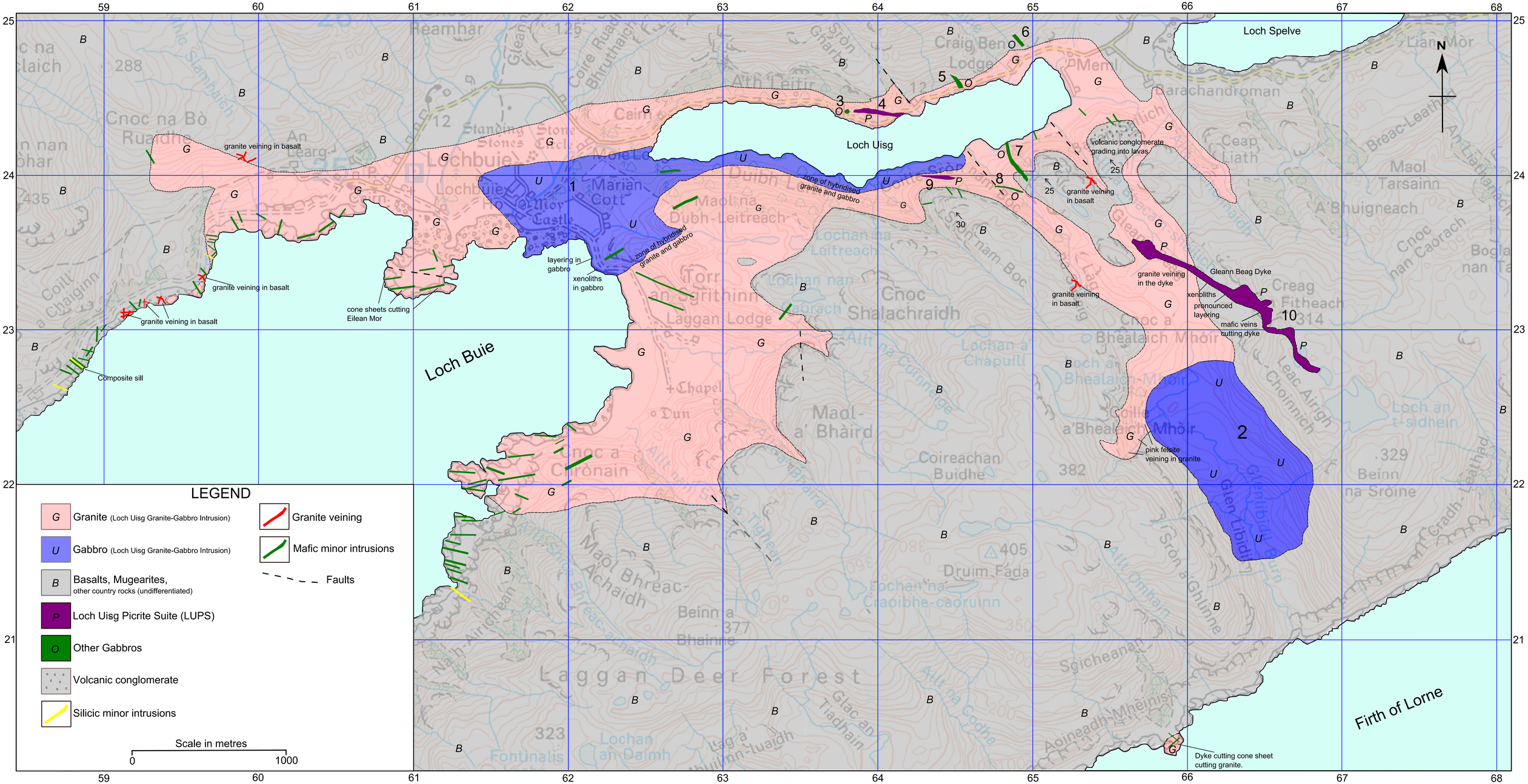
LEGEND
G Granite (Loch Uisg Granite-Gabbro Intrusion)
U Gabbro (Loch Uisg Granite-Gabbro Intrusion)
B Basalts, Mugearites, other country rocks (undifferentiated)
P Loch Uisg Picrite Suite (LUPS)
O Other Gabbros
Volcanic conglomerate
Silicic minor intrusions
Granite veining
Mafic minor intrusions
Faults
Scale in metres
0
1000
Loch Buie
Loch Uisg
Loch Spelve
Firth of Lorne
Laggan Deer Forest
granite veining in basalt
granite veining in basalt
granite veining in basalt
Composite sill
cone sheets cutting Eilean Mor
layering in gabbro
xenoliths in gabbro
zone of hybridised granite and gabbro
zone of hybridised granite and gabbro
volcanic conglomerate grading into lavas
granite veining in basalt
granite veining in basalt
granite veining in the dyke
Gleann Beag Dyke
xenoliths
pronounced layering
mafic veins cutting dyke
pink felsite veining in granite
Dyke cutting cone sheet cutting granite.
1
2
3
4
5
6
7
8
9
10
N